Déterminismes physiologiques, morphologiques et moléculaires de l'efficience d'utilisation de l'eau en lien avec la réponse à la sécheresse chez les peupliers : de la feuille à la plante entière

Maxime Durand

École doctorale SIReNa (Science et Ingénierie des Ressources Naturelles)

Thèse

Présentée et soutenue publiquement pour l'obtention du titre de

DOCTEUR DE L'UNIVERSITÉ DE LORRAINE

Mention : « Biologie et écologie des forêts et des agrosystèmes »

Par : Maxime DURAND

Déterminismes physiologiques, morphologiques et moléculaires de l'efficience d'utilisation de l'eau en lien avec la réponse à la sécheresse chez les peupliers: de la feuille à la plante entière.

5 septembre 2019

Membres du jury :

Président :	Pr. Yves JOLIVET	Professeur, Université de Lorraine, Nancy
Rapporteurs :	Dr. Evelyne COSTES	Directrice de Recherche, INRA, Montpellier
	Dr. Annabel PORTÉ	Directrice de Recherche, INRA, Bordeaux
Examinateurs :	Dr. Régis FICHOT	Maître de Conférences (HDR), Université d'Orléans, Orléans
	Dr. Catherine MASSONNET	Chargée de Recherche, INRA, Nancy
	Dr. Didier LE THIEC	Directeur de Recherche, INRA, Nancy
Membre invité :	Dr. Oliver BRENDEL	Chargé de Recherche (HDR), INRA, Nancy

UMR 1434 SILVA, Université de Lorraine – INRA – AgroParisTech, Centre INRA Grand-Est Nancy, 54280 Champenoux

À ma mère, Véronique

REMERCIEMENTS

Je remercie Evelyne Costes et Annabel Porté pour avoir accepté d'être les rapporteures de mon mémoire de thèse. Je souhaite remercier également Régis Fichot et Catherine Massonnet, pour leur participation à mon comité de suivi de thèse, ce jury et bien sûr pour leurs précieux conseils. Merci également à Guerric Le Maire pour son rôle dans mon comité de suivi.

Il y a maintenant quatre ans que mon aventure de thèse a commencé. J'ai rarement été aussi heureux que lorqu'on m'a annoncé que j'étais choisi pour le mener à bien. Les réponses négatives des concours précédents me renvoyaient à mes recherches antérieures infructueuses et m'ont fait subir un ascenseur émotionnel des plus intenses.

Je veux tout d'abord remercier Didier Le Thiec, mon directeur de thèse. Tu as été le premier à avoir cru en moi afin d'accomplir un travail de cette ampleur. Tu t'es acharné à trouver de nombreux financements pour me faire partir aux quatre coins du monde. Toutes les mesures qu'on a faites ensemble, des potentiels hydriques à 3 heures du matin, à l'écrasement des chenilles sur les feuilles de peupliers à 8 heures du soir, toutes les cinétiques d'échanges gazeux de l'aube au crépuscule par des températures parfois éprouvantes, tous ces moments resteront inoubliables pour moi. Tu as toujours été un exemple que j'ai tâché de suivre pendant ces quatre années et tu as su me remotiver quand j'avais des doutes sur le chemin à suivre. Didier, je ne pourrai jamais te rendre tout ce que tu m'as donné. Merci merci merci !

De la même façon, merci Oliver Brendel qui a assuré le co-encadrement avec Didier. Nombres de fois après avoir potassé un sujet pendant plusieurs heures, croyant enfin le comprendre, je suis allé te voir et tu as changé complètement ma manière d'aborder le sujet. Tu m'as fait me remettre en question sur tout ce que je croyais savoir. J'ai rarement eu des conversations aussi intéressantes et enrichissantes que celles que nous avons pu avoir ensemble. Merci de m'avoir mis sur les traces de Silvère. Cela m'a permis de poursuivre ses travaux de modélisation. Grâce à toi j'ai pu découvrir une nouvelle passion qui, j'espère, fera partie intégrante de ma future carrière.

Ces années de thèse ont été une sacrée aventure professionnelle. Au sein de l'équipe et de l'unité, les discussions, les réflexions et les échanges scientifiques ont été parfois surprenants, parfois brillants, mais toujours d'une excellente qualité. La bonne humeur a toujours été là et je veux remercier toutes les personnes qui ont su enrichir le quotidien du laboratoire.

Je veux remercier Cyril Buré, qui m'a aidé dans beaucoup de mesures, notamment pour suivre la croissance d'une centaine de peupliers, et qui a résolu nombre de problèmes sur les robots d'arrosage en serre. De la plantation des boutures à la récolte, rien de tout cela n'aurait pu se faire sans toi.

Un grand merci à David Cohen, Nathalie Aubry, Irène Hummel et Marie-Béatrice Bogeat-Triboulot pour votre générosité et votre bonne humeur à toute épreuve. Merci David, qui a été mon relai pendant la microdissection (128 000 stomates !). Nathalie, merci beaucoup pour ton travail énorme, et de qualité sur la quantification de l'expression

génique. Merci également a toi Irène qui m'a aidé à trouver du sens dans ce jeu de données presque trop complexe.

Je veux remercier Jean-Baptiste Lily et Patrick Gross, toujours venus à la rescousse pour résoudre les problèmes en serre et sur la LiCor. Même si vous êtes toujours très occupés, merci d'avoir trouvé le temps pour me dépanner. Merci Pascal Courtois pour toutes les mesures de sonde à neutrons qu'on a pu faire ensemble, parfois très tôt le matin.

Merci Nicolas Marron, qui m'a accompagné à une conférence en Argentine. Que de belles choses à voir, à manger et à boire ! Et bien sûr merci de m'avoir « sauvé la vie » lorque j'ai perdu ma carte de crédit à l'autre bout du monde.

Je souhaite aussi remercier Yves Jolivet pour m'avoir donné l'opportunité de faire de l'enseignement pendant ma thèse. Je suis réservé de nature et, me retrouver seul devant une classe d'étudiants était à la fois éprouvant, extrêmement formateur, et bien plus agréable que je n'aurais pu l'imaginer. Merci aussi à Dany Afif qui m'a accompagné à travers mes premiers enseignements et qui m'a aider à développer ma façon d'enseigner et surtout n'a pas hésité à me faire confiance afin d'en améliorer certains aspects. Merci également à tous les autres enseignants-chercheurs avec qui j'ai pu interagir : Mireille Cabané, Jean-Claude Pireaux, Pierrick Priaut et Sandrine Chauchard. Merci pour votre bienveillance et votre aide quand j'en ai eu besoin. Enfin, merci à Marie-Noëlle Vaultier, Anthony Gandin, Dominique Gérant, et tous ceux avec qui je n'ai pas travaillé directement mais qui ont su embellir le quotidien à travers une discussion, un repas, un échange.

Merci Christophe Rose pour la confiance que tu m'as accordé et le temps que tu as passé à me former à la microanalyse et à l'imagerie sous microscope électronique à balayage. Merci aussi pour ton aide dans le travail d'optimisation et de développement de nouvelles techniques pour réaliser plus de mesures et plus rapidement.

Je veux aussi remercier Pierre Montpied. Ton aide en statistique a été décisive pour traiter les données de mes designs expérimentaux parfois un peu trop complexes. Merci à toi et à Bruno Ferry également pour m'avoir fait confiance afin de concevoir un enseignement sur les statistiques. J'espère avoir été à la hauteur.

Merci Stéphane Ponton pour la chance que tu m'as donné en me prenant comme stagiaire de master il y a maintenant plus de quatre ans. A l'époque j'étais encore un peu perdu, avec pour seul objectif de donner le meilleur de moi-même afin d'avoir la chance de commencer une thèse à la fin de mon stage. Tes conseils résonnent encore dans mon esprit.

Pour leur accueil à l'institut Hawkesbury pour l'environnement de Sydney, je veux remercier Remko Duursma et Belinda Medlyn. Les discussions que nous avons eu pour faire fonctionner MAESPA sur mes données m'ont fait progresser rapidement, et les problèmes que nous avons rencontré ensemble étaient tellement fascinants qu'ils m'ont réveillé plusieurs fois au milieu de la nuit !

Le bureau dans lequel j'ai travaillé à l'INRA a toujours été bien rempli. Un énorme merci à tous ceux qui l'ont animé pendant ces quatre années. Pierre-Antoine Chuste (PAC) mon compagnon de pause-café, Théo Gérardin pour s'être creusé la tête ensemble sur le modèle dynamique et Chvan Youssef, merci pour tous ces moment mémorables et agréables que nous avons passé ensemble (Chvan j'attends toujours la recette de ton taboulet !). Merci également aux collègues doctorants et post-doctorants de la faculté :

Nicolas Dusart, Maxime Burst, Benjamin Turc, Adib Ouayjan et Ricardo Joffe pour tous ces moments de camaraderie au laboratoire et en dehors.

Je veux aussi remercier les trois stagiaires que j'ai encadré : Emmanuelle Ha, Mariétou Diouf et Fabrice Petel ainsi que les personnes sous contrats courts, qui ont participé aux expérimentations pour mesurer la taille des stomates, la surface foliaire des feuilles et suivre la croissance et les échanges gazeux des peupliers en serre et en pépinière. Merci à vous tous pour votre travail remarquable.

Merci à Laurence Le Maout, Adeline Vuillaume et Manon Malik pour m'avoir accompagné avec gentillesse à travers le labyrinthe administratif. Sans vous je ne suis pas certain que j'aurais réussi à signer mon contrat d'embauche !

Enfin, je veux adresser ces derniers remerciements à ma famille, pour avoir fait de moi la personne que je suis aujourd'hui. Maman, merci de tout mon cœur pour ton soutien indéfectible, pour m'avoir toujours poussé sans jamais douter. Sans toi je n'en serais pas là aujourd'hui. Merci Papa de m'avoir fait découvrir tant de nouvelles choses et d'avoir toujours cru en moi. Merci à mes grands-parents d'Heillecourt et d'Azelot, mes oncles, mes tantes, mes cousins et mes cousines. J'ai du mal à décrire avec des mots tout l'amour que j'ai pour vous.

Merci à vous tous, et à tous ceux que j'aurai le malheur d'oublier, d'avoir fait de ces quatre années un moment formidable !

Maxime

TABLE DES MATIÈRES

LISTE DES ABREVIATIONS COURAMMENT UTILISEES

Paramètres	Définition	Unités
A	Assimilation nette de CO_2	µmol m^{-2} s^{-1}
g_s	Conductance stomatique à la vapeur d'eau	mol m^{-2} s^{-1}
g_{bl}	Conductance de couche limite	mol m^{-2} s^{-1}
g_m	Conductance mésophylienne	mol m^{-2} s^{-1}
C_i	Concentration en CO_2 dans les cavités sous-stomatiques	ppm
C_a	Concentration en CO_2 atmosphérique	ppm
δ	Composition isotopique en carbone	‰
Δ	Discrimination isotopique en carbone	‰
Φ_c	Pertes en carbone indépendantes des processus foliaires	
Φ_w	Pertes en eau indépendantes de la transpiration foliaire	
WUE	Efficience d'utilisation de l'eau	mg g^{-1}
W_i	Efficience d'utilisation de l'eau intrinsèque (A/g_s)	µmol mol^{-1}
TE	Efficience de transpiration à l'échelle de la plante entière.	mg g^{-1}
g0 et G	Valeurs de g_s en régime permanent avant et après un changement environnemental	mol m^{-2} s^{-1}
τ	Temps de réponse stomatique (modèle dynamique)	s
λ	Délai de la réponse stomatique (modèle dynamique)	s
SL_{max}	Pente maximum au point d'inflexion (modèle dynamique)	mol m^{-2} s^{-2}
A_p	Aire de l'ouverture de l'ostiole	μm^2
GCL	Longueur des cellules de garde	µm
AGC	Aire des cellules de garde	µm
SD	Densité stomatique	mm^{-2}
TLA	Surface foliaire de la plante entière	cm^2 ou m^2
WU	Utilisation cumulée de l'eau à l'échelle de la plante entire	kgH_2O
E	Transpiration journalière moyenne de la plante entière par unité de surface foliaire	kgH_2O m^{-2} $jour^{-1}$
RH	Humidité relative	%
VPD	Déficit de pression en vapeur d'eau	kPa
ABA	Acide abscissique	
QTL	Locus de caractères quantitatifs : région du génome étroitement associé à un trait quantitatif.	

AVANT-PROPOS

Ces travaux de thèse ont été conduits au sein de l'unité mixte de recherche SILVA (Nancy, Grand-Est), et particulièrement dans l'équipe PhARE (Physiologie des Arbres et des Réponses à l'Environnement), sous la supervision de Didier Le Thiec et Oliver Brendel.

Le projet de thèse a été financé par la région Grand-Est et par le département EFPA (Écologie des Forêts, Prairies et milieux Aquatiques) de l'INRA. Ces travaux s'inscrivent au sein du projet européen WATBIO (http://www.watbio.eu/), pour la recherche des traits, et leurs déterminants moléculaires, impliqués dans la réponse à la sécheresse. Ils s'inscrivent également dans le projet Up-Trans, financé par le LabEx ARBRE (http://mycor.nancy.inra.fr/ARBRE/) et fait suite à plusieurs thèses au sein de l'unité mixte de recherche SILVA (Nancy, Grand-Est) et du Laboratoire de Biologie des Ligneux et des Grandes Cultures (Orléans, Centre-Val de Loire).

Pendant ces quatre ans, j'ai eu l'occasion de présenter mes résultats dans plusieurs colloques tels que l'école d'été du Plant Environment Physiology Group à Lisbonne, le symposium international IUFRO sur l'efficience d'utilisation de l'eau des arbres forestiers sous sécheresse à Nancy, et le symposium international IUFRO sur le peuplier à Buenos Aires. Une collaboration avec le "Hawkesbury Institute for the Environnement" de l'Université de Sydney en Australie m'a permis de travailler sur des questions de modélisation des échanges gazeux pendant un mois et demi avec Dr. Remko Duursma et Dr. Belinda Medlyn.

Les trois stagiaires et les nombreuses mains d'œuvre que j'ai eu l'occasion d'encadrer, ainsi que les 150 heures d'enseignement (et la formation associée) que j'ai eu la chance de donner à l'Université de Lorraine, m'ont permis d'améliorer mes compétences en pédagogie, mais surtout de découvrir une envie de partager le savoir.

Ces travaux de thèse vont permettre d'aboutir à quatre publications scientifiques, dont une est déjà publiée, deux autres sont soumises et la dernière est en cours d'écriture. Une liste complète de la production scientifique et technique réalisée pendant ces quatre années de thèse est disponible en annexe.

ÉTAT DE L'ART

ÉTAT DE L'ART

1. *Le peuplier*

1.1. L'histoire et le genre *Populus*

Les peupliers ont une longue histoire commune avec l'Homme, tous deux s'installant préférentiellement près des points d'eau. Il y a plus de 10 000 ans, les habitants de la rivière de l'Euphrate au Moyen-Orient utilisaient déjà du peuplier pour le chauffage et la construction de leurs habitations (Stettler, 2009), tout comme les Amérindiens Ojibwés 8 000 ans av. J.-C. (Hageneder, 2005) et les résidants de Youmulakekum, en Chine pendant la période précédant la dynastie Han (700-200 av. J.-C.). Dans la mythologie grecque, il est raconté que les dieux possédaient des couronnes tissées de peupliers tremble (*Populus tremula*, L.). À l'aube du 19e siècle, pendant leur traversée transcontinentale de l'océan atlantique au Pacifique, les explorateurs Lewis et Clark dépendaient des peupliers pour le chauffage, leurs canoés et leurs abris (DeVoto, 1997). Au milieu des années 1800 les peupliers servaient d'inspiration aux peintres impressionnistes français, comme Paul Cézanne (« *Les Peupliers* », 1880), Gustave Courbet (« *Marine, le peuplier* », 1875) ou Claude Monet et sa série de 23 tableaux prenant pour sujet des peupliers bordant la Seine. Le peuplier ayant un bois blanchâtre, il a été très utilisé pour la peinture sur panneau, par exemple il a servi de support pour la célèbre Joconde de Léonard de Vinci.

Le genre *Populus* est divisé en six sections (*Abaso*, *Aigeiros*, *Leucoides*, *Populus*, *Tacamahaca*, et *Turanga*), dont l'apparition est difficile à définir. La plus ancienne section (*Abaso*) daterait de la fin du Paléocène, d'après des empreintes de feuilles fossilisées de *Populus cinnamomoides* (Lesquereux) datant de 58 millions d'années (Collinson, 1992). La section *Leucoides* serait apparue pendant l'Eocène, puis *Tacamahaca* à la fin de l'Oligocène, *Aigeiros* au Miocène et *Populus* au Pliocène. Les peupliers noirs (*Populus nigra* L.) ont été introduits en Europe depuis la Perse (actuellement Iran) par l'intermédiaire de l'Italie vers 1750. Les peupliers de Virginie (*Populus deltoides* Bartr.) quant à eux, ont été introduits au 17e et 18e siècle depuis l'Amérique du Nord, sous plusieurs noms de cultivars.

Jusqu'au 20e siècle les peupliers plantés étaient principalement des espèces naturellement présentes, ou des hybrides spontanés issus d'espèces d'Europe et d'Amérique du Nord. L'hybridation entre espèces au sein ou entre sections est courante dans le genre *Populus* (Vanden Broeck *et al.*, 2005). La première hybridation contrôlée de peuplier a été réalisée par

A. Henry en 1912 (Henry, 1914), puis par la suite au jardin botanique de New York (Stout & Schreiner, 1933). Rapidement, le premier institut de recherche dédié à la création variétale de peupliers a vu le jour en Italie en 1937 dans la vallée de la rivière du Po (Dickmann, 2006). C'est à ce moment qu'est né le clone I214 (Jacometti, 1937), encore largement cultivé aujourd'hui de par le monde, et un des clones utilisés dans cette présente thèse. Des pénuries de bois au cours des années 1930 ont provoqué l'établissement d'une commission nationale du peuplier par le Ministère français de l'Agriculture. L'implication d'autres pays européens a permis dans un second temps d'étendre et de transformer cette commission en commission internationale pour le peuplier (IPC) sous la gouvernance de la FAO en 1958 (FAO, 1958).

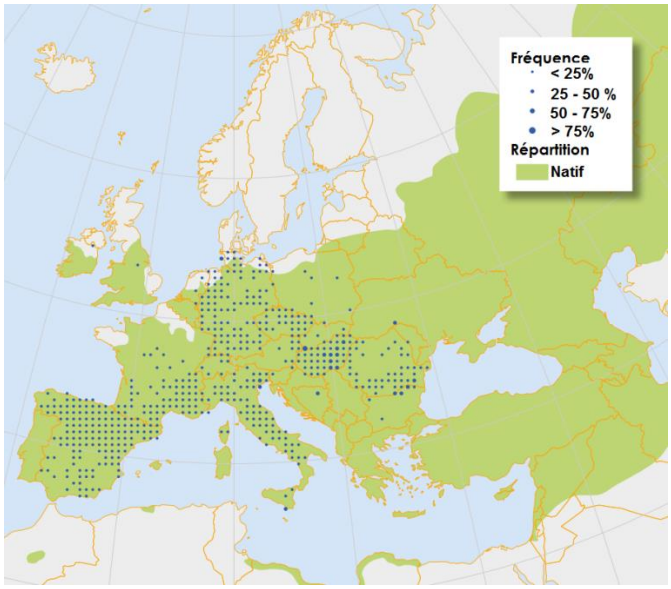

Figure 1. Aire de distribution de *Populus nigra* (L.) en Europe, Asie et Afrique. Les fréquences sont reportées à partir d'inventaires forestiers et la répartition depuis le programme européen EUFORGEN. D'après De Rigo *et al.* (2016).

1.2. Ecologie et répartition des peupliers

Au sein de la famille des *Salicaceae*, les peupliers sont des dicotylédones arbustives et dioïques, à feuillage caducifolié ou rarement semi-persistant. Les arbres portent des fleurs pistillées (femelle, produisant les graines) ou staminées (mâles, portant les pollens) réunies en chatons, sans calice ni corolle et s'allongeant depuis les bourgeons axiaux reproducteurs. Les feuilles de peupliers sont diverses, d'une espèce et d'un génotype à l'autre, peuvent changer avec l'âge et au sein d'un même arbre. Elles sont amphistomatiques, avec une densité stomatique très souvent supérieure sur la face abaxiale. La distribution géographique des peupliers s'étant des forêts boréales aux tropiques.

En France, l'espèce dominante à l'état naturel est le peuplier noir, ou peuplier d'Italie (*Populus nigra*), devant *Populus tremula* (L.) et *Populus alba* (L.). Sa distribution naturelle s'étend des îles britanniques au nord, aux côtes méditerranéennes au sud, jusqu'en Afrique du Nord. A l'est, elle atteint la Chine et le Kazakhstan (Fig. 1). Bien que son aire de répartition soit large, la présence des peupliers est rare à l'échelle géographique. Inféodés aux milieux humides à cause de leur forte consommation en eau et faible tolérance à l'ombrage, les peupliers sont des plantes pionnières courantes d'environnements perturbés. Nous les retrouvons peu en forêts denses, mais sont couramment répartis le long des rivières et dans des zones humides ripariennes ou alluviales (Fig. 2). La dynamique hydrogéomorphologique détermine l'hétérogénéité spatiale et temporelle de l'habitat riparien (Naiman *et al.*, 2005). Les peupliers au sein de la ripisylve jouent un rôle écologique essentiel. Le système racinaire des peupliers permet de maintenir la cohésion des sédiments, réduisant l'érosion des berges et limitant les dégâts des inondations. Ils permettent aussi de filtrer les eaux de ruissellement (épuration des nutriments excédentaires comme l'azote des eaux agricoles) et stimuler la biodiversité par la création d'habitats spécifiques (Stobrawa, 2014).

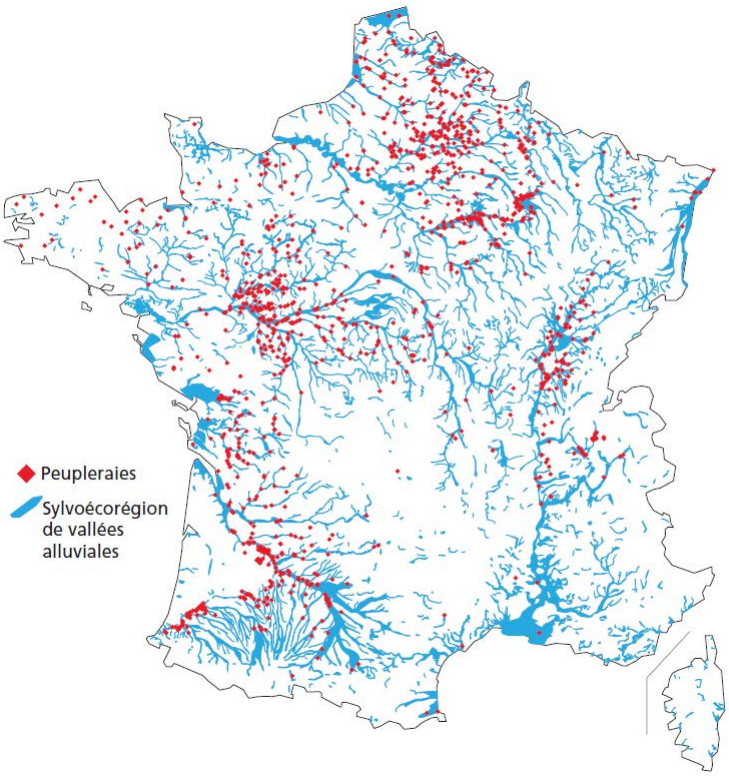

Figure 2. Répartition des peupleraies en France métropolitaine. D'après Du Puy et al. (2017).

Le génome du peuplier de l'Ouest (*Populus trichocarpa*, Torr. & Gray) a été séquencé en 2006 (Tuskan *et al.*, 2006), le troisième après *Arabidopsis thaliana* (L.) et *Oryza sativa* (L.). Avec

485 millions de paires de base, son génome est relativement petit, six fois plus petit que celui du maïs (*Zea mays*, L.). Même si la triploïdie et la tétraploïdie existent au sein de la section *Populus*, la plupart des espèces sont diploïdes (2n = 38; Isebrands & Richardson, 2014). Ces caractéristiques, ainsi que sa facilité de culture, sa capacité d'hybridation, de reproduction végétative et sa croissance rapide en font de fait le premier organisme modèle arbustif (Jansson & Douglas, 2007; Stobrawa, 2014).

1.3. Culture et risques associés

A la suite de la seconde guerre mondiale, la demande de produits dérivés du bois fut en hausse. La croissance de la population mondiale accélère également la propagation de ces hybrides à croissance rapide à travers le monde, notamment en Chine, en Inde, en Australie, au Brésil, au Chili, en Nouvelle Zélande et en Afrique du Sud (FAO, 1958). La superficie mondiale de peupliers est estimée à plus de 87 millions d'hectares, principalement au Canada, aux USA en Chine et en Russie (98% du total à eux quatre), dont 8.6 millions sont plantés essentiellement en Chine pour 88%. En France, la culture du peuplier représentait 236 000 ha en 2008 (Tableau 1), soit la plus grande surface de peupliers plantés en Europe (FAO, 2012).

Tableau 1. Superficie de peupliers à l'état naturel ou cultivé par pays. D'après FAO (2012). Les chiffres de la France sont ceux de 2008 puisque les données n'ont pas été actualisées dans le rapport de 2012.

Pays	Superficie total de peupliers (ha)	Superficie de peupliers plantés (ha)
Canada	30 360 400	44 128
Russie	24 757 000	0
États-Unis	17 698 300	45 000
Chine	12 900 000	7 570 000
Inde	362 700	700
France	275 800	236 000
Iran	185 000	150 000
Italie	143 655	101 430
Turquie	132 963	125 000
Espagne	119 600	105 000
Roumanie	73 240	47 942
Argentine	61 000	40 500

A l'état cultivé, les hybrides du peuplier noir avec un peuplier américain (*Populus deltoides*), les peupliers euraméricains (*Populus euramericana* ou *Populus canadensis*) sont les plus courants. D'autres hybrides, comme les peupliers interaméricains (*Populus deltoides* ×

trichocarpa) ont également été beaucoup utilisés pour leur vigueur et leur capacité de résistance aux pathogènes, et en particulier à la rouille foliaire. Cependant, de nouvelles virulences à la fin des années 1990 l'ont rendu fortement sensible à la rouille. Ainsi, il est aujourd'hui très peu utilisé comparé aux hybrides euraméricains (Thivolle-Cazat, 2002).

La propagation végétative des peupliers peut se faire à partir de simples tiges de bois, desquelles se formeront de nouvelles racines et tiges. Le bois de peuplier présente de nombreuses qualités qui permettent une grande diversité d'utilisations. Son anatomie poreuse se traduit par une certaine légèreté, un grain droit et une texture uniforme. Le bois n'est pas très rigide, faiblement résistant aux chocs et à la pliure, ce qui rend son travail, à la main ou par des machines, aisé. De plus il est facilement cloué, vissé ou collé. Parmi ses nombreuses utilisations, il peut servir à la fabrication de pulpes, de papiers, de contreplaqués, de panneaux composites, de bûches, de bois d'œuvre, de caisses, de boites, d'allumettes, de baguettes et de copeaux d'emballage. Il est notamment utilisé pour les emballages de camembert. La demande en bois et produits dérivés devraient augmenter de façon continue dans les années à venir atteignant une hausse de 20% d'ici 2060 (Fig. 3), conduite par la croissance démographique et économique ainsi que par des politiques publiques environnementales et énergétiques (FAO, 2018).

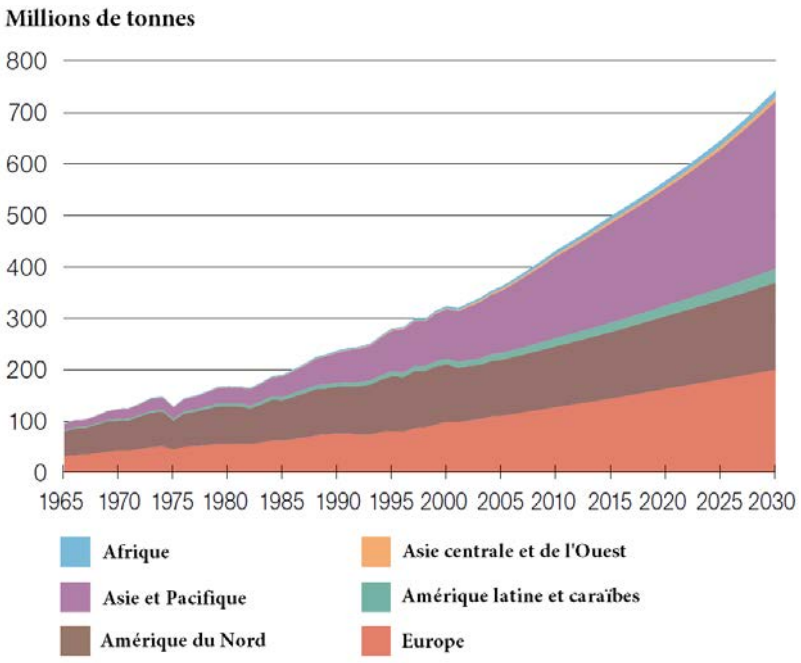

Figure 3. Production globale observée (1965-2005) et projetée (2005-2030) de papiers et cartons. D'après un rapport de la FAO sur l'état des forêts dans le monde (FAO, 2018)

2. Changements globaux et sécheresses

2.1. Changements climatiques observés

Dans un récent rapport du groupe d'experts intergouvernemental sur l'évolution du climat (IPCC, 2018), le comité rapporte que les hausses de température observées aujourd'hui à travers le globe de 0.8 à 1.2°C au-delà des températures de l'ère préindustrielle atteindront très probablement 1.5°C entre 2030 et 2052. Les zones continentales sont d'ailleurs sujettes à de plus fortes augmentations que les océans, notamment dans les hautes latitudes de l'hémisphère Nord. Ceci implique un accroissement de la fréquence et de l'intensité des extrêmes climatiques (Chevuturi *et al.*, 2018). Il faut noter que les conditions régionales spécifiques sont déterminantes pour une grande partie des impacts locaux des changements climatiques. En particulier les motifs de précipitations et de sécheresse, sont hautement dépendants du climat local.

Ces changements climatiques résultent essentiellement d'émissions de gaz à effet de serre (CO_2 principalement) d'origine anthropiques. Les concentrations de CO_2 dans l'atmosphère ont augmenté de 280 ppm en 1750, à l'aube de l'ère industrielle, à 390 ppm en 2011. Chaque décennie est marquée par une augmentation substantielle de la quantité d'émissions, avec une hausse moyenne de 1.9% par an dans les années 1980, 1% dans les années 1990 et 3.1% par an depuis 2000 (Peters *et al.*, 2012). Cette augmentation était à l'origine principalement due aux émissions liées à la déforestation et à des changements d'occupation des territoires. A partir de 1920, la part majoritaire des émissions de gaz à effet de serre provient de combustibles fossiles (Le Quéré *et al.*, 2013). De plus les émissions de méthane, un gaz à effet de serre émis en bien moindre quantité que le CO_2 mais ayant un potentiel de réchauffement global 25 fois supérieur, sont en forte augmentation depuis 2007 (Nisbet *et al.*, 2019).

Les efforts internationaux pour limiter l'augmentation des températures globales au-delà de 2°C semblent pour l'heure inconséquents au vu des prédictions d'émission de gaz à effet de serre (Fig. 4; Solomon *et al.*, 2009; IPCC, 2018). Les augmentations des émissions de méthane ne sont, par exemple, pas prévues dans les accords de Paris. Les objectifs fixés pourraient ainsi être plus complexes à atteindre.

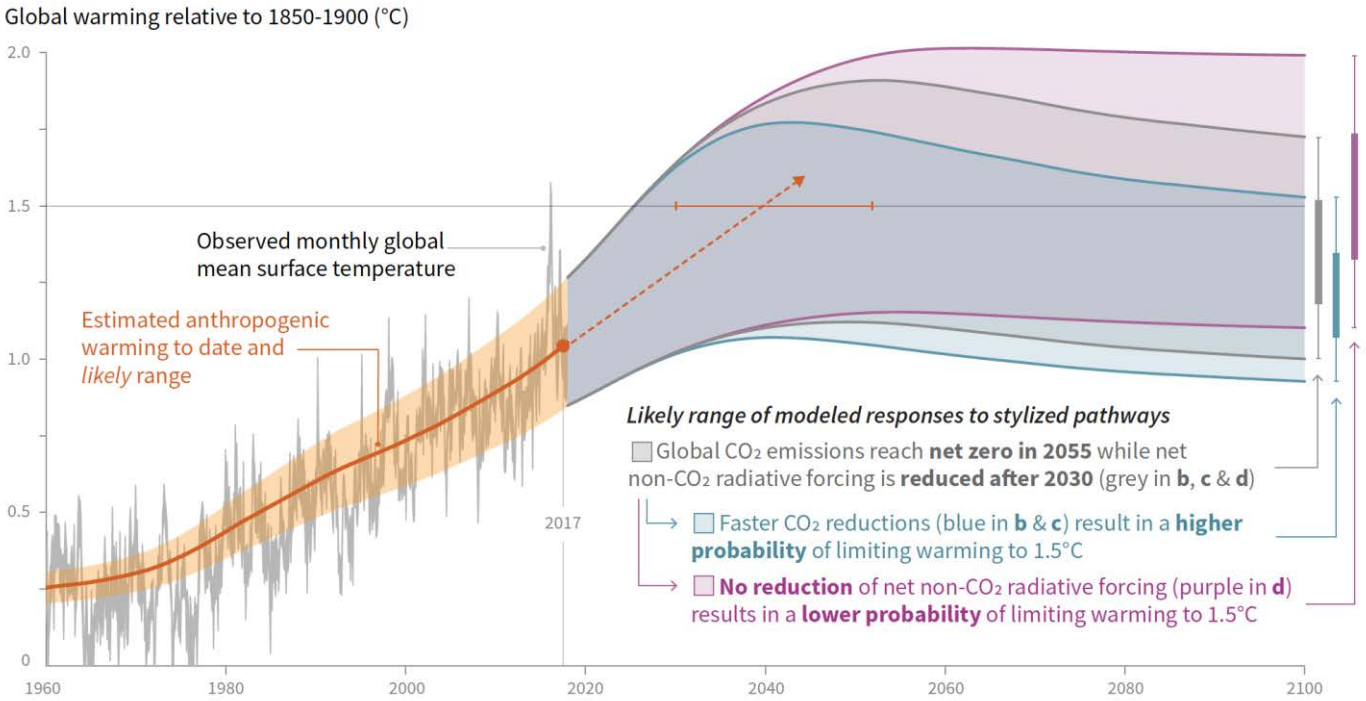

Figure 4. Evolution des températures globales observées et prédictions sous divers scénarii d'émissions anthropiques. Adapté d'après le rapport du GIEC sur les effets d'un réchauffement global d'1.5°C (IPCC, 2018).

2.2. Sécheresses édaphiques

Une sécheresse édaphique se définit comme un déficit hydrique prolongé mais temporaire (IPCC, 2018). De ce fait elle intervient de par le monde, aussi bien dans les régions les plus arides que les plus humides. Bien que le concept soit facile à déterminer, les sécheresses interviennent par le couplage de processus atmosphériques, hydrologiques et biogéophysiques. Ainsi, il est difficile de s'accorder sur une définition stricte et unifiée d'une sécheresse. Par conséquent le début et la fin, tout comme l'intensité ou la résistance à une sécheresse sont des paramètres complexes à caractériser. Enfin, une sécheresse est toujours définie sous le prisme des organismes qui la subissent. Ces caractéristiques forcent son étude à l'aide d'indices, et de seuils variant selon les régions considérées ou les objets d'étude.

Les fortes variations locales de précipitations, rendent difficile de déterminer avec certitude les tendances à l'échelle globale. Cependant, il est probable que les changements globaux induisent une augmentation de la fréquence et de l'intensité des sécheresses (IPCC, 2014), lié à des réductions des précipitations à l'échelle régionale associées, ou non, à une augmentation de l'évaporation induite par les hausses de températures (Dai, 2012). En Afrique, dans le sud de l'Europe, dans l'est et le sud de l'Asie et dans l'est de l'Australie la quantité de terrains sujets aux sécheresses s'est étendue significativement depuis 1950 (Dai, 2011). Les prédictions des

modèles de climat globaux prédisent une augmentation de l'aridité, et donc des sécheresses, dans les années à venir (Sheffield & Wood, 2008).

L'impact des sécheresses est considérable à la fois au niveau économique, humanitaire et environnemental (Touma *et al.*, 2015). La sécheresse de 2003 en Europe a causé à elle seule la perte d'environ 16 milliards d'euros et la canicule à proprement parlé 20 000 morts supplémentaires en France. Aux États-Unis, des épisodes de sécheresse de 2012 à 2013 dans les plaines centrales ont couté 12 milliards de dollars de dommages (Hoerling *et al.*, 2013). Des sécheresses en Ukraine et Russie en 2010 ont induit une baisse drastique de la production de blé, entraînant une hausse significative des prix mondiaux pour les pays importateurs comme l'Égypte ou la Tunisie, mettant en lumière les conséquences globales de sécheresses locales (Sternberg, 2011). Au-delà des pertes économiques, les sécheresses ont un impact sur les pénuries de nourriture et d'eau dans les pays les moins développés. Ces pénuries entraînent une hausse de la mortalité, des déplacements de masse de réfugiés d'un pays à l'autre et dans certain cas des conflits armés (Hsiang *et al.*, 2013).

2.3. Impacts sur les végétaux

L'impact des changements climatiques, en particulier des sécheresses sur les forêts et les végétaux en général, est une préoccupation centrale de la recherche agronomique actuelle. Les forêts occupent environ 30% des terres sur le globe, et sont étroitement liées au climat et à l'atmosphère avec lesquels elles échangent de l'eau, du CO_2, et divers composés (Bonan, 2008). Tous les effets des changements climatiques sur les forêts ne sont pas négatifs, par exemple l'élévation des concentrations atmosphériques en CO_2 pourrait augmenter la séquestration de carbone et la productivité des forêts (Allen *et al.*, 2015). Diverses espèces répondront de façon différente aux changements globaux, induisant des modifications de composition et de répartition des espèces au sein des écosystèmes forestiers (Etzold *et al.*, 2019). Cependant ces observations pourraient ne pas refléter les tendances globales puisqu'il n'existe pas de programme de surveillance systématique des forêts. Elles pourraient être le résultat d'une attention accrue récente de la communauté scientifique envers la mortalité des forêts (Allen *et al.*, 2010). De plus, différentes études divergent dans leurs méthodes et définitions de la sévérité des stress. Néanmoins, de récentes études montrent que certains écosystèmes forestiers pourraient déjà répondre aux changements climatiques. Le taux de mortalité des arbres est en hausse, en réponse aux augmentations des températures et aux sécheresses, même dans des écosystèmes normalement non limité par la disponibilité en eau (Allen *et al.*, 2010). D'autre

part l'impact des sécheresses, intensifié par les changements globaux (Allen *et al.*, 2015), entraîne généralement une diminution de la productivité primaire des forets (Ciais *et al.*, 2005).

La réponse des végétaux à la sécheresse est complexe. D'ordinaire, elles induisent une réduction de la production de biomasse, en particulier sur les espèces considérées comme grandes consommatrices d'eau comme l'eucalyptus (Coopman *et al.*, 2008) ou le peuplier (Fig. 5; Monclus *et al.*, 2006). La division et l'allongement cellulaire peuvent être inhibés en cas de stress hydrique prolongé (Hsiao, 1973). Au sein de la plante, l'eau est transportée sous tension des racines vers les feuilles par le xylème. C'est en fait sous l'effet de l'évaporation de l'eau dans les cavités sous-stomatiques que la colonne de sève brute est « tirée » des racines vers les feuilles. Sous cet état, l'eau est susceptible de se vaporiser puisque la pression au sein du xylème est plus négative que la pression de vapeur du liquide (Dixon & Joly, 1895). Lorsque ce phénomène de cavitation se produit, le vaisseau conducteur devient saturé en air, provoquant une embolie. Ce phénomène peut être induit par la sécheresse, alors appelé embolie estivale. Si une partie significative des vaisseaux conducteurs souffrent d'embolie, le fonctionnement hydraulique de la plante et sa capacité à alimenter les parties supérieures du végétal, comme les feuilles, ne peuvent être assurés adéquatement (Cruiziat *et al.*, 2002).

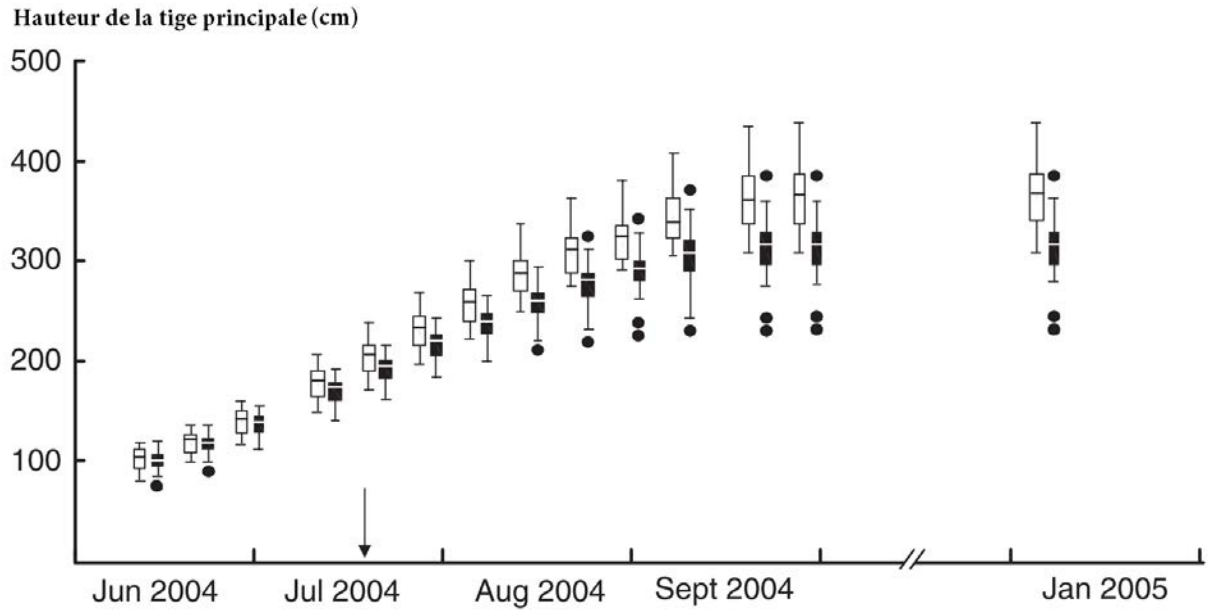

Figure 5. Dynamique de la hauteur de la tige principale chez 29 génotypes de peupliers euraméricains bien irrigués (boites blanches) ou sous sécheresse (boites noires). Les boites représentent la médiane, le premier et troisième quartile. Les barres verticales représentent les valeurs maximales et minimales. D'après Monclus et al. (2006).

Le comportement des espèces face à la sécheresse varie d'une espèce à l'autre. Nous pouvons qualifier des plantes capables de supporter une certaine dessiccation de tolérante à la sécheresse,

tandis que celles stockant une grande quantité d'eau tout en limitant les pertes, peuvent être qualifiées de résistantes. Une ancienne classification groupe les réponses au stress hydrique en plusieurs stratégies (Kearney & Shantz, 1911). L'échappement concerne les espèces « éphémères », ayant une période de croissance courte (quelques semaines) et des graines matures avant que la plante soit en contact avec un déficit hydrique. La stratégie d'évitement consiste à limiter l'épuisement de la réserve en eau. Cette économie d'eau peut faire intervenir un contrôle de la transpiration, notamment par la fermeture des stomates ou en limitant la surface foliaire susceptible de transpirer. En conséquence, le taux de croissance de ces plantes est généralement faible. Une autre possibilité implique un développement fort du système racinaire permettant une grande exploration et exploitation des réserves en eau du sol. Nous pouvons définir le comportement isohydrique d'une espèce selon sa régulation du potentiel hydrique foliaire de jour. Les plantes dites anisohydriques (orge, tournesol) montrent une diminution substantielle du potentiel hydrique foliaire lorsque le sol s'assèche, alors que les espèces isohydriques (maïs, peuplier) ont tendance à le maintenir (Tardieu & Simonneau, 1998). Ainsi les espèces anisohydriques seraient plus tolérantes à des déficits hydriques modérés, maintenant les échanges gazeux et donc l'assimilation de CO_2. Au contraire, un stress hydrique fort entraînerait des dommages irréversibles sur ces espèces (par exemple une embolie). Même si le lien entre le maintien du potentiel hydrique foliaire et la réponse stomatique à un déficit hydrique a été remis en question (Prieto *et al.*, 2010), ces comportements forment un gradient dans lequel le caractère d'isohydrie est comparé entre espèces ou génotypes.

Les problématiques liées à l'augmentation de la demande en bois entrent en conflit avec la projection de déclin de la productivité des forêts dans les années à venir. Exprimée simplement, la production de biomasse est issue de la transformation du CO_2 atmosphérique en sucres pendant le processus de photosynthèse dans les feuilles, tandis que les pertes en eau proviennent pour 99% de la transpiration des feuilles. Ces entrées de CO_2 et sorties d'H_2O s'effectuent au même endroit de la feuille, au sein des stomates.

3. *Stomates*

3.1. Rôles des stomates

Les stomates forment des pores sur l'épiderme des parties aériennes, principalement au niveau des feuilles. Ils sont composés d'une paire de cellules, dites de garde, avec un orifice central appelé ostiole en contact avec les espaces sous-stomatiques du mésophylle (Fig. 6). Ces cellules de garde peuvent modifier leur volume sous l'influence de divers facteurs endogènes et/ou

environnementaux. Ceci entraine des variations de l'ouverture de l'ostiole et par conséquent modifie les flux de CO_2 entrant et d'H_2O sortant de la feuille. Ces variations permettent ainsi de moduler deux processus cruciaux chez les végétaux : la photosynthèse et la transpiration. En 1977, Cowan & Farquhar proposent l'hypothèse que les mouvements stomatiques sont régulés de sorte que l'assimilation de CO_2 soit maximale pour des pertes en eau minimales.

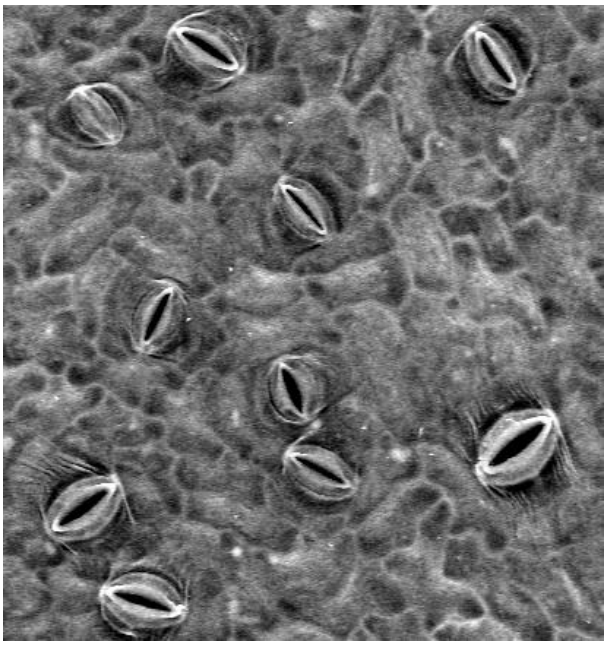

Figure 6. Stomates de la face abaxiale d'une feuille de peuplier euraméricain. Photographie prise au microscope électronique à balayage équipé d'un détecteur d'électrons rétrodiffusés. Grandissement x1000.

Ces échanges gazeux, dépendant du degré d'ouverture des stomates sont mesurés, par analogie de la loi d'Ohm, comme l'inverse d'une résistance, c'est-à-dire une conductance. Cette conductance stomatique (g_s) augmente ou diminue selon le degré d'ouverture des cellules de garde et les différences de pression entre les cavités sous-stomatiques et l'atmosphère. Une autre résistance à la diffusion de molécules entre la feuille et l'environnement, est la conductance de couche limite (g_{bl}). Cette conductance représente une couche d'air à la surface des feuilles qui n'est pas mélangé avec l'atmosphère. Elle est influencée par la vitesse du vent, la taille de la feuille et ses aspérités de surface (stomates dans des cavités, présence de poils). Cette couche prend son importance dans des houppiers denses, et dans des conditions de vent minimales. Dans ces conditions, l'environnement perçu par les cellules de garde est influencé par la couche limite, formant une boucle de rétroaction où les stomates sont influencés par leur propre transpiration et assimilation photosynthétique (Aphalo & Jarvis, 1993b). Ce phénomène

peut se produire au niveau de la feuille mais aussi de la plante entière, alors découplée de l'environnement (Jarvis & McNaughton, 1986).

3.2. Mécanismes d'ouverture et de fermeture des stomates

Les mouvements stomatiques sont provoqués par une déformation mécanique des parois des cellules de garde, induite par des mouvements d'eau entrant et sortant des cellules de garde. Ces flux d'eau ont pour origine une modification du gradient de potentiel électrochimique entre l'intérieur et l'extérieur de la cellule (Jones, 2014). Pendant l'ouverture stomatique, les pompes à protons ATPase-dépendante sur la membrane plasmique des cellules de garde expulsent vers l'apoplaste des ions H^+ (Kinoshita & Shimazaki, 1999). Cette augmentation de protons d'un seul côté de la membrane plasmique provoque une hyperpolarisation membranaire, qui a pour effet d'activer des canaux ioniques. Parmi eux, principalement des transporteurs de potassium (Humble & Raschke, 1971; Schroeder *et al.*, 1984), mais aussi de chlore et de malate qui permettent de tamponner les variations de pH liées aux mouvements de protons (Kim & Lee, 2007). L'ouverture stomatique peut aussi être maintenue par l'accumulation de sucres (Outlaw & Manchester, 1979). La fermeture stomatique peut faire intervenir une augmentation des pools de calcium cytosolique (McAinsh *et al.*, 1990). Elle s'effectue par la dépolarisation de la membrane plasmique induite par l'inactivation des pompes à protons (Kinoshita *et al.*, 1995). Les canaux entrant de potassium (Sato *et al.*, 2009) sont également inactivés, alors que des canaux sortant de potassium (Schroeder *et al.*, 1987; Schroeder & Hagiwara, 1989), de chlore et de malate sont activés (Vahisalu *et al.*, 2008; Geiger *et al.*, 2010).

La paroi des cellules de garde est dissymétrique, étant épaisse, rigide et cutinisée du côté de l'ostiole et fine du côté externe. De plus les microfibrilles de cellulose au sein de la paroi imposeraient une courbure anisotropique de par leur orientation radiale (Franks *et al.*, 1998). Les mouvements d'eau créent une force motrice responsable de l'augmentation du volume de ces cellules, un renforcement de la pression de turgescence et ainsi, un élargissement du diamètre de l'ostiole. Tous les stomates ne sont pas synchrones dans leurs mouvements. Les variations locales et les résistances à la diffusion latérale au sein des feuilles, peuvent entrainer des différences d'ouverture entre stomates, nécessitant d'observer le phénomène dans son ensemble (Fig. 6).

3.3. Facteurs induisant des mouvements stomatiques

Comme indiqué précédemment, les variations de l'ouverture des stomates sont régies par de nombreux facteurs environnementaux. Parmi eux, la lumière est la seule pour laquelle les

mécanismes de perception ont pu être identifiés. De manière générale, la plupart des plantes ouvrent leurs stomates en réponse à une augmentation de l'irradiance et les ferment à l'obscurité. Il faut séparer deux mécanismes de réponse à la lumière, dépendant de la longueur d'onde, qui agissent de concert (Shimazaki *et al.*, 2007). La lumière bleue agit comme un signal perçu par des phototropines, PHOT1 et PHOT2, récepteurs à la lumière bleue (Kinoshita *et al.*, 2001). Ces phototropines sont responsable de l'activation d'abord par phosphorylation des pompes ATPase-dépendantes (Sondergaard *et al.*, 2004; Yamauchi *et al.*, 2016), puis par la fixation de protéines 14-3-3 (Fig. 7; Palmgren, 2001). La réponse à la lumière bleue est rapide et nécessite une faible intensité lumineuse.

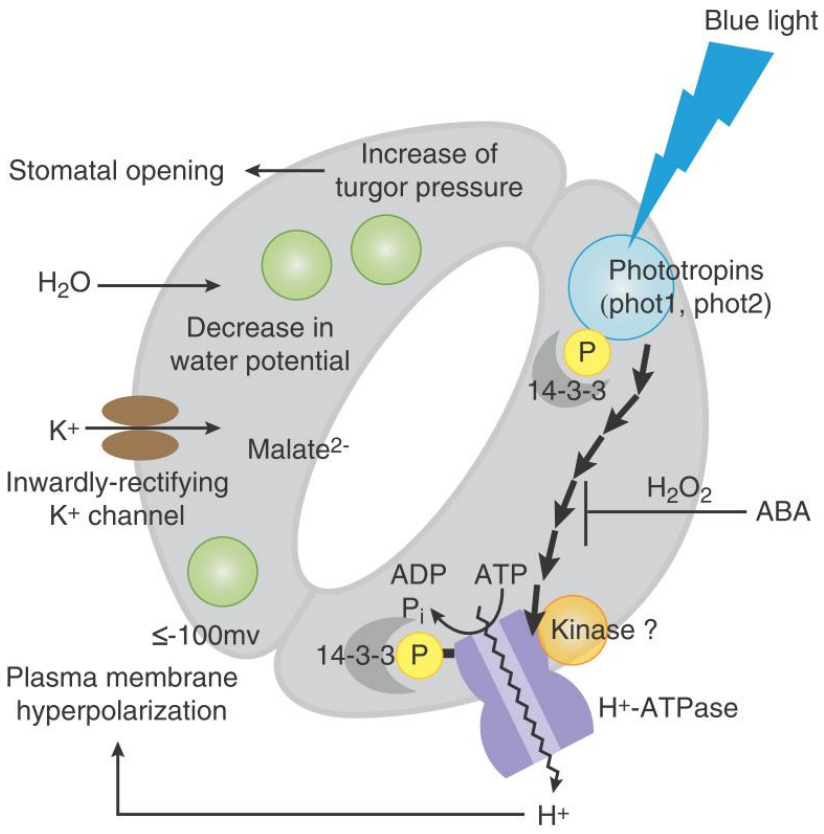

Figure 7. Ouverture stomatique en réponse à la lumière bleue. D'après Shimazaki et al. (2007).

Contrairement à la réponse à la lumière bleue, la réponse à la lumière rouge active la photosynthèse. Elle pourrait également être responsable de l'accumulation de sucres et de l'activation de transporteur de K^+ (Olsen *et al.*, 2002). Les mécanismes impliqués dans la perception et la signalisation de la lumière rouge sont encore peu connus mais pourraient faire intervenir, en partie, des variations de CO_2 dans les cavités sous-stomatiques (C_i) du mésophylle (Roelfsema *et al.*, 2002; Mott *et al.*, 2008; Lawson *et al.*, 2014). La réponse à la lumière rouge

agit de manière synergique avec la lumière bleue, produisant une ouverture stomatique plus grande que la somme des deux réponses (Assmann, 1988).

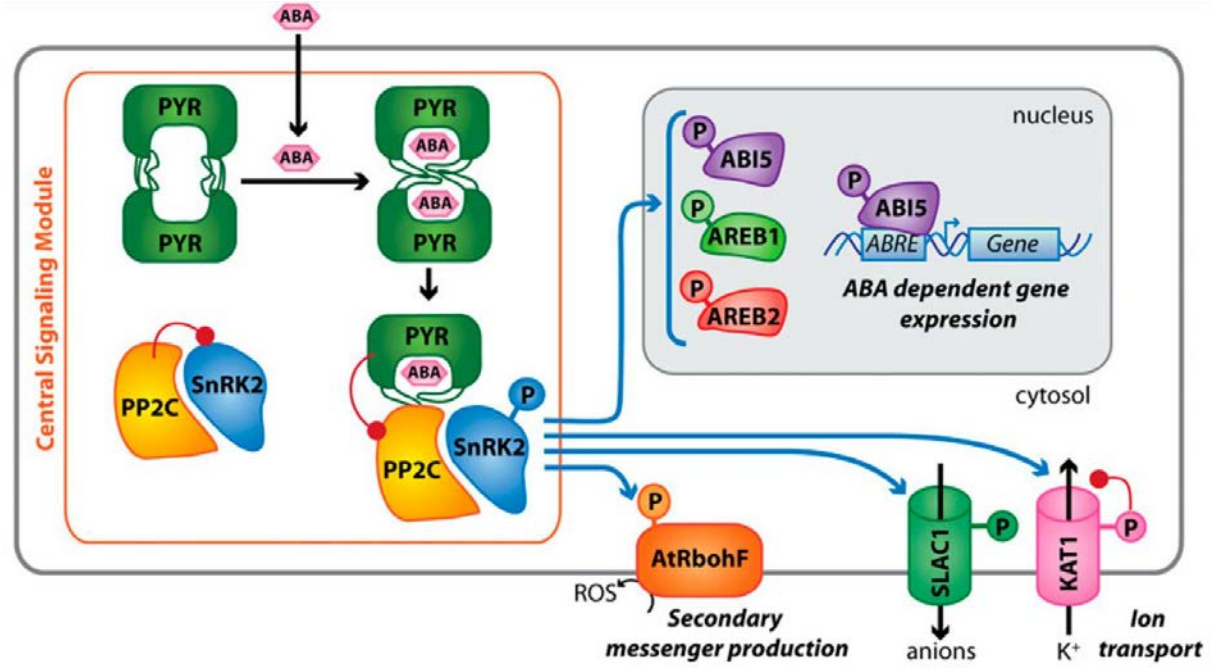

Figure 8. Voie de signalisation de l'acide abscissique. En absence d'ABA, les PP2C inhibent l'activité kinase de SnRK2 (OST1). Lorsque l'ABA se fixe à des dimères PYR/PYL, les complexes PP2C-SnRK2 se dissocient et inhibent l'activité des PP2C, libérant SnRK2. Les cibles de SnRK2 impliquent la régulation de canaux ioniques, de l'expression de gènes, et la production de messagers secondaires. D'après Hubbard *et al.* (2010).

En réponse à un déficit hydrique édaphique, les stomates se ferment, limitant les pertes en eau. Nous ne savons pas encore si les mécanismes responsables de la fermeture des stomates sont d'origine hydraulique ou hormonale (Rodriguez-Dominguez *et al.*, 2016). D'un côté, la diminution de pression de turgescence des cellules foliaires pourrait conduire à une rétroaction négative activement régulée (Sperry *et al.*, 2002; Buckley, 2005; Brodribb & Cochard, 2009). Ce mécanisme permettrait de retourner l'avantage mécanique de l'épiderme, contribuant à l'ouverture stomatique lorsque les pressions de turgescence diminuent (Franks *et al.*, 2001; Franks & Farquhar, 2007). D'un autre côté, la baisse de la conductance stomatique en sécheresse pourrait être induite avant tout, par des signaux hormonaux tels que l'acide abscissique (ABA, Fig. 8). L'ABA se déplacerait des racines vers les feuilles, étant générée indépendamment du statut hydrique foliaire (Davies & Zhang, 1991; Tardieu & Simonneau, 1998; Dodd, 2005). Les cellules de garde possèdent par ailleurs la voie complète de biosynthèse de l'ABA (Bauer *et al.*, 2013). En se fixant sur des récepteurs de la famille PYR/PYL, l'ABA inhibe des phosphatases de type PP2C encodées par le gène *ABI1* (Yoshida *et al.*, 2006; Park

et al., 2009). Se faisant, le facteur OST1 n'est plus réprimé, ce qui permet d'inactiver les canaux potassiques entrant, tels que KAT1 (Fig. 9; Sato *et al.*, 2009). Des transporteurs de type R et S, pour « rapid » et « slow » (Schroeder & Keller, 1992), tel que SLAC1 (type S) sont également activés (Geiger *et al.*, 2009). La réponse des stomates à un déficit hydrique d'origine atmosphérique, faisant varier le déficit de pression de vapeur d'eau entre la feuille et l'air extérieur (VPD), est peu connue. De la même façon que pour une réduction de la disponibilité en eau dans le sol, plusieurs mécanismes ont été proposés. La réponse stomatique au VPD a été liée à la fois à un mécanisme hydraulique passif et à une réponse activement régulée par l'ABA (Assmann *et al.*, 2000; Peak & Mott, 2011; Mc Adam & Brodribb, 2015).

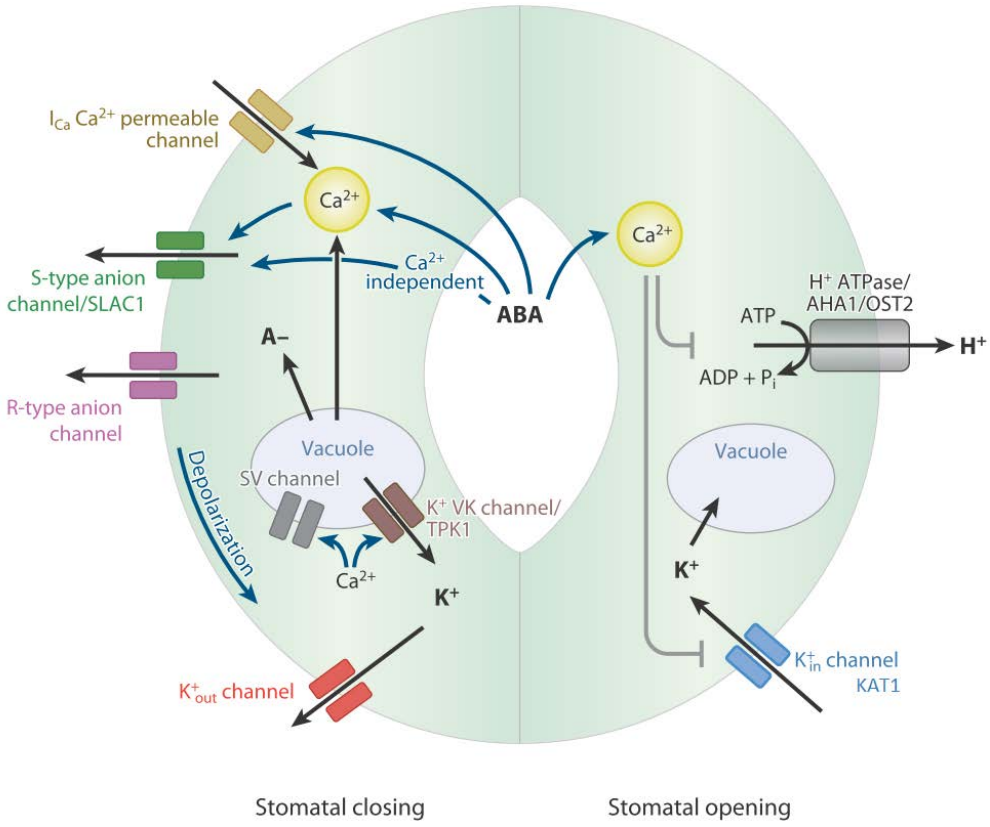

Figure 9. Fermeture stomatique liée à l'acide abscissique. A gauche, signalisation de l'ABA liée à la fermeture des stomates. A droite, signalisation de l'ABA liée à l'inhibition de l'ouverture stomatique. D'après Kim & Lee (2007).

3.4. Modélisation de la conductance stomatique

Modéliser pour prédire l'évolution de la conductance stomatique est une étape importante permettant d'évaluer les paradigmes actuels et de synthétiser notre compréhension des mécanismes responsables des mouvements stomatiques. Ces modèles peuvent s'intégrer par exemple aux modèles de climat globaux pour prédire l'évolution de la végétation et de la séquestration de carbone au sein des forêts (Franks *et al.*, 2018).

De nombreux modèles, dont très peu sont complètement mécanistes, ont été développés depuis une cinquantaine d'années (Damour *et al.*, 2010). Un des premiers modèles de conductance stomatique, proposé par Jarvis (1976), calcule g_s à partir de la conductance stomatique maximale, successivement limitée par l'ajout de fonctions empiriques environnementales (lumière, VPD, CO_2). Ce type de modèle, difficile à utiliser si nous considérons le nombre de paramètres à estimer pour chacune des fonctions, ne tient pas compte de potentielles interactions entre variables. D'autres modèles comme celui de Ball, Woodrow & Berry (1987) et plus tard affiné par Aphalo & Jarvis (1993a), utilisent la relation entre l'assimilation de CO_2 et la conductance stomatique, modulée par l'humidité de l'air :

$$g_s = g_0 + g_1 \left(\frac{A*RH}{C_a}\right) \quad (1)$$

Avec g_s la conductance stomatique, A l'assimilation nette de CO_2, RH l'humidité relative, C_a la concentration en CO_2 atmosphérique et g_0 et g_1 des paramètres empiriques. L'utilisation de l'humidité relative dans ce modèle est sujette à discussions, certains auteurs considérant que la réponse à l'humidité seule ne permet pas de tenir compte des interactions complexes avec la température (Aphalo & Jarvis, 1991). Ainsi le modèle de Leuning (1995), dérivé de celui de Ball & Berry utilise le VPD, lui-même dépendant de l'humidité relative et de la température :

$$g_s = g_0 + g_1 \left(\frac{A}{(C_a - \Gamma^*)\left(1 + {VPD}/{VPD_0}\right)}\right) \quad (2)$$

Avec Γ^* la concentration en CO_2 au point de compensation de l'assimilation en tenant compte de la respiration à l'obscurité, et VPD_0 un paramètre empirique. D'autres encore, tel que le modèle de Tuzet (2003), modifie la partie liée à l'humidité relative pour considérer l'impact du potentiel hydrique foliaire. Plus récemment, Medlyn *et al.* (2011) ont utilisé un modèle de photosynthèse simple dans lequel l'assimilation en CO_2 est supposée dépendre de C_i et de l'irradiance. En imposant la contrainte supplémentaire postulée par Cowan & Farquhar (1977), que la conductance est régulée pour maximiser la photosynthèse en regard des pertes en eau, les auteurs aboutissent à un modèle, curieusement proche de celui de Ball & Berry, de type :

$$g_s = g_0 + 1.6\left(1 + \frac{g_1}{\sqrt{VPD}}\right)\frac{A}{C_a} \quad (3)$$

Cependant, la relation entre A et g_s n'est pas aussi simple. La relation A et g_s n'est pas linéaire mais asymptotique (Wong *et al.*, 1979), impliquant une gamme de valeurs de g_s pour lesquelles A n'augmente plus. De plus, A et g_s sont à la fois liés par une boucle de rétroaction (Farquhar

et al., 1978), mais peuvent aussi réagir aux variables environnementales de manière indépendante l'un de l'autre (Bunce, 1988). Ainsi, même si la formulation des modèles de type Ball & Berry (équations 1, 2 et 3) sous-entend que A contrôle g_s, en réalité ni A ne contrôle g_s, ni g_s ne contrôle A et ni l'un ni l'autre ne peuvent vraiment être considérés comme déterminant. Une explication alternative de ce type de modèle est qu'il décrit plutôt la relation entre A et g_s (Aphalo & Jarvis, 1993a).

3.5. Dynamique des mouvements stomatiques

La plupart des modèles décrits précédemment sont définis en « régime permanent ». C'est-à-dire que pour un changement environnemental donné, A et g_s sont instantanément ajustés à leur nouvel environnement. Or, même si les variations de la photosynthèse sont très rapides, de l'ordre de la seconde, les variations de l'ouverture des stomates peuvent prendre quelques dizaines de minutes à plusieurs heures (Mc Ausland *et al.*, 2016). Ces variations temporelles de g_s induisent une hystérésis, ainsi elle est à la fois influencée par les variations du milieu extérieur mais également par son propre état antérieur (Ng & Jarvis, 1980). En considérant les variations naturelles de g_s lorsque les conditions environnementales sont maintenues stables (de Dios, 2017), auxquelles s'ajoutent en conditions naturelles les variations continues de l'irradiance, de la température, de C_a et de l'humidité de l'air, il est peu probable (ou rare) que g_s atteigne ou maintienne un régime permanent.

Les premiers essais de modélisation de ces dynamiques temporelles de g_s ont été réalisés en mesurant le temps entre le changement environnemental et le moment où g_s atteint un nouveau régime permanent (en conditions contrôlées stables), ou par régression de la partie linéaire de la réponse de g_s (revu par Vialet-Chabrand *et al.*, 2017). Ces approches posent un problème de comparaison entre différentes études évaluant la réponse de g_s par différents estimateurs. Afin d'intégrer la totalité de la réponse dynamique de g_s, les modèles les plus utilisés à l'heure actuelle décrivent empiriquement la forme de la variation de g_s par une équation exponentielle (Qu *et al.*, 2016) ou sigmoïdale (Vialet-Chabrand *et al.*, 2013). A partir de ces équations, différents paramètres empiriques décrivant le temps, la vitesse et l'amplitude de la réponse, peuvent être extraits. Le modèle sigmoïdal présente l'intérêt de pouvoir estimer un délai de la réponse stomatique (entre le changement environnemental et le début de la réponse de g_s), reporté chez plusieurs espèces (Barradas *et al.*, 1994; Vico *et al.*, 2011). Le modèle sigmoïde le plus utilisé aujourd'hui est celui développé par Vialet-Chabrand *et al.* (Vialet-Chabrand *et al.*, 2013; Mc Ausland *et al.*, 2016; Gérardin *et al.*, 2018) de type :

$$g_s = g_0 + (G - g_0)e^{-e^{(\frac{\lambda - t}{\tau})}} \quad (4)$$

Avec g_0 et G les valeurs de g_s respectivement avant et après le changement environnemental, t le temps, λ le délai de réponse, τ une constante de temps reflétant le temps de la réponse de g_s (Fig. 10 et 11) et « e » le nombre d'Euler (≈ 2.718). A partir de cette équation, la pente maximum de la régression, SL_{max}, peut être calculée :

$$SL_{max} = \frac{G - g_0}{\tau . e} \quad (5)$$

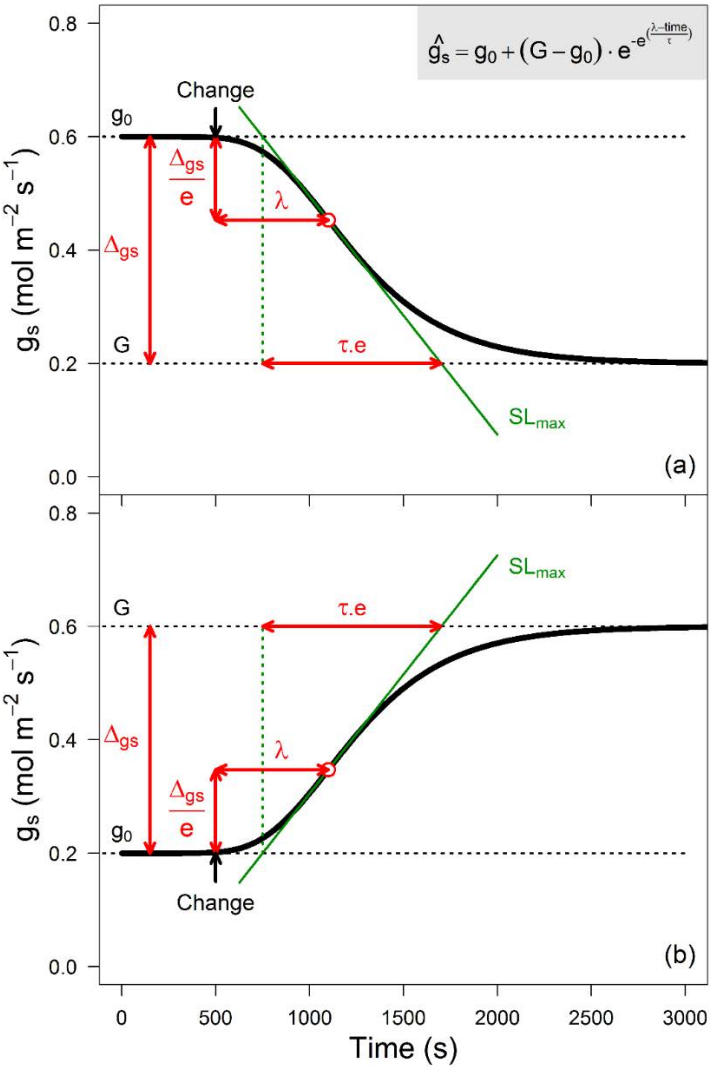

Figure 10. Description du modèle dynamique sigmoïde de Gérardin *et al.* (2018). (**a**) et (**b**) fermeture et ouverture stomatique, respectivement. La flèche noire montre le moment du changement environnemental. g_0 et G sont les valeurs de conductance stomatique (g_s) initiale et finale, respectivement. Δ_{gs} est l'amplitude de g_s, λ est le délai entre le changement environnemental et le moment où la pente est à un maximum (point blanc). SL_{max} est la tangente à ce point. En multipliant τ et e (≈ 2.718), nous obtenons le temps nécessaire pour modifier g_s de g0 à G si la vitesse était constante et égale à SL_{max}.

Cette équation illustre également la relation mathématique entre SL_{max} (vitesse), τ (temps) et l'amplitude ($G - g_0$). Seul λ est indépendant mathématiquement. Au-delà des contraintes inhérentes à un modèle descriptif empirique, ce modèle est spécifique à la condition environnementale testée. Comparer des résultats de ce modèle à des variations expérimentales de g_s nécessite la mise en place d'un protocole expérimental évaluant la dynamique temporelle de g_s par paliers sur une large gamme de variations. Son utilisation requiert également la résolution de plusieurs équations différentielles (pour calculer la vitesse de g_s à chaque instant de la simulation) et la définition de valeurs de g_s « cible », c'est-à-dire la valeur de g_s en régime permanent à l'instant donné si la réponse était instantanée (Vialet-Chabrand *et al.*, 2016).

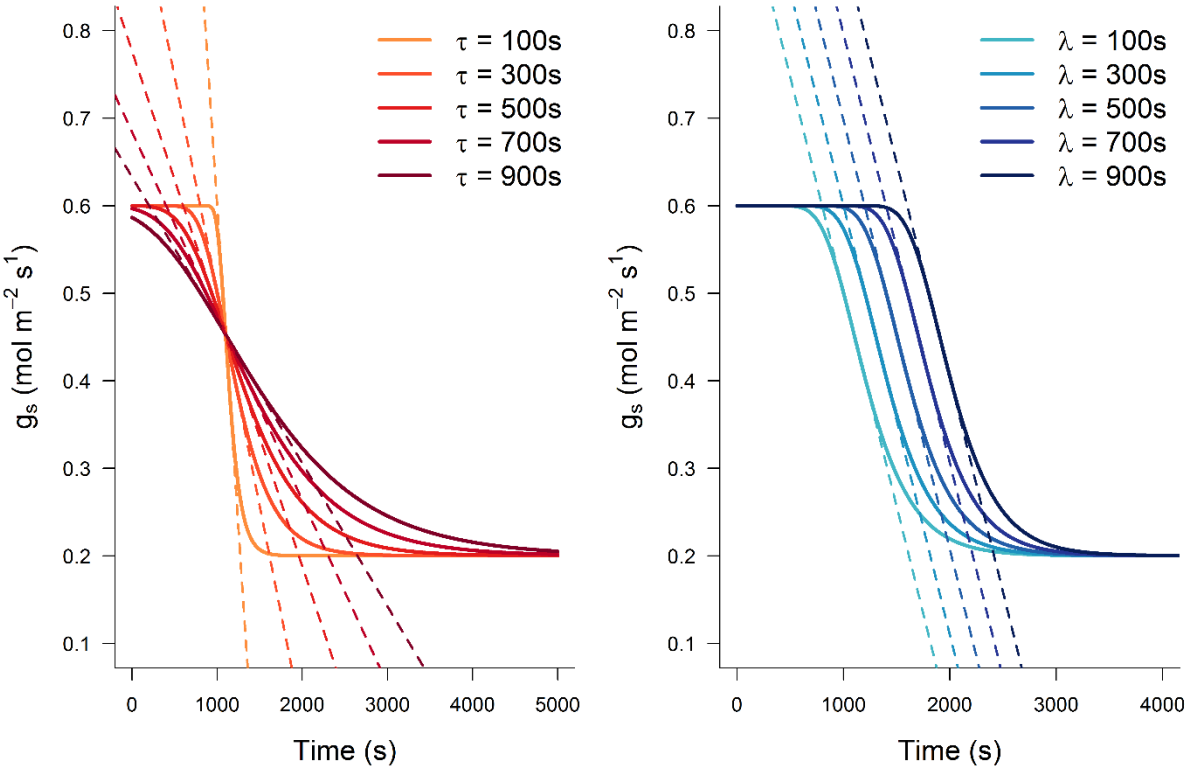

Figure 11. Illustration de la variation des paramètres τ (**a**) et λ (**b**) sur la dynamique temporelle de la conductance stomatique. g_0 = 0.6 mol m^{-2} s^{-1}, G = 0.2 mol m^{-2} s^{-1}, τ = 300s et λ = 100s sauf si mentionné autrement.

Quelques études ont pu mettre en évidence une diversité de la dynamique temporelle de g_s en réponse à la lumière (Mc Ausland *et al.*, 2016), au VPD (Males & Griffiths, 2017), au déficit hydrique et au CO_2 (Haworth *et al.*, 2018). Cependant, aujourd'hui nous ne connaissons pas les déterminants régissant cette diversité de dynamique stomatique. Il faut d'abord noter que g_s n'est pas linéairement liée à l'ouverture du pore stomatique (A_p, μm^2). La densité stomatique (SD, mm^{-2}) et la profondeur de l'ostiole (d_p, μm) participent également aux variations de g_s en

modifiant le chemin du CO_2 et de H_2O de la surface de la feuille jusqu'à la surface cellulaire où les gaz passent à l'état liquide. Nous pouvons relier ces différents paramètres à partir du modèle de Franks & Farquhar (2001) adapté du modèle de Brown & Escombe (1900) :

$$g_s = \frac{SD \times A_p \times {}^{D}/_{V}}{d_p + {}^{\pi}/_{2}\sqrt{{}^{A_p}/_{\pi}}} \quad (6)$$

Avec D la diffusivité de l'eau dans l'air (≈ 2.82×10^{-5} m^2 s^{-1}) et V le volume molaire de l'air (≈ 0.0244 m^3 mol^{-1}). La morphologie des cellules de garde, en forme d'haltère chez les monocotylédones et en forme de haricot chez les dicotylédones, et l'avantage mécanique de l'épiderme (en termes de pression de turgescence) par rapport aux cellules de garde pourraient aussi participer à la diversité des dynamiques stomatiques (Franks & Farquhar, 2007). La contribution de l'épiderme serait aussi en mesure d'être modifiée selon l'espacement des stomates et le nombre variable de cellules épidermiques de différentes tailles qui les entourent (Dow *et al.*, 2014). Des stomates encerclés par un faible nombre de cellules épidermiques seraient potentiellement susceptibles de ressentir une pression de turgescence plus faible. Le transport de solutés à travers les membranes, responsable des mouvements d'eau à travers les stomates pourraient également modifier la dynamique stomatique selon leur quantité et leur activité. Une hypothèse avancée par Drake *et al.* (2013) propose que des stomates de grande taille soient plus lents à répondre aux changements environnementaux. L'idée prend racine du fait que des petits objets possèdent une surface externe plus grande par rapport à leur volume, comparé à des gros objets. L'hypothèse ne fait pas consensus dans la littérature (Elliott-Kingston *et al.*, 2016; Mc Ausland *et al.*, 2016; Gérardin *et al.*, 2018; Kardiman & Ræbild, 2018) et présuppose que les flux de solutés à travers les cellules de garde soient uniformes, une fois normalisés par la surface des cellules de garde (Lawson & Blatt, 2014; Raven, 2014).

Cette diversité de dynamique stomatique entrainerait différents impacts. Des stomates plus rapides quand les conditions ne sont plus propices (par ex. le passage d'un nuage diminuant l'assimilation de CO_2) permettraient d'économiser des pertes en eau au moment de la fermeture stomatique (Fig. 12). Economiser l'eau du sol en fermant ses stomates plus rapidement lors d'épisodes de sécheresse permettrait de limiter l'épuisement des ressources du sol (Mc Ausland *et al.*, 2016). Lorsque les conditions deviennent favorables à nouveau, une ouverture plus rapide pourrait capitaliser sur l'augmentation de l'assimilation en CO_2. Cette dissymétrie de l'impact de la dynamique stomatique en réponse à un changement de lumière entre l'ouverture et la

fermeture pourrait influencer le rapport entre A et g_s, modifiant le coût hydrique de la photosynthèse (Ooba & Takahashi, 2003).

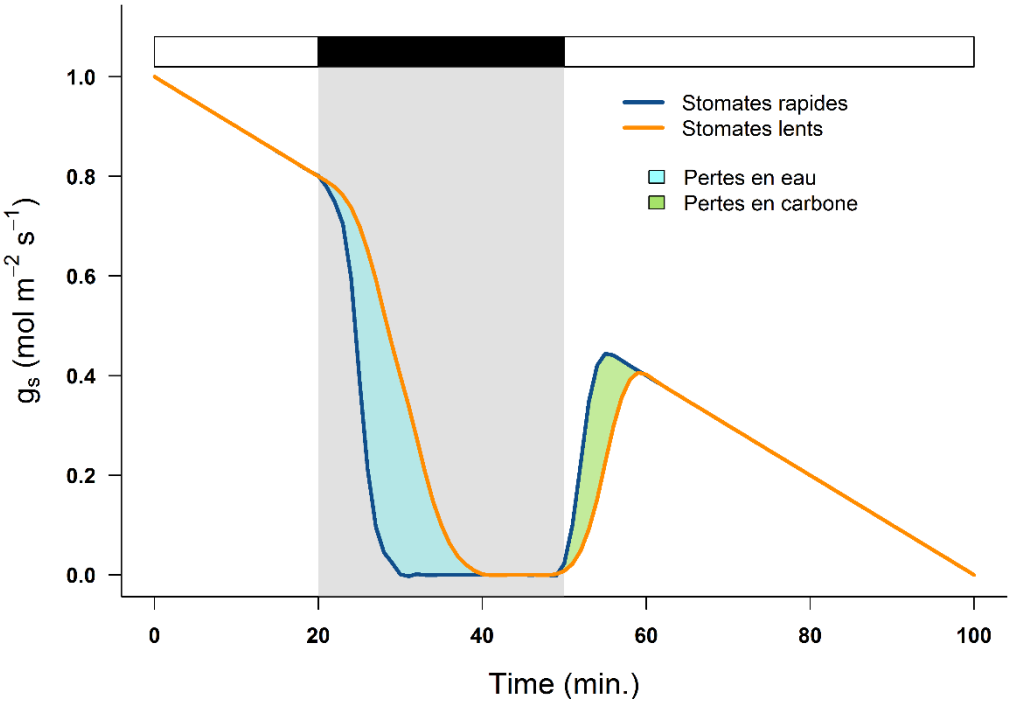

Figure 12. Illustration des impacts théoriques de la dynamique stomatique sur les pertes en eau et en carbone. La zone noire et grisée correspond au passage d'un nuage, réduisant la photosynthèse et induisant une fermeture des stomates.

4. *Efficience d'utilisation de l'eau*

4.1. Définitions et composants à différentes échelles

Nous avons vu précédemment que le rapport entre A et g_s n'est pas fixe, et les mécanismes régissant ces deux processus peuvent être régulés conjointement ou indépendamment. Ce ratio est appelé l'efficience d'utilisation de l'eau (WUE). C'est un trait complexe, définissable à plusieurs échelles (Fig. 13). Au niveau de la feuille, le rapport A/g_s est communément appelé l'efficience d'utilisation de l'eau intrinsèque (W_i). C'est un trait hautement variable selon les variations environnementales puisque défini de manière instantanée. Nous pouvons aussi décrire le flux de CO_2 de l'atmosphère vers la feuille comme le produit entre la conductance stomatique au CO_2 (g_c) et la différence entre C_a et C_i tel que :

$$A = g_c(C_a - C_i) \quad (7)$$

Puisque la diffusion de l'eau dans l'air est 1.6 fois plus rapide que celle du CO_2 ($g_s = 1.6g_c$),

nous pouvons remplacer le numérateur du ratio A/g_s par l'équation (7) et le dénominateur par $1.6g_c$. En simplifiant par g_c nous obtenons :

$$W_i = \frac{A}{g_s} = \frac{(C_a - C_i)}{1.6} = \frac{C_a\left(1 - {}^{C_i}/_{C_a}\right)}{1.6} \quad (8)$$

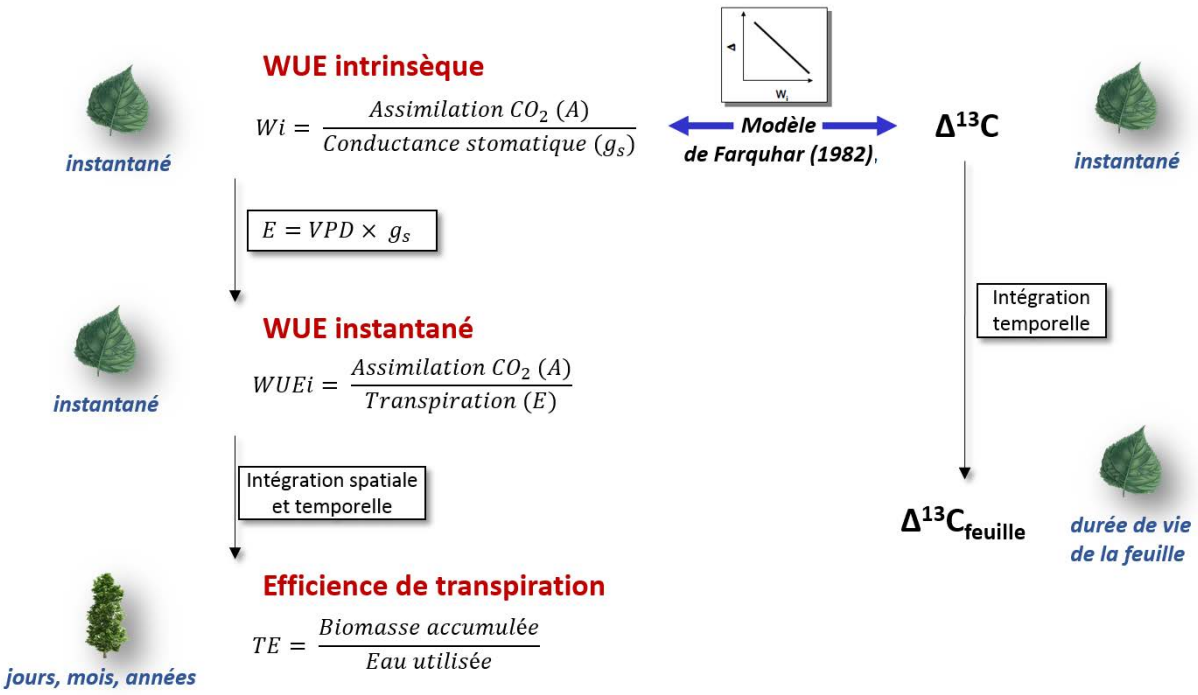

Figure 13. Illustration des différentes intégrations spatiales et temporelles de l'efficience d'utilisation de l'eau.

Nous pouvons également calculer WUE au niveau foliaire en considérant la transpiration foliaire (E) de manière similaire à l'équation (7), comme le produit de g_s et de la différence de pression en vapeur d'eau entre la feuille (e_i) et l'atmosphère (e_a) tel que VPD = e_i - e_a. Cette définition assume une conductance de couche limite, g_{bl}, infinie (c'est-à-dire une résistance nulle). Le rapport A/E (W_{inst}) représente alors le ratio des flux entrant de CO_2 sur les flux sortant d'H_2O. En modifiant l'équation (8) pour inclure le VPD nous obtenons (Farquhar & Richards, 1984):

$$W_{inst} = \frac{A}{E} = \frac{(C_a - C_i)}{1.6\,(e_i - e_a)} = \frac{C_a\left(1 - {}^{C_i}/_{C_a}\right)}{1.6\,(e_i - e_a)} \quad (9)$$

L'efficience d'utilisation de l'eau est utilisée aussi bien en agronomie qu'en foresterie. Dans ces domaines, WUE est souvent mesurée au niveau de la plante entière ou de l'écosystème (Navarro *et al.*, 2018). Ces dernières années, les prévisions économiques et climatiques prévoyant une augmentation de la demande en bois (voir paragraphe 1.3) et des sécheresses

(voir paragraphe 2.2), conduisent à une augmentation du nombre d'études visant à améliorer la production de biomasse par rapport à la consommation en eau (Condon *et al.*, 2004). Ce ratio est appelé l'efficience de transpiration (TE). Il est défini à l'échelle de la plante entière et sur une période de temps donnée, et est intrinsèquement relié aux définitions à l'échelle foliaire de WUE. Cependant, de nombreux autres processus interviennent sur WUE au niveau de la plante entière par rapport à la feuille, entraînant des pertes de carbone (Φ_c) et d'eau (Φ_w) non associées à la photosynthèse (Farquhar *et al.*, 1989). Φ_c tient compte des gains de carbone par les tiges photosynthétiques ou les fruits immatures et des pertes en carbone par la respiration des organes autres que les feuilles (tiges, racines, fruits). Φ_w comprend les pertes d'eau de la plante entière de nuit et des organes autres que les feuilles de jour (Farquhar & Richards, 1984; Cernusak *et al.*, 2007). En incluant ces termes à l'équation (9) nous obtenons une estimation instantanée de WUE, TE_{inst} :

$$TE_{inst} = \frac{C_a(1+\varphi_c)\left(1-{}^{C_i}/_{C_a}\right)}{1.6(e_i-e_a)(1+\varphi_w)} \quad (10)$$

La mesure de TE est laborieuse, nécessitant la détermination précise des gains de biomasse et les pertes en eau cumulées (WU) sur une période souvent longue (semaines, années). Sa mesure sur des jeunes plants en pot demande la pesée régulière de chaque plante et la détermination, destructive, de la biomasse produite (Rasheed *et al.*, 2013). Sur des arbres adultes, l'estimation de l'eau consommée peut se faire à partir de mesures du flux de sève. La biomasse produite est souvent difficile à estimer, en particulier au niveau des racines et fait souvent intervenir des estimations à partir du diamètre ou du volume du tronc (Olbrich *et al.*, 1993; Navarro *et al.*, 2018).

4.2. Intérêt et utilisation des isotopes de carbone

Le carbone possède quatre isotopes. Deux sont radioactifs (^{11}C et ^{14}C) et deux sont stables (^{12}C et ^{13}C). L'abondance naturelle du ^{13}C approche 1.1% (contre 98.9% pour ^{12}C). Au sein de la matière organique, différents processus discriminent contre le ^{13}C au profit du ^{12}C. Etudier ces processus de discrimination revient à comparer le ratio d'isotopes ^{13}C par rapport au ^{12}C. Par convention le ratio isotopique $^{13}C/^{12}C$ est rapporté à un standard international, la Vienna Pee Dee Belemnite (Gonfiantini, 1984) pour en déterminer la composition isotopique (δ):

$$\delta = \frac{1000 \times \left(\frac{^{13}C}{^{12}C_{ech}} - \frac{^{13}C}{^{12}C_{std}}\right)}{\frac{^{13}C}{^{12}C_{ech}}} \quad (11)$$

Le rapport isotopique pour le carbone de la matière organique est toujours inférieur à celui du standard. Cette composition isotopique provenant d'un échantillon biologique (δ_{ech}), peut être comparée à celle du milieu source, c'est-à-dire de l'atmosphère au moment où l'échantillon s'est développé (δ_{air}). De cette façon, les processus de discrimination propre à l'organisme (Δ) pourront être mis en lumière :

$$\Delta = \frac{1000(\delta_{air} - \delta_{ech})}{1000 + \delta_{ech}} \quad (12)$$

Chez les végétaux, les sources principales de discrimination au niveau des feuilles sont les premières réactions de carboxylation par la ribulose-1,5-bisphosphate carboxylase (Rubisco, ≈27-30‰) et par la diffusion du CO_2 de l'atmosphère vers les cavités sous-stomatiques (≈4.4‰). Il existe plusieurs autres processus, d'importance moindre mais non négligeable, tel que la diffusion du CO_2 dans la phase liquide (Brugnoli & Farquhar, 2000), la photorespiration et la respiration de jour (Gillon & Griffiths, 1997). En 1982, Farquhar *et al.* (1982) développent un modèle permettant de lier la discrimination du ^{13}C au moment de l'entrée du CO_2 dans la feuille et le rapport C_i/C_a. Cette relation n'est pas instantanée mais intégrée dans le temps et pondérée par l'assimilation de CO_2. Elle prend la forme:

$$\Delta = a + (b - a)\frac{C_i}{C_a} \quad (13)$$

Avec « a » la discrimination contre le $^{13}CO_2$ lors de la diffusion gazeuse de la surface de la feuille aux cavités sous stomatiques et « b » la discrimination contre le $^{13}CO_2$ pendant la carboxylation (Farquhar *et al.*, 1982). Le ratio C_i/C_a reflète le ratio entre la demande et la disponibilité en CO_2. Puisqu'il apparait à la fois dans l'équation (8) et (13), nous pouvons établir une corrélation négative théorique entre Δ et W_i. Cette corrélation a été validée de façon expérimentale chez de nombreuses espèces herbacées (Farquhar *et al.*, 1989; Anyia *et al.*, 2007) et arborées (Ponton *et al.*, 2002; Marguerit *et al.*, 2014). Lorsque cette relation n'est pas apparente, la cause principale est souvent un problème de correspondance entre l'intégration temporelle de Δ et la mesure instantanée de W_i par échange gazeux foliaires. Il est également possible qu'un décalage entre les valeurs prédites par le modèle et les valeurs mesurées soit observé. Ce décalage provient majoritairement de résistances au cheminement du CO_2 des cavités sous-stomatiques aux sites de carboxylation au niveau des chloroplastes. De la même façon que les autres résistances aux flux de CO_2, nous nous y référons communément à travers la conductance du mésophylle (g_m), qui n'est pas prise en compte dans le modèle simple de

discrimination. Le modèle complet, bien plus compliqué, a été décrit quelques années plus tard (Farquhar & Richards, 1984):

$$\Delta = a_b \frac{C_a - C_s}{C_a} + a \frac{C_s - C_i}{C_a} + (b_s + a_l) \frac{C_i - C_c}{C_a} + b \frac{C_c}{C_a} - f \frac{\Gamma^*}{C_a} - e' \frac{R_d}{A + R_d} \frac{C_c - \Gamma^*}{C_a} \qquad (14)$$

Avec a_b, a et a_l les fractionnements associés à la diffusion du $^{13}CO_2$ à travers la couche limite, les stomates et dans l'eau, respectivement. b_s est le fractionnement du $^{13}CO_2$ à son entrée en solution à 25°C. C_s et C_c sont les concentrations en CO_2 à la surface des feuilles et aux sites de carboxylation, respectivement. e' et f sont les fractionnements liés à la respiration de jour et à la photorespiration, respectivement. Enfin, R_d est le taux de la respiration « au noir » de jour.

Δ peut être mesuré sur divers échantillons végétaux impliquant différent processus biochimiques et physiologiques ayant potentiellement des fractionnements isotopiques post-photosynthétiques (Fig. 14; Bowling *et al.*, 2008). L'étude de la composition isotopique sur ces différents compartiments intègre les processus de discrimination isotopique au moment de leur formation. Ainsi, les tiges et les feuilles sont composées, entre autre, de cellulose, d'hémicellulose et de lignine, mis en place pendant la formation des tissus. D'autres réserves carbonées, notamment les sucres solubles et l'amidon sont les premiers produits de la photosynthèse, et ont un turnover de quelques jours et d'une semaine, respectivement (Brugnoli & Farquhar, 2000). L'abondance relative des différents composés carbonés et leur contribution à la composition isotopique de la feuille entière peuvent créer une discordance entre le signal et les valeurs réelles du ratio A/g_s (Bowling *et al.*, 2008). La respiration et la photorespiration ont aussi un impact sur la composition isotopique, qui peut différer selon l'espèce et les conditions environnementales (Ghashghaie *et al.*, 2001; Ghashghaie *et al.*, 2003).

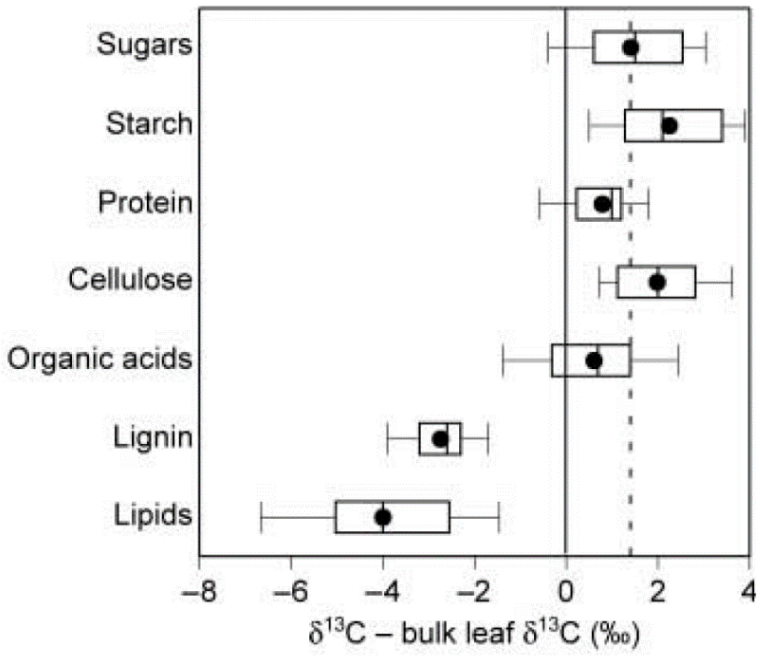

Figure 14. Composition isotopique de différents composés de plantes vasculaires C_3, relativement à la composition isotopique de la feuille entière (ligne noire). La ligne pointillée représente la composition isotopique moyenne des sucres solubles. Les lignes verticales des boites montrent les 10^e, 25^e, 50^e (médiane), 75^e, et 90^e centiles et le point noir la moyenne. D'après Bowling et al. (2008).

La détection de régions génomiques (QTL, « quantitative trait loci ») impliquées dans la régulation de traits phénotypiques quantitatifs permet d'étudier le lien entre différents traits, selon leur co-localisation. Des déterminants génétiques de l'efficience d'utilisation de l'eau, ont pu être mis en évidence chez plusieurs espèces pérennes (Brendel *et al.*, 2002; Casasoli *et al.*, 2004; Marguerit *et al.*, 2014). Chez le chêne, un QTL lié à l'efficience d'utilisation de l'eau (Brendel *et al.*, 2008) a été co-localisé avec un QTL lié à la densité stomatique (Gailing *et al.*, 2008). Ces résultats suggèrent un contrôle génétique de WUE, en association avec la régulation stomatique chez cette espèce (Roussel *et al.*, 2009a; Roussel *et al.*, 2009b).

PROBLEMATIQUE ET OBJECTIFS DE RECHERCHE

Les augmentations de température, de l'intensité et de la durée des sécheresses présentent un problème majeur pour la culture du peuplier. Sa grande consommation en eau limite généralement sa répartition dans les zones humides. Par ailleurs la demande industrielle en produits de bois ne cesse d'augmenter et contraint les populiculteurs à installer des plantations en zones mésophiles dans la vallée de la Loire et de la Garonne. Ces territoires sont susceptibles de subir des sécheresses plus longues et plus intenses qu'en zones alluviales. Le concept d'efficience d'utilisation de l'eau apparaît ainsi essentiel afin d'améliorer ou maintenir la croissance des peupliers tout en réduisant leur consommation d'eau.

A travers l'étude des traits anatomiques, physiologiques et moléculaires liés à l'efficience d'utilisation de l'eau, les connaissances des déterminants et de la variabilité génotypique de W_i chez le peuplier, se sont développées (Marron, 2003; Monclus, 2006; Chamaillard, 2011; Rasheed, 2012). Un lien fort entre W_i et g_s a été identifié chez les peupliers, suggérant que d'autres traits stomatiques tels que leur taille, leur densité et leur vitesse d'ouverture et de fermeture pourraient être impliqués. Ces traits pourraient être liés à des déterminants moléculaires (Berger & Altmann, 2000; Masle *et al.*, 2005) et influencer les différences génotypiques et sous sécheresse d'efficience d'utilisation de l'eau. Cette dernière semblerait être sous contrôle génétique chez plusieurs espèces arborées (Brendel *et al.*, 2008; Marguerit *et al.*, 2014). Chez les peupliers, de précédentes études ont montré que les différences d'efficience à l'échelle de la feuille sont comparables à celles au niveau de la plante entière (Rasheed *et al.*, 2013), et sont maintenues à différents niveaux de VPD (Rasheed *et al.*, 2015) et avec l'âge (Rasheed *et al.*, 2011). Puisque de nombreux traits peuvent influencer la comparaison de résultats à différentes échelles, il nous apparait nécessaire d'examiner cette problématique à différentes échelles et sous différentes conditions environnementales.

L'objectif général de la thèse est d'améliorer notre compréhension de la variabilité de la réponse au déficit hydrique chez les peupliers. Plus spécifiquement, nous souhaitons répondre aux questions suivantes :

1. Existe-il des différences de dynamique des mouvements stomatiques liées aux variables environnementales (lumière, VPD) entre génotypes et selon leur état hydrique ? Et quelle est leur influence sur les variations de TE entre génotypes et en condition de sécheresse ?

2. Est-ce que les différences de dynamique stomatiques potentiellement observées sont liées à des déterminants physiologiques, morphologiques et/ou moléculaires ?

3. Pouvons-nous mettre en évidence une différence de ces déterminants et de leurs contributions relatives à WUE en conditions contrôlées par rapport aux conditions naturelles ?

4. Comment les déterminants décrits dans les questions précédentes et traités au niveau de la feuille contribuent à WUE à l'échelle de la plante entière ?

Pour répondre à ces questions, nous avons mis en place deux plantations de peupliers, l'une en serre et l'autre en pépinière, destinées à subir une sécheresse édaphique. Les mêmes génotypes de peupliers (deux différents clones de *Populus euramericana* et deux de *Populus nigra*) ont été utilisés sur les deux dispositifs. Ils ont été choisis sur la base de leur sensibilité différente à la sécheresse et dans le but de comparer entre génotypes et espèces.

L'expérience en serre a pour but, dans un premiers temps, de quantifier la dynamique temporelle des mouvements stomatiques en réponse à un changement d'irradiance et de VPD. Ceci sur les quatre génotypes de peuplier et en réponse à la sécheresse. Différents traits mesurés au niveau foliaire et au niveau de la plante entière ont servi à établir à la fois, les déterminants principaux de cette dynamique stomatique, et l'impact au niveau de la plante entière. Dans un deuxième temps, des prélèvements foliaires ont permis d'étudier le contenu en éléments et l'expression génique au sein des cellules de garde. Ces mesures ont été réalisées séparément sur chacune des faces de la feuille et à deux moments de la journée (matin et après-midi). Elles ont pour but d'examiner d'une part leur variabilité génotypique, et d'autre part leurs variations, en lien avec g_s, induites par les conditions endogènes (face de la feuille) et environnementales (sécheresse, moment de la journée).

L'expérience en pépinière servira de point de comparaison, par rapport à l'expérimentation en serre. L'efficience de transpiration, et Δ mesurée sur la feuille entière, ainsi que leurs composants (production de biomasse, assimilation de CO_2, eau utilisée, conductance stomatique, transpiration), seront quantifiés et la dynamique temporelle des mouvements stomatiques sera évaluée afin de mettre en lumière des différences, ou des correspondances, entre niveaux d'organisation (feuille, plante entière) et entre conditions environnementales et les causes sous-jacentes.

REFERENCES

Allen CD, Breshears DD, McDowell NG. 2015. On underestimation of global vulnerability to tree mortality and forest die-off from hotter drought in the Anthropocene. *Ecosphere* **6**(8): 55.

Allen CD, Macalady AK, Chenchouni H, Bachelet D, McDowell N, Vennetier M, Kitzberger T, Rigling A, Breshears DD, Hogg EH, et al. 2010. A global overview of drought and heat-induced tree mortality reveals emerging climate change risks for forests. *Forest Ecology and Management* **259**(4): 660-684.

Anyia AO, Slaski JJ, Nyachiro JM, Archambault DJ, Juskiw P. 2007. Relationship of carbon isotope discrimination to water use efficiency and productivity of barley under field and greenhouse conditions. *Journal of Agronomy and Crop Science* **193**(5): 313-323.

Aphalo PJ, Jarvis PG. 1991. Do stomata respond to relative humidity? *Plant, Cell & Environment* **14**(1): 127-132.

Aphalo PJ, Jarvis PG. 1993a. An analysis of Ball's empirical-model of stomatal conductance. *Annals of Botany* **72**(4): 321-327.

Aphalo PJ, Jarvis PG. 1993b. The boundary-layer and the apparent responses of stomatal conductance to wind-speed and to the mole fractions of CO2 and water-vapor in the air. *Plant Cell and Environment* **16**(7): 771-783.

Assmann SM. 1988. Enhancement of the stomatal response to blue light by red light, reduced intercellular concentrations of CO2, and low vapor pressure differences. *Plant Physiology* **87**(1): 226-231.

Assmann SM, Snyder JA, Lee YRJ. 2000. ABA-deficient (aba1) and ABA-insensitive (abi1-1, abi2-1) mutants of Arabidopsis have a wild-type stomatal response to humidity. *Plant Cell and Environment* **23**(4): 387-395.

Ball JT, Woodrow I, Berry J 1987. A model predicting stomatal conductance and its contribution to the control of photosynthesis under different environmental conditions. In: Biggins J ed. *Progress in Photosynthesis Research*: Springer Netherlands, 221-224.

Barradas VL, Jones HG, Clark JA. 1994. Stomatal responses to changing irradiance in Phaseolus vulgaris L. *Journal of Experimental Botany* **45**(7): 931-936.

Bauer H, Ache P, Lautner S, Fromm J, Hartung W, Al-Rasheid KAS, Sonnewald S, Sonnewald U, Kneitz S, Lachmann N, et al. 2013. The stomatal response to reduced relative humidity requires guard cell-autonomous ABA synthesis. *Current Biology* **23**(1): 53-57.

Berger D, Altmann T. 2000. A subtilisin-like serine protease involved in the regulation of stomatal density and distribution in Arabidopsis thaliana. *Genes & Development* **14**(9): 1119-1131.

Bonan GB. 2008. Forests and climate change: forcings, feedbacks, and the climate benefits of forests. *Science* **320**(5882): 1444-1449.

Bowling DR, Pataki DE, Randerson JT. 2008. Carbon isotopes in terrestrial ecosystem pools and CO2 fluxes. *New Phytologist* **178**(1): 24-40.

Brendel O, Le Thiec D, Scotti-Saintagne C, Bodenes C, Kremer A, Guehl JM. 2008. Quantitative trait loci controlling water use efficiency and related traits in Quercus robur L. *Tree Genetics & Genomes* **4**(2): 263-278.

Brendel O, Pot D, Plomion C, Rozenberg P, Guehl JM. 2002. Genetic parameters and QTL analysis of delta(13)C and ring width in maritime pine. *Plant Cell and Environment* **25**(8): 945-953.

Brodribb TJ, Cochard H. 2009. Hydraulic failure defines the recovery and point of death in water-stressed conifers. *Plant Physiology* **149**(1): 575-584.

Brown HT, Escombe F. 1900. Static diffusion of gases and liquids in relation to the assimilation of carbon and translocation in plants. *Annals of Botany* **14**(3): 537-542.

Brugnoli E, Farquhar GD 2000. Photosynthetic fractionation of carbon isotopes. In: Leegood RC, Sharkey TD, von Caemmerer S eds. *Photosynthesis: physiology and metabolism.* . Dordrecht: Kluwer Academic Publishers, 399-434.

Buckley TN. 2005. The control of stomata by water balance. *New Phytologist* **168**(2): 275-291.

Bunce JA. 1988. Nonstomatal inhibition of photosynthesis by water stress. Reduction in photosynthesis at high transpiration rate without stomatal closure in field-grown tomato. *Photosynthesis Research* **18**(3): 357-362.

Casasoli M, Pot D, Plomion C, Monteverdi MC, Barreneche T, Lauteri M, Villani F. 2004. Identification of QTLs affecting adaptive traits in Castanea sativa Mill. *Plant Cell and Environment* **27**(9): 1088-1101.

Cernusak LA, Winter K, Aranda J, Turner BL, Marshall JD. 2007. Transpiration efficiency of a tropical pioneer tree (Ficus insipida) in relation to soil fertility. *Journal of Experimental Botany* **58**(13): 3549-3566.

Chamaillard S. 2011. *Efficience d'utilisation de l'eau chez le peuplier noir (Populus nigra L.) : variabilité et plasticité en réponse aux variations de l'environnement* PhD, Université d'Orléans Orléans.

Chevuturi A, Klingaman NP, Turner AG, Hannah S. 2018. Projected changes in the Asian-Australian monsoon region in 1.5°C and 2.0°C global-warming scenarios. *Earth's Future* **6**(3): 339-358.

Ciais P, Reichstein M, Viovy N, Granier A, Ogee J, Allard V, Aubinet M, Buchmann N, Bernhofer C, Carrara A, et al. 2005. Europe-wide reduction in primary productivity caused by the heat and drought in 2003. *Nature* **437**(7058): 529-533.

Collinson ME. 1992. The early fossil record of the Saliceae. *Proceedings of the Royal Society of Edinburgh* **98B**: 155-167.

Condon AG, Richards RA, Rebetzke GJ, Farquhar GD. 2004. Breeding for high water-use efficiency. *Journal of Experimental Botany* **55**(407): 2447-2460.

Coopman RE, Jara JC, Bravo LA, Sáez KL, Mella GR, Escobar R. 2008. Changes in morpho-physiological attributes of Eucalyptus globulus plants in response to different drought hardening treatments. *Electronic Journal of Biotechnology* **11**(2): 30-39.

Cowan IR, Farquhar GD. 1977. Stomatal function in relation to leaf metabolism and environment. *Symposia of the Society for Experimental Biology* **31**: 471-505.

Cruiziat P, Cochard H, Améglio T. 2002. Hydraulic architecture of trees: main concepts and results. *Ann. For. Sci.* **59**(7): 723-752.

Dai A. 2012. Increasing drought under global warming in observations and models. *Nature Climate Change* **3**: 52.

Dai AG. 2011. Drought under global warming: a review. *Wiley Interdisciplinary Reviews-Climate Change* **2**(1): 45-65.

Damour G, Simonneau T, Cochard H, Urban L. 2010. An overview of models of stomatal conductance at the leaf level. *Plant Cell and Environment* **33**(9): 1419-1438.

Davies WJ, Zhang JH. 1991. Root signals and the regulation of growth and development of plants in drying soil. *Annual Review of Plant Physiology and Plant Molecular Biology* **42**: 55-76.

de Dios VR. 2017. Circadian regulation and diurnal variation in gas exchange. *Plant Physiology* **175**(1): 3-4.

de Rigo D, Enescu C, Houston Durrant T, Caudullo G 2016. Populus nigra in Europe: distribution, habitat, usage and threats. In: San-Miguel-Ayanz J, de Rigo D, Caudullo G, Houston Durrant T, Mauri A eds. *European Atlas of Forest Tree Species*. Luxembourg: Publication Office of the European Union.

DeVoto B. 1997. *The journals of Lewis and Clark.* New York: Houghton Mifflin Company.

Dickmann DI. 2006. Silviculture and biology of short-rotation woody crops in temperate regions: then and now. *Biomass and Bioenergy* **30**(696-705).

Dixon HH, Joly J. 1895. On the ascent of sap. *Philosophical Transactions of the Royal Society of London. B* **186**: 563-576.

Dodd IC. 2005. Root-to-shoot signalling: assessing the roles of 'up' in the up and down world of long-distance signalling in planta. *Plant and Soil* **274**(1-2): 251-270.

Dow GJ, Berry JA, Bergmann DC. 2014. The physiological importance of developmental mechanisms that enforce proper stomatal spacing in Arabidopsis thaliana. *New Phytologist* **201**(4): 1205-1217.

Drake PL, Froend RH, Franks PJ. 2013. Smaller, faster stomata: scaling of stomatal size, rate of response, and stomatal conductance. *Journal of Experimental Botany* **64**(2): 495-505.

Du Puy S, Derrière N, Wurpillot S. 2017. IGN, ed. *La forêt plantée en France: état des lieux*. La feuille de l'inventaire forestier: Institut natianal de l'information géographique et forestière.

Elliott-Kingston C, Haworth M, Yearsley JM, Batke SP, Lawson T, McElwain JC. 2016. Does size matter? Atmospheric CO2 may be a stronger driver of stomatal closing rate than stomatal size in taxa that diversified under low CO2. *Frontiers in Plant Science* **7**.

Etzold S, Ziemińska K, Rohner B, Bottero A, Bose AK, Ruehr NK, Zingg A, Rigling A. 2019. One century of forest monitoring data in Switzerland reveals species- and site-specific trends of climate-induced tree mortality. *Frontiers in Plant Science* **10**(307).

FAO. 1958. nations Faaootu, ed. *Poplars in forestry and land use*. Rome.

FAO. 2012. Forest Assessment MaCD, ed. *Improving lives with poplars and willows. Synthesis of country progress reports. 24th session of the international poplar commission, Dehradun, India, 30 Oct-2 Nov 2012. Working Paper IPC/12.* Rome: FAO.

FAO. 2018. Muller E, Kushlin A, Linhares-Juvenal T, Muchoney D, Wertz-Kanounnikoff S, Henderson-Howat D, eds. *The state of the world's forests*. Rome, Italy.

Farquhar GD, Dubbe DR, Raschke K. 1978. Gain of feedback loop involving carbon dioxide and stomata - Theory and measurement. *Plant Physiology* **62**(3): 406-412.

Farquhar GD, Ehleringer JR, Hubick KT. 1989. Carbon isotope discrimination and photosynthesis. *Annual Review of Plant Physiology and Plant Molecular Biology* **40**: 503-537.

Farquhar GD, O'Leary MHO, Berry J. 1982. On the relationship between carbon isotope discrimination and the intercellular carbon dioxide concentration in leaves. *Australian Journal of Plant Physiology* **9**: 121-137.

Farquhar GD, Richards RA. 1984. Isotopic composition of plant carbon correlates with water-use efficiency of wheat genotypes. *Functional Plant Biology* **11**(6): 539-552.

Franks PJ, Bonan GB, Berry JA, Lombardozzi DL, Holbrook NM, Herold N, Oleson KW. 2018. Comparing optimal and empirical stomatal conductance models for application in Earth system models. *Global Change Biology* **24**(12): 5708-5723.

Franks PJ, Buckley TN, Shope JC, Mott KA. 2001. Guard cell volume and pressure measured concurrently by confocal microscopy and the cell pressure probe. *Plant Physiology* **125**(4): 1577-1584.

Franks PJ, Cowan IR, Farquhar GD. 1998. A study of stomatal mechanics using the cell pressure probe. *Plant, Cell & Environment* **21**(1): 94-100.

Franks PJ, Farquhar GD. 2001. The effect of exogenous abscisic acid on stomatal development, stomatal mechanics, and leaf gas exchange in Tradescantia virginiana. *Plant Physiology* **125**(2): 935-942.

Franks PJ, Farquhar GD. 2007. The mechanical diversity of stomata and its significance in gas-exchange control. *Plant Physiology* **143**(1): 78-87.

Gailing O, Langenfeld-Heyser R, Polle A, Finkeldey R. 2008. Quantitative trait loci affecting stomatal density and growth in a Quercus robur progeny: implications for the adaptation to changing environments. *Global Change Biology* **14**(8): 1934-1946.

Geiger D, Scherzer S, Mumm P, Marten I, Ache P, Matschi S, Liese A, Wellmann C, Al-Rasheid KAS, Grill E, et al. 2010. Guard cell anion channel SLAC1 is regulated by CDPK protein kinases with distinct Ca2+ affinities. *Proceedings of the National Academy of Sciences of the United States of America* **107**(17): 8023-8028.

Geiger D, Scherzer S, Mumm P, Stange A, Marten I, Bauer H, Ache P, Matschi S, Liese A, Al-Rasheid KAS, et al. 2009. Activity of guard cell anion channel SLAC1 is controlled by drought-stress signaling kinase-phosphatase pair. *Proceedings of the National Academy of Sciences* **106**(50): 21425-21430.

Gérardin T, Douthe C, Flexas J, Brendel O. 2018. Shade and drought growth conditions strongly impact dynamic responses of stomata to variations in irradiance in Nicotiana tabacum. *Environmental and Experimental Botany* **153**: 188-197.

Ghashghaie J, Badeck F-W, Lanigan G, Nogués S, Tcherkez G, Deléens E, Cornic G, Griffiths H. 2003. Carbon isotope fractionation during dark respiration and photorespiration in C3 plants. *Phytochemistry Reviews* **2**(1): 145-161.

Ghashghaie J, Duranceau M, Badeck FW, Cornic G, Adeline MT, Deleens E. 2001. δ13C of CO2 respired in the dark in relation to δ13C of leaf metabolites: comparison between Nicotiana sylvestris and Helianthus annuus under drought. *Plant, Cell & Environment* **24**(5): 505-515.

Gillon JS, Griffiths H. 1997. The influence of (photo)respiration on carbon isotope discrimination in plants. *Plant, Cell & Environment* **20**(10): 1217-1230.

Gonfiantini R. 1984. I.A.E.A Advisory group meeting on stable isotope reference samples for geochemical and hydrological investigations. *Chemical Geology* **46**(1): 85.

Hageneder F. 2005. *The meaning of trees.* San Francisco, CA: Chronicle Books.

Haworth M, Marino G, Cosentino SL, Brunetti C, De Carlo A, Avola G, Riggi E, Loreto F, Centritto M. 2018. Increased free abscisic acid during drought enhances stomatal sensitivity and modifies stomatal behaviour in fast growing giant reed (Arundo donax L.). *Environmental and Experimental Botany* **147**: 116-124.

Henry A. 1914. A new hybrid poplar. . *Gardeners' Chronicle* **Series III**(56): 257-258.

Hoerling M, Schubert S, Mo KC. 2013. *An interpretation of the origins of the 2012 central great plains drought assessment report.*: NOAA Drought Task Force.

Hsiang SM, Burke M, Miguel E. 2013. Quantifying the influence of climate on human conflict. *Science* **341**(6151): 1235367.

Hsiao TC. 1973. Plant responses to water stress. *Annual Review of Plant Physiology and Plant Molecular Biology* **24**: 519-570.

Hubbard KE, Nishimura N, Hitomi K, Getzoff ED, Schroeder JI. 2010. Early abscisic acid signal transduction mechanisms: newly discovered components and newly emerging questions. *Genes & Development* **24**(16): 1695-1708.

Humble GD, Raschke K. 1971. Stomatal opening quantitatively related to potassium transport: evidence from electron probe analysis. *Plant Physiology* **48**(4): 447-453.

IPCC. 2014. Meyer L, Brinkman S, van Kesteren L, Leprince-Ringuet N, van Boxmeer F, eds. *Climate change 2014: Synthesis report. Contribution of working groups I, II and III to the fifth assessment report of the intergovernmental panel on climate change*. Geneva, Switzerland: Cambridge University Press.

IPCC. 2018. Masson-Delmotte V, Pörtner HO, Skea J, Panmao Z, Roberts D, Shukla PR, Pirani A, Moufouma-Okia W, Péan C, Pidcock R, Connors S, Mattews JBR, Chen Y, Zhou

XH, Gomis MI, Lonnoy E, Mauycock T, Tignor M, Waterfield T, eds. *Global warming of 1.5°C. An IPCC special report on the impacts of global warming of 1.5°C above pre-industrial levels and related global greenhouse gas emission pathways, in the context of strengthening the global response to the threat of climate change, sustainable development, and efforts to eradicate poverty*. Switzerland: Intergovernmental Panel on Climate Change. .

Isebrands JG, Richardson J. 2014. *Poplars and willows : trees for society and the environment*. Boston, Rome CABI and FAO.

Jacometti G 1937. I nuovi pioppi italiani. Atti del convegno di pioppicoltori in Casale Monferrato (11 luglio1937). . *Comitato Nazionale Forestale*. Roma.

Jansson S, Douglas CJ. 2007. Populus: A model system for plant biology. *Annual Review of Plant Biology* **58**: 435-458.

Jarvis PG. 1976. Interpretation of variations in leaf water potential and stomatal conductance found in canopies in field. *Philosophical Transactions of the Royal Society of London Series B-Biological Sciences* **273**(927): 593-610.

Jarvis PG, McNaughton KG 1986. Stomatal control of transpiration: scaling up from leaf to region. In: MacFadyen A, Ford ED eds. *Advances in Ecological Research*: Academic Press, 1-49.

Jones HG. 2014. *Plants and microclimate: A quantitative approach to environmental plant physiology, 3rd edition*. Cambridge: Cambridge Univ Press.

Kardiman R, Ræbild A. 2018. Relationship between stomatal density, size and speed of opening in Sumatran rainforest species. *Tree Physiology* **38**(5): 696-705.

Kearney TH, Shantz HL. 1911. The water economy of dry land crops. . *U.S. Department of Agriculture Yearbook for 1911*: 351-361.

Kim DJ, Lee JS. 2007. Current theories for mechanism of stomatal opening: Influence of blue light, mesophyll cells, and sucrose. *Journal of Plant Biology* **50**(5): 523-526.

Kinoshita T, Doi M, Suetsugu N, Kagawa T, Wada M, Shimazaki K-i. 2001. phot1 and phot2 mediate blue light regulation of stomatal opening. *Nature* **414**(6864): 656-660.

Kinoshita T, Nishimura M, Shimazaki K. 1995. Cytosolic concentration of Ca2+ regulates the plasma membrane H+-ATPase in guard cells of fava bean. *The Plant Cell* **7**(8): 1333-1342.

Kinoshita T, Shimazaki Ki. 1999. Blue light activates the plasma membrane H(+)-ATPase by phosphorylation of the C-terminus in stomatal guard cells. *The EMBO journal* **18**(20): 5548-5558.

Lawson T, Blatt MR. 2014. Stomatal size, speed, and responsiveness impact on photosynthesis and water use efficiency. *Plant Physiology* **164**(4): 1556-1570.

Lawson T, Simkin AJ, Kelly G, Granot D. 2014. Mesophyll photosynthesis and guard cell metabolism impacts on stomatal behaviour. *New Phytologist* **203**(4): 1064-1081.

Le Quéré C, Andres RJ, Boden T, Conway T, Houghton RA, House JI, Marland G, Peters GP, van der Werf GR, Ahlström A, et al. 2013. The global carbon budget 1959–2011. *Earth Syst. Sci. Data* **5**(1): 165-185.

Leuning R. 1995. A critical-appraisal of a combined stomatal-photosynthesis model for C3 plants. *Plant Cell and Environment* **18**(4): 339-355.

Males J, Griffiths H. 2017. Specialized stomatal humidity responses underpin ecological diversity in C3 bromeliads. *Plant Cell and Environment* **40**(12): 2931-2945.

Marguerit E, Bouffier L, Chancerel E, Costa P, Lagane F, Guehl JM, Plomion C, Brendel O. 2014. The genetics of water-use efficiency and its relation to growth in maritime pine. *Journal of Experimental Botany* **65**(17): 4757-4768.

Marron N. 2003. *Écophysiologie des peupliers euraméricains en réponse à la sécheresse.* PhD, Université d'Orléans Orléans.

Masle J, Gilmore SR, Farquhar GD. 2005. The ERECTA gene regulates plant transpiration efficiency in Arabidopsis. *Nature* **436**(7052): 866-870.

Mc Adam SAM, Brodribb TJ. 2015. The evolution of mechanisms driving the stomatal response to vapor pressure deficit. *Plant Physiology* **167**(3): 833-843.

Mc Ausland L, Vialet-Chabrand S, Davey P, Baker NR, Brendel O, Lawson T. 2016. Effects of kinetics of light-induced stomatal responses on photosynthesis and water-use efficiency. *New Phytologist* **211**(4): 1209-1220.

McAinsh MR, Brownlee C, Hetherington AM. 1990. Abscisic acid-induced elevation of guard cell cytosolic Ca2+ precedes stomatal closure. *Nature* **343**(6254): 186-188.

Medlyn BE, Duursma RA, Eamus D, Ellsworth DS, Prentice IC, Barton CVM, Crous KY, de Angelis P, Freeman M, Wingate L. 2011. Reconciling the optimal and empirical approaches to modelling stomatal conductance. *Global Change Biology* **17**(6): 2134-2144.

Monclus R. 2006. *Efficience d'utilisation de l'eau et tolérance à la sécheresse chez le peuplier.* PhD, Université d'Orléans Orléans.

Monclus R, Dreyer E, Villar M, Delmotte FM, Delay D, Petit JM, Barbaroux C, Le Thiec D, Brechet C, Brignolas F. 2006. Impact of drought on productivity and water use efficiency in 29 genotypes of Populus deltoides x Populus nigra. *New Phytologist* **169**(4): 765-777.

Mott KA, Sibbernsen ED, Shope JC. 2008. The role of the mesophyll in stomatal responses to light and CO2. *Plant Cell and Environment* **31**(9): 1299-1306.

Naiman RJ, Décamps H, McClain ME. 2005. Riparia - ecology, conservation and management of streamside communities. *Aquatic Conservation: Marine and Freshwater Ecosystems* **17**(6): 657-657.

Navarro A, Portillo-Estrada M, Arriga N, Vanbeveren SPP, Ceulemans R. 2018. Genotypic variation in transpiration of coppiced poplar during the third rotation of a short-rotation bio-energy culture. *GCB Bioenergy* **10**(8): 592-607.

Ng PAP, Jarvis PG. 1980. Hysteresis in the response of stomatal conductance in Pinus sylvestris L needles to light - Observations and a hypothesis. *Plant Cell and Environment* **3**(3): 207-216.

Nisbet EG, Manning MR, Dlugokencky EJ, Fisher RE, Lowry D, Michel SE, Myhre CL, Platt M, Allen G, Bousquet P, et al. 2019. Very strong atmospheric methane growth in the 4 years 2014-2017: implications for the paris agreement. *Global Biogeochemical Cycles* **33**(3): 318-342.

Olbrich BW, Le Roux D, Poulter AG, Bond WJ, Stock WD. 1993. Variation in water use efficiency and δ13C levels in Eucalyptus grandis clones. *Journal of Hydrology* **150**(2): 615-633.

Olsen RL, Pratt RB, Gump P, Kemper A, Tallman G. 2002. Red light activates a chloroplast-dependent ion uptake mechanism for stomatal opening under reduced CO2 concentrations in Vicia spp. *New Phytologist* **153**(3): 497-508.

Ooba M, Takahashi H. 2003. Effect of asymmetric stomatal response on gas-exchange dynamics. *Ecological Modelling* **164**(1): 65-82.

Outlaw WH, Manchester J. 1979. Guard cell starch concentration quantitatively related to stomatal aperture. *Plant Physiology* **64**(1): 79-82.

Palmgren MG. 2001. Plant plasma membrane H+-ATPases: powerhouses for nutrient uptake. *Annual Review of Plant Physiology and Plant Molecular Biology* **52**(1): 817-845.

Park S-Y, Fung P, Nishimura N, Jensen DR, Fujii H, Zhao Y, Lumba S, Santiago J, Rodrigues A, Chow T-fF, et al. 2009. Abscisic acid inhibits PP2Cs via the PYR/PYL family of ABA-binding START proteins. *Science (New York, N.Y.)* **324**(5930): 1068-1071.

Peak D, Mott KA. 2011. A new, vapour-phase mechanism for stomatal responses to humidity and temperature. *Plant Cell and Environment* **34**(1): 162-178.

Peters GP, Andrew RM, Boden T, Canadell JG, Ciais P, Le Quéré C, Marland G, Raupach MR, Wilson C. 2012. The challenge to keep global warming below 2 °C. *Nature Climate Change* **3**: 4.

Ponton S, Dupouey J-L, Nathalie B, Dreyer E. 2002. Comparison of water-use efficiency of seedlings from two sympatric oak species: Genotype x environment interactions. *Tree Physiology* **22**: 413-422.

Prieto JA, Lebon E, Ojeda H. 2010. Stomatal behavior of different grapevine cultivars in response to soil water status and air water vapor pressure deficit. *Journal International Des Sciences De La Vigne Et Du Vin* **44**(1): 9-20.

Qu MN, Hamdani S, Li WZ, Wang SM, Tang JY, Chen Z, Song QF, Li M, Zhao HL, Chang TG, et al. 2016. Rapid stomatal response to fluctuating light: an under-explored mechanism to improve drought tolerance in rice. *Functional Plant Biology* **43**(8): 727-738.

Rasheed F. 2012. *Components of transpiration efficiency in poplars : genetic diversity, stability with age and scaling from leaf to whole plant level.* PhD, AgroParisTech Nancy.

Rasheed F, Dreyer E, Richard B, Brignolas F, Brendel O, Le Thiec D. 2015. Vapour pressure deficit during growth has little impact on genotypic differences of transpiration efficiency at leaf and whole-plant level: an example from Populus nigra L. *Plant Cell & Environment* **38**(4): 670-684.

Rasheed F, Dreyer E, Richard B, Brignolas F, Montpied P, Le Thiec D. 2013. Genotype differences in C-13 discrimination between atmosphere and leaf matter match differences in transpiration efficiency at leaf and whole-plant levels in hybrid Populus deltoides x nigra. *Plant Cell and Environment* **36**(1): 87-102.

Rasheed F, Richard B, Le Thiec D, Montpied P, Paillassa E, Brignolas F, Dreyer E. 2011. Time course of delta C-13 in poplar wood: genotype ranking remains stable over the life cycle in plantations despite some differences between cellulose and bulk wood. *Tree Physiology* **31**(11): 1183-1193.

Raven JA. 2014. Speedy small stomata? *Journal of Experimental Botany* **65**(6): 1415-1424.

Rodriguez-Dominguez CM, Buckley TN, Egea G, de Cires A, Hernandez-Santana V, Martorell S, Diaz-Espejo A. 2016. Most stomatal closure in woody species under moderate drought can be explained by stomatal responses to leaf turgor. *Plant Cell and Environment* **39**(9): 2014-2026.

Roelfsema MRG, Hanstein S, Felle HH, Hedrich R. 2002. CO2 provides an intermediate link in the red light response of guard cells. *Plant Journal* **32**(1): 65-75.

Roussel M, Dreyer E, Montpied P, Le-Provost G, Guehl JM, Brendel O. 2009a. The diversity of C-13 isotope discrimination in a Quercus robur full-sib family is associated with differences in intrinsic water use efficiency, transpiration efficiency, and stomatal conductance. *Journal of Experimental Botany* **60**(8): 2419-2431.

Roussel M, Le Thiec D, Montpied P, Ningre N, Guehl J-M, Brendel O. 2009b. Diversity of water use efficiency among Quercus robur genotypes: contribution of related leaf traits. *Annals of Forest Science* **66**(4): 408-408.

Sato A, Sato Y, Fukao Y, Fujiwara M, Umezawa T, Shinozaki K, Hibi T, Taniguchi M, Miyake H, Goto DB, et al. 2009. Threonine at position 306 of the KAT1 potassium channel is essential for channel activity and is a target site for ABA-activated SnRK2/OST1/SnRK2.6 protein kinase. *Biochemical Journal* **424**: 439-448.

Schroeder JI, Hagiwara S. 1989. Cytosolic calcium regulates ion channels in the plasma membrane of Vicia faba guard cells. *Nature* **338**: 427.

Schroeder JI, Hedrich R, Fernandez JM. 1984. Potassium-selective single channels in guard cell protoplasts of Vicia faba. *Nature* **312**(5992): 361-362.

Schroeder JI, Keller BU. 1992. Two types of anion channel currents in guard cells with distinct voltage regulation. *Proceedings of the National Academy of Sciences of the United States of America* **89**(11): 5025-5029.

Schroeder JI, Raschke K, Neher E. 1987. Voltage dependence of K+ channels in guard-cell protoplasts. *Proceedings of the National Academy of Sciences* **84**(12): 4108-4112.

Sheffield J, Wood EF. 2008. Projected changes in drought occurrence under future global warming from multi-model, multi-scenario, IPCC AR4 simulations. *Climate Dynamics* **31**(1): 79-105.

Shimazaki K-i, Doi M, Assmann SM, Kinoshita T 2007. Light regulation of stomatal movement. *Annual Review of Plant Biology*, 219-247.

Solomon S, Plattner G-K, Knutti R, Friedlingstein P. 2009. Irreversible climate change due to carbon dioxide emissions. *Proceedings of the National Academy of Sciences of the United States of America* **106**(6): 1704-1709.

Sondergaard TE, Schulz A, Palmgren MG. 2004. Energization of transport processes in plants. Roles of the plasma membrane H+-ATPase. *Plant Physiology* **136**(1): 2475-2482.

Sperry JS, Hacke UG, Oren R, Comstock JP. 2002. Water deficits and hydraulic limits to leaf water supply. *Plant Cell and Environment* **25**(2): 251-263.

Sternberg T. 2011. Regional drought has a global impact. *Nature* **472**(7342): 169-169.

Stettler RF. 2009. *Cottonwood and the river of time.* . Seattle, WA: University of Washington Press.

Stobrawa K. 2014. *Poplars (Populus spp.): ecological role, applications and scientific perspectives in the 21st century*.

Stout AB, Schreiner EJ. 1933. Results of a project in hybridizing poplars. . *Journal of Heredity* **24**: 216-229.

Tardieu F, Simonneau T. 1998. Variability among species of stomatal control under fluctuating soil water status and evaporative demand: modelling isohydric and anisohydric behaviours. *Journal of Experimental Botany* **49**: 419-432.

Thivolle-Cazat A. 2002. A. T-C, ed. *Disponibilité en bois de peuplier en France de 2002 à 2020. Rapport AFOCEL*. Paris, France: Commission Nationale du Peuplier.

Touma D, Ashfaq M, Nayak MA, Kao S-C, Diffenbaugh NS. 2015. A multi-model and multi-index evaluation of drought characteristics in the 21st century. *Journal of Hydrology* **526**: 196-207.

Tuskan GA, DiFazio S, Jansson S, Bohlmann J, Grigoriev I, Hellsten U, Putnam N, Ralph S, Rombauts S, Salamov A, et al. 2006. The genome of black cottonwood, Populus trichocarpa (Torr. and Gray). *Science* **313**(5793): 1596-1604.

Tuzet A, Perrier A, Leuning R. 2003. A coupled model of stomatal conductance, photosynthesis and transpiration. *Plant Cell and Environment* **26**(7): 1097-1116.

Vahisalu T, Kollist H, Wang Y-F, Nishimura N, Chan W-Y, Valerio G, Lamminmäki A, Brosché M, Moldau H, Desikan R, et al. 2008. SLAC1 is required for plant guard cell S-type anion channel function in stomatal signalling. *Nature* **452**: 487.

Vanden Broeck A, Villar M, Van Bockstaele E, Van Slycken J. 2005. Natural hybridization between cultivated poplars and their wild relatives: evidence and consequences for native poplar populations. *Annals of Forest Science* **62**(7): 601-613.

Vialet-Chabrand S, Dreyer E, Brendel O. 2013. Performance of a new dynamic model for predicting diurnal time courses of stomatal conductance at the leaf level. *Plant Cell and Environment* **36**(8): 1529-1546.

Vialet-Chabrand S, Matthews J, McAusland L, Blatt MR, Griffiths H, Lawson T. 2017. Temporal dynamics of stomatal behavior: modeling and implications for photosynthesis and water use. *Plant Physiology* **174**(2): 603-613.

Vialet-Chabrand S, Matthews JSA, Brendel O, Blatt MR, Wang Y, Hills A, Griffiths H, Rogers S, Lawson T. 2016. Modelling water use efficiency in a dynamic environment: An example using Arabidopsis thaliana. *Plant Science* **251**: 65-74.

Vico G, Manzoni S, Palmroth S, Katul G. 2011. Effects of stomatal delays on the economics of leaf gas exchange under intermittent light regimes. *New Phytologist* **192**(3): 640-652.

Wong SC, Cowan IR, Farquhar GD. 1979. Stomatal conductance correlates with photosynthetic capacity. *Nature* **282**(5737): 424-426.

Yamauchi S, Takemiya A, Sakamoto T, Kurata T, Tsutsumi T, Kinoshita T, Shimazaki K. 2016. The plasma membrane H+-ATPase AHA1 plays a major role in stomatal opening in response to blue light. *Plant Physiology* **171**(4): 2731-2743.

Yoshida R, Umezawa T, Mizoguchi T, Takahashi S, Takahashi F, Shinozaki K. 2006. The regulatory domain of SRK2E/OST1/SnRK2.6 interacts with ABI1 and integrates abscisic acid (ABA) and osmotic stress signals controlling stomatal closure in Arabidopsis. *Journal of Biological Chemistry* **281**(8): 5310-5318.

CHAPITRE I

Altération des dynamiques stomatiques induite par un changement d'irradiance et du déficit de pression en vapeur d'eau sous sécheresse : impact sur l'efficience de transpiration chez le peuplier

CHAPITRE I :

Altération des dynamiques stomatiques induite par un changement d'irradiance et du déficit de pression en vapeur d'eau sous sécheresse : impact sur l'efficience de transpiration chez le peuplier.

Présentation synthétique de l'article

Contexte

La demande actuelle de produits issus du bois est en augmentation, favorisée notamment par la croissance économique et la mise en place de politiques publiques environnementales. La productivité des plantations de peupliers est fortement dépendante de la disponibilité en eau du sol, qui pourrait être limitée par l'augmentation probable de l'intensité et la fréquence des sécheresses, favorisée par les changements climatiques. Au niveau des feuilles, les flux de CO_2 entrant pour la photosynthèse et les pertes en H_2O par transpiration sont régulés par les stomates. Cependant, la dynamique temporelle des mouvements stomatiques est bien plus lente que celle de la photosynthèse, induisant un découplage des deux flux, et modifiant l'efficience d'utilisation de l'eau. Nous avons posé l'hypothèse que les variations génotypiques de la dynamique stomatique contribuaient significativement aux différences d'efficience de transpiration chez le peuplier par le biais de la transpiration.

Objectifs

Par la quantification de la dynamique stomatique de quatre génotypes de peupliers en réponse à un changement de lumière et de VPD sous sécheresse, nous examinerons : (1) la variabilité génotypique de la dynamique temporelle de la conductance stomatique, (2) l'impact de la sécheresse sur la dynamique stomatique, (3) les déterminants foliaires de la dynamique stomatique, et en particulier la morphologie des stomates et (4) l'impact de cette dynamique à l'échelle de la plante entière.

Stratégie

Deux génotypes de peupliers euraméricains (Carpaccio et I214) et deux génotypes de peupliers noirs (6J29 et N38) ont été plantés en serre à partir de boutures. Après 60 jours de croissance, le contenu en eau du sol sur une moitié des peupliers a été réduit de 27.9% à 18.3%. Des récoltes, ainsi que l'utilisation d'un automate de pesées et d'arrosages ont permis de mesurer la biomasse produite, la transpiration et l'efficience d'utilisation de l'eau. Des prélèvements foliaires ont été destinés à la mesure de différents traits morphologiques stomatiques (taille et

densité). La dynamique stomatique a été quantifiée à l'aide de systèmes d'échanges gazeux, permettant le contrôle des variables environnementales. Ces dernières sont maintenus stables, à l'exception de l'irradiance et du VPD. Leur variation soudaine a provoqué des mouvements stomatiques que nous avons enregistré. Ces données ont été ensuite ajustées à un modèle sigmoïdal afin d'extraire plusieurs paramètres de la dynamique, servant à la comparaison entre traitements.

Résultats

Nous avons observé une forte variabilité génotypique de la dynamique stomatique en réponse à un changement d'irradiance et du VPD. De manière générale, les mouvements stomatiques étaient plus rapides chez les peupliers euraméricains que chez les peupliers noirs, en particulier en réponse à un changement de VPD. Le génotype I214 était toujours le plus rapide à fermer ses stomates, comparé aux autres génotypes. La sécheresse a allongé significativement le délai de la réponse stomatique après une diminution de l'irradiance. Cependant, seul I214 a montré une diminution de la vitesse maximale de la fermeture des stomates liée à une réduction de l'irradiance et du VPD en sécheresse. Le plus souvent les différences entre régimes hydriques et entre génotypes ont été observées pendant la fermeture des stomates plutôt que pendant leur ouverture. La vitesse des stomates, et d'autres paramètres associés (temps, délais), ont pu être corrélés significativement et positivement à la densité et l'index stomatique. De plus, la taille des stomates (longueur des cellules de garde, aire des stomates à la surface des feuilles) était corrélée négativement à la vitesse de changement de la conductance stomatique. La plupart des corrélations ont été observées avec les données anatomiques des stomates de la face adaxiale de la feuille et en réponse au VPD. Enfin, la transpiration de la plante entière était corrélée négativement avec la vitesse des stomates, bien que les peupliers présentant les stomates les plus rapides aient une consommation en eau plus importante.

Conclusions

Cette étude est à notre connaissance la première montrant le lien suspecté entre la dynamique des stomates et la transpiration de la plante entière. Cependant, puisque les plantes les plus grandes étaient aussi celles qui consommaient le plus d'eau, nous n'avons pas pu observer un effet semblable sur l'efficience d'utilisation de l'eau de la plante entière. La dynamique stomatique était corrélée avec la morphologie des stomates, mettant en lumière leur rôle, en particulier dans la réponse au VPD plutôt qu'à l'irradiance, chez les peupliers. L'absence de corrélation entre les paramètres dynamiques en réponse à l'irradiance et au VPD montre également que les mécanismes physiologiques des mouvements stomatiques, spécifiques à la

variable environnementale, induisent une vitesse propre. Enfin, nous avons montré que la sécheresse pouvait ralentir la dynamique stomatique, contrairement à quelques précédentes études sur des espèces plus tolérantes à la sécheresse (Haworth *et al.*, 2018).

Article: Altered stomatal dynamics induced by changes in irradiance and vapour-pressure deficit under drought: impacts on the whole plant transpiration efficiency of poplar genotypes

Publié dans New Phytologist (2019)

MAXIME DURAND[1] • OLIVER BRENDEL[1] • CYRIL BURÉ[1] • DIDIER LE THIEC[1]

[1] *Inra, Université de Lorraine, AgroParisTech, SILVA, F-54280 Champenoux, France*

Corresponding author:

Didier Le Thiec

Email: didier.lethiec@inra.fr

Telephone: (+33) 3 83 39 40 98

Accepté: 20 janvier 2019

DOI: 10.1111/nph.15710

New Phytologist

Research

Altered stomatal dynamics induced by changes in irradiance and vapour-pressure deficit under drought: impacts on the whole-plant transpiration efficiency of poplar genotypes

Maxime Durand, Oliver Brendel, Cyril Buré and Didier Le Thiec

INRA, Université de Lorraine, AgroParisTech, SILVA, F-54280 Champenoux, France

Author for correspondence:
Didier Le Thiec
Tel: +33 3 83 39 40 98
Email: didier.lethiec@inra.fr

Received: *21 August 2018*
Accepted: *20 January 2019*

New Phytologist (2019)
doi: 10.1111/nph.15710

Key words: drought, kinetics of stomatal responses, light, *Populus*, stomatal conductance, vapour-pressure deficit (VPD), water use efficiency (WUE).

Summary

• Recent findings were able to show significant variability of stomatal dynamics between species, but not much is known about factors influencing stomatal dynamics and its consequences on biomass production, transpiration and water-use efficiency (WUE).

• We assessed the dynamics of stomatal conductance (g_s) to a change of irradiance or vapour-pressure deficit (VPD) in two *Populus euramericana* and two *Populus nigra* genotypes grown under control and drought conditions. Our objectives were to determine the diversity of stomatal dynamics among poplar genotypes, and if soil water deficit can alter it. Physiological and morphological factors were investigated to find their potential links with stomatal morphology, WUE and its components at the whole-plant level.

• We found significant genotypic variability of g_s dynamics to both irradiance and VPD. Genotypes with faster stomatal dynamics were correlated with higher stomatal density and smaller stomata, and the implications of these correlations are discussed.

• Drought slowed g_s dynamics, depending on genotype and especially during stomatal closing. This finding is contrary to previous research on more drought-tolerant species. Independently of the treatment, faster stomatal dynamics were negatively correlated with daily whole-plant transpiration, presenting new evidence of a previously hypothesized contribution of stomatal dynamics to whole-plant water use.

Introduction

Droughts, or temporary soil water deficits, are likely to increase in intensity and frequency as a result of global changes (IPCC, 2014). Since 1950, the amount of land subjected to droughts has significantly expanded in Africa, southern Europe, eastern and southern Asia, and eastern Australia (Dai, 2011). Current global climate models predict a decline in soil moisture and a rising frequency of short- and long-term droughts in the future (Sheffield & Wood, 2008).

Although a decrease in soil moisture will induce a reduction in plant biomass production (Monclus *et al.*, 2006; Coopman *et al.*, 2008), wood demand has risen and will most likely continue to rise, driven by demography, economic growth and environmental as well as energy policies (FAO, 2018). This divergence in trends will further impact populations, economies and the environment in the coming years as even regional droughts have global impact (Sternberg, 2011). In order to mitigate the effects of drought on growth a promising strategy is to improve whole-plant transpiration efficiency (*TE*) (Condon *et al.*, 2004), the amount of biomass produced for a given amount of water used (see Supporting Information Table S1 for a full list of abbreviations).

Poplar productivity is closely linked to water availability (Tschaplinski & Blake, 1989). Although poplars are naturally found in riparian ecosystems due to their high water requirements, poplar cultivation extends to mesophyte habitats where they are more frequently subjected to soil water deficits. Monclus *et al.* (2005, 2006) showed in hybrid poplars that even a moderate drought induced a large reduction of biomass even though ^{13}C discrimination, a proxy of leaf-level intrinsic water use efficiency (W_i), the ratio between net CO_2 assimilation (A) and stomatal conductance to water vapour (g_s; Farquhar & Richards, 1984) was highly variable, driven mainly by g_s as opposed to productivity traits.

At the leaf level, stomata are at the interface between the atmosphere and the leaf. They play a central role in regulating A used by photosynthetic processes, and H_2O losses by transpiration. A long-standing theory of stomatal behaviour proposed that g_s is balanced in order to maximize A and minimize water loss (Cowan & Farquhar, 1977). However, A and g_s are not always tightly coupled (Knapp & Smith, 1990). First, the often-reported correlation between A and g_s is not linear (Wong *et al.*, 1979), which results in a range of high g_s at which A does not improve further. Secondly, diurnal changes of g_s are several orders of magnitude slower than those of A, excluding modifications of

carboxylation and electron transport rates. This results in a decoupling of A and g_s following an environmental change (Kaiser & Kappen, 2000), prompting large variations of W_i. Although g_s is often studied under steady-state conditions (Damour *et al.*, 2010), recent investigations suggest that g_s rarely reaches a steady state in naturally changing environments (Rayment *et al.*, 2000; Vialet-Chabrand *et al.*, 2013). Stomatal dynamics appear, therefore, as a limiting factor in the control of A and transpiration. Faster stomata, by enabling a closer tracking of environmental conditions, could function more closely to an optimal stomatal behaviour described by Cowan & Farquhar (1977). Moreover, faster stomatal closing could limit the rate at which soil moisture is exhausted by the plant, preventing or at least moving back an edaphic drought event. Plants living in drier habitats seem to have on average faster stomatal response when irradiance change (Vico *et al.*, 2011). However, the direct impact of drought appears to be species-specific (Gerardin *et al.*, 2018; Haworth *et al.*, 2018).

Despite multiple studies showing the diversity of stomatal dynamics across species (Vico *et al.*, 2011; Dumont *et al.*, 2013; Mc Ausland *et al.*, 2016; Qu *et al.*, 2016; Males & Griffiths, 2017), the main drivers of these differences are still unclear. Drake *et al.* (2013) proposed that the lower surface-to-volume ratio of larger stomata may cause slower movements of water in and out of the guard cells which would translate into slower aperture changes. Some authors were able to establish a correlation between stomatal size, density and speed of response to irradiance (Drake *et al.*, 2013; Haworth *et al.*, 2016; Xiong *et al.*, 2018). However, this hypothesis might only be relevant in specific cases allowing for a wide diversity of stomatal sizes but similar morphologies (Raven, 2014; Elliott-Kingston *et al.*, 2016; Lawson & Vialet-Chabrand, 2019). If vapour-pressure deficit (VPD) and irradiance-induced stomatal dynamics are correlated, it would suggest that a common factor may drive these two responses (e.g. stomatal morphology).

We quantified the stomatal speed of closing and opening in response to a step change in irradiance and VPD in four poplar genotypes from two species *Populus nigra* and *Populus nigra x deltoides* (*Populus euramericana*). We subjected them to two contrasting water availabilities in order to answer the following questions: (1) Do parameters related to irradiance and VPD-induced stomatal dynamics vary among poplar genotypes?; (2) Does soil water deficit increase the speed of stomatal response?; (3) Are stomatal dynamics in response to irradiance and VPD related?; (4) Is the speed of stomatal response negatively correlated with stomatal size and positively with stomatal density?; and (5) Is faster stomatal response associated with lower transpiration, water use and thus higher TE?

Materials and Methods

Plant material and growth conditions

Four poplar genotypes were used throughout our experiment. Carpaccio and I214 are commercially available *Populus deltoides* × *nigra* (Moench.) clones, whereas 6J29 and N38 are *P. nigra* (L.) genotypes originating from natural populations in France (Drôme 6; FR-6) and Italy (La Zelata; IT1), respectively. Poplar clones were chosen for their common use for wood production (*P. euramericana*), contrasted natural distribution (*P. nigra*) and diversity of drought tolerance. I214 and 6J29 are generally found to be sensitive to drought (Table S2; Chen *et al.*, 1997; Giovannelli *et al.*, 2007; Muller & Lambs, 2009; Viger *et al.*, 2016). The two species were selected to serve as a basis for comparison between traditionally planted against naturally occurring species of *Populus*. 64 shoot cuttings were planted in 10-l pots with drainage holes and a saucer filled by 9.5 kg (± 1.5%) of a sand:peat mixture (1 : 1, v/v) maintained constant at a volumetric soil water content (*SWC*) of 27.9% on the 91st day of the year. The soil was fertilized by adding 20 mg of slow-release nutritive granules (Nutricote T100, 13 : 13 : 13 NPK and micronutrients; Fertil SAS, Boulogne-Billancourt, France) and 1 g l^{-1} $CaMg(CO_3)_2$. To limit soil evaporation, 1.4 kg of white marble gravel (8–12 mm) covered each pot. Four additional nonplanted pots (two for each water treatment) also were used to estimate soil evaporation. Cuttings grew in a fully automated glasshouse at INRA-Nancy (48°45′09.3″N, 6°20′27.6″E; Champenoux, France) for 60 d under natural light. Environmental conditions in the glasshouse were affected by weather conditions, but the temperature was regulated to have a free range between 15 and 25°C. In order to maintain the *SWC* constant (Fig. S1), pots were weighed at least three times a day (QC65EDE-D; Sartorius-AG Göttingen, Germany; accuracy: ± 0.1 g) and watered back to a reference mass calculated for each pot with a weighting and watering robot to 85% of field capacity for the control plants. The mass difference over 24 h, to which soil evaporation was subtracted, was assumed to represent daily water use. Cumulated water use (*WU*) was computed for each plant over the duration of the experiment. Diameter and height of each plant were measured once a week throughout the experiment.

Transpiration efficiency and drought set-up

On the 151st day of the year, watering on half of the plants (chosen randomly) was stopped until a volumetric *SWC* of 18.3% was reached. The target value was reached after 2 d. The control of *SWC* was based on pot mass and a calibration between volumetric *SWC* measured by Time Domain Reflectometry (HD2; IMKO, Ettlingen, Germany) and pot mass. New reference masses for each plant were computed by fitting a linear regression between the total pot mass and SWC ($R^2 > 0.8$). The drought was maintained for 25 d, reference masses were adjusted each week to take the plant growth into account.

Four individuals per genotype and the remaining 48 trees were harvested, respectively, before and after the drought period. Leaves, stems and roots were oven-dried at 60°C until they reached a constant dry mass which was recorded in order to estimate initial and final biomass in each compartment. Biomass increment was computed for each individual from the difference between the harvested dry mass and mean genotypic biomass estimated at the start of the experiment. Whole-plant *TE* was

New Phytologist

Research 3

computed per individual as total biomass increment (*DMT*) over *WU*. Total leaf area (*TLA*) was estimated twice during the experiment by measuring each leaf width and fitting an allometric relationship between leaf area and leaf width ($R^2 > 0.98$ for every genotype). Additionally, *TLA* of the trees was measured during both harvests right before drying (Li-3000A; LiCor, Lincoln, NE, USA). Because *TLA* and plant height were highly correlated ($R^2 > 0.97$), we estimated *TLA* for each day of the experiment from splined weekly measures of plant height. By dividing for each day and each individual, their daily *WU* by their daily estimated *TLA*, we were able to calculate daily whole-plant transpiration (see Fig. 1). The average of these computations over the drought period is later referred to as E.

Leaf gas exchange

On the 161st day of the year, we monitored the diurnal dynamics of gas exchange (A and g_s) every hour from 05:30 to 18:00 h (local time) on five replicates per genotype and water treatment (i.e. 40 individuals) on the first fully expanded leaf at the start of the drought using a portable photosynthesis system (Li-6200; LiCor).

All other gas exchange measurements used the same leaves and four intercalibrated Li-6400XT portable photosynthesis systems (LiCor) in order to control environmental factors inside the leaf cuvette. Unless stated otherwise, vapour pressure deficit (VPD) is considered to be leaf-to-air. Leaves were first left to acclimatize inside the leaf cuvette (Photosynthetic Active Radiation, PAR, 1000 µmol m^{-2} s^{-1}; CO_2 concentration, 400 ppm; leaf temperature, 25°C; VPD, 1 kPa; flow, 600 µmol s^{-1}) until g_s reached a steady-state (SS_0; defined here as a variation < 5% over 5 min). At this point, PAR was switched to 200 µmol m^{-2} s^{-1} and g_s was recorded every 45 s until it reached a new steady-state (SS_1). PAR was then switched back to 1000 µmol m^{-2} s^{-1} until g_s reached the last steady-state (SS_2). The same protocol was used for the stomatal response curves to a change of VPD except that PAR was fixed at 1000 µmol m^{-2} s^{-1} and VPD was switched from 1 to 3 kPa and then back to 1 kPa. VPD pressures were chosen because they are regularly encountered in the field and to assure strong repeatability of the experiment. The magnitude of change in g_s was defined as the difference in g_s between two steady states (i.e. between SS_1 and SS_0 for closing or SS_2 and SS_1 for opening).

Stomatal morphology

Leaves used in gas exchange measurements were sampled on the 172nd day of the year and immediately frozen into liquid nitrogen. Leaves were then freeze-dried following Dumont *et al.* (2014). In order to study both sides of the leaves two discs of 78.54 mm^2 were sampled from each leaf with a stamper. Discs were then platinum-coated to avoid charging effects (EM ACE600; Leica, Wetzlar, Germany), placed under a scanning electron microscope (ΣIGMA-VP; Carl Zeiss Microscopy, Oberkochen, Germany) coupled with a backscattered secondary electron detector at accelerating voltage of 20 kV. The working distance was set at 9 mm and the magnification at ×500, leading to a resolution of 0.279 μm^2 per pixel. Sixteen pictures covering an area of 3.44 mm^2 were used to measure stomatal density (*SD*) by manual counting using ImageJ software, excluding stomata overlapping in the margins of the picture. Stomatal index (*SI*) was computed as *SD* over the total number of cells (i.e. stomatal and epidermal cells). Length and surface area of the guard cells (*GCL* and *AGC*, respectively) was measured on 48 randomly chosen stomata per discs using the ImageJ software and calculated following de Boer *et al.* (2016).

Model description

Stomatal response curves were fitted using a sigmoidal model (Vialet-Chabrand *et al.*, 2013). Our goal was to empirically

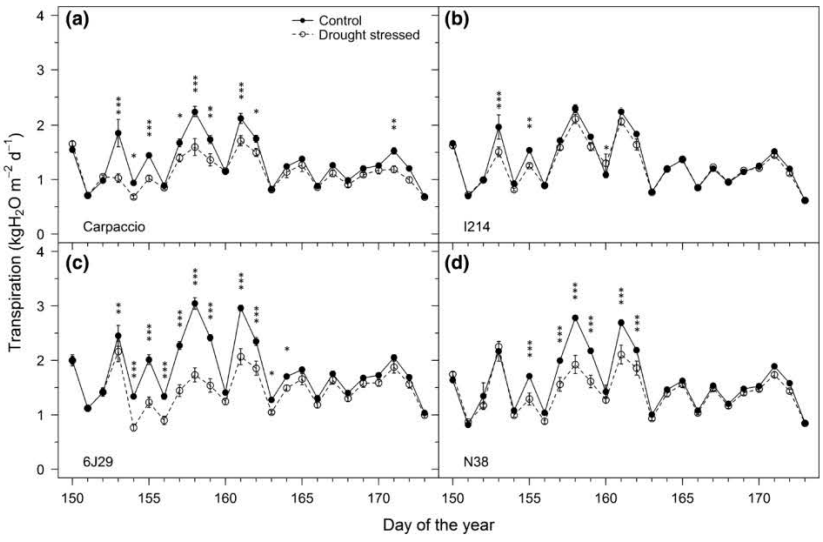

Fig. 1 Daily transpiration per unit leaf area of two *Populus deltoides* × *nigra* (a) Carpaccio and (b) I214, and two *Populus nigra* genotypes (c) 6J29 and (d) N38 under contrasting water availability. The drought experiment started on the 151st day. Closed and open circles are (respectively) for control and drought-stressed treatments (means ± SE). Significant differences between water treatments for each date is shown ($n = 6$). *, $P < 0.05$; **, $P < 0.01$; ***, $P < 0.001$.

describe g_s dynamics to evaluate the specific parts of the g_s response and assess differences among genotypes. By nature, the model has no predictive value. It takes the form:

$$\widehat{g_s} = g_0 + (G - g_0)e^{-e^{\left(\frac{\lambda - t}{\tau}\right)}} \quad \text{Eqn 1}$$

($\widehat{g_s}$, the fitted g_s; g_0 and G, steady-state values of g_s (mol m^{-2} s^{-1}) at the start and end of the curve (respectively); τ, a time constant (s); λ, lag time (s); t, time (s)). Further details regarding the model parameters can be found in Gerardin *et al.* (2018) and in Fig. S2. From these parameters an estimator of the speed of the stomatal response, the maximum slope (SL_{max}), can be calculated as:

$$\mathrm{SL}_{\max} = \frac{G - g_0}{\tau \times e} \quad \text{Eqn 2}$$

(e, Euler's number ($e \approx 2.718$)). The fitting procedure used R/NLMINB function (R Core Team, 2017) with uniform random starting values for τ and λ (Fig. S3). We used the equation linking stomatal aperture (A_p) and SD with g_s (Franks & Farquhar, 2001), of the form:

$$\widehat{g_s} = \frac{SD \times A_p \times \frac{D}{V}}{d_p + \frac{\pi}{2}\sqrt{\frac{A_p}{\pi}}} \quad \text{Eqn 3}$$

(D, diffusivity of water in air (2.82×10^{-5} m^2 s^{-1}); V, molar volume of air (0.0244 m^3 mol^{-1}); d_p, pore depth, assumed to be equal to half of the guard cell width (de Boer *et al.*, 2016)). By re-purposing Eqn 1 to simulate changes of aperture instead of g_s and re-calculating g_s with Eqn 3 we were able to compare theoretically the dynamics of A_p and g_s simultaneously and the interplay with SD.

Statistical analysis

Statistics were done using R 3.4.3 (R Core Team, 2017, all data used are available in Table S4). A type 2 two-way ANOVA was used to detect significant differences among the four genotypes and the two water treatments. Normality and homoscedasticity were checked by a Shapiro–Wilk normality test and a Levene test, respectively. Post-hoc contrast analyses were performed to test differences between modalities for each factor. Diurnal gas exchange measurements ($n = 5$) and daily transpiration ($n = 6$) were tested with a type 2 two-way repeated ANOVA design with genotypes and water treatments as between-subjects factors and the time as within-subjects factors. Normality of the residuals at each repeated measurements was checked by a Shapiro–Wilk normality test and sphericity was checked with Mauchly tests. When sphericity was violated, we used the Greenhouse–Geisser correction. Correlations were computed by performing ANCOVA with stomatal dynamics parameters as dependent variables, water treatment as categorical independent variable and either stomatal morphology, whole-plant growth parameters or other stomatal dynamics parameters as continuous independent variables ($n = 24$). Partial R^2 for the continuous independent variables were computed and P-values were adjusted to control the false discovery rate. Significant differences were considered at $P < 0.05$ for all tests.

Results

Growth and gas-exchange in relation to water availability

Our experimental drought induced significant differences of growth and water use (for all tests, $n = 6$). Before, no significant differences were found between treatments (Table S3). Height increment was decreased for all genotypes compared to the control trees, from 13% for I214 and up to 32% for 6J29 (Table 1). We also found a small overall 12% decrease in diameter increments. *DMT* was the highest for I214 and the lowest for N38 control trees which summed up to a mean difference of 18.9 g between the two genotypes. *DMT* was similar between water treatments for Carpaccio and N38 but was reduced by 25% in I214 and 6J29 mainly due to a decline of root (by 12.7 g) and leaf (by 9.4 g) dry mass increments, respectively. *TLA* was marginally lower in drought-stressed trees compared to the control except for 6J29 which showed a significant 39% decrease. Drought also reduced *WU* by 4.2, 2.0, 4.9 and 2.5 kgH_2O for Carpaccio, I214, 6J29 and N38, respectively. I214 showed the lowest reduction in *WU* (12%), whereas 6J29 showed the highest (30%). Consequently, we found that drought induced a 14% decline of *TE* in I214 but a significant increase for Carpaccio and N38 (41% and 26%, respectively). In summary, although drought had a similar effect among poplar genotypes by reducing growth and water use, the magnitude of the response was different and led to distinct modifications of *TE*.

Values of E ranged from 0.62 to 3.04 kgH_2O m^{-2} d^{-1} across all genotypes and water treatments ($n = 6$; Fig. 1). On average over the drought period, all genotypes had a significantly lower transpiration in the drought-stressed trees compared to the control (Table 1). More precisely, transpiration was significantly reduced on 9, 2, 11 and 6 out of the 23 d in Carpaccio, I214, 6J29 and N38, respectively. Daily fluctuations of transpiration were strongly linked with fluctuations of global radiation and atmospheric VPD (Fig. S4) that drove the potential evapotranspiration (Fig. S5a). There was a decreasing trend of whole-plant transpiration during the experiment (Fig. S5b), which may have resulted from leaf ageing, changes of the immediate light environment or naturally developing *SD* gradients with height. This could explain why significant differences between water treatments were found mostly in the first 13 d, where potential evapotranspiration also was at the highest.

As for the daily gas-exchange dynamic ($n = 5$; Fig. 2), A was higher among black poplars compared to the two hybrids with a mean maximum of 16.0, 19.0, 24.1 and 25.4 µmol m^{-2} s^{-1} for Carpaccio, I214, 6J29 and N38, respectively. Only isolated differences of A between control and drought-stressed trees were found for 6J29 and N38. In essence, I214 was the only genotype

Table 1 Growth, biomass production and water use of two *Populus deltoides* × *nigra* (Carpaccio and I214) and two *Populus nigra* genotypes (6J29 and N38) under contrasting water availability

Genotype	Treatment	*H* (cm)	*D* (mm)	*DMT* (g)	*DML* (g)	*DMS* (g)	*DMR* (g)	*WU* (kgH_2O)	*E* ($kgH_2O\ m^{-2}\ d^{-1}$)	*TLA* (cm^2)	*TE* ($g\ l^{-1}$)
Carpaccio	Control	70 ± 6.9 a	5.1 ± 1 a	77.7 ± 9.2 ab	26.9 ± 2.9 ab	31.1 ± 1.8 ab	19.7 ± 8.9 bcd	20.4 ± 1 a	1.25 ± 0.08 d	2857 ± 504 b	3.81 ± 0.47 d
	Drought	55 ± 2.5 b	4.1 ± 0.6 b	87.5 ± 16.6 a	27.8 ± 4.8 a	30.3 ± 5.7 b	29.5 ± 8.8 b	16.2 ± 0.6 b	1.01 ± 0.11 f	2711 ± 144 b	5.38 ± 0.94 bc
I214	Control	69.3 ± 4.3 a	4.8 ± 0.6 ab	91.6 ± 10.2 a	22.1 ± 2.2 cde	29.5 ± 2.8 b	40.1 ± 9.1 a	16.3 ± 0.6 b	1.25 ± 0.03 d	2420 ± 197 bc	5.63 ± 0.63 b
	Drought	60.1 ± 3.7 b	4.2 ± 0.5 ab	69.6 ± 12.7 bc	19.2 ± 2.7 ef	23 ± 2.8 c	27.4 ± 7.8 bc	14.3 ± 0.8 c	1.14 ± 0.1 e	2139 ± 261 c	4.85 ± 0.74 c
6J29	Control	67.4 ± 3.2 a	5.1 ± 1 a	79.5 ± 8.4 ab	25.5 ± 2.5 abc	35.6 ± 4.2 a	18.4 ± 4.6 cd	16.1 ± 1.5 b	1.73 ± 0.07 a	3448 ± 600 a	4.94 ± 0.22 bc
	Drought	46 ± 3.8 c	4.5 ± 0.6 ab	61.4 ± 5.8 c	16.1 ± 3.5 f	29.7 ± 3.6 b	15.7 ± 5.7 d	11.2 ± 1.1 d	1.4 ± 0.1 c	2094 ± 333 c	5.31 ± 0.19 bc
N38	Control	72.4 ± 4.5 a	3.9 ± 0.5 b	72.7 ± 7.1 bc	23.1 ± 2.1 bcd	30.4 ± 2 b	19.2 ± 3.9 cd	13.5 ± 0.7 c	1.53 ± 0.07 b	2537 ± 220 bc	5.4 ± 0.5 bc
	Drought	59 ± 5.4 b	3.9 ± 0.4 b	72.6 ± 7.2 bc	20.7 ± 2.2 de	29 ± 2.5 b	22.9 ± 6.7 bcd	11 ± 0.3 d	1.34 ± 0.09 cd	2220 ± 187 c	6.83 ± 0.22 a
P-value	Genotype	< 0.001	0.022	0.016	< 0.001	< 0.001	< 0.001	< 0.001	< 0.001	0.001	< 0.001
	Treatment	< 0.001	0.005	0.01	< 0.001	< 0.001	ns	< 0.001	< 0.001	< 0.001	< 0.001
	Interaction	0.014	ns	0.001	0.001	ns	0.003	< 0.001	0.025	< 0.001	< 0.001

Values reported are means ± standard deviation of the difference between the end and the start of the drought ($n = 6$). ANOVA factors were considered significant when $P < 0.05$. Letters show significant differences by *post hoc* contrast among the eight groups (four genotypes + two water treatments). *H*, plant height increment; *D*, main stem diameter increment; *DMT*, total dry mass increment; *DML*, leaf dry mass increment; *DMS*, stem dry mass increment; *DMR*, root dry mass increment; *WU*, cumulated water use during the drought period; *TLA*, total leaf area increment; *E*, average daily whole-plant transpiration during the drought period per unit leaf area; *TE*, transpiration efficiency; ns, not significant.

that did not show the typical afternoon stomatal closure more strongly in the drought treatment, leading to similar W_i. By contrast, W_i was significantly higher in the Carpaccio and N38 drought-stressed trees compared to the control for most of the afternoon and a similar trend can be seen in 6J29 (not significant).

Stomatal morphology

The leaves used for stomatal morphology also were used for gas-exchange measurements. As such, they were fully mature before the start of the drought so a potential drought effect could not be tested. Stomatal morphology showed more contrasts between leaf sides ($_{ab}$, abaxial; $_{ad}$, adaxial) in the black poplars compared to the hybrids (for all tests, $n = 6$). Although *GCL* was similar between leaf sides in the hybrid poplars, GCL_{ad} was (respectively) 4.9 and 2.4 μm higher in 6J29 and N38 compared to GCL_{ab} (Table 2). AGC_{ad} was marginally lower compared to AGC_{ab} for Carpaccio and I214, whereas it was 34 and 20% higher for 6J29 and N38, respectively. Overall 6J29 had the largest stomata (292.3 and 392.5 μm^2 for AGC_{ab} and AGC_{ad}, respectively) and I214 the smallest (258.3 and 233.1 μm^2 for AGC_{ab} and AGC_{ad}, respectively).

For all genotypes, SD_{ab} was higher than SD_{ad}. I214 had the highest *SD* on both leaf sides and 6J29 and N38 had similar *SD* on both adaxial and abaxial leaves. Concurrently, *SI* was found to be significantly different across all genotypes and leaf sides. Overall, genotypes with larger stomata (higher *GCL* and *AGC*) tended to be associated with lower *SD* and *SI*.

Stomatal dynamics induced by a step change of irradiance

Lowering the PAR reduced *A* and g_s on all genotypes and water treatments with a higher relative reduction of g_s in the drought-stressed trees ($n = 6$ for all tests; Table S5). The magnitude of g_s change ranged from 0.21 to 0.29 $mol\ m^{-2}\ s^{-1}$ and from 0.16 to 0.41 $mol\ m^{-2}\ s^{-1}$ for the closing and opening processes, respectively (Fig. 3, S6). Only I214 showed a significant 37% lower magnitude during the stomatal opening in the drought-stressed trees compared to the control. The maximum slope of stomatal closing ($SL_{max,d}$) was the highest for I214 and the lowest for 6J29 both for control and drought-stressed trees (I214: 421 and 260 $\mu mol\ m^{-2}\ s^{-2}$; 6J29: 180 and 148 $\mu mol\ m^{-2}\ s^{-2}$ for control and drought-stressed trees, respectively). In addition, drought-stressed I214 trees showed a significant 38% reduction of the $SL_{max,d}$ compared to the control. τ during stomatal closing (τ_d) was the lowest in I214 both for control (258 s) and drought-stressed trees (339 s) and the highest in N38 for the control (504 s) and in 6J29 for the drought-stressed trees (614 s). Although the ANOVA returned a significant genotype effect ($P = 0.02$), *post hoc* comparisons were unable to show any significant genotypic differences of τ given the intragroup variance. Similarly, we found an overall 87% increase of λ during stomatal closing (λ_d) in the drought-stressed treatment compared to the control on average for all genotypes ($P < 0.001$) but post-hoc comparisons were again unable to identify

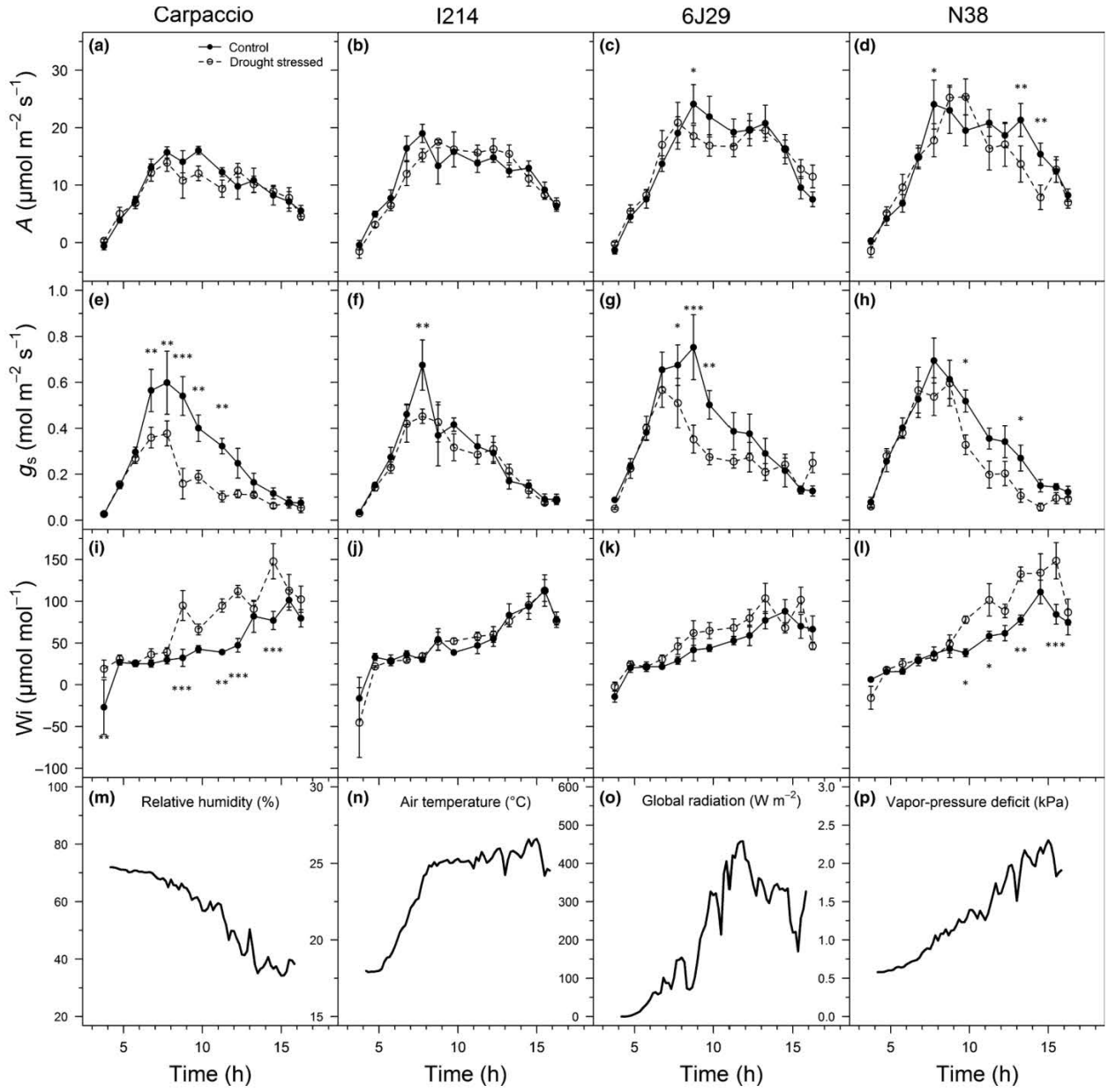

Fig. 2 Gas-exchange dynamic of two *Populus deltoides* × *nigra* (a, e, i) Carpaccio and (b, f, j) I214, and two *Populus nigra* genotypes (c, g, k) 6J29 and (d, h, l) N38 under contrasting water availability. (a–d) Net CO_2 assimilation (A), (e–h) stomatal conductance to water vapour (g_s), and (i–l) intrinsic water use efficiency (W_i). (m) Relative humidity, (n) air temperature, (o) global radiation and (p) atmospheric vapour-pressure deficit inside the glasshouse are also reported. Closed and open circles are (respectively) for control and drought-stressed treatments (means ± SE). All measurements were done on the 161st day of the year (9 June 2016), including the meteorological data. Significant differences between water treatments for each date is shown ($n = 5$). *, $P < 0.05$; **, $P < 0.01$; ***, $P < 0.001$.

differences between water treatments for any specific genotype. Neither genotype nor water treatment had any significant impact on τ, λ nor SL_{max} during the stomatal opening (τ_i, λ_i and $SL_{max,I}$, respectively). Overall, stomatal dynamics in the drought treatment were slower during stomatal closing and similar during stomatal opening.

Stomatal dynamics induced by a step change of VPD

Compared to the irradiance response, the step change in VPD prompted an almost complete closure of the stomata, which resulted in different magnitudes of g_s response between genotypes because of differences in g_s at SS_0 (for all tests $n = 6$; Table S5).

Table 2 Stomatal morphology measurements of two *Populus deltoides* × *nigra* (Carpaccio and I214) and two *Populus nigra* genotypes (6J29 and N38) for each of the two leaf sides

Genotype	Leaf side	GCL (μm)	AGC (μm^2)	SD (mm^{-2})	SI (%)
Carpaccio	Abaxial	26.7 ± 0.8 c	279.5 ± 20.3 cd	142.8 ± 12.5 c	10.9 ± 0.8 b
	Adaxial	27.1 ± 1.1 c	261.4 ± 22.8 de	84.8 ± 7 e	5.9 ± 0.3 f
I214	Abaxial	27.4 ± 1.3 c	258.3 ± 26.1 de	191.1 ± 27.4 a	11.9 ± 0.7 a
	Adaxial	26.5 ± 1.2 c	233.1 ± 26.7 e	116.5 ± 10.4 d	6.7 ± 0.5 e
6J29	Abaxial	29 ± 1.4 b	292.3 ± 35.1 c	149.9 ± 13.5 bc	7.7 ± 0.7 d
	Adaxial	33.9 ± 1.4 a	392.5 ± 61.1 a	64.9 ± 4.8 f	4.8 ± 0.3 g
N38	Abaxial	26.8 ± 0.7 c	271.2 ± 20.8 cd	155.6 ± 14.1 b	8.6 ± 0.8 c
	Adaxial	29.2 ± 0.8 b	326.4 ± 41.5 b	59.5 ± 4.1 f	4.1 ± 0.4 h
P value	Genotype	< 0.001	< 0.001	< 0.001	< 0.001
	Leaf side	< 0.001	< 0.001	< 0.001	< 0.001
	Interaction	< 0.001	< 0.001	< 0.001	< 0.001

Values reported are means ± standard deviation ($n = 6$). ANOVA factors were considered significant when $P < 0.05$. Letters show significant differences by post-hoc contrast among the eight groups (four genotypes + two leaf sides). GCL, guard cell length; AGC, guard cell surface area; SD, stomatal density; SI, stomatal index.

The magnitude of g_s change ranged from 0.53 to 0.12 mol m^{-2} s^{-1} and from 0.11 to 0.26 mol m^{-2} s^{-1} for the closing and opening processes, respectively (Fig. 4, S7). Magnitude of stomatal closing was overall higher in the control compared to the drought-stressed treatment ($P = 0.017$), whereas only I214 showed a significant 35% lower magnitude during the stomatal opening in the drought-stressed trees compared to the control. Similar to the irradiance response, $SL_{max,d}$ was the highest for I214 and the lowest for 6J29, differing by a factor of 10 and 6.8 for control and drought-stressed trees, respectively (I214: 1112 and 603 μmol m^{-2} s^{-2}; 6J29: 110 and 88 μmol m^{-2} s^{-2} for control and drought-stressed trees, respectively). In addition, drought-stressed I214 trees showed a significant 46% reduction of $SL_{max,d}$ compared to the control. Overall, black poplars tended to have a lower SL_{max} than hybrid poplars both during the closing and opening processes. Black poplars also showed values of both parameters τ_d and λ_d 4.7 and 3.1 times higher (respectively) than the hybrid poplars. There was a similar trend between species during the stomatal opening although not as pronounced. Overall, *VPD*-induced stomatal closing tended to be slower under drought, led by a smaller magnitude of g_s change but similar τ and λ. Differences between species also were more pronounced during the *VPD* change than during the irradiance change.

Comparisons between irradiance and *VPD*-induced stomatal dynamics

Significant differences in the stomatal dynamics parameters between irradiance and *VPD* responses were found mostly in the black poplars (for all tests $n = 6$). τ_d and τ_i were significantly lower during an irradiance change for 6J29 and N38 for both water treatments ($P < 0.003$) except for τ_d in the N38 drought-stressed trees and τ_i in the N38 control trees ($P = 0.98$ and 0.05, respectively). λ_d was significantly lower during an irradiance change for 6J29 and N38 for both water treatments ($P < 0.008$), whereas all genotypes and water treatments had a λ_i significantly lower during an irradiance change ($P < 0.03$) except for the I214 control trees ($P = 0.31$). $SL_{max,d}$ was, however, significantly lower during an irradiance change only for I214 control and drought-stressed trees ($P < 0.001$), whereas $SL_{max,i}$ was significantly higher only in the 6J29 control ($P = 0.03$) despite visible trends of higher $SL_{max,d}$ and $SL_{max,i}$ on both black poplars. Dynamics parameters were mostly uncorrelated between irradiance and VPD responses. Only λ_d and $SL_{max,d}$ but neither τ_d, τ_i, λ_i nor $SL_{max,i}$ showed significant positive correlation ($P = 0.05$, 0.09, 0.04, 0.16, 6.49×10^{-7} and 0.37, respectively, for τ_d, τ_i, λ_d, λ_i, $SL_{max,d}$ and $SL_{max,i}$).

Correlations between stomatal dynamics and morphology

No correlation was found between stomatal morphology and dynamic parameters when including a genotype effect in the statistical model. Thus, correlations were intergenotypic but not intragenotypic in nature ($n = 24$ for all tests). Except for $SL_{max,i}$ and SD_{ad} ($P = 0.03$), none of the dynamic parameters of irradiance-induced stomatal opening were significantly correlated with stomatal morphology parameters ($P > 0.06$ in all cases; Fig. 5, S8). However, τ_d was negatively correlated with SD_{ad} and SI_{ad} ($P = 0.006$ and 0.033, respectively). Additionally, $SL_{max,d}$ was positively correlated with *SD* and *SI* on both leaf sides and negatively correlated with *GCL* and *AGC* on the adaxial side only.

As for the VPD response, most of the significant correlations between stomatal dynamics parameters and stomatal morphology occurred on parameters measured on the adaxial side of the leaf. Although both τ and λ during stomatal closing and opening were significantly positively correlated with GCL_{ad}, and AGC_{ad} ($P < 0.003$ in all cases), only GCL_{ab} was positively correlated with τ_d, τ_i and λ_i ($P = 0.013$, 0.003 and 0.013, respectively). τ and λ during both stomatal closing and opening also were negatively correlated with SD_{ad} and SI_{ad}. Only SI_{ab} was negatively correlated with τ and λ during both stomatal opening and closing ($P < 0.003$). SL_{max} during both opening and closing was positively correlated with *SD* and *SI* on both leaf sides (except between SD_{ab} and $SL_{max,i}$, $P = 0.83$) and negatively correlated with GCL_{ad} and AGC_{ad}. Overall, a higher *SD* or *SI*, as well as smaller stomata, tended to result in faster responses.

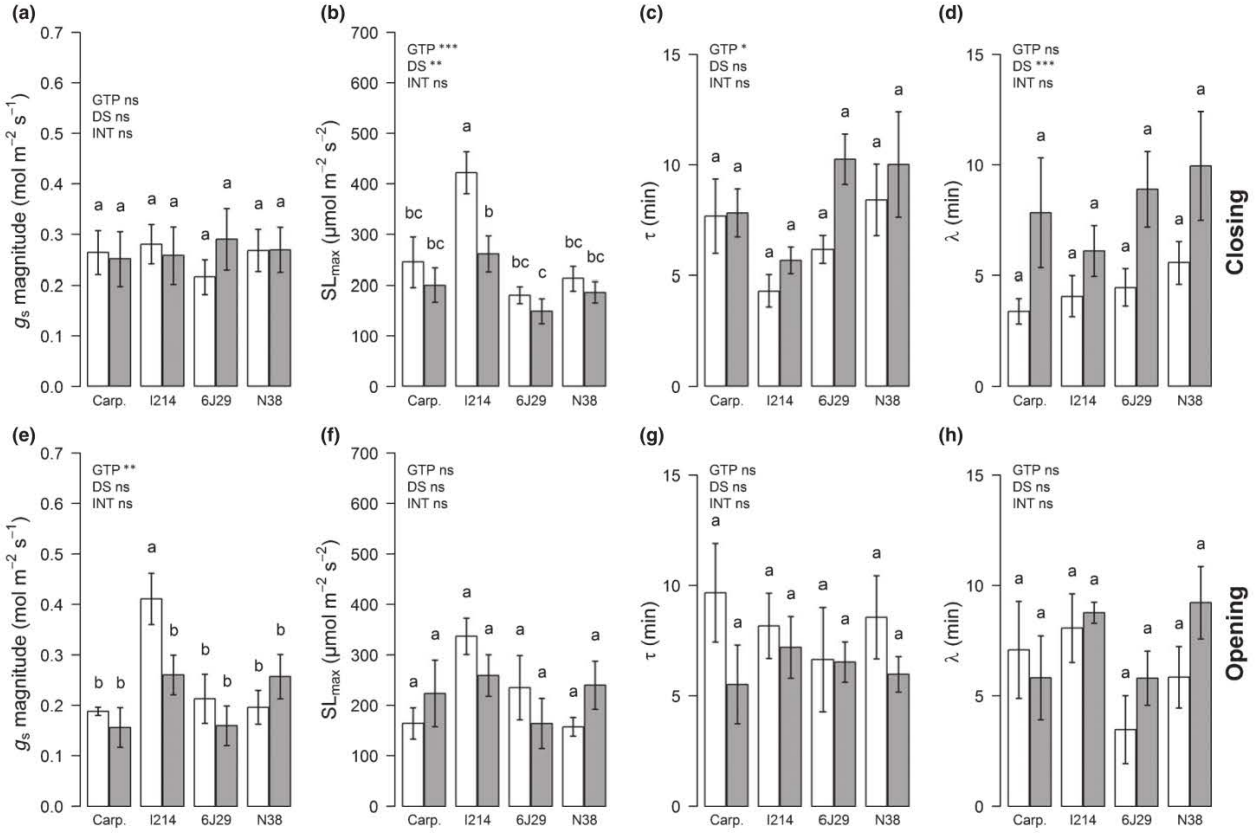

Fig. 3 Dynamic parameters of the stomatal conductance to water vapour (g_s) response to (a–d) a decrease or (e–h) an increase of irradiance for two *Populus deltoides* × *nigra* (Carpaccio and I214) and two *Populus nigra* genotypes (6J29 and N38) under contrasting water availability. Values are means ± SE. Open and closed bars are control and drought-stressed treatments, respectively. Letters show significant differences by post-hoc contrast among the eight groups (four genotypes + two treatments). Results of two-way ANOVA are given for main effects (GTP, genotype; DS, drought stress) and interaction (INT), $n = 6$. τ, time constant; λ, lag time; SL_{max}, maximum slope of the g_s response. *, $P < 0.05$; **, $P < 0.01$; ***, $P < 0.001$; ns, not significant.

Correlations between stomatal dynamics, growth and water use

Similarly to correlations between stomatal morphology and dynamics parameters, correlations presented here are intergenotypic but not intragenotypic in nature as no significant correlation was found when including a genotype effect into the statistical model ($n = 24$ for all tests). There were significant but weak correlations during stomatal closing between whole-plant growth and dynamic parameters derived from a step change of irradiance (Fig. 6, S8). *DMT* was positively correlated with SL_{max} and negatively with τ_i ($P < 0.04$). $SL_{max,d}$ also was negatively correlated with *E* ($P = 0.02$). Overall, stronger and more numerous correlations were found between whole-plant growth and dynamic parameters derived from a step change of VPD. Although τ and λ were positively correlated with *E*, we found a negative correlation with *E* and SL_{max} (in all cases, $P < 0.001$). *WU* was negatively correlated with τ_d, λ_d and λ_i ($P < 0.001$, $P < 0.001$ and $P = 0.022$, respectively) and positively with $SL_{max,i}$ ($P = 0.01$). *DMT* also was negatively correlated with τ_d and positively with $SL_{max,i}$ ($P < 0.05$). *TE* was only found to be positively correlated with λ_d during the VPD response. Overall, slower responding stomata were related to higher transpiration but lower water use and biomass production.

Discussion

Genotypic variability

Most current gas-exchange models use a steady-state approach to compute stomatal conductance (g_s) (Damour *et al.*, 2010) which can lead to significant discrepancies between the observed and modeled data (Stegemann *et al.*, 1999; Vialet-Chabrand *et al.*, 2013). Assessing the effect of water availability on the dynamics of g_s among different poplar genotypes and its potential links with stomatal morphology and transpiration efficiency (*TE*) will help us further our understanding of guard cell functioning on whole-plant water use and improve current models.

In the present study, we fitted a dynamic model to describe the g_s response to a step change of irradiance or vapour-pressure

New Phytologist

Research 9

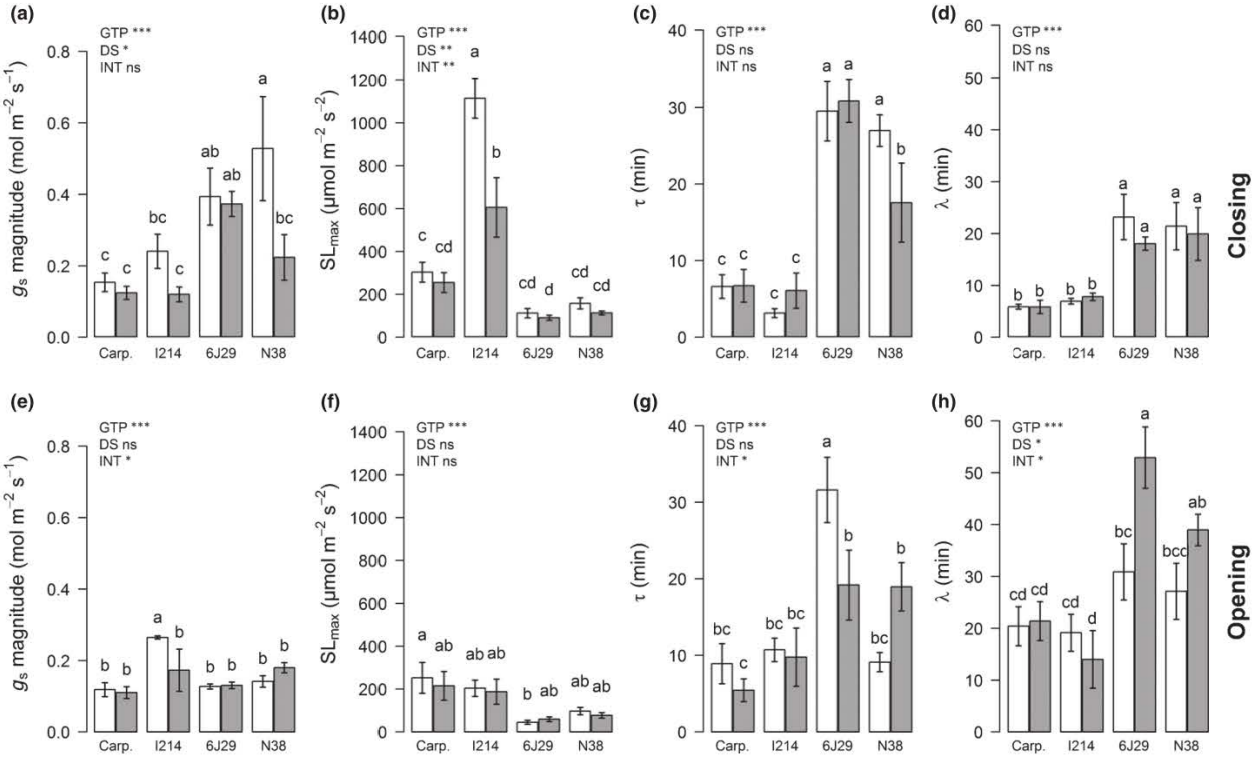

Fig. 4 Dynamic parameters of the stomatal conductance to water vapour (g_s) response to (a–d) a decrease or (e–h) an increase of vapour-pressure deficit for two *Populus deltoides* × *nigra* (Carpaccio and I214) and two *Populus nigra* genotypes (6J29 and N38) under contrasting water availability. Values are means ± SE. Open and closed bars are control and drought-stressed treatments, respectively. Letters show significant differences by post-hoc contrast among the eight groups (four genotypes + two treatments). Results of two-way ANOVA are given for main effects (GTP, genotype; DS, drought stress) and interaction (INT), $n = 6$. τ, time constant; λ, lag time; SL_{max}, maximum slope of the g_s response. *, $P < 0.05$; **, $P < 0.01$; ***, $P < 0.001$; ns, not significant.

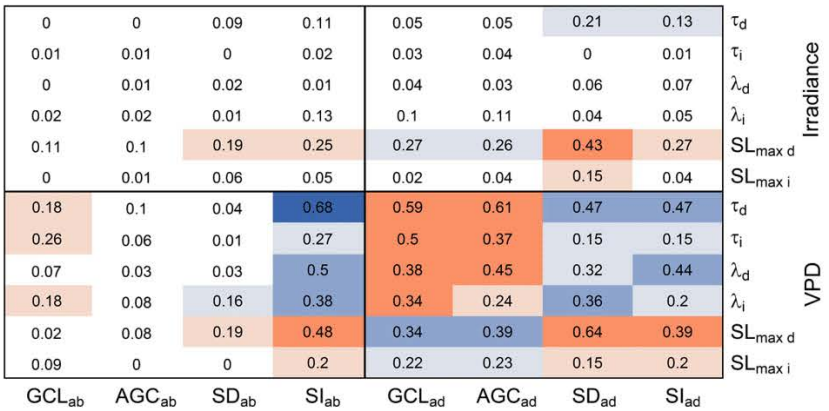

Fig. 5 Correlation matrix between dynamic parameters of stomatal conductance to water vapour (g_s) response to a decrease or an increase of irradiance or vapour-pressure deficit (VPD) and stomatal morphological parameters for two *Populus deltoides* × *nigra* (Carpaccio and I214) and two *Populus nigra* genotypes (6J29 and N38). Subscripts $_d$ and $_i$ are, respectively, for stomatal closing and opening to irradiance or VPD and $_{ab}$ and $_{ad}$ are (respectively) for the abaxial and adaxial side of the leaf. Partial R^2 of the residual variability once the treatment effect is accounted for are shown ($n = 24$). Correlations were considered significant at $P < 0.05$ and are highlighted in orange or blue for positive and negative relationships, respectively. White cells are nonsignificant correlations. *GCL*, guard cell length; *AGC*, guard cell surface area; *SD*, stomatal density, *SI*, stomatal index. τ, λ and SL_{max} are parameters of the sigmoidal model.

deficit (VPD). Through the analysis of the model parameters, we found during a change of irradiance that the genotype I214 had a significantly higher maximum slope of stomatal closing ($SL_{max,d}$) but not $SL_{max,i}$ compared to the other genotypes both as a response to irradiance and VPD. Moreover, the parameters τ_d and λ_d in the VPD response were significantly higher in the two *Populus nigra* genotypes, indicating a trend of a slower stomatal response despite having a higher magnitude of g_s change compared to the two *P. euramericana* clones. This trend on closing parameters is consistent with the literature because previous investigations on poplar genotypes also found significant differences in the speed of stomatal closure to an increase in VPD and similar stomatal opening dynamics to either to an increase in blue or red light (Dumont *et al.*, 2013). Significant variability among species in irradiance or VPD-induced stomatal dynamics also have been found previously over a wide diversity of taxa, lifeforms and ecologies (Grantz & Zeiger, 1986; Elliott-Kingston *et al.*, 2016; Mc Ausland *et al.*, 2016; Males & Griffiths, 2017; Kardiman & Ræbild, 2018) suggesting species-specific mechanisms of stomatal dynamics. It should be noted that λ is not related to the magnitude of g_s change and thus will always induce a longer g_s response. On the contrary stomatal dynamics differing in SL_{max} and τ only (same g_s magnitude and λ) will result in a marginal amount of water saved overall, given the sigmoidal nature of the stomatal response. The higher amount of water lost in the first part of the curve will be balanced mostly by the lower amount of water lost in the late part of the curve. Thus, λ is the main parameter contributing to the variation in the amount of water lost. These considerations could contribute to the observed similar *E* among the hybrid poplar genotypes despite them having considerable differences in SL_{max} but not λ whereas the two *P. nigra* genotypes show a higher *E*.

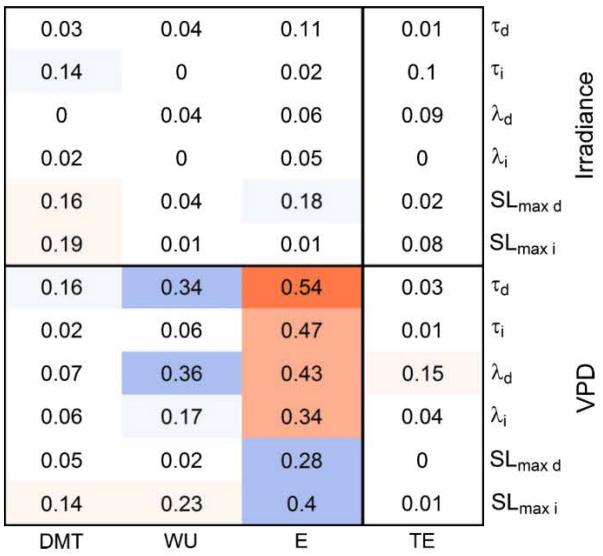

Fig. 6 Correlation matrix between dynamic parameters of stomatal conductance to water vapour (g_s) response to a decrease or an increase of irradiance or vapour-pressure deficit (VPD) and whole-plant growth traits during the drought period for two *Populus deltoides* × *nigra* (Carpaccio and I214) and two *Populus nigra* genotypes (6J29 and N38). Subscripts $_d$ and $_i$ are (respectively) for stomatal closing and opening to irradiance or VPD. Partial R^2 of the residual variability once the treatment effect is accounted for are shown ($n = 24$). Correlations were considered significant at $P < 0.05$ and are highlighted in orange or blue for positive and negative relationships, respectively. White cells are nonsignificant correlations. *DMT*, total dry mass increments; *WU*, cumulated water use; *E*, average daily whole-plant transpiration per square metre, *TE*, transpiration efficiency. τ, λ and SL_{max} are parameters of the sigmoidal model.

Water availability altered stomatal dynamics

Under drought, we observed a trend of increasing τ_d and decreasing $SL_{max,d}$ as a result of an irradiance change, the latter being only significant in I214. Additionally, for the irradiance response, λ_d was almost doubled for all genotypes. Several accounts on crops and trees reported a reduced stomatal closing time and either an increased or a decreased stomatal opening time with increasing leaf water potential (Davies & Kozlowski, 1975; Barradas *et al.*, 1994), SWC (Gerardin *et al.*, 2018; Haworth *et al.*, 2018) and in drier climates (Vico *et al.*, 2011). It has been hypothesized that a faster stomatal closure would prevent unnecessary water loss when conditions become unfavourable (Davies & Kozlowski, 1975). This appears contrary to our results despite some studies being difficult to compare as response times give an incomplete picture of the full g_s response that includes time, magnitude and speed. Poplars are mostly restricted to riparian ecosystems where water availability is rarely limited. Species sensitive to drought might lack the ability to adjust stomatal dynamics in order to track light more efficiently when water availability decreases. Despite the clear reduction of soil water content, I214 exhibited only a marginal reduction of operating g_s and *E* (Figs 1, 2). Although not much is known about the water use of I214, similar daily water use was reported on individuals growing over a mean water table of 1.45 or 3.54 m deep (Muller & Lambs, 2009). Furthermore, λ may be related to the initial perception and signalization of the changing environmental condition, whereas τ and SL_{max} relate to the actual speed at which guard cells modify their aperture by solutes and water movements as suggested by Gerardin *et al.* (2018). Following this assumption would lead to conclude that under drought poplar genotypes exhibit a delayed activation of mechanisms during stomatal closure when irradiance is decreasing.

As for the VPD-induced stomatal dynamics, I214 had a $SL_{max,d}$ halved following a rise in VPD under drought compared to the control, whereas τ_d doubled even though the magnitude of the g_s response was smaller than in the control treatment. Unlike N38 which had a lower τ_d under drought due to a lower magnitude of g_s change. Under fluctuating irradiance a slowly adjusting g_s can be beneficial by limiting the cost of stomatal opening and maintaining high conductance when conditions return to high light (Vico *et al.*, 2011). However, changes of VPD are usually slow and steady over several hours. A slow stomatal response could mean that the plant is rarely synchronized with its environment, always lagging behind. In angiosperms, stomatal response to VPD has been linked to both a passive hydraulic and actively regulated abscissic acid response (Assmann *et al.*, 2000; Peak &

Mott, 2011; Mc Adam & Brodribb, 2015). The trend of increasing λ_i in both *P. nigra* genotypes, whereas τ_i is reduced in 6J29 but increased in N38, suggests genotype-dependent mechanisms of stomatal control.

Stomatal dynamics are linked with their morphologies

Drake *et al.* (2013) proposed the idea that smaller stomata could have faster response times than larger stomata because of their greater membrane surface area : volume ratio. In our study, faster stomata were associated with higher *SD*, *SI* and lower *AGC*, thus corroborating Drake's observations. There is, however, no consensus over a definite negative correlation between stomatal size and speed in the current literature (Drake *et al.*, 2013; Elliott-Kingston *et al.*, 2016; Haworth *et al.*, 2016; Mc Ausland *et al.*, 2016; Gerardin *et al.*, 2018; Kardiman & Ræbild, 2018; Xiong *et al.*, 2018). There is a number of reasons why such correlations might not be detected. Other factors can influence stomatal movements such as guard cell geometry, osmotic shuttling, mechanical advantage and stomatal spacing (Franks & Farquhar, 2007; Dow *et al.*, 2014). In the present study, *SI* was strongly negatively correlated with stomatal closing time on both sides of the leaf and for both irradiance and VPD responses. Similar results were found in *Nicotiana tabacum* grown under shade or drought conditions (Gerardin *et al.*, 2018) suggesting that stomatal response speed could also be influenced by the number of epidermal cells around the guard cells. Stomata surrounded by only a few epidermal cells could experience a reduced epidermal cell turgor pressure than stomata surrounded by a higher number of epidermal cells. Lastly, the underlying assumption behind Drake's hypothesis that solute fluxes through the guard cell walls are uniform when normalized to surface area across species is arguable (Lawson & Blatt, 2014; Raven, 2014). Because stomatal response to irradiance and VPD have different dynamics (Dumont *et al.*, 2013; Haworth *et al.*, 2018) and were mostly uncorrelated in our study, the suspected link between stomatal size and speed may depend on the environmental change. It could, for example, play a major role in the passive hydraulic response to VPD. If, as Drake suggested, size is a driver of variation in stomatal speed, the speed of guard cell movement (i.e. aperture change) but not necessarily the speed of g_s (depending on *SD*) change should be negatively correlated with stomatal size. Focusing on the speed of g_s change only could lead to inaccurate conclusions. We found a range of *SD* and τ for which one species shows a faster stomatal aperture change but a slower g_s change compared to the other, considering a fixed step change of g_s, pore depth and λ (Fig. 7), suggesting that the speed of guard cell movement can be decoupled from the speed of g_s change. Indeed, smaller, more numerous stomata could show a higher SL_{max} for the same change in aperture compared with larger, fewer stomata because of their higher *SD*. Similarly, given an equal speed of aperture change, fewer and larger stomata will have a bigger aperture. For a similar change in g_s, they will be required to reduce their aperture further than more numerous smaller stomata which will increase τ and reduce SL_{max}. Thus, where possible, future research should account for *SD* when assessing differences in stomatal dynamics.

Stomatal dynamics are linked with productivity and water use

It has been suggested that faster stomatal dynamics, by allowing a better tracking of the surrounding environmental conditions,

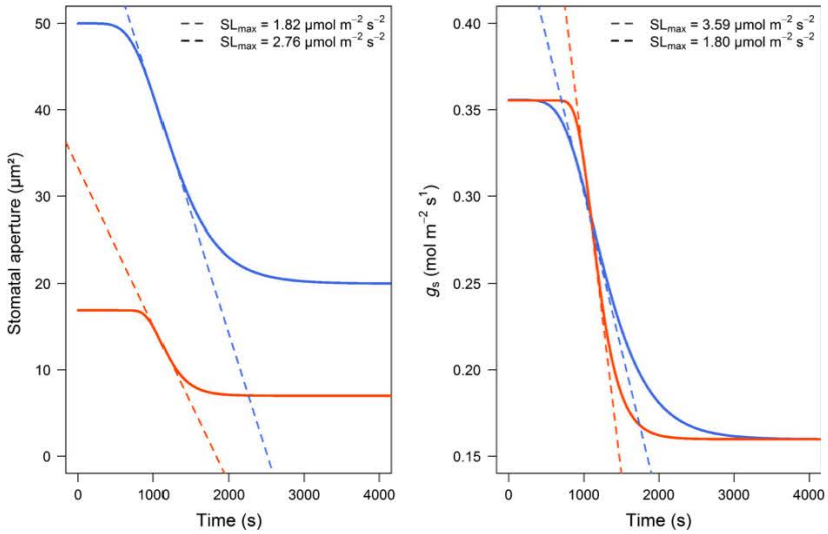

Fig. 7 Simulation of the dynamics of stomatal aperture and stomatal conductance (g_s) reduction for two hypothetical species (blue and orange straight lines) during stomatal closing. Maximum slopes of aperture or g_s change are shown in dashed lines. Both species have identical starting and ending g_s (from 0.355 to 0.160 mol m^{-2} s^{-1}), λ (100 s) and pore depth (5 µm). Stomatal density is 150 and 65 mm^{-2} and τ (time constant of the sigmoidal model) is 200 and 400 s, respectively, for the orange and blue species. Note the faster rate of stomatal aperture reduction and the slower rate of g_s reduction in the blue species compared to the orange one.

may limit water loss and maximize carbon gain (Knapp & Smith, 1990; Vico *et al.*, 2011). In agreement with this idea, we found *E* tended to be positively correlated with stomatal response times and negatively with speed of g_s change, which was more pronounced during stomatal closing than opening. This is to our knowledge the first instance of a reported correlation between whole-plant transpiration and stomatal dynamics, highlighting the need to account for g_s dynamics in order to accurately model water use from leaf gas exchange data. Moreover, we found weak positive correlations between SL_{max} and *DMT*. However, genotypes with a higher *DMT* also had a higher *TLA* and *WU*. Both also were negatively correlated with VPD-related stomatal response times. This points to others factors being primarily responsible for differences in whole-plant biomass production and water use between genotypes. In particular, the meteorological conditions notably drove the variations of transpiration. More work is needed to confirm if similar results would have been reached under different environments (e.g. in natural conditions).

In conclusion, our findings showed significant genotypic differences in stomatal dynamics related to changes of both irradiance and VPD which add to previous investigations highlighting the wide inter- and intraspecific diversity of stomatal dynamics across many vascular plants. We found the VPD response to be slower than irradiance, which could result from the slower variation of VPD in natural conditions compared to irradiance. However, this result should be taken cautiously because accurate comparisons between stresses should account for different stress levels. Soil water deficit altered stomatal dynamics differently among poplar genotypes, but overall had a slow-down effect on stomatal response to changes of irradiance and VPD. By contrast to previous findings showing a faster stomatal response to an increased soil water deficit in drought-tolerant species, our findings draw attention to a potentially detrimental effect in drought-sensitive species. It also adds to recent findings showing a diversity of stomatal dynamics with different light acclimation during growth (Matthews *et al.*, 2018). This calls for further investigations on the variability over time, environmental change, growth conditions and canopy layers of such dynamics measurement among individual plants. Although our results showed significant correlations between stomatal response speed and morphology, further research investigating a potential link between stomatal size and speed should focus on the speed of stomatal aperture change as *SD* drives the magnitude of aperture change and thus also the speed of the g_s response. Finally, although higher whole-plant transpiration was associated with slower stomatal response to VPD, the contribution of leaf-level stomatal dynamics is one of many factors governing whole-plant water use and carbon gain.

Acknowledgements

This work was conducted in the frame of the WATBIO (Development of improved perennial biomass crops for water-stressed environments), a collaborative research project funded from the European Union's Seventh Programme for research, technological development and demonstration under grant agreement no. 311929. The research received funding from the French National Research Agency through the Laboratory of Excellence ARBRE (ANR-12- LABXARBRE-01). MD received a PhD scholarship from the Région Lorraine and EFPA (INRA research department). We thank the nursery of Guéméné Penfao for providing the euramerican poplar cuttings. The authors acknowledge Marc Villar and Catherine Bastien from the UR0588-INRA Unit for access to the referenced *Populus nigra* clones 6J29 and N38. Lastly, we want to thank the editor and the three reviewers for their conscientious effort in helping improving our manuscript. The authors declare that the research was conducted in the absence of any commercial or financial relationships that could be construed as a potential conflict of interest.

Author contributions

MD, CB and DLT contributed to the data collection; MD, OB and DLT contributed to the experimental design, data analysis and interpretation as well as the writing of the manuscript.

ORCID

Oliver Brendel https://orcid.org/0000-0003-3252-0273
Maxime Durand https://orcid.org/0000-0002-8991-3601
Didier Le Thiec https://orcid.org/0000-0002-4204-551X

References

Assmann SM, Snyder JA, Lee YRJ. 2000. ABA-deficient (aba1) and ABA-insensitive (abi1-1, abi2-1) mutants of *Arabidopsis* have a wild-type stomatal response to humidity. *Plant, Cell & Environment* **23**: 387–395.

Barradas VL, Jones HG, Clark JA. 1994. Stomatal responses to changing irradiance in *Phaseolus vulgaris* L. *Journal of Experimental Botany* **45**: 931–936.

de Boer HJ, Price CA, Wagner-Cremer F, Dekker SC, Franks PJ, Veneklaas EJ. 2016. Optimal allocation of leaf epidermal area for gas exchange. *New Phytologist* **210**: 1219–1228.

Chen SL, Wang SS, Altman A, Huttermann A. 1997. Genotypic variation in drought tolerance of poplar in relation to abscisic acid. *Tree Physiology* **17**: 797–803.

Condon AG, Richards RA, Rebetzke GJ, Farquhar GD. 2004. Breeding for high water-use efficiency. *Journal of Experimental Botany* **55**: 2447–2460.

Coopman RE, Jara JC, Bravo LA, Sáez KL, Mella GR, Escobar R. 2008. Changes in morpho-physiological attributes of *Eucalyptus globulus* plants in response to different drought hardening treatments. *Electronic Journal of Biotechnology* **11**: 30–39.

Cowan IR, Farquhar GD. 1977. Stomatal function in relation to leaf metabolism and environment. *Symposia of the Society for Experimental Biology* **31**: 471–505.

Dai AG. 2011. Drought under global warming: a review. *Wiley Interdisciplinary Reviews-Climate Change* **2**: 45–65.

Damour G, Simonneau T, Cochard H, Urban L. 2010. An overview of models of stomatal conductance at the leaf level. *Plant, Cell & Environment* **33**: 1419–1438.

Davies WJ, Kozlowski TT. 1975. Stomatal responses to changes in light intensity as influenced by plant water stress. *Forest Science* **21**: 129–133.

Dow GJ, Berry JA, Bergmann DC. 2014. The physiological importance of developmental mechanisms that enforce proper stomatal spacing in *Arabidopsis thaliana*. *New Phytologist* **201**: 1205–1217.

Drake PL, Froend RH, Franks PJ. 2013. Smaller, faster stomata: scaling of stomatal size, rate of response, and stomatal conductance. *Journal of Experimental Botany* **64**: 495–505.

Dumont J, Cohen D, Gerard J, Jolivet Y, Dizengremel P, Le Thiec D. 2014. Distinct responses to ozone of abaxial and adaxial stomata in three Euramerican poplar genotypes. *Plant, Cell & Environment* **37**: 2064–2076.

Dumont J, Spicher F, Montpied P, Dizengremel P, Jolivet Y, Le Thiec D. 2013. Effects of ozone on stomatal responses to environmental parameters (blue light, red light, CO_2 and vapour pressure deficit) in three *Populus deltoides* x *Populus nigra* genotypes. *Environmental Pollution* **173**: 85–96.

Elliott-Kingston C, Haworth M, Yearsley JM, Batke SP, Lawson T, McElwain JC. 2016. Does size matter? Atmospheric CO_2 may be a stronger driver of stomatal closing rate than stomatal size in taxa that diversified under low CO_2. *Frontiers in Plant Science* **7**: 1253.

FAO. 2018. Quantifying the contributions of forests to the sustainable development goals. Chapter 2. In: Muller E, Kushlin A, Linhares-Juvenal T, Muchoney D, Wertz-Kanounnikoff S, Henderson-Howat D, eds. *The state of the world's forests*. Rome, Italy: FAO, 7–72.

Farquhar GD, Richards RA. 1984. Isotopic composition of plant carbon correlates with water-use efficiency of wheat genotypes. *Functional Plant Biology* **11**: 539–552.

Franks PJ, Farquhar GD. 2001. The effect of exogenous abscisic acid on stomatal development, stomatal mechanics, and leaf gas exchange in *Tradescantia virginiana*. *Plant Physiology* **125**: 935–942.

Franks PJ, Farquhar GD. 2007. The mechanical diversity of stomata and its significance in gas-exchange control. *Plant Physiology* **143**: 78–87.

Gerardin T, Douthe C, Flexas J, Brendel O. 2018. Shade and drought growth conditions strongly impact dynamic responses of stomata to variations in irradiance in *Nicotiana tabacum*. *Environmental and Experimental Botany* **153**: 188–197.

Giovannelli A, Deslauriers A, Fragnelli G, Scaletti L, Castro G, Rossi S, Crivellaro A. 2007. Evaluation of drought response of two poplar clones (*Populus* x *canadensis* Monch 'I-214' and *P-deltoides* Marsh. 'Dvina') through high resolution analysis of stem growth. *Journal of Experimental Botany* **58**: 2673–2683.

Grantz DA, Zeiger E. 1986. Stomatal responses to light and leaf-air water-vapor pressure difference show similar kinetics in sugarcane and soybean. *Plant Physiology* **81**: 865–868.

Haworth M, Killi D, Materassi A, Raschi A, Centritto M. 2016. Impaired stomatal control is associated with reduced photosynthetic physiology in crop species grown at elevated CO_2. *Frontiers in Plant Science* **7**: 1568–1581.

Haworth M, Marino G, Cosentino SL, Brunetti C, De Carlo A, Avola G, Riggi E, Loreto F, Centritto M. 2018. Increased free abscisic acid during drought enhances stomatal sensitivity and modifies stomatal behaviour in fast growing giant reed (*Arundo donax* L.). *Environmental and Experimental Botany* **147**: 116–124.

IPCC. 2014. Summary for policy makers. In: Meyer L, Brinkman S, van Kesteren L, Leprince-Ringuet N, van Boxmeer F, eds. *Climate change 2014: synthesis report. Contribution of working groups I, II and III to the fifth assessment report of the intergovernmental panel on climate change*. Geneva, Switzerland: Cambridge University Press, 7.

Kaiser H, Kappen L. 2000. *In situ* observation of stomatal movements and gas exchange of *Aegopodium podagraria* L. in the understorey. *Journal of Experimental Botany* **51**: 1741–1749.

Kardiman R, Ræbild A. 2018. Relationship between stomatal density, size and speed of opening in Sumatran rainforest species. *Tree Physiology* **38**: 696–705.

Knapp AK, Smith WK. 1990. Stomatal and photosynthetic responses to variable sunlight. *Physiologia Plantarum* **78**: 160–165.

Lawson T, Blatt MR. 2014. Stomatal size, speed, and responsiveness impact on photosynthesis and water use efficiency. *Plant Physiology* **164**: 1556–1570.

Lawson T, Vialet-Chabrand S. 2019. Speedy stomata, photosynthesis and plant water use efficiency. *New Phytologist* **221**: 93–98.

Males J, Griffiths H. 2017. Specialized stomatal humidity responses underpin ecological diversity in C_3 bromeliads. *Plant, Cell & Environment* **40**: 2931–2945.

Matthews JSA, Vialet-Chabrand S, Lawson T. 2018. Acclimation to fluctuating light impacts the rapidity of response and diurnal rhythm of stomatal conductance. *Plant Physiology* **176**: 1939–1951.

McAdam SAM, Brodribb TJ. 2015. The evolution of mechanisms driving the stomatal response to vapor pressure deficit. *Plant Physiology* **167**: 833–843.

McAusland L, Vialet-Chabrand S, Davey P, Baker NR, Brendel O, Lawson T. 2016. Effects of kinetics of light-induced stomatal responses on photosynthesis and water-use efficiency. *New Phytologist* **211**: 1209–1220.

Monclus R, Dreyer E, Delmotte FM, Villar M, Delay D, Boudouresque E, Petit JM, Marron N, Brechet C, Brignolas F. 2005. Productivity, leaf traits and carbon isotope discrimination in 29 *Populus deltoides* x *P-nigra* clones. *New Phytologist* **167**: 53–62.

Monclus R, Dreyer E, Villar M, Delmotte FM, Delay D, Petit JM, Barbaroux C, Le Thiec D, Brechet C, Brignolas F. 2006. Impact of drought on productivity and water use efficiency in 29 genotypes of *Populus deltoides* x *Populus nigra*. *New Phytologist* **169**: 765–777.

Muller E, Lambs L. 2009. Daily variations of water use with vapor pressure deficit in a plantation of I214 poplars. *Water* **1**: 32–42.

Peak D, Mott KA. 2011. A new, vapour-phase mechanism for stomatal responses to humidity and temperature. *Plant, Cell & Environment* **34**: 162–178.

Qu MN, Hamdani S, Li WZ, Wang SM, Tang JY, Chen Z, Song QF, Li M, Zhao HL, Chang TG *et al.* 2016. Rapid stomatal response to fluctuating light: an under-explored mechanism to improve drought tolerance in rice. *Functional Plant Biology* **43**: 727–738.

R Core Team. 2017. *R: a language and environment for statistical computing*. Vienna, Austria: R Foundation for Statistical Computing. [WWW document] URL https://www.R-project.org/ [accessed 2018].

Raven JA. 2014. Speedy small stomata? *Journal of Experimental Botany* **65**: 1415–1424.

Rayment MB, Loustau D, Jarvis PG. 2000. Measuring and modeling conductances of black spruce at three organizational scales: shoot, branch and canopy. *Tree Physiology* **20**: 713–723.

Sheffield J, Wood EF. 2008. Projected changes in drought occurrence under future global warming from multi-model, multi-scenario, IPCC AR4 simulations. *Climate Dynamics* **31**: 79–105.

Stegemann J, Timm H-C, Küppers M. 1999. Simulation of photosynthetic plasticity in response to highly fluctuating light: an empirical model integrating dynamic photosynthetic induction and capacity. *Trees* **14**: 145–160.

Sternberg T. 2011. Regional drought has a global impact. *Nature* **472**: 169.

Tschaplinski TJ, Blake TJ. 1989. Water relations, photosynthetic capacity, and root shoot partitioning of photosynthates as determinants of productivity in hybrid poplar. *Canadian Journal of Botany* **67**: 1689–1697.

Vialet-Chabrand S, Dreyer E, Brendel O. 2013. Performance of a new dynamic model for predicting diurnal time courses of stomatal conductance at the leaf level. *Plant, Cell & Environment* **36**: 1529–1546.

Vico G, Manzoni S, Palmroth S, Katul G. 2011. Effects of stomatal delays on the economics of leaf gas exchange under intermittent light regimes. *New Phytologist* **192**: 640–652.

Viger M, Smith HK, Cohen D, Dewoody J, Trewin H, Steenackers M, Bastien C, Taylor G. 2016. Adaptive mechanisms and genomic plasticity for drought tolerance identified in European black poplar (*Populus nigra* L.). *Tree Physiology* **36**: 909–928.

Wong SC, Cowan IR, Farquhar GD. 1979. Stomatal conductance correlates with photosynthetic capacity. *Nature* **282**: 424–426.

Xiong D, Douthe C, Flexas J. 2018. Differential coordination of stomatal conductance, mesophyll conductance and leaf hydraulic conductance in response to changing light across species. *Plant, Cell & Environment* **41**: 436–450.

Supporting Information

Additional Supporting Information may be found online in the Supporting Information section at the end of the article.

Fig. S1 Relative extractable water inside the pots during the drought experiment.

Fig. S2 Summary of the parameters derived from a sigmoidal adjustment of a change in stomatal conductance.

Fig. S3 Time course of stomatal conductance and fitted curves.

Fig. S4 Meteorological data in the glasshouse during the drought experiment.

Fig. S5 Drivers of whole-plant transpiration during the drought experiment as explained by a statistical model including the genotype, water treatment, potential evapotranspiration and day of the year effect.

Fig. S6 Sigmoidal adjustments used to derive the parameters τ, λ, SL_{max} and the magnitude of irradiance-induced stomatal conductance change for the four poplar genotypes, Carpaccio, I214, 6J29 and N38.

Fig. S7 Sigmoidal adjustments used to derive the parameters τ, λ, SL_{max} and the magnitude of VPD-induced stomatal conductance change for the four poplar genotypes, Carpaccio, I214, 6J29 and N38.

Fig. S8 Correlations between dynamic parameters of g_s response to a decrease or an increase of VPD and either stomatal morphological parameters or average daily whole-plant transpiration.

Table S1 Summary of parameters referred to within the text and their units.

Table S2 Information on the four genotypes used in the study.

Table S3 Growth, biomass production and water use of the four poplar genotypes, Carpaccio, I214, 6J29 and N38 before the drought.

Table S4 Dataset used for statistical analysis.

Table S5 Steady-state values of the dynamic gas-exchange response to a decrease and increase of irradiance and VPD of the four poplar genotypes, Carpaccio, I214, 6J29 and N38.

Please note: Wiley Blackwell are not responsible for the content or functionality of any Supporting Information supplied by the authors. Any queries (other than missing material) should be directed to the *New Phytologist* Central Office.

DONNÉES SUPPLÉMENTAIRES

Table S1 Summary of parameters referred to within the text and their units.

	Definition	**Unit**
Parameters		
DMT	Total plant dry mass increment	g
TLA	Total leaf area increment	cm^2
WU	Cumulated water use during the drought	kgH_2O
E	Average daily whole plant transpiration per leaf area	$kgH_2O\ m^{-2}\ d^{-1}$
TE	Transpiration efficiency	$g\ l^{-1}$
A	Net CO_2 assimilation	$\mu mol\ m^{-2}\ s^{-1}$
g_s	Stomatal conductance to water vapor	$mol\ m^{-2}\ s^{-1}$
Wi	Intrinsic water use efficiency	$\mu mol\ mol^{-1}$
τ	Time constant of the stomatal response	s or min
λ	Lag time of the stomatal response	s or min
SL_{max}	Maximum slope of the stomatal response	$mol\ m^{-2}\ s^{-2}$
GCL	Guard cell length	µm
AGC	Guard cell area	μm^2
SD	Stomatal density	cm^{-2}
SI	Stomatal index	%
Subscripts		
d	Denote stomatal closing response to irradiance or VPD.	
i	Denote stomatal opening response to irradiance or VPD.	
ab	Specify that the parameter was measured on the abaxial side of the leaf.	
ad	Specify that the parameter was measured on the adaxial side of the leaf.	

Haworth M, Marino G, Cosentino SL, Brunetti C, De Carlo A, Avola G, Riggi E, Loreto F, Centritto M. 2018. Increased free abscisic acid during drought enhances stomatal sensitivity and modifies stomatal behaviour in fast growing giant reed (Arundo donax L.). *Environmental and Experimental Botany* **147**: 116-124.

Table S2 Information on the four genotypes used in the study.

Genotype	Species	Sex	Source of the base material	Origin	Mother	Father	Reference
Carpaccio	*Populus deltoides x nigra*	Female	Seed obtained by controlled crossing	Centro di Sperimentazione Agricola e Forestale, Via Casalotti 300, I-00166 Roma, Italy	P. deltoides '2900/958' (Stoneville 1,Mississipi, USA)	P. nigra 'Italica M' (United Kingdom)	a
I214	*Populus deltoides x nigra*	Female	Seed obtained by controlled crossing	Jacometti Giovanni, Istituzione per il Miglioramento del Pioppo, Villafranca Piemonte (TO), Italy	'canadese bianco'	'Caroliniano prodigioso' (Parco di Miradolo, Pinerolo TO, Italy)	b, c
6J29	*Populus nigra*	-	Sampling in the field	Ramière, Drôme (Rhône), France	-	-	d, e
N38	*Populus nigra*	-	Sampling in the field	Ticino (Po), Italy	-	-	e

a: **Gras M.A., Mughini G. 1988.** Osservazioni sul comportamento produttivo di alcuni cloni di Populus x euramericana di recente selezione in Italia centrale. Informatore Agrario. **49**(64) : 45-47

b: **Jacometti G. 1937.** I nuovi pioppi italiani. Atti del convegno di pioppicoltori in Casale Monferrato (11 luglio1937). Comitato Nazionale Forestale, Roma. 39-50

c: **Ministère de l'Agriculture et de l'Alimentation. 2008.** Conseils d'utilisation des ressources génétiques forestières: Populus ssp. – Peupliers cultivés. [WWW document] URL http://agriculture.gouv.fr/sites/minagri/files/documents//Peupliers2008.pdf/ [accessed 24 October 2011].

d: **Chamaillard S. 2011.** Efficience d'utilisation de l'eau chez le peuplier noir (Populus nigra L.) : variabilité et plasticité en réponse aux variations de l'environnement. PhD thesis, Université d'Orléans, Orléans, France.

e: **Viger M, Smith HK, Cohen D, Dewoody J, Trewin H, Steenackers M, Bastien C, Taylor G. 2016.** Adaptive mechanisms and genomic plasticity for drought tolerance identified in European black poplar (Populus nigra L.). *Tree Physiology* **36**(7): 909-928.

Table S3 Growth, biomass production and water use of two *Populus deltoides* × *nigra* (Carpaccio and I214) and two *Populus nigra* genotypes (6J29 and N38) before the drought. Values reported are means ± standard deviation (n = 6). ANOVA factors were considered significant when $p < 0.05$. Letters show significant differences by post-hoc contrasts among the eight groups (4 genotypes + 2 water treatments). DMT, DML, DMS, DMR and TE were measured on separate individuals harvested before the drought.

Genotype	Treatment	H (cm)	D (mm)	DMT (g)	DML (g)	DMS (g)	DMR (g)	WU (kgH_2O)	E ($kgH_2O\ m^{-2}\ d^{-1}$)	TLA (cm^2)	TE ($g.l^{-1}$)
Carpaccio	control	127.1 ± 8.1 a	10.1 ± 0.9 a	80.97 ± 5.24 a	34.34 ± 5.28 a	32.18 ± 1.64 a	14.46 ± 1.68 a	12.6 ± 1.6 a	2.2 ± 0.1 bcd	3183 ± 323 a	5.37 ± 0.37 a
	drought	128.2 ± 6.1 a	10.2 ± 0.9 a					13.7 ± 0.7 a	2.2 ± 0.1 bc	3282 ± 270 a	
I214	control	110.9 ± 4.2 b	10.2 ± 0.8 a	63.85 ± 3.19 b	22.59 ± 1.36 b	24.23 ± 1.41 b	17.02 ± 0.64 a	9.9 ± 1.1 b	2 ± 0.2 d	2495 ± 477 b	5.48 ± 0.23 a
	drought	108.2 ± 4.9 b	9.6 ± 1.2 ab					10.0 ± 0.6 b	2.1 ± 0.1 cd	2485 ± 193 b	
6J29	control	93.3 ± 4 c	8.2 ± 0.4 c	25.16 ± 4.59 c	11.14 ± 2.27 c	9.09 ± 2.01 c	4.92 ± 1.11 b	5.8 ± 1.0 c	3.2 ± 0.4 a	1121 ± 209 cd	3.71 ± 0.19 c
	drought	91.8 ± 4.6 c	7.7 ± 0.6 c					5.5 ± 0.5 c	3 ± 0.2 a	988 ± 89 d	
N38	control	80.8 ± 9.1 d	8.1 ± 0.7 c	29.09 ± 6.13 c	13.55 ± 2.52 c	9.98 ± 2.19 c	5.57 ± 1.66 b	5.3 ± 1.0 c	2.1 ± 0.1 cd	1290 ± 189 cd	4.25 ± 0.29 b
	drought	80.7 ± 5.8 d	8.6 ± 0.6 bc					6.0 ± 0.5 c	2.4 ± 0.1 b	1352 ± 178 c	
P value	Genotype	<0.001	<0.001	<0.001	<0.001	<0.001	<0.001	<0.001	<0.001	<0.001	<0.001
	Treatment	ns	ns					ns	ns	ns	
	Interaction	ns	ns					ns	ns	ns	

H, plant height; D, main stem diameter; DMT, total dry mass; DML, leaf dry mass; DMS, stem dry mass; DMR, root dry mass; WU, cumulated water use; TLA, total leaf area; E, average daily transpiration per unit leaf area; TE, transpiration efficiency; ns, not significant.

Table S5 Steady-state values of the dynamic gas-exchange response to a decrease and increase of irradiance and VPD of the four poplar genotypes, Carpaccio, I214, 6J29 and N38 (means ± standard deviation, n = 6). Steady-states values were recorded before any change in irradiance of VPD (SS_0), after the first step change in irradiance or VPD (SS_1) and after last the step change in irradiance or VPD (SS_2). ΔSS shows statistical differences between SS_0 and SS_2 from post-hoc comparisons of a linear model including the genotype, water treatment and steady-state effect. ANOVA factors were considered significant when $p < 0.05$. Letters show significant differences by post-hoc contrast among the eight groups (4 genotypes + 2 treatments).

	Genotype	Treatment	A (µmol m^{-2} s^{-1})				g_s (mol m^{-2} s^{-1})				Wi (µmol mol^{-1})			
			SS_0	SS_1	SS_2	ΔSS	SS_0	SS_1	SS_2	ΔSS	SS_0	SS_1	SS_2	ΔSS
Irradiance	Carpaccio	control	17.6 ± 3.2 de	7.5 ± 3 ab	16.9 ± 3.4 de	ns	0.6 ± 0.08 bc	0.33 ± 0.11 b	0.55 ± 0.09 bcd	ns	29.5 ± 4 b	25.8 ± 14.4 cd	31.2 ± 7.3 b	ns
		drought	15.1 ± 3.9 e	7.4 ± 2.3 ab	15.6 ± 3.6 e	ns	0.4 ± 0.22 bc	0.15 ± 0.12 c	0.31 ± 0.19 e	ns	44.2 ± 17.3 ab	67.7 ± 36.7 ab	63.9 ± 31.4 a	ns
	I214	control	22.4 ± 0.5 abc	9.7 ± 0.8 a	21.9 ± 2 abc	ns	0.59 ± 0.17 bc	0.31 ± 0.16 b	0.73 ± 0.21 ab	ns	40.8 ± 12.7 ab	40.5 ± 24.8 bcd	33.1 ± 13.9 b	ns
		drought	18.5 ± 2.5 cde	8.4 ± 0.4 ab	18.4 ± 3.5 cde	ns	0.36 ± 0.12 c	0.11 ± 0.04 c	0.38 ± 0.1 cde	ns	54.2 ± 13.2 ab	92.2 ± 47.4 a	50.2 ± 8.4 ab	ns
	6J29	control	23.1 ± 1.1 ab	9.1 ± 1 a	22.9 ± 0.8 ab	ns	0.9 ± 0.27 a	0.61 ± 0.12 a	0.82 ± 0.17 a	ns	27.7 ± 8.3 b	15.5 ± 3.5 d	28.9 ± 5.6 b	ns
		drought	19.8 ± 3.8 bcd	8.6 ± 0.9 ab	19.2 ± 3.2 bcde	ns	0.46 ± 0.19 bc	0.17 ± 0.05 c	0.33 ± 0.1 e	ns	49.9 ± 21.2 ab	53.9 ± 16.7 bc	60.2 ± 10.6 a	ns
	N38	control	23.8 ± 3.4 a	9.3 ± 0.9 a	23.7 ± 3.7 a	ns	0.64 ± 0.18 ab	0.38 ± 0.11 b	0.57 ± 0.15 bc	ns	39.7 ± 12.9 ab	26.2 ± 6.5 cd	43.5 ± 10.3 ab	ns
		drought	20.6 ± 1.7 abcd	6.3 ± 0.4 b	20.5 ± 1.8 abcd	ns	0.37 ± 0.13 bc	0.06 ± 0.01 c	0.36 ± 0.13 de	ns	63 ± 26.6 a	100.5 ± 11.5 a	64 ± 24.1 a	ns
	p value	Genotype	<0.001	0.033	0.001		ns	0.001	ns		ns	0.017	ns	
		Treatment	0.001	0.005	0.002		<0.001	<0.001	<0.001		0.001	<0.001	<0.001	
		Interaction	ns	ns	ns		ns	0.019	ns		ns	ns	ns	
VPD	Carpaccio	control	13.6 ± 1.6 d	8.6 ± 2.5 bc	12.7 ± 1.3 cd	ns	0.24 ± 0.04 b	0.1 ± 0.03 ab	0.22 ± 0.03 b	ns	57.8 ± 11.4 ab	89.9 ± 9 bc	60.3 ± 10.4 ab	ns
		drought	12.4 ± 2.4 d	8.2 ± 1.5 bc	12 ± 1.2 d	ns	0.24 ± 0.03 b	0.09 ± 0.03 ab	0.2 ± 0.05 b	ns	52.4 ± 13.5 b	98.1 ± 20.4 abc	63.7 ± 13.1 ab	ns
	I214	control	14.9 ± 2.6 cd	5.9 ± 2.3 c	15.4 ± 1.8 bc	ns	0.29 ± 0.04 b	0.06 ± 0.03 b	0.36 ± 0.07 a	ns	52.7 ± 13.6 b	102.8 ± 9 abc	43.1 ± 4.4 b	ns
		drought	14.2 ± 2.9 d	6 ± 2.8 c	13.8 ± 4.4 cd	ns	0.18 ± 0.04 b	0.06 ± 0.04 b	0.24 ± 0.16 b	ns	79.5 ± 15 a	112.4 ± 21.6 ab	71.3 ± 27.1 ab	ns
	6J29	control	18.2 ± 2.1 bc	10.3 ± 0.9 b	15 ± 2.9 bcd	0.04	0.52 ± 0.22 a	0.13 ± 0.03 a	0.25 ± 0.03 b	<0.001	38.7 ± 11.5 b	84.1 ± 17 c	62 ± 16.1 ab	0.01
		drought	24 ± 2 a	14 ± 1.8 a	21.2 ± 2.6 a	ns	0.5 ± 0.11 a	0.13 ± 0.03 a	0.26 ± 0.04 ab	<0.001	49.6 ± 8.7 b	112.7 ± 15.5 ab	82.6 ± 8.4 a	0.001
	N38	control	21.3 ± 3 ab	10.7 ± 3.3 b	19.1 ± 2.1 a	ns	0.62 ± 0.31 a	0.1 ± 0.03 ab	0.23 ± 0.05 b	<0.001	44.1 ± 25.9 b	111.8 ± 12.3 abc	87.6 ± 28 a	<0.001
		drought	20.4 ± 5.9 ab	8.3 ± 1.9 bc	18 ± 1.8 ab	ns	0.29 ± 0.16 b	0.07 ± 0.02 b	0.25 ± 0.04 b	ns	77.8 ± 20.7 a	122.1 ± 24.2 a	72.9 ± 14.8 ab	ns
	p value	Genotype	<0.001	<0.001	<0.001		<0.001	<0.001	0.014		0.009	0.017	0.014	
		Treatment	ns	ns	ns		0.022	ns	ns		0.002	0.007	ns	
		Interaction	0.02	0.02	0.001		ns	ns	ns		0.023	ns	0.032	

A, net CO_2 assimilation; g_s, stomatal conductance to water vapor; Wi, intrinsic water use efficiency; ns, not significant.

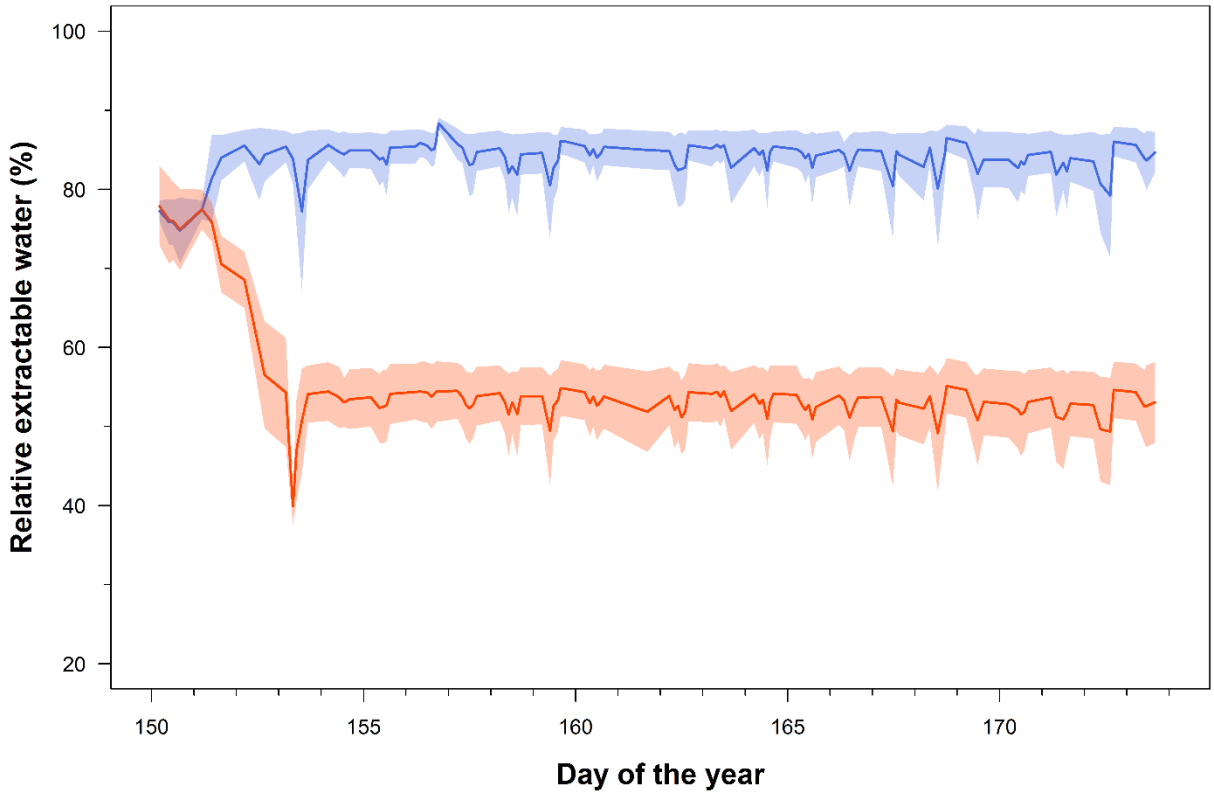

Figure S1. Relative extractable water (REW) inside the pots during the drought experiment. REW was calculated as the difference between the volumetric soil water content (SWC) in the soil and the volumetric SWC at the permanent wilting point (SWC = 3%) divided by the difference between SWC at field capacity (32.8%) and SWC at the permanent wilting point. The drought experiment started on the 151st day. The blue and orange lines are the average of control and drought-stressed trees respectively. The blue and orange areas show the standard deviation between trees.

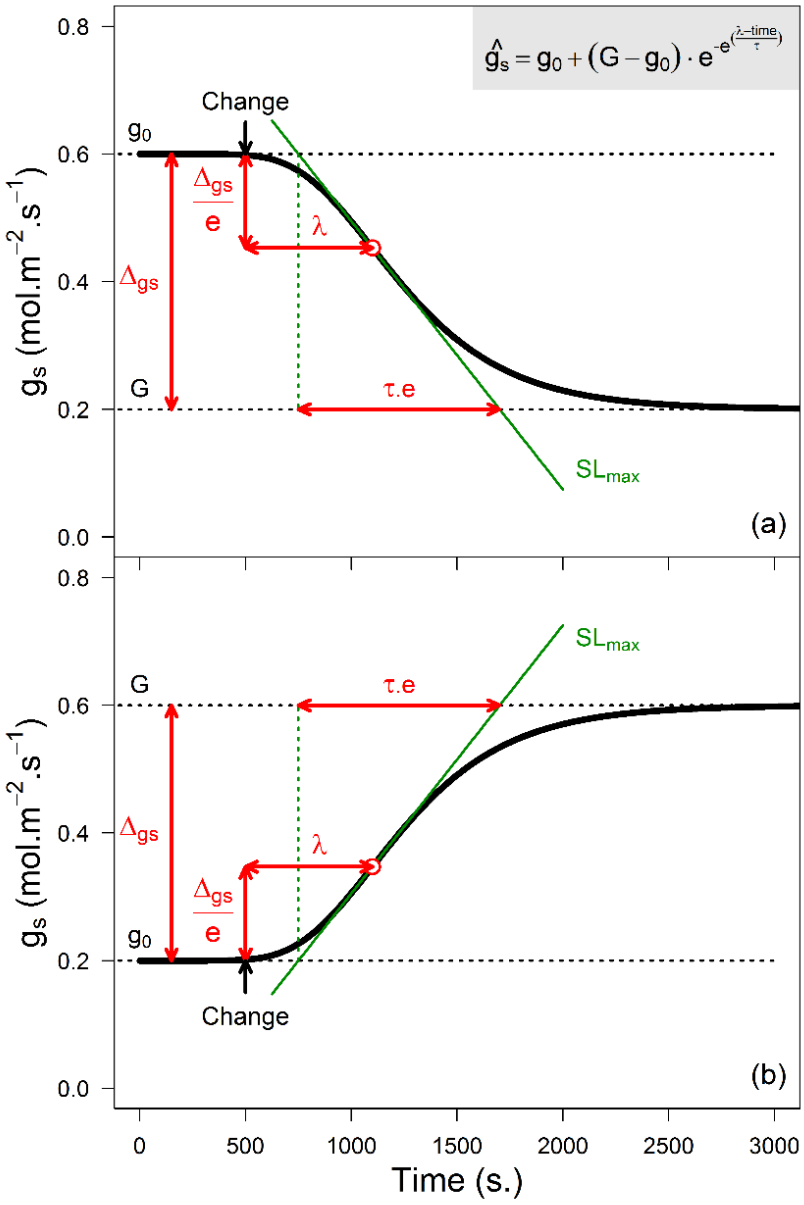

Figure S2. Summary of the parameters derived from a sigmoidal adjustment of a change in stomatal conductance. (a) Stomatal closing and (b) stomatal opening. The black arrow show the time at which either irradiance or VPD was modified. g_0 and G are the stomatal conductance values at the start and the end of the curve, respectively. Δgs is the magnitude of stomatal conductance change. λ is the time between the environmental change and the moment where the change of stomatal conductance is at a maximum (white dot). SLmax is the tangent to this point and is calculated as Δgs/(τ·e) where e ≈ 2.718. By multiplying τ and e, we find the time to get from g0 to G if the speed of change was equal to SLmax.

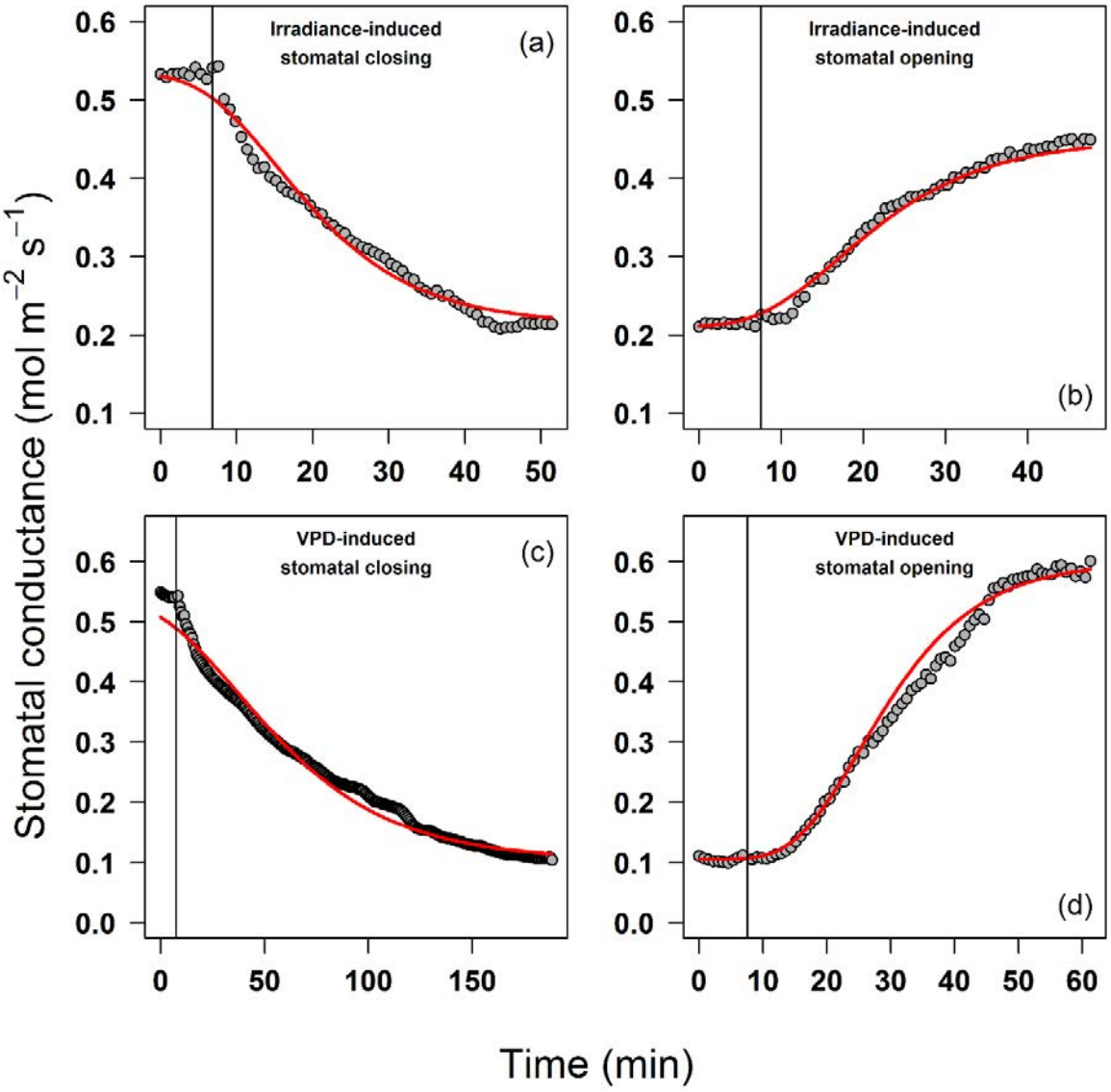

Figure S3. Time course of stomatal conductance and fitted curves. Irradiance-induced stomatal closing (**a**) and opening (**b**). VPD-induced stomatal closing (**c**) and opening (**d**). Measured stomatal conductance data is shown in gray and the fitted curve in red. The vertical line show the moment of the environmental change.

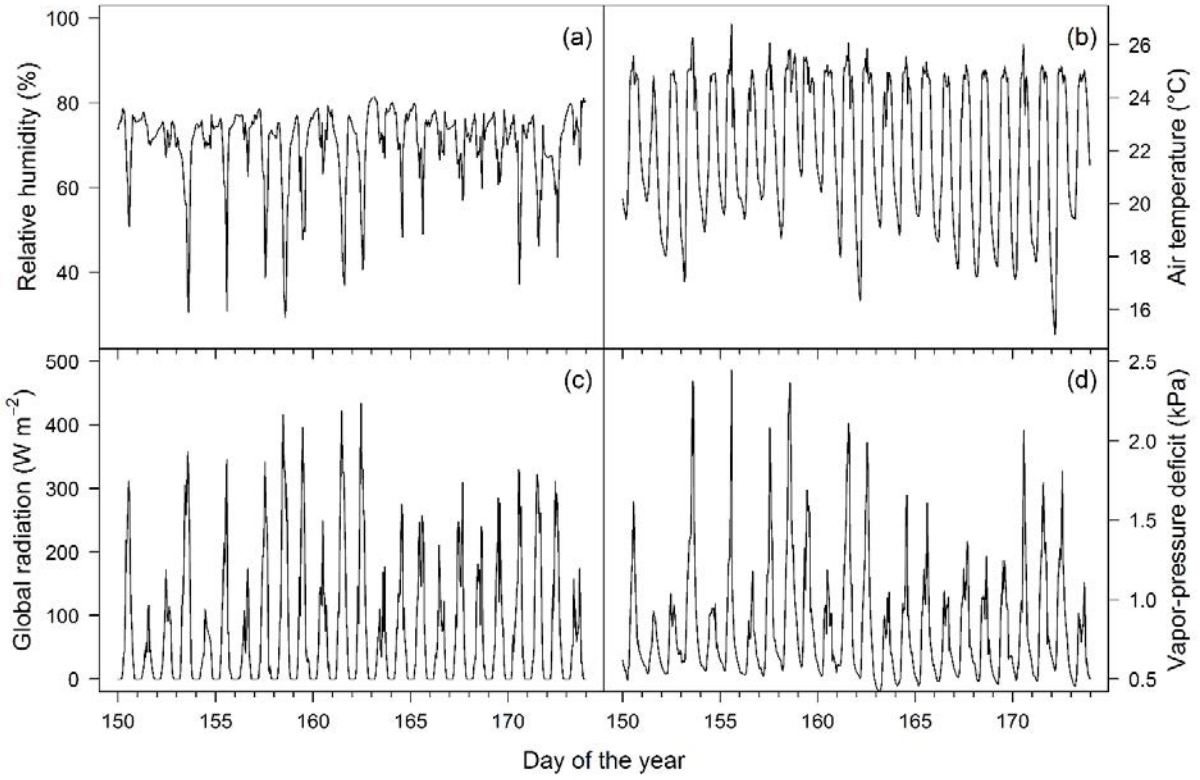

Figure S4. Meteorological data in the glasshouse during the drought experiment. (**a**) Relative humidity (%), (**b**) air temperature (°C), (**c**) global radiation (W m^{-2}), (**d**) atmospheric vapor-pressure deficit (kPa). The drought experiment started on the 151st day.

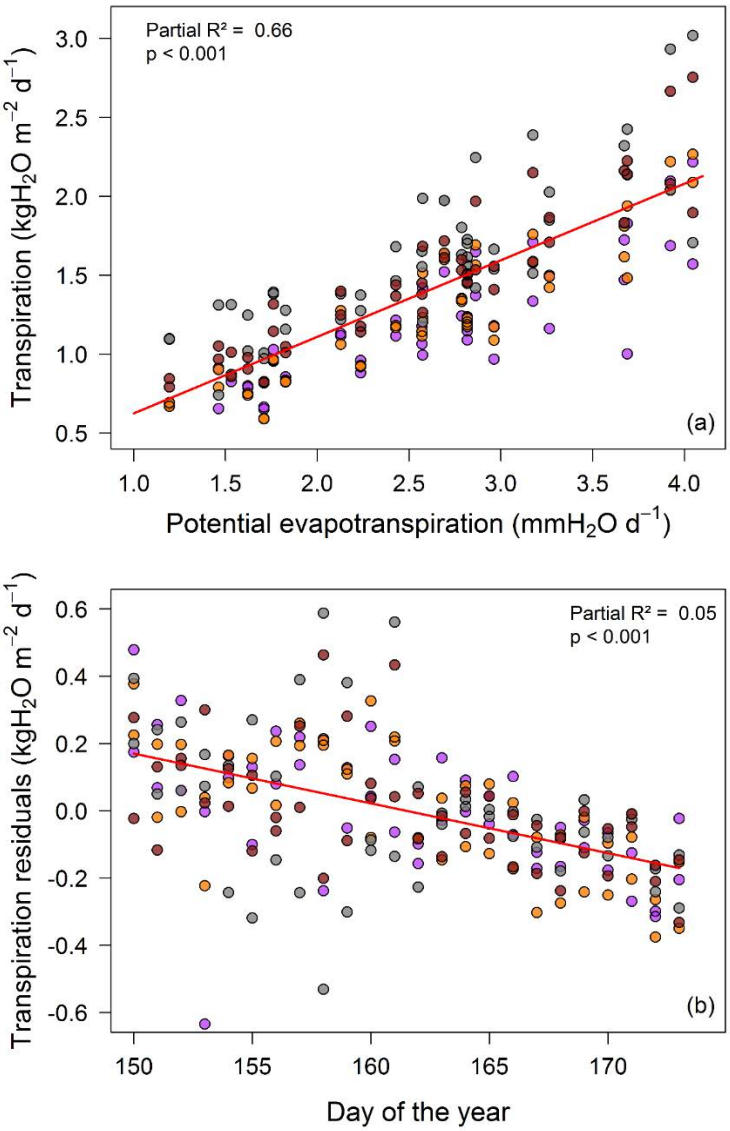

Figure S5. Drivers of whole-plant transpiration during the drought experiment as explained by a statistical model including the genotype, water treatment, potential evapotranspiration and day of the year effect. (**a**) Correlation between the daily whole-plant transpiration and potential evapotranspiration. (**b**) Correlation between the daily whole-plant transpiration residual variability once the genotype, water treatment and potential evapotranspiration effect are accounted for and the day of the year. Partial R^2 and *p* value for each effect is shown (n = 24). Correlations were considered significant at $p < 0.05$ and a regression line was drawn. Potential evapotranspiration was computed using the Penman equation following and adapted by Shuttleworth (2007) with the wind speed recorded at 0.19 m s^{-1} in the glasshouse. Purple, orange, gray and red dots are for Carpaccio, I214, 6J29 and N38 respectively.

Shuttleworth WJ. 2007. Putting the "vap" into evaporation. *Hydrol. Earth Syst. Sci.* **11**(1): 210-244.

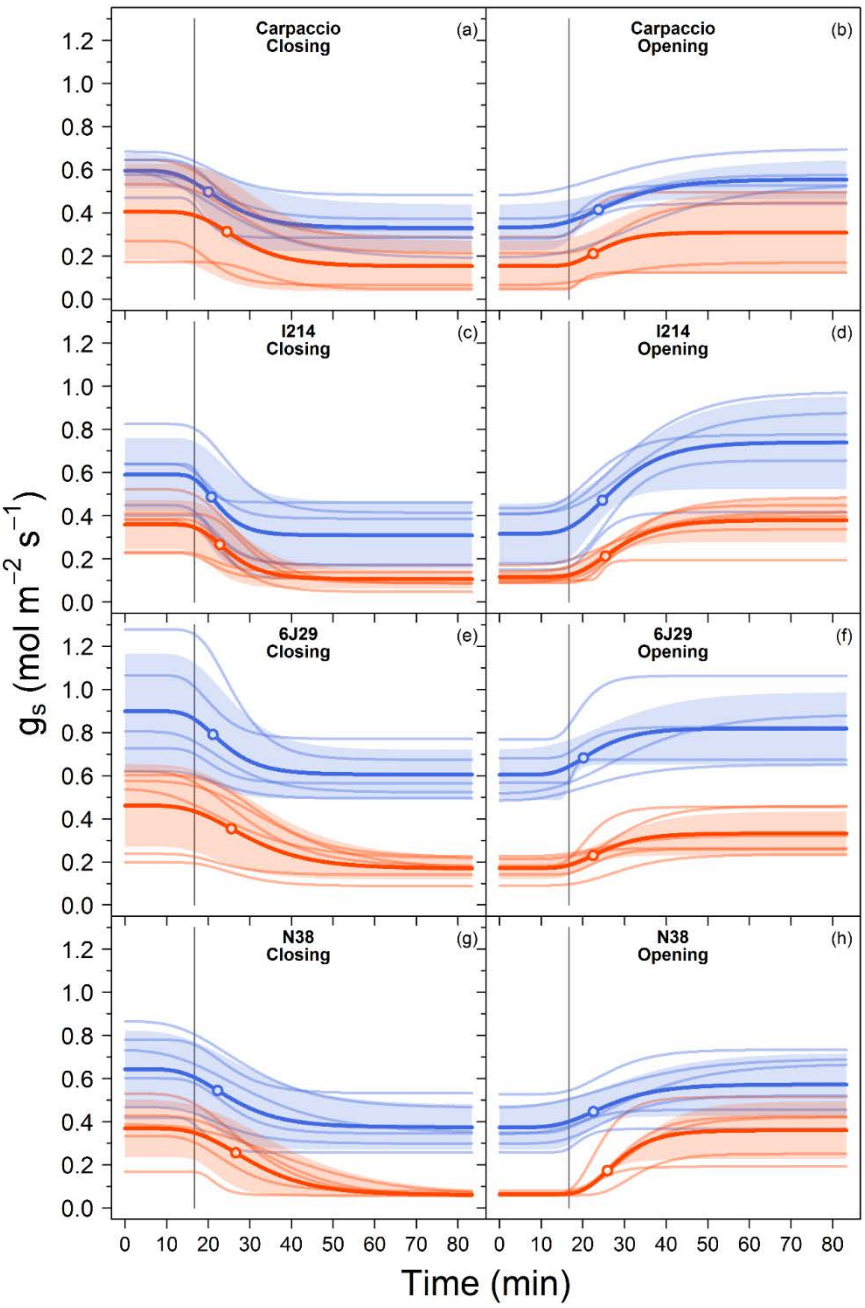

Figure S6. Sigmoidal adjustments used to derive the parameters τ, λ, SL_{max} and the magnitude of stomatal conductance change for the four poplar genotypes, Carpaccio (**a**, **b**), I214 (**c**, **d**), 6J29 (**e**, **f**) and N38 (**g**, **h**). Stomatal closing (**a**, **c**, **e**, **g**) and opening (**b**, **d**, **f**, **h**) to a decrease or an increase of irradiance, respectively. Blue and orange are for control and drought-stressed trees, respectively. The average sigmoidal response for both water treatments is drawn in bold with the colored areas showing the standard deviation. The white dot show the moment where the change in stomatal conductance is at a maximum. The vertical gray line shows when the environmental change happened.

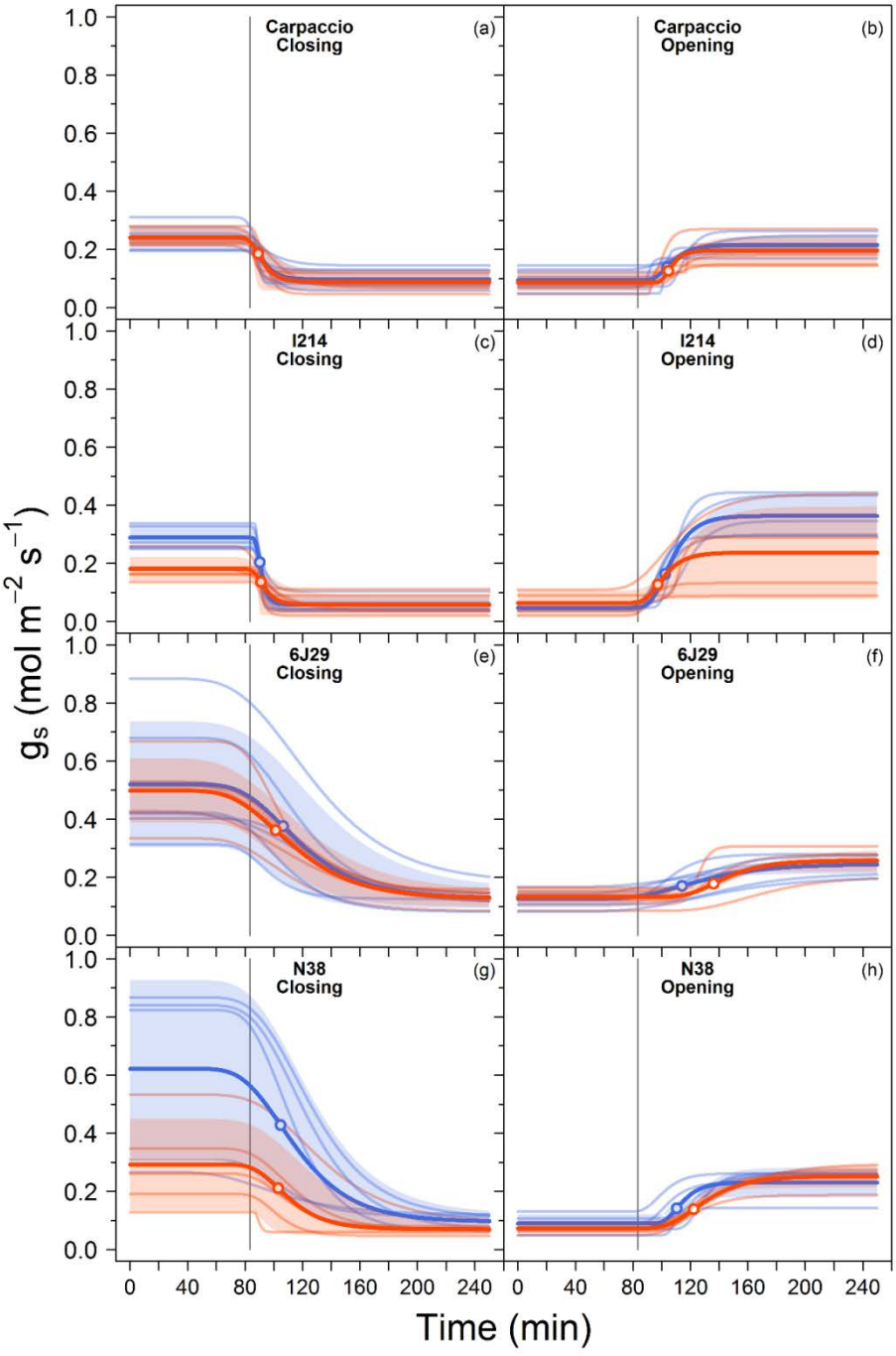

Figure S7. Sigmoidal adjustments used to derive the parameters τ, λ, SL_{max} and the magnitude of stomatal conductance change for the four poplar genotypes, Carpaccio (**a**, **b**), I214 (**c**, **d**), 6J29 (**e**, **f**) and N38 (**g**, **h**). Stomatal closing (**a**, **c**, **e**, **g**) and opening (**b**, **d**, **f**, **h**) to an increase or a decrease of VPD, respectively. Blue and orange are for control and drought-stressed trees, respectively. The average sigmoidal response for both water treatments is drawn in bold with the colored areas showing the standard deviation. The white dot show the moment where the change in stomatal conductance is at a maximum. The vertical gray line shows when the environmental change happened.

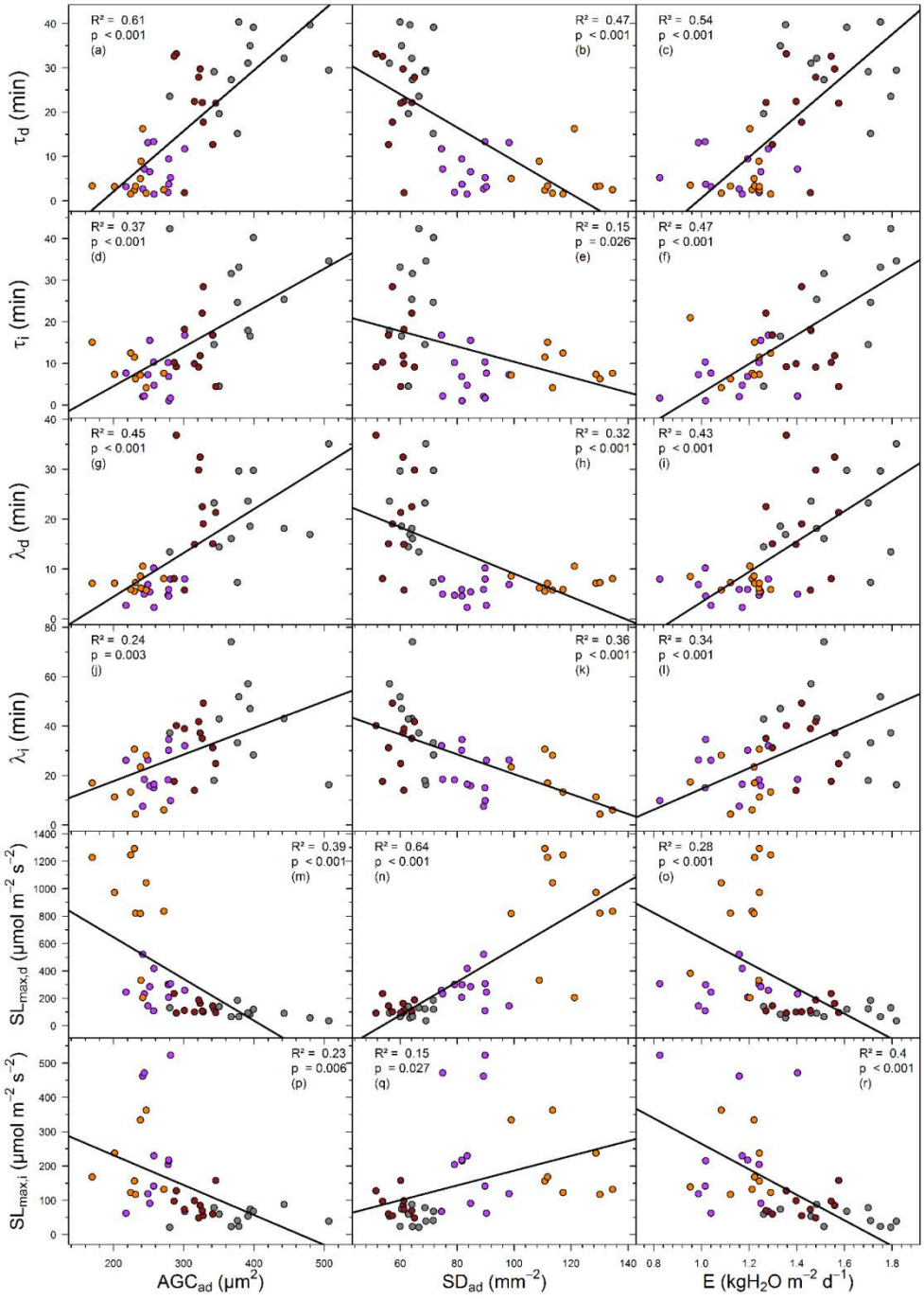

Figure S8. Correlations between dynamic parameters of g_s response to a decrease (τ_i, λ_i and $SL_{max,i}$) or an increase (τ_d, λ_d and $SL_{max,d}$) of VPD and stomatal size on the adaxial side of the leaf (AGC_{ad}; **a**, **d**, **g**, **j**, **m**, **p**), stomatal density on the adaxial side of the leaf (SD_{ad}; **b**, **e**, **h**, **k**, **n**, **q**) or the average daily whole-plant transpiration per square meter (E; **c**, **f**, **i**, **l**, **o**, **r**). Partial R^2 and *p* value of the residual variability once the treatment effect is accounted for are shown (n = 24). Correlations were considered significant at $p < 0.05$ and a regression line was drawn. τ, λ and SL_{max} are parameters of the sigmoidal model. Purple, orange, gray and red dots are for Carpaccio, I214, 6J29 and N38 respectively.

Transition

Dans ce chapitre, nous avons pu voir que les dynamiques stomatiques présentaient une variabilité génotypique, qui était modifiée sous sécheresse. Les variations de la taille et de la densité des stomates semblent être impliquées plutôt dans la diversité des réponses au VPD, potentiellement liées à une réponse hydraulique passive des stomates aux variations de VPD. Enfin, nous avons montré que les dynamiques stomatiques influencent la transpiration de la plante entière, cependant nous n'avons pas pu mettre en évidence un effet sur l'efficience de transpiration. En effet, les génotypes avec la plus faible transpiration avaient également la plus forte surface foliaire, et ainsi la plus grande consommation en eau. Ainsi les différences de surface foliaire entre génotype et traitement peuvent contrebalancer la régulation stomatique à l'échelle de la feuille. L'efficience de transpiration peut être déterminée par des variations de la biomasse produite, de l'eau consommée ou des deux à la fois, agissant soit de manière opposée ou avec des ampleurs différentes. Il nous apparait ainsi essentiel de comprendre les traits qui vont piloter l'efficience d'utilisation de l'eau à différentes échelles, et d'analyser si ces déterminants sont similaires lorsque les conditions environnementales sont modifiées. En conditions naturelles, l'environnement est très différent de celui observé en conditions contrôlées. La présence du vent peut limiter l'impact de la transpiration foliaire sur sa propre régulation stomatique (c'est-à-dire favoriser le couplage du houppier avec l'atmosphère). Les conditions de lumière, de température et d'humidité de l'air peuvent aussi varier bien plus fortement qu'en conditions contrôlées. De plus, l'âge des plantes est généralement plus élevé. Ces conditions peuvent favoriser une régulation et un développement stomatique différent (taille et densité des stomates).

C'est pourquoi nous avons quantifié l'efficience d'utilisation de l'eau en conditions naturelles au niveau de la feuille et de la plante entière sur les quatre génotypes utilisés dans le chapitre précédent. Ceci afin de comparer WUE et ses déterminants à différents échelles entre des conditions contrôlées (serre) et naturelles (pépinière). L'efficience de transpiration a été estimée à partir de capteurs de flux de sève, de récolte de biomasse et d'allométries de croissance pour estimer la surface foliaire de la plante entière. L'efficience d'utilisation de l'eau intrinsèque a été mesurée par discrimination isotopique du carbone 13 (Δ), et par mesures d'échanges gazeux foliaires (A/g_s).

CHAPITRE II

Efficience d'utilisation de l'eau au niveau de la feuille et de la plante entière : est-ce que les résultats obtenus en conditions contrôlées sont conservés en conditions naturelles ?

CHAPITRE II :

Efficience d'utilisation de l'eau au niveau de la feuille et de la plante entière : est-ce que les résultats obtenus en conditions contrôlées sont conservés en conditions naturelles ?

Présentation de l'article

Contexte

Compte tenu de l'augmentation probable de l'intensité et de la fréquence des sécheresses induites par les changements climatiques, et de la demande en bois entrainée par la croissance économique et les politiques publiques environnementales, il apparait nécessaire de maintenir ou d'améliorer la production de biomasse tout en réduisant l'utilisation d'eau des arbres plantés. Ce ratio est appelé l'efficience d'utilisation de l'eau (WUE). Défini à plusieurs échelles spatiales (foliaire, plante entière) et à partir de multiples estimateurs, ce trait n'est aujourd'hui pas utilisé lors de sélection variétale. Avant cela, il est essentiel d'évaluer la stabilité de WUE dans différentes conditions de croissance.

Objectifs

A partir d'expérimentations en conditions contrôlées (serre) et naturelles (pépinière), sous des régimes hydriques distincts, et sur plusieurs génotypes de peupliers, nous avons mesuré plusieurs estimateurs de WUE et de ses composants. Nos objectifs étaient : (1) d'analyser les différences ou concordances de WUE au niveau foliaire et de la plante entière en conditions hydriques non-limitantes entre la serre et la pépinière, (2) d'identifier si la sécheresse modifie cette relation entre conditions de croissance et (3) de déterminer les processus sous-jacents pilotant WUE à l'échelle de la feuille et de la plante entière en conditions contrôlées et naturelles.

Stratégie

Deux génotypes de peupliers euraméricains (Carpaccio et I214) et deux génotypes de peupliers noirs (6J29 et N38) ont été utilisés à la fois en serre et en pépinière. L'expérimentation en serre a été détaillée dans un article précédemment publié (Chapitre I). En pépinière, un dispositif d'exclusion des pluies couvrant 85% de la surface au sol a été mis en place à l'aide de bâches imperméables et de gouttières permettant l'évacuation des eaux de pluie. Des récoltes et des capteurs de flux de sève ont permis d'estimer la production de biomasse, la transpiration et le WUE des plantes entières (TE). De plus, des mesures d'échanges gazeux et la détermination de

la discrimination isotopique du carbone 13 (Δ) ont servi à l'estimation de WUE à l'échelle foliaire.

Résultats

Notre dispositif d'exclusion des pluies a permis de diminuer significativement le contenu en eau du sol. Dans ce dispositif, la conductance stomatique et l'assimilation nette de CO_2 au niveau foliaire étaient également réduites, tout comme la transpiration à l'échelle de la plante entière. L'efficience d'utilisation de l'eau au niveau de la feuille et de la plante entière a été augmentée dans la parcelle sous exclusion des pluies. Malgré cela, les peupliers appartenant à ce dispositif présentaient une production de biomasse plus forte que chez les peupliers témoins. Le classement génotypique était relativement maintenu entre l'expérimentation en serre et en pépinière en ce qui concerne la transpiration, Δ et TE, même si l'impossibilité d'établir des paires a limité notre analyse corrélative. En général seul un des génotypes, différent selon la variable considérée, montrait un changement modifiant son classement par rapport aux autres génotypes. Ce classement était plus fortement modifié par un changement de disponibilité en eau que par des différences de conditions de croissance. Δ au niveau foliaire était corrélée négativement avec TE, plus fortement en conditions naturelles qu'en conditions contrôlées, suggérant qu'une plus forte efficience au niveau foliaire était associée à une plus forte efficience au niveau de la plante entière. De plus, TE n'était jamais corrélée négativement avec la production de biomasse quelle que soient les conditions de croissance, même si sa détermination était plutôt pilotée par la consommation en eau en serre et par la production de biomasse en pépinière.

Conclusions

Bien que notre dispositif d'exclusion des pluies ait fonctionné, la production de biomasse plus importante sous ces conditions suggère que d'autres facteurs ont interagi avec notre traitement. Nous posons l'hypothèse que les différences de contenu en azote dans le sol et dans les feuilles depuis 2015 pourraient expliquer en partie cette croissance. Puisque ces différences étaient observables dès 2015, avant la mise en place de notre dispositif d'exclusion des pluies, nous avançons l'idée que le contenu en azote du sol aurait pu être déjà différent au moment de la plantation. Cet effet, associé à des sécheresses répétées modifiant potentiellement l'assimilation d'azote par la plante et l'effet de la pose des bâches, limitant le lessivage de l'azote et augmentant les températures du sol, pourrait ainsi favoriser la production de biomasse en dépit de la réduction de l'eau dans le sol. Nos résultats montrent que WUE semble relativement stable entre conditions de croissance. Par ailleurs, l'absence de corrélation négative entre WUE et la

production de biomasse, ainsi que la bonne relation entre WUE au niveau foliaire et de la plante entière à la fois en conditions contrôlées et naturelles suggère que WUE pourrait être utilisée comme trait pour la sélection de génotypes plus efficients dans leur utilisation de l'eau, mais sans impacter leur production de biomasse. Néanmoins les différences observées entre traitements hydriques supposent une diversité de la réponse à la sécheresse qui devrait être prise en compte dans les stratégies de sélection.

Article: Leaf-level and whole-plant water-use efficiency: do results reached in controlled conditions still hold in natural environments?

Soumis à Agricultural and forest meteorology.

MAXIME DURAND[1] • OLIVER BRENDEL[1] • CYRIL BURÉ[1] • PASCAL COURTOIS[1] • JEAN-BAPTISTE LILY[1] • ANDRÉ GRANIER[1] • DIDIER LE THIEC[1]

[1] *Inra, Université de Lorraine, AgroParisTech, SILVA, F-54280 Champenoux, France*

Corresponding author:

Didier Le Thiec

Email: didier.lethiec@inra.fr

Telephone: (+33) 3 83 39 40 98

ABSTRACT

• Water use efficiency (WUE), the amount of biomass produced with regards to the water used, has not yet been used as a breeding trait to select poplar genotypes with simultaneously high productivity and conservation of water. Before its application as a selection target, WUE or its estimators need to be stable across growing conditions.

• We compared the WUE and its components of two *Populus euramericana* (Moench.) and two *Populus nigra* (L.) genotypes grown either in a glasshouse or in the field, both under contrasting water availability.

• Genotype ranking was fairly stable for transpiration, carbon isotopic discrimination (Δ) and whole plant WUE (TE) between the glasshouse and the field. Moreover, increased WUE measured as Δ or TE was not associated with lower biomass production, further suggesting that WUE may be used as breeding target in glasshouses for genotype selection without impacting the whole plant biomass production.

• However, reduced water availability modified the genotype ranking more significantly than growing conditions, suggesting a plasticity of poplar response to drought that should be considered in breeding strategies.

KEYWORDS

drought, Populus, stomatal conductance, transpiration, carbon isotopic discrimination

INTRODUCTION

Increased intensity and frequency of short and long-term droughts is an expected consequence of global changes (Dai, 2012; IPCC, 2014), as is predicted by current global climate change models (Sheffield & Wood, 2008). The amount of land exposed to droughts has risen significantly around the globe since 1950 (Dai, 2011). This will likely cause enduring environmental, economic and humanitarian consequences on societies and ecosystems (Touma *et al.*, 2015). Since climate and forests are interconnected (Bonan, 2008), each influencing the other, the effect of a reduction of soil moisture on forests, while complex, is a key element in global change research.

A decrease in plant productivity is commonly found as a response to a decline in soil water availability (Ciais *et al.*, 2005; Monclus *et al.*, 2006; Coopman *et al.*, 2008). A trend that is in contrast with the foreseen rise in wood demand, driven by economic growth in conjunction with energy and environmental policies (FAO, 2018). This divergence motivates plantation managers to extend their cultivation of trees species such as poplars away from their natural distribution in riparian ecosystems (Stobrawa, 2014), due to their high water requirements (Tschaplinski & Blake, 1989), to mesophyte habitats where soil water deficits are more frequent. Maintaining or increasing wood production while reducing water use appears therefore as a major challenge for the coming decades (Hamdy *et al.*, 2003; Condon *et al.*, 2004).

The concept of water-use efficiency (WUE) can be defined at the whole-plant scale as the transpiration efficiency (TE, the amount of biomass produced for a given amount of water used over a defined period of time). Since biomass production originates from CO_2 assimilation (A) into the leaves and the majority of water is lost by leaf transpiration, driven by stomatal conductance (g_s) and the leaf-to-air vapour-pressure deficit (VPD), we can define WUE at the leaf level intrinsically as the ratio of A over g_s (W_i).

Currently, commercial genotypes of hybrid poplars were selected mainly on a basis of high productivity, resistance to pathogens and suitable wood properties but not for high WUE (Monclus *et al.*, 2006). If WUE is to be used as a breeding trait, reducing water use must not come at the expense of wood production. Given the asymptotic relationship between A and g_s at the leaf level, there is a range of high g_s for which A does not improve further (Wong *et al.*, 1979). Therefore, a reduction of g_s does not always cause a similar reduction of A, making improvements of W_i possible.

At the whole-plant scale, methods for measuring TE demand a labor-intensive account of the water used, often limiting its widespread use in large-scale experiments. This makes it not realistically applicable to large screenings for cultivar improvement. Indirect estimations of WUE by measuring the composition of stable carbon isotopes (δ, the ratio of ^{13}C to ^{12}C in a biological sample relative to an international standard, Pee Dee Belemnite) enables the comparisons of δ in the sample of interest relative to the one of the atmosphere (Δ). Differences of δ between the two arise from processes of discriminations which provide insights into leaf gas exchange processes and may be useful as a proxy to W_i (Farquhar *et al.*, 1982). Δ has been negatively related to W_i in C_3 crops (Farquhar *et al.*, 1989; Anyia *et al.*, 2007) and trees (Ponton *et al.*, 2002; Roussel *et al.*, 2009b). In poplars Δ has been negatively linked with W_i and TE in black and hybrid poplars (Rasheed *et al.*, 2013; Rasheed *et al.*, 2015). However, some studies reported a lack of correlation with TE (Turner *et al.*, 2007; Devi *et al.*, 2011). Δ is a leaf-level assimilation rate-weighted temporal integration of the A/g_s ratio. Unlike TE, Δ does therefore not take into account possible carbon gains through photosynthetic stems, carbon losses by respiration (apart from leaves during the day) and water losses at night or during the day in organs other than leaves (Farquhar *et al.*, 1989; Hubick & Farquhar, 1989). Because of the different spatiotemporal integrations of WUE estimators (Δ, W_i, TE), understanding how and under which circumstances they are related can be complex.

An important consideration regarding the usefulness of WUE in selecting genotypes for improved WUE but similar or enhanced biomass production, is the stability of genotypic differences across growing conditions. Because TE is laborious to measure, experiments are often conducted in pot experiments in glasshouses. However, in controlled conditions the environment is widely different than in the field, with plants rarely experiencing high winds or pathogens as well as often being limited in the range of global radiation, temperature and humidity they are subjected to. Comparisons of WUE in controlled and field conditions are scarce in the literature. Some studies were able to establish a correlation or similar genotype ranking between growing conditions of Δ or WUE in grass species (Johnson & Bassett, 1991) and crops (Ehdaie *et al.*, 1991; Anyia *et al.*, 2007) while others reported a weak correlation (Lambrides *et al.*, 2004) in sunflowers or not at all in three wheat species (Frank *et al.*, 1987). In oaks, field grown genotypes with high or low Δ had a similar ranking when planted in a glasshouse (Roussel *et al.*, 2009b), which manifested as differences of TE as well (Roussel *et al.*, 2009a). To our knowledge, field estimations of TE are rare but extensive progress could be

gained from understanding to what degree WUE estimators from genotypes planted in glasshouses influence TE in the field.

In this context, we investigated the biomass production, water use, TE and Δ of poplar genotypes grown in the field. Poplars were either irrigated or not, with the latter growing under a rainfall exclusion system. Our aim was to compare this data with a similar drought experiment using the same poplar genotypes, previously published in Durand *et al.* (2019) in order to answer the questions: (1) Is leaf-level and whole-plant WUE similar among well-watered poplar genotypes when grown in a glasshouse or in the field? (2) Does soil water deficit modify our assessment under well-watered conditions? (3) What are the underlying processes driving WUE at the leaf and whole-plant scale in controlled and field conditions?

MATERIAL & METHOD

Plant material and experimental design

We used four poplar genotypes throughout the experiment. Carpaccio and I214 are commercially available *Populus deltoides* × *nigra* (Moench.) clones, while 6J29 and N38 are *Populus nigra* (L.) genotypes originating from natural populations in France (Drôme 6; FR-6) and Italy (La Zelata; IT1), respectively. Clones were selected to compare them with a previous glasshouse experiment (Durand *et al.*, 2019) and for their diversity of drought tolerance, I214 and 6J29 being usually found to be drought-sensitive (Chen *et al.*, 1997; Giovannelli *et al.*, 2007; Muller & Lambs, 2009; Viger *et al.*, 2016). The glasshouse drought experiment is explained in details in Durand *et al.* (2019). In the field, 144 shoot cuttings were planted in June 2nd 2014 by groups of three along six parallel rows spaced 5 m apart. A single randomly selected genotype was use for each group of three trees. Within and between groups on a row, poplars were separated by 1 m and 4 m, respectively (Fig. S1). The plantation was setup in a nursery at INRA-Nancy (48°45′09.3″N, 6°20′27.6″E; Champenoux, France). The plot had a 6° slope southeastward.

The studied site is characterized by gray marls of the Jurassic inferior (Lotharingian) era, a deep homogenous swelling heavy clay soil (52% silt, 40% clay, 8% sand). On average, the soil had a pH of 7.1, an organic matter content of 33.3 g kg^{-1}, a total nitrogen content of 1.66 g kg^{-1} and a C/N ratio of 11.6.

Rainfall exclusion setup

Each tree was equipped with a water-dripping system, each dispensing 50 l per day. Waterings on the three more elevated rows relative to the slope stopped in May 26th 2015, to limit surface runoff of water to the rows below. In April 2016, covers 1.5 meters-wide were placed on the ground on each side of the three rows where irrigation was stopped (Fig. S1), covering 85% of the total ground area. Covers were two-fold, one was green to mirror soil optical properties and limit the rise of temperature under the covers (green canvas mulch, Triangle-outillage, Ennevelin, France), the other was impermeable to liquids but not to gases preventing rainfall to reach the ground but not soil evaporation to escape into the atmosphere (Berner France, Saint-Julien-du-Sault, France). Gutters were placed on the downward side of each cover to evacuate water to the bottom of the site (PVC, First Corp, Altare, Italy).

1.6 and 0.9 meters-long neutron probe access tubes (ten of each, aluminum, closed at their base) were installed, evenly spaced on the rows of the plot (Fig. S1), in order to quantify volumetric

soil water content (SWC) every 10 cm in depth (TROXLER TX 4301, Research Triangle Park, NC, USA). Calibration of each tube was performed following Normand (1974) by simultaneously measuring at each depth the wet soil bulk density (Gamma probe, Campbell, CPN 501 DR), the neutron counting speed of the soil (neutron probe) and the gravimetric soil moisture by taking soil samples during the installation and subsequently measuring the ponderal water content.

Measurements were performed once each month, in May 17th, June 23rd, July 18th and August 22nd 2017. For the last three dates, predawn leaf water potentials (Ψ_p) were measured on the same day (4:00 to 5:00 h, local time) on six randomly-chosen non-senescent leaves of each genotype and water regime (*i.e.* 48 leaves) with a Scholander pressure bomb (SKPM-1400, Skye Instruments LTD, Llandrindod Wells, UK).

Sapflow

Whole-tree water use (WU) was inferred from sapflow measurements using the thermal dissipation technique. Probes 20 millimeters-long were installed on July 11th 2017 20 cm above ground in the main stems in the North direction to estimate the sapflow per unit of sapwood area (*i.e.* sap flux density), following Granier (1985; 1987). Six probes per genotype and water regime were used (*i.e.* 48 probes). Probes were enclosed in aluminum sheets to protect them from direct radiation and rainfall. They were removed on September 3rd 2017, after 55 days. WU per tree was then computed by scaling sap flux density from transversal cross-section at sensor height since harvests revealed the absence of heartwood, which is common in young trees.

Monitoring and harvests

Meteorological variables were measured in a meteorological station 190 m away from the planted poplars. The station was equipped with a data logger (Campbell 21X, Campbell Scientific Ltd), temperature and atmospheric relative humidity (Vaisala HMP45), global radiation (pyranometer Kipp and Zonen CMP6), wind speed (contact anemometer, Campbell Scientific A100) and rainfall sensors (tipping bucket rain gauge, Precis Mecanique 3030).

Diameter at 1.3 m (DBH) and height (H) of each tree were measured once each week during the growing season from 2015 to 2017. In April 18th 2016 and September 4th 2017 harvests were conducted to measure the above-ground biomass (DM_T), separated in leaves (DM_L) and stems (DM_S). The first harvest was done before bud-break so only the woody biomass was measured. Every tree used for the sapflow experiment was used in the second harvest. One of

each group of three trees was used for each harvest (*i.e.* 48 trees). Leaves and stems were oven-dried at 60°C until they reached a constant dry mass to estimate the biomass in each compartment before the covers were installed and after the sapflow experiment. Using an exponential relationship between H and woody biomass for each genotype (RMSE < 26 g), we were able to compute the biomass in April 2016 for each tree harvested in September 2017 (Fig. S2a). From this data, we fitted a second order polynomial relationship between tree height and woody biomass for each combination of genotype and treatment (RMSE < 229 g). This enabled us to estimate the woody biomass of each of the 48 trees used for sapflow measurements at the start of the sapflow experiment using their measured height at the time (Fig. S2b). TE was estimated from estimation of above-ground biomass between the start and the end of the sapflow experiment, divided by WU. As such it did not integrate root biomass. TE from the glasshouse experiment was also re-calculated without the root biomass to be able to consistently compare the two experiments.

Total leaf area (TLA) was estimated twice during the experiment. The first one was performed in the first week of July 2017, right before the sapflow sensors installation. We fitted a third order polynomial between the number of leaves and the total leaf area (estimated from leaf width, Fig. S3) on each branch for two trees of each combination of genotype and treatment (*i.e.* eight trees). Then we estimated the total leaf area on 19 trees by counting the number of leaves on each branch and summing the computed leaf area of the tree. A second estimation of leaf area was performed by fitting a linear relationship between leaf mass and area from 50 leaves per tree harvested in September 2017 (R^2 > 0.94, Li-3000A, LI-COR, Lincoln, NE, USA). Using this relationship we were able to estimate leaf mass per area (LMA), TLA from DM_L on the 48 harvested trees in September 4th and DM_L from the TLA estimated at the start of the sapflow experiment (July 11th).

Since the sapwood area (SA), calculated from DBH measurements, was highly correlated with TLA (using both dates for each genotype, R^2 > 0.91), we estimated TLA for each tree and each day of the sapflow experiment from splined weekly measurements of SA. Furthermore, by dividing for each day and each individual, their daily WU (from sapflow measurements) by their daily estimated TLA, we were able to calculate daily whole-plant transpiration per unit area (E, Fig. 1).

Leaf gas exchange

We assessed the photosynthetic capacity by measuring CO_2 assimilation and internal CO_2 concentration (C_i) along discrete steps of [CO_2] using the LI-6800 portable photosynthesis

system (LI-COR, Lincoln, NE, USA). Conditions inside the leaf cuvette was as follows: leaf temperature of 25°C, saturating irradiance of 1500 µmol m^{-2} s^{-1}, leaf-to-air VPD of 1.6 kPa, fan speed of 10000 rpm, flowrate of 1000 µmol s^{-1} with an overpressure of 0.1 kPa. Before starting, we waited for g_s to reach a steady-state. Infrared gas analysers were matched after every step changes of [CO_2] which were in order: 400, 1800, 1500, 1200, 1000, 800, 600, 400, 250, 200, 150, 100, 50, 0 and 400 ppm. Maximum carboxylation rate (Vc_{max}), maximum electron-transport rate (J_{max}) and maximum CO_2 assimilation at saturating C_i (A_{max}) were estimated using the "plantecophys" R package (Duursma, 2015; R Core Team, 2019), using the Michaelis-Menten constants for CO_2 (K_c), and O_2 (K_o) and the CO_2 photo-compensation point (Γ*) of Bernacchi *et al.* (2001).

On July 18th and August 22nd 2017 we monitored diurnal dynamics of gas exchange (A and g_s) from 5:30 and 6:30 h to 15:30 and 16:30 h (universal time), respectively. This was done on six replicates per genotype and treatment (*i.e.* 48 individuals) on sun leaves facing the south-east direction using two intercalibrated portable photosynthesis systems (Li-6200, LI-COR Inc., Lincoln, NE, USA).

Carbon isotopic discrimination

Mature leaves were sampled in the field at the end of August 2015 and 2017 and in the glasshouse during the leaf sampling described in Durand *et al.* (2019). In the field, leaves grew under the rainfall exclusion setup, but they were fully mature before the start of the drought in the glasshouse. All sampled leaves were oven-dried for 48 h at 70°C and grounded into a fine powder. 1.0 ± 0.1 mg subsamples were weighed into tin capsules and δ was measured with a coupled isotope ratio mass spectrometer (Thermo-Finnigan; Delta S, Bremen, Germany). $^{13}C/^{12}C$ ratios were computed relative to the Vienna Pee Dee Belemnite international standard. Isotopic composition of the air in the glasshouse was -9.61 ‰, derived from isotopic compositions of two *Zea mays* (L.) planted in the glasshouse at the time, following Marino & McElroy (1991). In the field the isotopic composition of the air was -8.73 ‰, estimated from its evolution over the past three centuries following Bonal *et al.* (2011). Isotopic discrimination was estimated as $\Delta = (\delta_{air} - \delta_{leaf}) / (1 + \delta_{leaf} / 1000)$.

Statistics

Statistics were done using R 3.5.2 (R Core Team, 2019). Significant differences among the four genotypes and the two treatments was tested with type two Two-Way ANOVA. A similar but repeated ANOVA design with genotypes and treatments as between-subjects factors and the time as within-subjects factor was used for diurnals gas exchange and daily whole-plant

transpiration (n = 5-6). Differences of soil water content was tested with Student tests at every depth (n = 10). Correlations were computed by performing linear regressions (n = 48), using genotype-treatment means when comparing field and glasshouse data because pairing could not be established between trees (n = 8). Normality, homoscedasticity and sphericity were checked by Shapiro-Wilk normality tests, Levene tests and Mauchly tests, respectively. When sphericity was violated we used the Greenhouse-Geisser correction. Significant differences between modalities of each factors were tested by post-hoc contrast analysis and *P* values were adjusted to control for the false discovery rate. Significant differences were considered at $P < 0.05$ for all tests.

RESULTS

Water relations in the field

Our experimental rainfall exclusion design proved successful in reducing the SWC. On May 17th 2017, the mean SWC ranged from 47 to 35.9% from 20 to 150 cm in depth with no significant difference between irrigated and the rainfall exclusion plot at any depth (data not shown). Both plots showed a decrease of SWC on June 23rd, which was larger in the rainfall exclusion plot. This led to significant differences of SWC between plots in most of the first 120 cm ($P < 0.04$, except at 70 and 80 cm, Fig. 2). At this date, Ψ_p was marginally lower in the rainfall exclusion trees than in the irrigated ($P = 0.05$). During the following month SWC continued to decrease in the rainfall exclusion plot causing larger differences between the two plots in the first 130 cm ($P < 0.007$) on July 18th. Ψ_p was also significantly lower in the rainfall exclusion trees than in the irrigated for all genotypes ($P < 0.02$). More rainfall during the month of August (Fig. S4**c**) led to a small increase of SWC on both plots in the first 100 cm on August 22nd (but a continued decrease below this depth). Nonetheless, we found significant differences of SWC between plots in the first 140 cm. Ψ_p was however similar between irrigated and rainfall exclusion trees, except for Carpaccio which showed a more negative Ψ_p in the rainfall exclusion trees than in the irrigated ones (Fig. 2).

Sapflow sensors recorded the flow of ascending sap in the main stem, from which we can infer plant water use (WU), between July 14th and August 31st (Table 1). Whole-plant water use was higher in the rainfall exclusion hybrid poplars than in the irrigated by 34 and 58% for Carpaccio and I214 ($P < 0.03$). A similar but not significant trend was found in the black poplars ($P > 0.23$). However, whole-plant daily transpiration per leaf area (E) was overall significantly lower in rainfall exclusion trees. Post-hoc comparisons were able to detect significant differences of E in Carpaccio and 6J29 but not in I214 and N38 (Table 1). When investigating differences of E on specific days, transpiration in the irrigated trees was almost always higher than in the rainfall exclusion trees for every genotype (Fig. 1). Despite this, we were able to detect significant differences of transpiration between water regimes only in 15, 2, 8 and 0 days for Carpaccio, I214, 6J29 and N38 respectively, because of the high individual variability of whole-plant transpiration.

At the leaf level, diurnal gas exchange measurements on July 18th and August 22nd showed a clear reduction of g_s for every genotype throughout the day except early in the morning ($P < 0.001$, Fig. 3**e-h**, Fig. 4**e-h**). On July 18th, stomata of the rainfall exclusion trees, regardless of

genotype, were completely closed from 10:00 until the end of the day, while those of the irrigated trees continued to decrease during the afternoon. Overall, g_s was similar between the four genotypes at this date ($P = 0.45$). On August 22nd, Carpaccio rainfall exclusion trees were almost completely closed throughout the day similarly to July 18th (Fig. 4**e**), while the other three genotypes showed different extents at which g_s was reduced under rainfall exclusion with N38 exhibiting the second strongest and 6J29 the smallest reduction of g_s. Overall, g_s was also reduced in the rainfall exclusion trees but to a smaller degree than on July 18th (Fig. 4**e-h)**.

Biomass and photosynthesis in the field

At the whole-plant scale at the end of the growth period in 2017, we found H, DM_S and DM_L to be overall higher in the rainfall exclusion than in the irrigated trees ($P < 0.001$, Table S1). While post-hoc comparisons were not always able to show significant genotypic differences, the lack of interaction between the genotype and treatment effect ($P > 0.05$) highlights the similar trend in every genotype. In April 2016, there were no such differences between treatments ($P > 0.19$). Growth and biomass accumulation in 2017 show these differences were in part, established during the summer 2017 (Table 1). Growth was 23 to 60% higher for height and 43 to 154% for DBH in the rainfall exclusion than in the irrigated trees, depending on genotype. DM_T and DM_S, although similar among genotypes, were also more than doubled in the rainfall exclusion than in the irrigated trees with a mean total biomass accumulation of 2.43 kg in the former and 1.04 kg in the latter. Moreover, even though LMA was 8.4 to 12.6% higher in the rainfall exclusion than in the irrigated trees depending on genotype ($P < 0.001$ but not significant in Carpaccio with post hoc comparisons), both DM_L and TLA were overall higher in the rainfall exclusion trees as well (DM_L: 203 and 446 g, TLA: 2.05 and 2.94 m^2, for irrigated and rainfall exclusion trees respectively). However the high individual variability prevented us from detecting significant genotypic-specific differences between treatments by post-hoc comparisons.

At the leaf level, photosynthetic capacity measurements showed a significant increase in Vc_{max} by 32, 28 and 27% in Carpaccio, I214 and N38 rainfall exclusion trees compared the irrigated ones. There was a similar but not significant trend in 6J29 (Fig. 5**a**, $P = 0.009$, 0.006, 0.385, 0.007 for Carpaccio, I214, 6J29 and N38 respectively). Yet, 6J29 exhibited in irrigated conditions a Vc_{max} as high as the other three genotypes under rainfall exclusion. J_{max} had a comparable trend with an overall higher J_{max} in the rainfall exclusion trees but post-hoc comparisons were not able to show genotypic-specific differences (Fig. 5**b**). A_{max} did not show any significant difference between treatments (Fig. 5**c**, $P = 0.67$). Genotypic differences were

significant and similar among the three parameters tested ($P = 0.002$, 0.011 and 0.009 for Vc_{max}, J_{max} and A_{max} respectively). Carpaccio had the lowest Vc_{max}, J_{max} and A_{max} while 6J29 had the highest both under irrigated and rainfall exclusion conditions. Leaf nitrogen content were also increased in the trees that were not irrigated in 2015 and under rainfall exclusion in 2017, when compared to the irrigated ones ($P < 0.001$ in both cases, Fig. S5). In the glasshouse, leaf nitrogen also tended to be increased under drought ($P = 0.057$, data not shown).

Despite this trend of higher photosynthetic capacity in the rainfall exclusion than in the irrigated trees, CO_2 assimilation during our gas exchange diurnals was lower under rainfall exclusion. On July 18th, A decreased more rapidly in the rainfall exclusion than in the irrigated trees from 7:00 h onwards in the hybrid poplars and from 8:30 h onwards in the black poplars (Fig. 3**a-d**). On August 22nd, the reduction of A in the rainfall exclusion plants was still visible but to a smaller degree depending on the concurrent decrease of g_s (Fig. 4**a-h**). I214 and 6J29 exhibited a decrease of A under rainfall exclusion, mostly in the early morning, which was much smaller than in Carpaccio and N38. Akin to photosynthetic capacity data, Carpaccio showed overall the lowest and 6J29 the highest CO_2 assimilation.

Water use efficiency and comparisons between the glasshouse and field experiment

Regarding the intrinsic WUE (W_i) during the gas exchange diurnals on July 18th, most of the significant differences between treatments were found for times were g_s approached zero and thus W_i increased very strongly (Fig. 3**i-l**, Fig. 4**i-l**). Similarly to A and g_s, no genotypic difference of W_i was found at this date. On August 22nd, W_i remained relatively constant in the irrigated trees while it increased in the afternoon on rainfall exclusion trees. As a result, W_i tended to be higher in the early morning in irrigated trees because of a similar g_s but higher A. The reverse was found in the afternoon in I214 and N38, resulting from a larger decrease of g_s than A when comparing them to the irrigated trees.

As a consequence of the respectively large increase in biomass accumulation and the moderate increase in water use in the rainfall exclusion poplars when compared to the irrigated ones, TE was overall 78% higher under rainfall exclusion than in irrigated conditions (2.78 and 4.96 g l^{-1}, for irrigated and rainfall exclusion respectively). On the contrary, Δ was significantly reduced by 13, 12, 6.5 and 10% in the rainfall exclusion trees when comparing to the irrigated trees, for Carpaccio, I214, 6J29 and N38 respectively. Overall, hybrid poplars tended to have a lower TE than black poplars under irrigated conditions (not significant). Under rainfall exclusion, this trend was illustrated by the significant difference between Carpaccio and N38, having the lowest and highest TE, respectively ($P < 0.05$). Correspondingly, this tendency was reversed

when comparing genotypic differences in Δ, with Carpaccio and I214 exhibiting the highest Δ and N38 the lowest, under both irrigated and rainfall exclusion conditions. 6J29 showed the smallest increase of TE (47%) and the smallest decrease of Δ (6.5%) under rainfall exclusion. Furthermore, we found a negative correlation between of TE and Δ among treatments and genotypes in the field ($P < 0.001$, $R^2 = 0.39$, Fig. 6**b**), driven mainly by the water regime. By contrast, TE and Δ was found to be nearly significantly negatively correlated in the glasshouse experiment ($P = 0.087$, $R^2 = 0.04$, Fig. 6**a**) because of the high combined Δ and TE of 6J29, also found in the field experiment (without 6J29 in the glasshouse, $P = 0.001$, $R^2 = 0.25$). Components of TE were also different under controlled and field conditions. In the field, TE was not correlated with water use ($P = 0.21$, Fig. 7**d**), but positively and strongly with biomass accumulation ($P < 0.001$, $R^2 = 0.62$, Fig. 7**b**) while the reverse was true in the glasshouse experiment. TE was negatively correlated with water use ($P < 0.001$, $R^2 = 0.40$, Fig. 7**c**) but not with biomass accumulation ($P = 0.93$, Fig. 7**a**). Similar results were found when taking the water regime into account using an ANCOVA statistical design.

Unexpectedly, despite this divergence we found TE values in the field to be close to the one we found in the glasshouse experiment. Well-watered trees tended to have a higher transpiration efficiency in the glasshouse while we found the inverse for water-limited trees (Fig. 8**a**). Only N38 well-watered trees were significantly lower in the field than in the glasshouse ($P = 0.02$) whereas water-limited I214 and N38 were significantly higher in the field than in the glasshouse ($P < 0.004$). By contrast, Δ in the field was always lower than in the glasshouse for every combination of genotype and treatment ($P < 0.001$), by 11 and 19% on average for irrigated and rainfall exclusion trees, respectively (Fig. 8**b**). This was similar to the lower E in the field than in the glasshouse (Fig. 8**c**), also exhibited by every combination of genotype and treatment, by 24, 28, 34 and 49% for Carpaccio, I214, 6J29 and N38 respectively ($P < 0.001$).

Correlations of traits between the glasshouse and the field are difficult considering no pairing can be established between trees. As such our only alternative is to correlate genotypes and treatments means. This has the effect of reducing the number of observations by a factor of 6 (equal to the number of replicates in each conditions), thus reducing the statistical power to detect significant correlations, even though each calculated mean is informed by six replicates. As a result, correlations of TE, Δ and E between the field and glasshouse experiment were not statistically significant (P = 0.18, 0.05 and 0.14, respectively) despite the discernable positive trends and the relatively strong correlation coefficients ($R^2 = 0.15$, 0.40 and 0.21, respectively, Fig. 8). By randomly pairing greenhouse and field data by genotype and water regime a million

times (similar to a bootstrap with replacement), we found 92, 97 and 92% of *P* values under the 0.05 threshold and R^2 of 0.22, 0.23 and 0.19 for TE, Δ and E, respectively (Fig. S6).

Genotype ranking between the field and glasshouse experiment was fairly maintained, with typically only one genotype switching order between the field and glasshouse conditions. For example from lowest to highest TE in irrigated trees, the order Carpaccio, I214 and 6J29 was similar in the field and in the glasshouse (Fig. 8**a**). Likewise in rainfall exclusion trees, the order Carpaccio, 6J29 and N38 was found in both conditions. Overall, N38 frequently had the highest TE and always had the lowest Δ in both conditions and for both treatments (Fig. 8**a-b**). On the contrary, Carpaccio irrigated trees had the lowest TE and the highest Δ in both conditions. 6J29 also had the highest E in both conditions for both treatments (Fig. 8**c**).).

DISCUSSION

Water use efficiency has a major potential to help select and breed new individuals with similar or increased biomass production and lower water consumption. However, estimating WUE is not an easy task. Further research is needed to better understand if and under which conditions different spatiotemporally-integrated estimators of WUE are related. In this study we investigated the water use efficiency and its components at the leaf and whole plant scale of four poplar genotypes in the field under irrigation or a rainfall exclusion setup. This data was also compared to a preceding study in a glasshouse in order to explore the links between leaf-level and whole-plant WUE in each condition and across them.

Rainfall exclusion effect in the field

A major and unexpected result of our study was the increased biomass and leaf area production in the rainfall exclusion trees as compared to the irrigated ones. The moderate but significant reduction of soil water content and lower predawn leaf water potential we found in the rainfall exclusion plot (Fig. 2) is usually associated with a reduced biomass production in poplar genotypes, driven by stomatal closure (Monclus *et al.*, 2006). In our experiment at the leaf level, stomatal opening was substantially lower in the rainfall exclusion trees (Fig. 3-4), as theory predicts, decreasing both transpiration and CO_2 assimilation but increasing W_i. Despite this, the higher biomass production was most likely amplified by the exponential growth with increased tree size, as larger trees have larger leaf area and thus a higher number of photosynthetic organs. The increased photosynthetic capacity (V_{cmax}), mitigating the reduced CO_2 assimilation prompted by stomatal closure may have also contributed, to a lower degree, to the higher biomass production in the rainfall exclusion plot compared to the irrigated one. The observed leaf-level trend of lower transpiration per unit area (E) when water is limited was also seen at the whole plant scale, with different magnitude of decrease depending on genotype (Fig. 1). A number of factors could explain this genotypic difference, such as leaf aging (Reich, 1984), differences of stomatal density in newly developing leaves or with leaf position in the canopy (Ceulemans *et al.*, 1995) and differences in the physiology of shaded leaves compared to sun leaves (Campany *et al.*, 2016).

Another consideration is the increased nitrogen content in leaves in 2015 which was maintained in 2017 (Fig. S5). A slight trend of higher nitrogen in the soil was also found in 2017, however not significant. Nitrogen availability in known to stimulate growth (Gruber & Galloway, 2008), and has a complex relationship with soil water availability. As the soil dries, the rate of both

diffusion and mass flow to the roots is reduced leading to a decrease of permeability of roots to nutrients (Oren & Sheriff, 1995), counteracted somewhat by the increased concentration of the soil solution (Nye *et al.*, 1979). In maize roots, response to drought resulted in an overexpression of nearly all genes involved in nitrogen uptake and assimilation (Wang *et al.*, 2017). When plant growth is manly limited by water, theory suggests that allocating more nitrogen per leaf area would raise CO_2 assimilation when stomatal conductance and leaf area production declines (Farquhar *et al.*, 2002), which is in accordance with our results of higher nitrogen content and photosynthetic capacity in the rainfall exclusion trees in the field and the similar trend observed in the glasshouse. Mooney *et al.* (1978) found an increased nitrogen content in eucalyptus species living in dryer habitats and other reports show a similar trend under drought in beech (Sánchez-Gómez *et al.*, 2013) and willows (Weih *et al.*, 2011), driven by a higher leaf mass per area under drought, which is similar to our findings (Table 1, Fig. S5). This increased nitrogen content was hypothesized to be a functional adaptation rather than a passive effect of reduced water availability (Weih *et al.*, 2011), potentially relevant as a breeding target for poplars.

This response may have interacted with the covers installed in the rainfall exclusion plot. Placing covers permeable to water on the soil, like traditional mulch, is known to increase soil water content (Walsh *et al.*, 1996b), a rise in temperature of 1 to 2°C in the firsts 10 cm of soil but not in the air 5 cm above the surface (Ham *et al.*, 1993; Walsh *et al.*, 1996b), and an increased nitrate content in the soil because of the lower weed competition and lower leaching (Walsh *et al.*, 1996a). This results in an increased growth and biomass production when compared to grass or mixed flora covers. In our setup the soil water content was reduced under the covers (Fig. 2), which may have been promoted by increased soil evaporation induced by the increase in soil surface temperature. However the amount of reflected light and rise in temperature caused by the covers is largely dependent on the cover color (Hostetler *et al.*, 2007) which was green in our case, similar to the grass cover in the irrigated plot.

Poplar roots can have associations with ectomycorrhizal and with vesicular-arbuscular mycorrhizal fungi but can be limited by high soil nitrogen and temperature (Block *et al.*, 2006), and by low water availability (Nickel *et al.*, 2017). However, root systems were found to be related to the main stem diameter in poplars, depending on soil fertility (Fortier *et al.*, 2015). Following this assumption would lead to a probable higher root biomass in the rainfall exclusion trees than in the irrigated ones, even if mycorrhization may be limited under the canvas. Carbon allocation to roots was found to be increased both under drought (Tschaplinski *et al.*, 1998) and

under low soil nitrogen (Fortier *et al.*, 2015). Furthermore, under high nitrogen but low water availability, root proliferation was enhanced in different poplar hybrids (Ibrahim *et al.*, 1998), increasing levels of carotenoids, proline, ABA and consequently, drought tolerance (Song *et al.*, 2019). This has the additional result of decreasing leaf gas exchange (Liu & Dickmann, 1996; Song *et al.*, 2019). These mechanisms may have strengthened the drought tolerance of the rainfall exclusion trees subjected to repeated summer droughts.

Carbon isotope discrimination as a leaf-level estimator of transpiration efficiency

Numerous studies have found a negative relationship between Δ and WUE in C_3 crops and trees species, in accordance with theory (see: Brugnoli & Farquhar, 2000; Roussel *et al.*, 2009b). More specifically, Δ measured in soluble sugars was negatively correlated with TE in six hybrid poplar genotypes (Rasheed *et al.*, 2013) and several black poplar genotypes (Rasheed *et al.*, 2015; Bogeat-Triboulot *et al.*, 2019; Durand *et al.*, 2019) grown in a glasshouse. This is in agreement with our study showing the negative relationship between Δ and TE across hybrid and black poplar genotypes in the field (Fig. 6**b**). In the glasshouse, our weaker and nearly significant trend may be explained by a number of factors. First, the sampled leaves were already mature at the start of the drought so that other measurements could be performed on the same leaves (Durand *et al.*, 2019). This likely led to the observed small range (2 ‰) of Δ values in the glasshouse. The trend may have been driven by leaf starch and soluble sugars as they are known to more closely reflect the daily assimilation-weighted average of C_i over atmospheric CO_2 concentrations (C_i/C_a; Brugnoli *et al.*, 1988) . Second, Δ and TE involve different spatial and temporal integration. At the leaf level the link between Δ and C_i/C_a could be modified by cuticular and mesophyll conductance (Brugnoli & Farquhar, 2000), fractionation during respiration and photorespiration (Gillon & Griffiths, 1997), leaf physiology (*e.g.* sun/shade) and leaf age causing different metabolisms and chemical compositions (Gutierrez & Meinzer, 1994). All of which are susceptible to have genotypic-specific variations and/or be altered under stress. At the whole-plant level, Δ does not include neither carbon lost through respiration by non-photosynthetic organs or at night by the whole plant, nor water losses during the night by stomata or by other organs during the day (Farquhar *et al.*, 1989; Hubick & Farquhar, 1989). 6J29 appears to deviate to the upper right in Fig. 6 both in controlled and field conditions by having the highest combined TE and Δ, the latter being usually associated with lower WUE. A possible explanation may be that the higher photosynthetic capacity found in this genotype may result from differences of mesophyll conductance compared with the other genotypes, shifting the relation between Δ and TE as well.

For WUE to be considered as a breeding trait, the optimization of plant water use should not be at the cost of biomass production. In our glasshouse experiment TE was negatively correlated with water use but not with biomass production (Fig. 7**a-c**), suggesting genotypes with higher TE associated with reduced stomatal conductance without a concurrent and proportional reduction in assimilation rate. The mild drought carried out likely shifted from the asymptotic part of the A-g_s relationship (Wong *et al.*, 1979) thereby decreasing water use at a trivial cost of CO_2 assimilation. Many studies reported a positive (Voltas *et al.*, 2006; Rasheed *et al.*, 2013; Bogeat-Triboulot *et al.*, 2019) or an absence of correlation (Marron *et al.*, 2005; Monclus *et al.*, 2005; Monclus *et al.*, 2006; Rasheed *et al.*, 2015) between WUE estimators and biomass production in black and hybrid poplars as well as in other species (Hubick *et al.*, 1986; Virgona & Farquhar, 1996). Both enabling the possibility of selecting genotypes with improved TE and productivity. Negative correlations between WUE and productivity are somewhat counter intuitive since for a given WU, the higher the productivity, the higher WUE. For the correlation to be negative, a higher productivity has to be met with an even higher WU so that WUE gets lower despite the higher productivity. Thus it predicates upon a negative correlation between TE and water use so that increments of biomass production would require a larger increment in water use. Such cases exists, often under drought (Read *et al.*, 1991; Ray *et al.*, 1999), or when comparing genotypes with contrasting growth adaptation to dryer climates (Zhang *et al.*, 2004), but not necessarily (Ehdaie & Waines, 1993). However in the field, the more productive trees were also under reduced water availability, hence under stomatal control (Fig. 3-4) which led to higher TE and lower Δ when compared with the not water-limited but less productive trees.

Stability of transpiration efficiency across growing conditions

Genotypic means of TE were mostly similar between in the field and the glasshouse experiment. This is in agreement with investigations on the stability of poplar genotype ranking with age (Rasheed *et al.*, 2011) and different VPD treatments (Rasheed *et al.*, 2015), which make part of the distinctions between our glasshouse and field experiment. For black poplars specifically, N38 when grown in a glasshouse and in the field tend to have a lower TE and a higher Δ than 6J29, in agreement with previous drought experiments (Bogeat-Triboulot *et al.*, 2019; Durand *et al.*, 2019). These findings of relatively stable transpiration efficiency across wildly different environmental conditions and age suggests that selecting poplar genotypes with higher WUE and higher productivity in glasshouses may be viable for poplar plantation in the field. By contrast Δ, despite a near significant correlation was systematically and largely higher in the glasshouse than in the field, similar to previous studies on wheat (Ehdaie *et al.*, 1991) and barley

(Anyia *et al.*, 2007). This difference is not likely to be related to differences in the isotopic composition of the air as it was 1‰ higher in the field (δ = -9.61 and -8.73‰ for glasshouse and field air respectively). Accurate estimations of air δ are difficult, and soil respiration may have interacted with the air to further modify δ depending on species and environmental conditions (Ghashghaie *et al.*, 2001; Xu *et al.*, 2004). Apart from differences of leaf sampling between experiments, these differences of Δ may be rooted in differences of g_s between the two environments. Genotype ranking of whole-plant daily transpiration was also fairly maintained, except for N38 between the glasshouse and the field experiment. While comparisons of VPD experienced between the two growing conditions are difficult, diurnals gas exchange data performed in similar instrumental conditions, and during solar noon in summer on a cloudless sky, suggests a lower g_s in the field (Fig. 3-4) as compared to the glasshouse (Durand *et al.*, 2019), further reduced by the decreased water availability. This lower g_s would contribute to a higher W_i and thus a lower Δ, in agreement with our findings. Little is known about the stability of WUE between field and glasshouse experiment, with only a handful of studies showing either a strong (Ehdaie *et al.*, 1991), a weak (Lambrides *et al.*, 2004), a trend (Johnson & Bassett, 1991) or no correlation at all (Frank *et al.*, 1987).

This highlights the need for future studies to investigate the drivers behind these contrasting patterns. For example differences of stomatal dynamics along the day has been found to impact whole-plant transpiration in poplar genotypes, partly linked to variation in stomatal density and sizes (Durand *et al.*, 2019). Under field and glasshouse conditions, stomatal density, size and speed and their relation to transpiration and WUE may be different. The higher wind speed in the field than in the glasshouse may lead to widely different boundary layer conductance of the leaf, changing the relation between variations of environmental conditions and leaf transpiration. This highlights the need for future studies to investigate the drivers behind these contrasting patterns so that the opportunity to breed plants for improved water use does not remain beyond our reach forever.

ACKNOWLEDGEMENTS

This work was conducted in the frame of the WATBIO (Development of improved perennial biomass crops for water-stressed environments), a collaborative research project funded from the European Union's Seventh Programme for research, technological development and demonstration under grant agreement No. 311929. The research received funding from the French National Research Agency through the Laboratory of Excellence ARBRE (ANR-12-LABXARBRE-01). M.D. received a Ph.D. scholarship from the Lorraine Région and EFPA (INRA research department). We thank the nursery of Guéméné Penfao for providing the euramerican poplar cuttings. The authors acknowledge Marc Villar and Catherine Bastien from the UR0588-INRA Unit for access to the referenced Populus nigra clones 6J29 and N38 as well as Joseph Levillain, David Cohen and Irène Hummel for their technical help.

CONFLICT OF INTEREST

The authors declare that the research was conducted in the absence of any commercial or financial relationships that could be construed as a potential conflict of interest.

AUTHOR CONTRIBUTION

MD, CB, JBL, PC and DLT contributed to the data collection. MD, OB, AG and DLT contributed to the experimental design. MD, OB, DLT, JBL and AG contributed to data analysis and interpretation. All contributors were involved in the writing of the manuscript.

REFERENCES

Anyia AO, Slaski JJ, Nyachiro JM, Archambault DJ, Juskiw P. 2007. Relationship of carbon isotope discrimination to water use efficiency and productivity of barley under field and greenhouse conditions. *Journal of Agronomy and Crop Science* **193**(5): 313-323.

Bernacchi CJ, Singsaas EL, Pimentel C, Portis AR, Long SP. 2001. Improved temperature response functions for models of Rubisco-limited photosynthesis. *Plant Cell & Environment* **24**(2): 253-259.

Block RMA, Rees KCJ, Knight JD. 2006. A review of fine root dynamics in Populus plantations. *Agroforestry Systems* **67**(1): 73-84.

Bobich EG, Barron-Gafford GA, Rascher KG, Murthy R. 2010. Effects of drought and changes in vapour pressure deficit on water relations of Populus deltoides growing in ambient and elevated CO2. *Tree Physiology* **30**(7): 866-875.

Bogeat-Triboulot MB, Buré C, Gérardin T, Chuste PA, Le Thiec D, Hummel I, Durand M, Wildhagen H, Douthe C, Molins A, et al. 2019. Additive effects of high growth rate and low transpiration rate drive differences in whole plant transpiration efficiency among black poplar genotypes. *Environmental and Experimental Botany* **In press**.

Bonal D, Ponton S, Le Thiec D, Richard B, Ningre N, Hérault B, Ogée J, Gonzalez S, Pignal M, Sabatier D, et al. 2011. Leaf functional response to increasing atmospheric CO2 concentrations over the last century in two northern Amazonian tree species: a historical δ13C and δ18O approach using herbarium samples. *Plant, Cell & Environment* **34**(8): 1332-1344.

Bonan GB. 2008. Forests and climate change: forcings, feedbacks, and the climate benefits of forests. *Science* **320**(5882): 1444-1449.

Brugnoli E, Farquhar GD 2000. Photosynthetic fractionation of carbon isotopes. In: Leegood RC, Sharkey TD, von Caemmerer S eds. *Photosynthesis: physiology and metabolism.* . Dordrecht: Kluwer Academic Publishers, 399-434.

Brugnoli E, Hubick KT, von Caemmerer S, Wong SC, Farquhar GD. 1988. Correlation between the carbon isotope discrimination in leaf starch and sugars of C3 plants and the ratio of intercellular and atmospheric partial pressures of carbon dioxide. *Plant Physiology* **88**(4): 1418-1424.

Campany CE, Tjoelker MG, von Caemmerer S, Duursma RA. 2016. Coupled response of stomatal and mesophyll conductance to light enhances photosynthesis of shade leaves under sunflecks. *Plant Cell & Environment* **39**(12): 2762-2773.

Ceulemans R, Praet L, Jiang XN. 1995. Effects of CO2 enrichment, leaf position and clone on stomatal index and epidermal cell density in poplar (Populus). *New Phytologist* **131**(1): 99-107.

Chen SL, Wang SS, Altman A, Huttermann A. 1997. Genotypic variation in drought tolerance of poplar in relation to abscisic acid. *Tree Physiology* **17**(12): 797-803.

Ciais P, Reichstein M, Viovy N, Granier A, Ogee J, Allard V, Aubinet M, Buchmann N, Bernhofer C, Carrara A, et al. 2005. Europe-wide reduction in primary productivity caused by the heat and drought in 2003. *Nature* **437**(7058): 529-533.

Condon AG, Richards RA, Rebetzke GJ, Farquhar GD. 2004. Breeding for high water-use efficiency. *Journal of Experimental Botany* **55**(407): 2447-2460.

Coopman RE, Jara JC, Bravo LA, Sáez KL, Mella GR, Escobar R. 2008. Changes in morpho-physiological attributes of Eucalyptus globulus plants in response to different drought hardening treatments. *Electronic Journal of Biotechnology* **11**(2): 30-39.

Dai A. 2012. Increasing drought under global warming in observations and models. *Nature Climate Change* **3**: 52.

Dai AG. 2011. Drought under global warming: a review. *Wiley Interdisciplinary Reviews-Climate Change* **2**(1): 45-65.

Devi MJ, Bhatnagar-Mathur P, Sharma KK, Serraj R, Anwar SY, Vadez V. 2011. Relationships between transpiration efficiency and its surrogate traits in the rd29A:DREB1A transgenic lines of groundnut. *Journal of Agronomy and Crop Science* **197**(4): 272-283.

Di Baccio D, Minnocci A, Sebastiani L. 2010. Leaf structural modifications in Populus × euramericana subjected to Zn excess. *Biologia Plantarum* **54**(3): 502-508.

Durand M, Brendel O, Buré C, Le Thiec D. 2019. Altered stomatal dynamics induced by changes in irradiance and vapour-pressure deficit under drought: impact on the whole plant transpiration efficiency of poplar genotypes. *New Phytologist* **222**: 1789-1802.

Duursma RA. 2015. Plantecophys - An R package for analysing and modelling leaf gas exchange data. *Plos One* **10**(11).

Ehdaie B, Hall AE, Farquhar GD, Nguyen HT, Waines JG. 1991. Water-use efficiency and carbon isotope discrimination in Wheat. *Crop Science* **31**(5): 1282-1288.

Ehdaie B, Waines JG. 1993. Variation in water-use efficiency and its components in Wheat .1. Well-watered pot experiment. *Crop Science* **33**(2): 294-299.

FAO. 2018. Muller E, Kushlin A, Linhares-Juvenal T, Muchoney D, Wertz-Kanounnikoff S, Henderson-Howat D, eds. *The state of the world's forests*. Rome, Italy.

Farquhar GD, Buckley T, Miller J. 2002. Optimal stomatal control in relation to leaf area and nitrogen content. *Silva Fennica* **36**(3).

Farquhar GD, Ehleringer JR, Hubick KT. 1989. Carbon isotope discrimination and photosynthesis. *Annual Review of Plant Physiology and Plant Molecular Biology* **40**: 503-537.

Farquhar GD, O'Leary MHO, Berry J. 1982. On the relationship between carbon isotope discrimination and the intercellular carbon dioxide concentration in leaves. *Australian Journal of Plant Physiology* **9**: 121-137.

Fortier J, Truax B, Gagnon D, Lambert F. 2015. Plastic allometry in coarse root biomass of mature hybrid poplar plantations. *Bioenergy Research* **8**(4): 1691-1704.

Frank AB, Barker RE, Berdahl JD. 1987. Water-use efficiency of grasses grown under controlled and field conditions. *Agronomy Journal* **79**.

Ghashghaie J, Duranceau M, Badeck FW, Cornic G, Adeline MT, Deleens E. 2001. δ13C of CO2 respired in the dark in relation to δ13C of leaf metabolites: comparison between Nicotiana sylvestris and Helianthus annuus under drought. *Plant, Cell & Environment* **24**(5): 505-515.

Gillon JS, Griffiths H. 1997. The influence of (photo)respiration on carbon isotope discrimination in plants. *Plant, Cell & Environment* **20**(10): 1217-1230.

Giovannelli A, Deslauriers A, Fragnelli G, Scaletti L, Castro G, Rossi S, Crivellaro A. 2007. Evaluation of drought response of two poplar clones (Populus x canadensis Monch 'I-214' and P-deltoides Marsh. 'Dvina') through high resolution analysis of stem growth. *Journal of Experimental Botany* **58**(10): 2673-2683.

Granier A. 1985. A new method of sapflow measurement in tree stems. *Annales Des Sciences Forestieres* **42**(2): 193-200.

Granier A. 1987. Evaluation of transpiration in a Douglas-fir stand by means of sapflow measurements. *Tree Physiology* **3**(4): 309-319.

Gruber N, Galloway JN. 2008. An Earth-system perspective of the global nitrogen cycle. *Nature* **451**: 293.

Gutierrez MV, Meinzer FC. 1994. Carbon isotope discrimination and photosynthetic gas exchange in coffee hedgerows during canopy development. *Functional Plant Biology* **21**: 207-219.

Ham JM, Kluitenberg GJ, Lamont WJ. 1993. Optical-properties of plastic mulches affect the field temperature regime. *Journal of the American Society for Horticultural Science* **118**(2): 188-193.

Hamdy A, Ragab R, Scarascia-Mugnozza E. 2003. Coping with water scarcity: water saving and increasing water productivity. *Irrigation and Drainage* **52**(1): 3-20.

Hetherington AM, Woodward FI. 2003. The role of stomata in sensing and driving environmental change. *Nature* **424**(6951): 901-908.

Hostetler GL, Merwin I, Brown MG, Padilla-Zakour O. 2007. Influence of geotextile mulches on canopy microclimate, yield, and fruit composition of cabernet franc. *American Journal of Enology and Viticulture* **58**: 431-442.

Hubick KT, Farquhar GD. 1989. Carbon isotope discrimination and the ratio of carbon gained to water lost in Barley cultivars. *Plant Cell & Environment* **12**(8): 795-804.

Hubick KT, Farquhar GD, Shorter R. 1986. Correlation between water-use efficiency and carbon isotope discrimination in diverse peanut (arachis) germplasm. *Australian Journal of Plant Physiology* **13**(6): 803-816.

Ibrahim L, Proe MF, Cameron AD. 1998. Interactive effects of nitrogen and water availabilities on gas exchange and whole-plant carbon allocation in poplar. *Tree Physiology* **18**(7): 481-487.

IPCC. 2014. Meyer L, Brinkman S, van Kesteren L, Leprince-Ringuet N, van Boxmeer F, eds. *Climate change 2014: Synthesis report. Contribution of working groups I, II and III to the fifth assessment report of the intergovernmental panel on climate change*. Geneva, Switzerland: Cambridge University Press.

Johnson RC, Bassett LM. 1991. Carbon isotope discrimination and water use efficiency in four cool-season grasses. *Crop Science* **31**.

Lambrides CJ, Chapman SC, Shorter R. 2004. Genetic variation for carbon isotope discrimination in sunflower: association with transpiration efficiency and evidence for cytoplasmic inheritance. *Crop Science* **44**.

Liu ZJ, Dickmann DI. 1996. Effects of water and nitrogen interaction on net photosynthesis, stomatal conductance, and water-use efficiency in two hybrid poplar clones. *Physiologia Plantarum* **97**(3): 507-512.

Marino BD, McElroy MB. 1991. Isotopic composition of atmospheric CO2 inferred from carbon in C4 plant cellulose. *Nature* **349**(6305): 127-131.

Marron N, Villar M, Dreyer E, Delay D, Boudouresque E, Petit JM, Delmotte FM, Guehl JM, Brignolas F. 2005. Diversity of leaf traits related to productivity in 31 Populus deltoides x Populus nigra clones. *Tree Physiology* **25**(4): 425-435.

Monclus R, Dreyer E, Delmotte FM, Villar M, Delay D, Boudouresque E, Petit JM, Marron N, Brechet C, Brignolas F. 2005. Productivity, leaf traits and carbon isotope discrimination in 29 Populus deltoides x P-nigra clones. *New Phytologist* **167**(1): 53-62.

Monclus R, Dreyer E, Villar M, Delmotte FM, Delay D, Petit JM, Barbaroux C, Le Thiec D, Brechet C, Brignolas F. 2006. Impact of drought on productivity and water use efficiency in 29 genotypes of Populus deltoides x Populus nigra. *New Phytologist* **169**(4): 765-777.

Mooney HA, Ferrar PJ, Slatyer RO. 1978. Photosynthetic capacity and carbon allocation patterns in diverse growth forms of Eucalyptus. *Oecologia* **36**(1): 103-111.

Muller E, Lambs L. 2009. Daily variations of water use with vapor pressure deficit in a plantation of I214 poplars. *Water* **1**(1): 32.

Nickel UT, Winkler JB, Mühlhans S, Buegger F, Munch JC, Pritsch K. 2017. Nitrogen fertilisation reduces sink strength of poplar ectomycorrhizae during recovery after drought more than phosphorus fertilisation. *Plant and Soil* **419**(1): 405-422.

Normand M. 1974. Méthode d'étalonnage d'un humidimètre à neutrons utilisant les mesures de densité du densimètre gamma associé.: 53-69.

Nye PH, Tinker PB, Boast CW. 1979. Solute movement in the soil-root system. *Soil Science* **127**(4): 254.

Oren R, Sheriff DW 1995. Water and nutrient acquisition by roots and canopies. In: Smith WK, Hinckley TM eds. *Resource physiology of conifers. acquisition, allocation, and Utilization,*. San Diego, United States: Academic Press, Inc., 39-74.

Ponton S, Dupouey J-L, Nathalie B, Dreyer E. 2002. Comparison of water-use efficiency of seedlings from two sympatric oak species: Genotype x environment interactions. *Tree Physiology* **22**: 413-422.

Rasheed F, Dreyer E, Richard B, Brignolas F, Brendel O, Le Thiec D. 2015. Vapour pressure deficit during growth has little impact on genotypic differences of transpiration efficiency at leaf and whole-plant level: an example from Populus nigra L. *Plant Cell & Environment* **38**(4): 670-684.

Rasheed F, Dreyer E, Richard B, Brignolas F, Montpied P, Le Thiec D. 2013. Genotype differences in C-13 discrimination between atmosphere and leaf matter match differences in transpiration efficiency at leaf and whole-plant levels in hybrid Populus deltoides x nigra. *Plant Cell and Environment* **36**(1): 87-102.

Rasheed F, Richard B, Le Thiec D, Montpied P, Paillassa E, Brignolas F, Dreyer E. 2011. Time course of delta C-13 in poplar wood: genotype ranking remains stable over the life cycle in plantations despite some differences between cellulose and bulk wood. *Tree Physiology* **31**(11): 1183-1193.

Ray IM, Townsend MS, Muncy CH, Henning JA. 1999. Heritabilities of water-use efficiency traits and correlations with agronomic traits in water-stressed alfalfa. *Crop Science* **39**(2): 494-498.

Read JJ, Johnson DA, Asay KH, Tieszen LL. 1991. Carbon isotope discrimination, gas-exchange, and water-use efficiency in crested Wheatgrass clones. *Crop Science* **31**(5): 1203-1208.

Reich PB. 1984. Loss of stomatal function in ageing hybrid poplar leaves. *Annals of Botany* **53**(5): 691-698.

Roussel M, Dreyer E, Montpied P, Le-Provost G, Guehl JM, Brendel O. 2009a. The diversity of C-13 isotope discrimination in a Quercus robur full-sib family is associated with differences in intrinsic water use efficiency, transpiration efficiency, and stomatal conductance. *Journal of Experimental Botany* **60**(8): 2419-2431.

Roussel M, Le Thiec D, Montpied P, Ningre N, Guehl J-M, Brendel O. 2009b. Diversity of water use efficiency among Quercus robur genotypes: contribution of related leaf traits. *Annals of Forest Science* **66**(4): 408-408.

Sánchez-Gómez D, Robson TM, Gascó A, Gil-Pelegrín E, Aranda I. 2013. Differences in the leaf functional traits of six beech (Fagus sylvatica L.) populations are reflected in their response to water limitation. *Environmental and Experimental Botany* **87**: 110-119.

Sheffield J, Wood EF. 2008. Projected changes in drought occurrence under future global warming from multi-model, multi-scenario, IPCC AR4 simulations. *Climate Dynamics* **31**(1): 79-105.

Song JY, Wang Y, Pan YH, Pang JY, Zhang X, Fan JF, Zhang Y. 2019. The influence of nitrogen availability on anatomical and physiological responses of Populus alba x P-glandulosa to drought stress. *BMC Plant Biology* **19**.

Stobrawa K. 2014. *Poplars (Populus spp.): ecological role, applications and scientific perspectives in the 21st century*.

Touma D, Ashfaq M, Nayak MA, Kao S-C, Diffenbaugh NS. 2015. A multi-model and multi-index evaluation of drought characteristics in the 21st century. *Journal of Hydrology* **526**: 196-207.

Tschaplinski TJ, Blake TJ. 1989. Water relations, photosynthetic capacity, and root shoot partitioning of photosynthates as determinants of productivity in hybrid poplar. *Canadian Journal of Botany-Revue Canadienne De Botanique* **67**(6): 1689-1697.

Tschaplinski TJ, Tuskan GA, Gebre GM, Todd DE. 1998. Drought resistance of two hybrid Populus clones grown in a large-scale plantation. *Tree Physiology* **18**(10): 653-658.

Turner NC, Palta JA, Shrestha R, Ludwig C, Siddique KHM, Turner DW. 2007. Carbon isotope discrimination is not correlated with transpiration efficiency in three cool-season grain legumes (pulses). *Journal of Integrative Plant Biology* **49**(10): 1478-1483.

Viger M, Smith HK, Cohen D, Dewoody J, Trewin H, Steenackers M, Bastien C, Taylor G. 2016. Adaptive mechanisms and genomic plasticity for drought tolerance identified in European black poplar (Populus nigra L.). *Tree Physiology* **36**(7): 909-928.

Virgona JM, Farquhar GD. 1996. Genotypic variation in relative growth rate and carbon isotope discrimination in sunflower is related to photosynthetic capacity. *Australian Journal of Plant Physiology* **23**(2): 227-236.

Voltas J, Serrano L, Hernandez M, Peman J. 2006. Carbon isotope discrimination, gas exchange and stem growth of four euramerican hybrid poplars under different watering regimes. *New Forests* **31**(3): 435-451.

Walsh BD, MacKenzie AF, Buszard DJ. 1996a. Soil nitrate levels as influenced by apple orchard floor management systems. *Canadian Journal of Soil Science* **76**(3): 343-349.

Walsh BD, Salmins S, Buszard DJ, MacKenzie AF. 1996b. Impact of soil management systems on organic dwarf apple orchards and soil aggregate stability, bulk density, temperature and water content. *Canadian Journal of Soil Science* **76**(2): 203-209.

Wang H, Yang Z, Yu Y, Chen S, He Z, Wang Y, Jiang L, Wang G, Yang C, Liu B, et al. 2017. Drought enhances nitrogen uptake and assimilation in maize roots. *Agronomy Journal* **109**(1): 39-46.

Weih M, Bonosi L, Ghelardini L, Rönnberg-Wästljung AC. 2011. Optimizing nitrogen economy under drought: increased leaf nitrogen is an acclimation to water stress in willow (Salix spp.). *Annals of Botany* **108**(7): 1347-1353.

Wong SC, Cowan IR, Farquhar GD. 1979. Stomatal conductance correlates with photosynthetic capacity. *Nature* **282**(5737): 424-426.

Xu Cy, Lin Gh, Griffin KL, Sambrotto RN. 2004. Leaf respiratory CO2 is 13C-enriched relative to leaf organic components in five species of C3 plants. *New Phytologist* **163**(3): 499-505.

Zhang X, Zang R, Li C. 2004. Population differences in physiological and morphological adaptations of Populus davidiana seedlings in response to progressive drought stress. *Plant Science* **166**(3): 791-797.

TABLES

Table 1 Growth, biomass production and water use of two Populus deltoides × nigra (Carpaccio and I214) and two Populus nigra genotypes (6J29 and N38) under irrigated or a rainfall exclusion setup in the field. Values reported are means ± standard deviation of the difference between the end and the start of the experiment (n = 6). ANOVA factors were considered significant when $P < 0.05$. Letters show significant differences by post-hoc contrast among the eight groups (4 genotypes + 2 water treatments).

Genotype	Treatment	H (cm)	DBH (mm)	DM_T (g)	DM_S (g)	DM_L (g)	TLA (m^2)	LMA (g mm^{-2})	WU (kgH_2O)	E (kgH_2O m^{-2} d^{-1})	TE ($g.l^{-1}$)	$\Delta^{13}C$ (‰)
Carpaccio	irrigated	53 ± 11 a	3.3 ± 0.1 a	911 ± 531 a	684 ± 425 a	239 ± 58 a	2.59 ± 0.71 ab	0.95 ± 0.05 a	429 ± 163 ab	1 ± 0.09 de	2.26 ± 0.79 a	21.57 ± 0.55 e
	rainfall excl.	85 ± 17 cde	8.4 ± 1.9 d	2571 ± 1125 b	1960 ± 742 b	622 ± 324 b	5.79 ± 3.59 b	1.03 ± 0.07 ab	574 ± 63 c	0.73 ± 0.12 ab	4.02 ± 1.61 bc	18.72 ± 0.7 b
I214	irrigated	56 ± 9 ab	5 ± 1.6 ab	954 ± 407 a	638 ± 343 a	190 ± 50 a	2.06 ± 0.66 ab	0.95 ± 0.09 a	346 ± 74 a	0.89 ± 0.04 bcd	2.55 ± 0.57 ab	21.09 ± 0.34 de
	rainfall excl.	88 ± 21 de	8.5 ± 1.9 d	2563 ± 798 b	2133 ± 706 b	446 ± 266 ab	3.99 ± 2.55 ab	1.06 ± 0.07 bc	545 ± 88 bc	0.82 ± 0.16 abc	5.07 ± 0.65 cd	18.66 ± 0.43 b
6J29	irrigated	80 ± 10 cd	5.5 ± 0.4 bc	1216 ± 506 a	928 ± 399 a	235 ± 139 a	2.18 ± 1.37 ab	0.95 ± 0.11 a	391 ± 99 a	1.13 ± 0.12 e	3.39 ± 1.55 ab	20.74 ± 0.38 d
	rainfall excl.	98 ± 11 e	8.5 ± 1.3 d	2437 ± 497 b	2021 ± 341 b	415 ± 223 ab	3.48 ± 1.97 ab	1.07 ± 0.03 bc	468 ± 52 abc	0.95 ± 0.05 cd	4.98 ± 1.17 cd	19.39 ± 0.41 c
N38	irrigated	71 ± 8 bc	4.9 ± 0.6 ab	1084 ± 360 a	802 ± 405 a	148 ± 117 a	1.36 ± 1.07 a	1.05 ± 0.03 b	345 ± 84 a	0.8 ± 0.19 abc	2.93 ± 0.69 ab	19.99 ± 0.42 c
	rainfall excl.	99 ± 10 e	7 ± 1.7 cd	2139 ± 558 b	1840 ± 591 b	300 ± 199 ab	2.5 ± 1.74 ab	1.14 ± 0.02 c	351 ± 71 a	0.67 ± 0.09 a	5.75 ± 0.41 d	17.95 ± 0.93 a
P value	Genotype	**0.001**	ns	ns	ns	ns	ns	**0.001**	**0.002**	**< 0.001**	**0.049**	**< 0.001**
	Treatment	**< 0.001**	**< 0.001**	**< 0.001**	**< 0.001**	**0.001**	**0.005**	**< 0.001**	**< 0.001**	**< 0.001**	**< 0.001**	**< 0.001**
	Interaction	ns	ns	ns	ns	ns	ns	ns	ns	ns	ns	**0.014**

H, plant height increment; D, main stem diameter increment at 1.3 m; DM_T, total dry mass increment; DM_S, stem dry mass increment; DM_L, leaf dry mass increment; WU, cumulated water use; TLA, total leaf area increment; E, average daily whole-plant transpiration per unit leaf area; TE, transpiration efficiency; $\Delta^{13}C$, carbon isotopic discrimination from bulk leaves; ns, not significant.

FIGURES

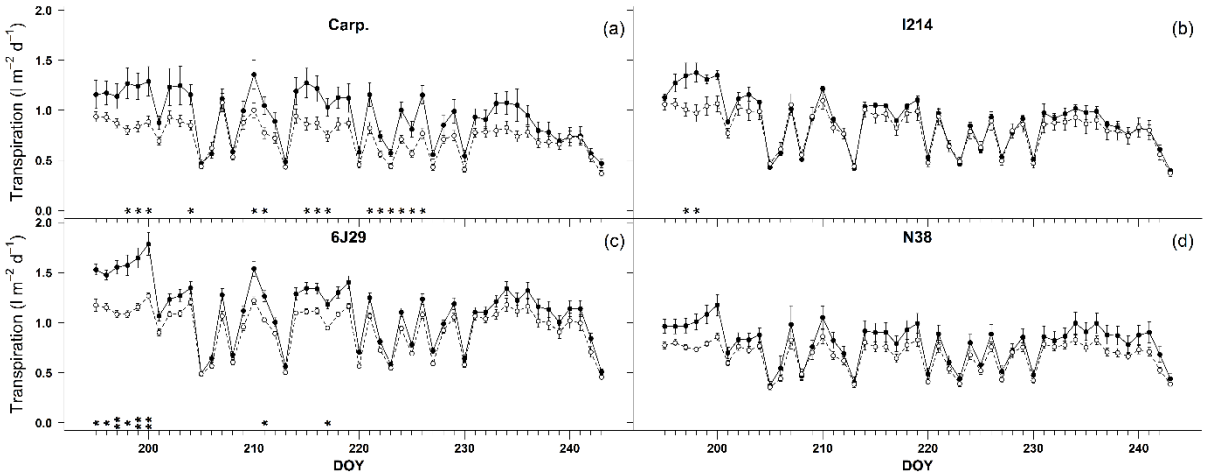

Figure 1. Daily transpiration per unit leaf area of two *Populus deltoides* × *nigra* Carpaccio (**a**), I214 (**b**) and two *Populus nigra* genotypes 6J29 (**c**), N38 (**d**) under irrigation or a rainfall exclusion setup in the field in 2017. Black and white circles are respectively for irrigated and rainfall exclusion trees (means ± standard error). Significant differences between water treatments for each date is shown (n = 6). *, $P < 0.05$; **, $P < 0.01$; ***, $P < 0.001$; ns, not significant.

.

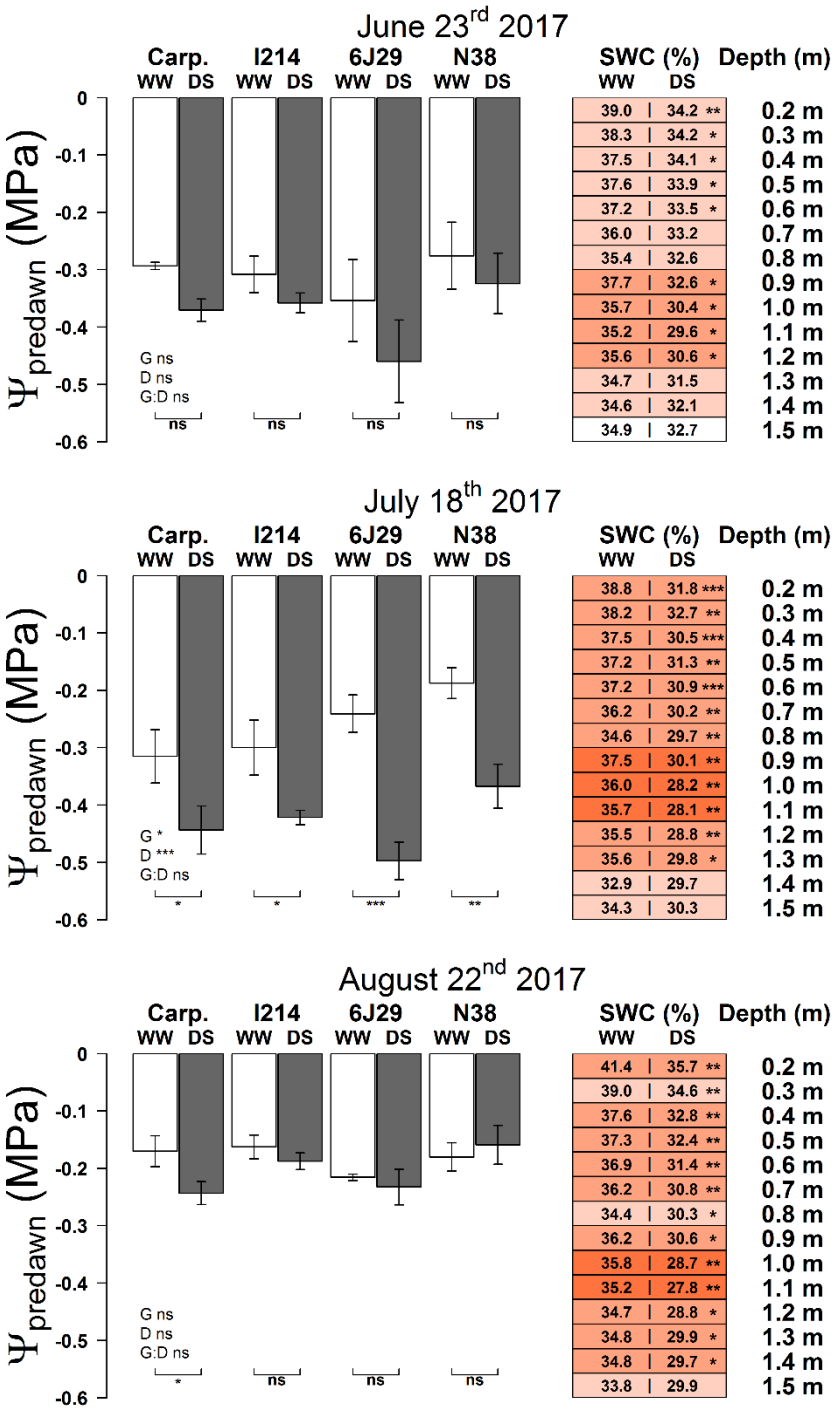

Figure 2. Predawn leaf water potential (left side) of two *Populus deltoides* × *nigra* (Carpaccio and I214) and two *Populus nigra* genotypes (6J29 and N38) and soil water content (right side) under irrigation or a rainfall exclusion setup in the field at three dates. Values reported are means ± standard error (n = 6). WW and DS is for irrigated and rainfall exclusion trees respectively (white and gray bars respectively). Mean soil water content (SWC) is shown for each 10cm in depth with stronger colors indicating stronger differences between treatments. Results of two-way ANOVA are given for main effects (G: genotype; D: water treatment) and interaction (G:D). Significant differences between water treatments are reported. *, $P < 0.05$; **, $P < 0.01$; ***, $P < 0.001$; ns, not significant.

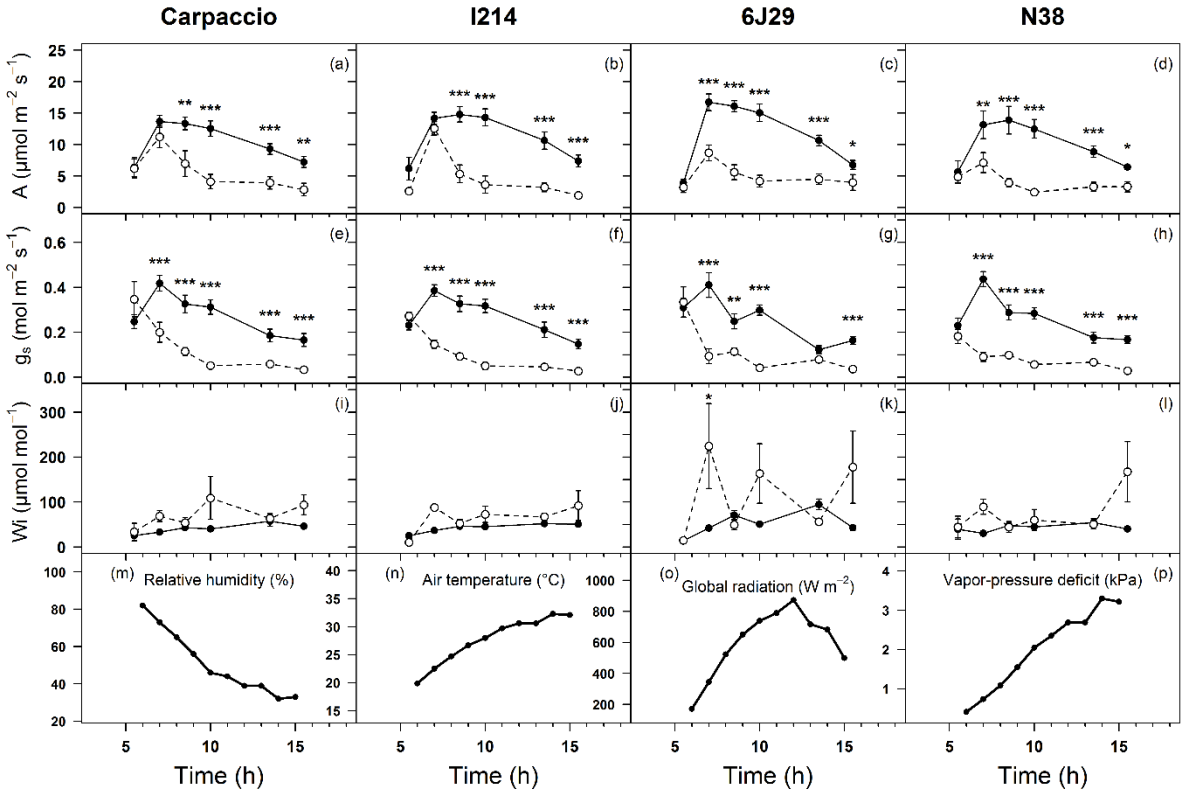

Figure 3. Gas-exchange dynamic of two *Populus deltoides* × *nigra* Carpaccio (**a**, **e** and **i**), I214 (**b**, **f** and **j**), and two *Populus nigra* genotypes 6J29 (**c**, **g** and **k**), N38 (**d**, **h** and **l**) under irrigation or a rainfall exclusion setup in the field. (**a**) to (**d**): net CO_2 assimilation, (**e**) to (**h**): stomatal conductance to water vapour and (**i**) to (**l**): intrinsic water use efficiency. Relative humidity (**m**), air temperature (**n**), global radiation (**o**) and atmospheric vapour-pressure deficit (**p**) in the field are also reported. Black and white circles are respectively for irrigated and rainfall exclusion trees (means ± standard error). All measurements were done on the 199st day of the year (July 18th), including the meteorological data. Significant differences between water treatments for each time is shown (n = 4-6). *, $P < 0.05$; **, $P < 0.01$; ***, $P < 0.001$; ns, not significant.

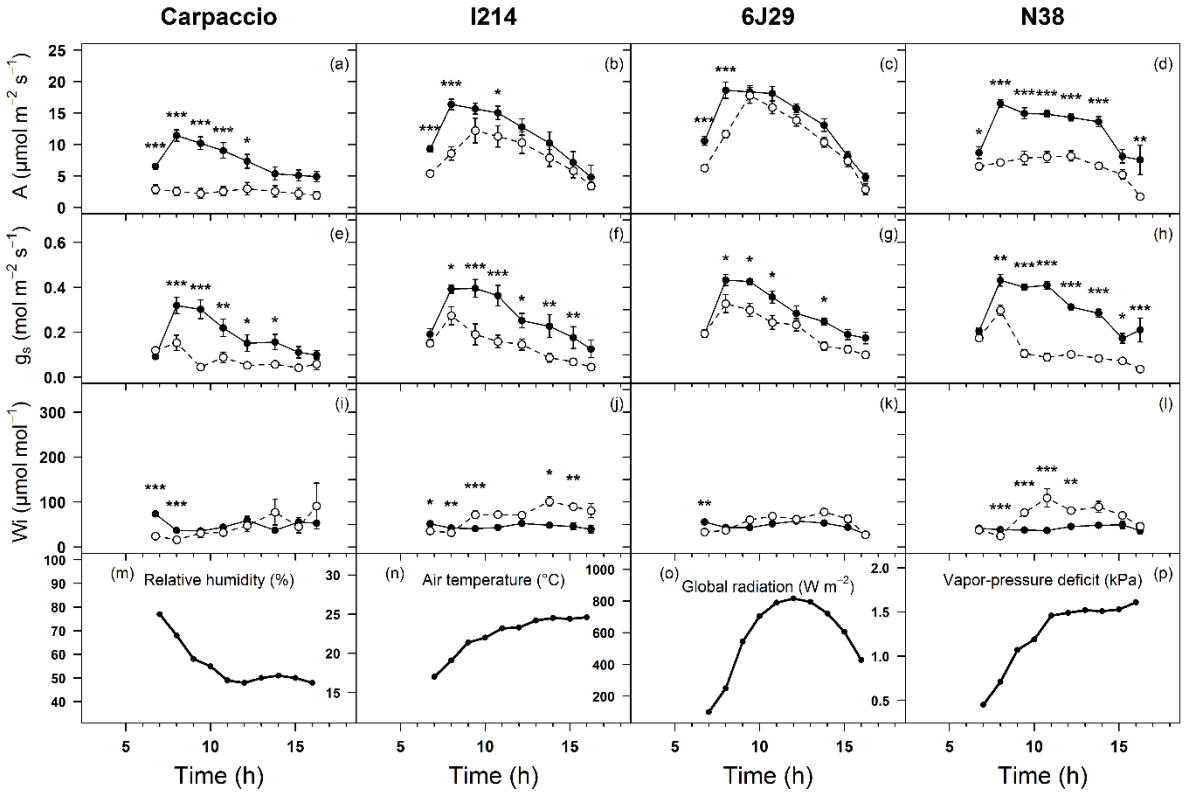

Figure 4. Gas-exchange dynamic of two *Populus deltoides* × *nigra* Carpaccio (**a**, **e** and **i**), I214 (**b**, **f** and **j**), and two *Populus nigra* genotypes 6J29 (**c**, **g** and **k**), N38 (**d**, **h** and **l**) under irrigation or a rainfall exclusion setup in the field. (**a**) to (**d**): net CO_2 assimilation, (**e**) to (**h**): stomatal conductance to water vapour and (**i**) to (**l**): intrinsic water use efficiency. Relative humidity (**m**), air temperature (**n**), global radiation (**o**) and atmospheric vapour-pressure deficit (**p**) in the field are also reported. Black and white circles are respectively for irrigated and rainfall exclusion trees (means ± standard error). All measurements were done on the 234st day of the year (August 22nd), including the meteorological data. Significant differences between water treatments for each time is shown (n = 4-6). *, $P < 0.05$; **, $P < 0.01$; ***, $P < 0.001$; ns, not significant.

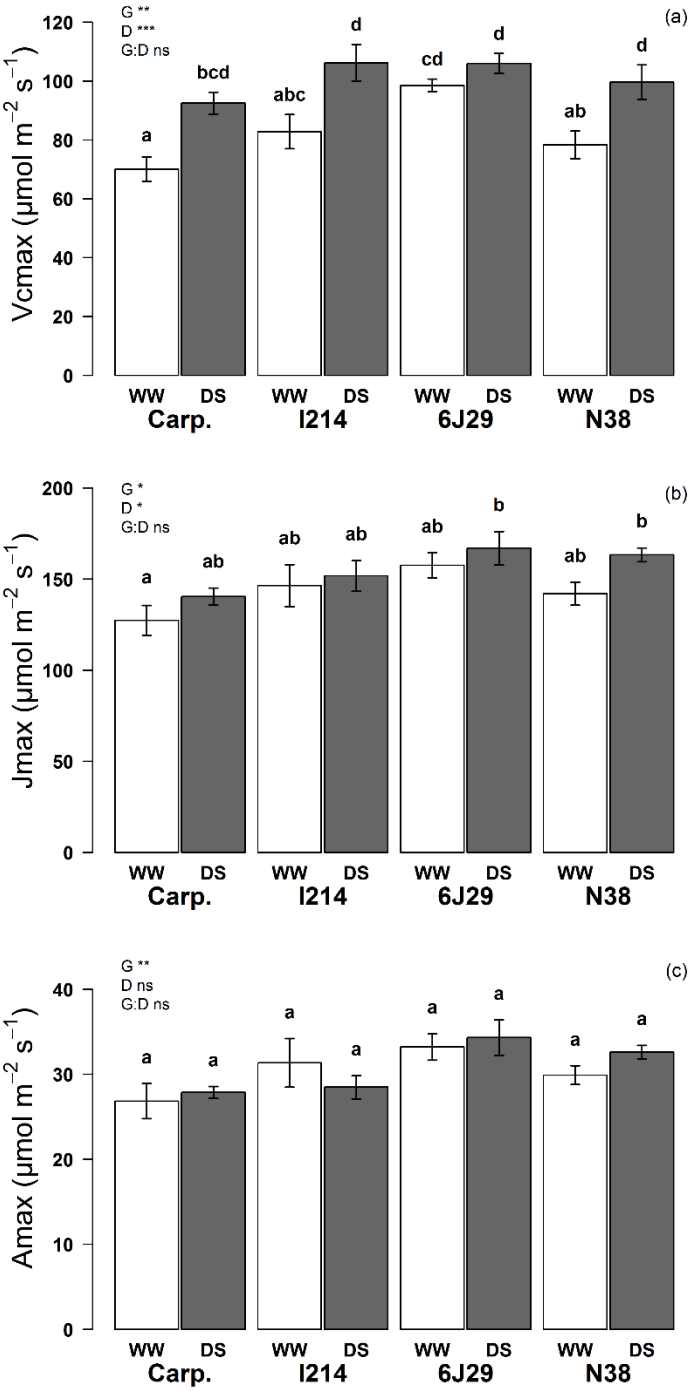

Figure 5. Photosynthetic capacity data of two *Populus deltoides* × *nigra* (Carpaccio and I214) and two *Populus nigra* genotypes (6J29 and N38) under irrigation or a water exclusion setup in the field. a) Maximum rate of rubisco carboxylation (V_{cmax}) b) maximum rate of electron transport (J_{max}) c) maximum CO_2 assimilation under saturating CO_2 concentration (A_{max}). Values reported are means ± standard error (n = 6**).** WW and DS is for irrigated and rainfall exclusion trees respectively (white and gray bars respectively). Results of two-way ANOVA are given for main effects (G: genotype; D: water treatment) and interaction (G:D). Significant differences between water treatments are reported. ***,** P < 0.05; **, P < 0.01; ***, P < 0.001; ns, not significant.

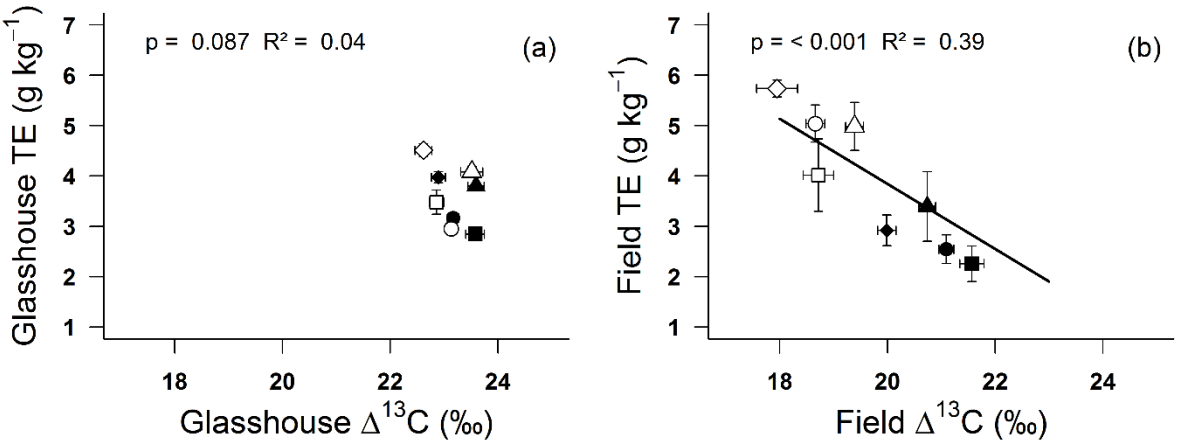

Figure 6. Correlations between a glasshouse and a field experiment on two *Populus deltoides* × *nigra* (Carpaccio and I214) and two *Populus nigra* genotypes (6J29 and N38) under well-watered or reduced water availability. a) Transpiration efficiency and carbon isotopic discrimination in the glasshouse experiment b) Transpiration efficiency and carbon isotopic discrimination in the field experiment. Closed and open symbols are for well-watered and reduced water availability, respectively. Squares, circles, triangles and diamonds are for Carpaccio, I214, 6J29 and N38, respectively. Values reported are means ± standard error (n = 6). *P* and R^2 values are shown.

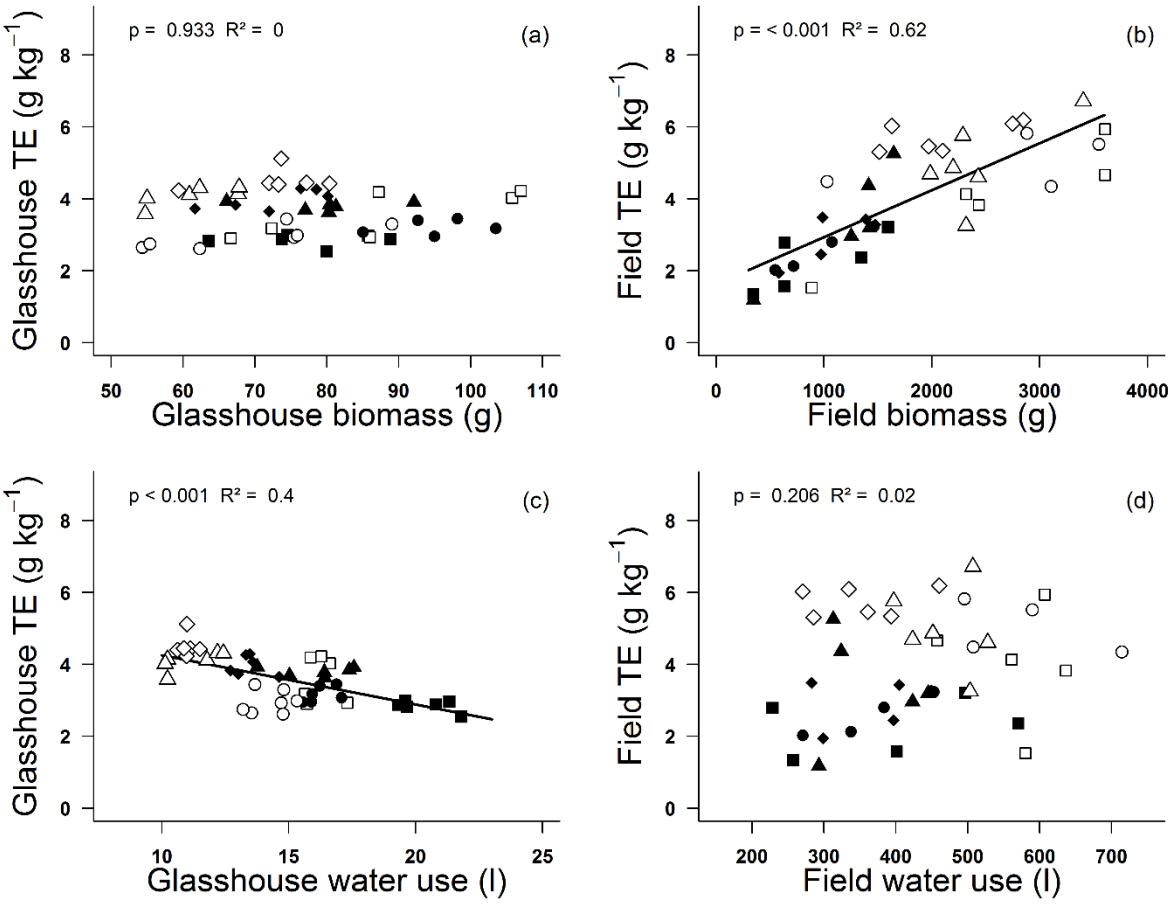

Figure 7. Correlations on two *Populus deltoides* × *nigra* (Carpaccio and I214) and two *Populus nigra* genotypes (6J29 and N38) under well-watered or reduced water availability either in a glasshouse or a field experiment. a) Transpiration efficiency and biomass production in the glasshouse b) Transpiration efficiency and whole-plant water use in the glasshouse c) Transpiration efficiency and biomass production in the field d) Transpiration efficiency and whole-plant water use in the field. Closed and open symbols are for well-watered and reduced water availability, respectively. Squares, circles, triangles and diamonds are for Carpaccio, I214, 6J29 and N38, respectively. *P* and R^2 values are shown.

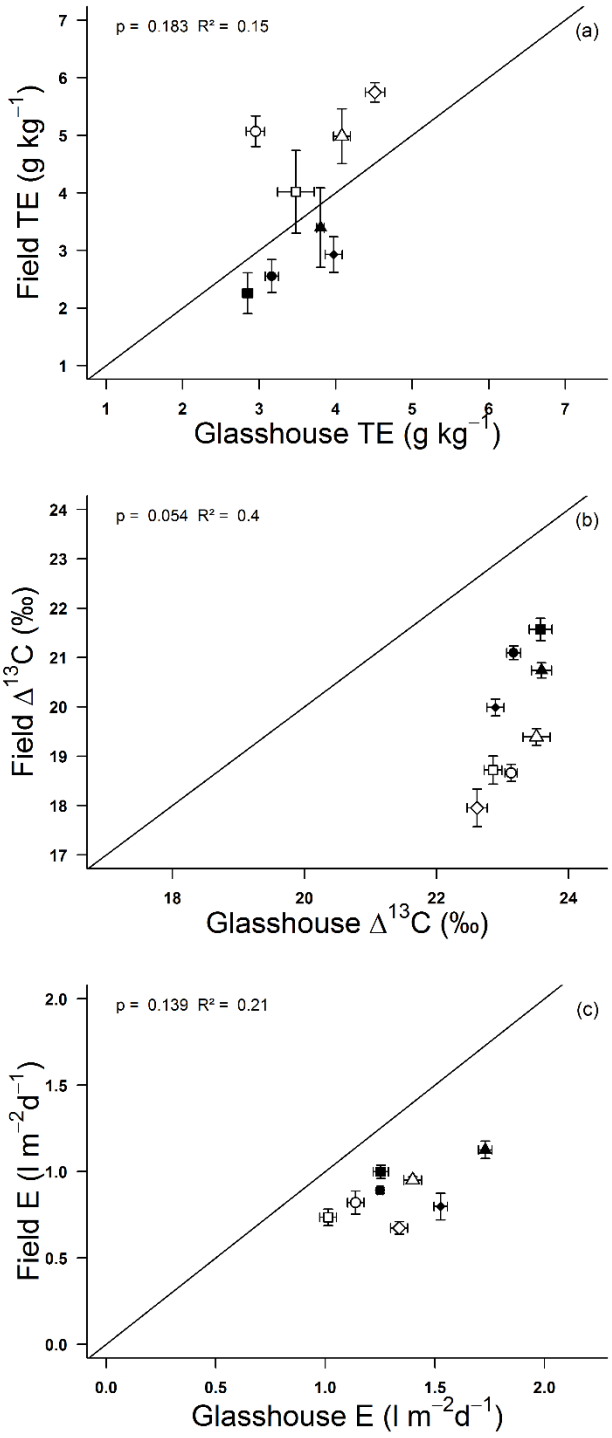

Figure 8. Correlations between a glasshouse and a field experiment on two *Populus deltoides* × *nigra* (Carpaccio and I214) and two *Populus nigra* genotypes (6J29 and N38) under well-watered or reduced water availability. a) Transpiration efficiency b) Carbon isotopic discrimination c) Mean daily whole-plant transpiration per unit leaf area. Closed and open symbols are for well-watered and reduced water availability, respectively. Squares, circles, triangles and diamonds are for Carpaccio, I214, 6J29 and N38, respectively. Values reported are means ± standard error (n = 6). *P* and R^2 values are shown. The straight continuous line shows the 1:1 regression line.

DONNÉES SUPPLÉMENTAIRES

Table S1. Growth and biomass production of two *Populus deltoides* × *nigra* (Carpaccio and I214) and two *Populus nigra* genotypes (6J29 and N38) under irrigation or a water exclusion setup in the field. Values reported are means ± standard deviation (n = 5-6). ANOVA factors were considered significant when $p < 0.05$. Letters show significant differences by *post-hoc* contrast analysis among the eight groups (4 genotypes + 2 water treatments) for each harvest (2016 and 2017).

Harvest	Genotype	Treatment	H (cm)	DMs (g)	DML (g)
September 2017	Carpaccio	control	520 ± 25 ab	3124 ± 616 a	988 ± 153 a
		drought	590 ± 38 c	6266 ± 1075 c	2102 ± 257 c
	I214	control	480 ± 27 a	2449 ± 555 a	811 ± 185 a
		drought	521 ± 48 ab	5675 ± 2465 c	1826 ± 547 bc
	6J29	control	518 ± 29 ab	2715 ± 642 a	835 ± 187 a
		drought	546 ± 18 b	4869 ± 608 bc	1537 ± 186 b
	N38	control	505 ± 24 ab	2601 ± 482 a	960 ± 230 a
		drought	513 ± 15 ab	3909 ± 932 ab	1501 ± 269 b
	P value	Genotype	**< 0.001**	**0.024**	**0.015**
		Treatment	**< 0.001**	**< 0.001**	**< 0.001**
		Interaction	ns	ns	ns
April 2016	Carpaccio	control	229 ± 44 a	336 ± 193 a	
		drought	232 ± 45 a	326 ± 178 a	
	I214	control	211 ± 25 a	173 ± 55 a	
		drought	216 ± 30 a	205 ± 109 a	
	6J29	control	246 ± 23 a	245 ± 87 a	
		drought	219 ± 23 a	180 ± 49 a	
	N38	control	230 ± 14 a	218 ± 53 a	
		drought	202 ± 28 a	174 ± 61 a	
	P value	Genotype	ns	**0.018**	
		Treatment	ns	ns	
		Interaction	ns	ns	

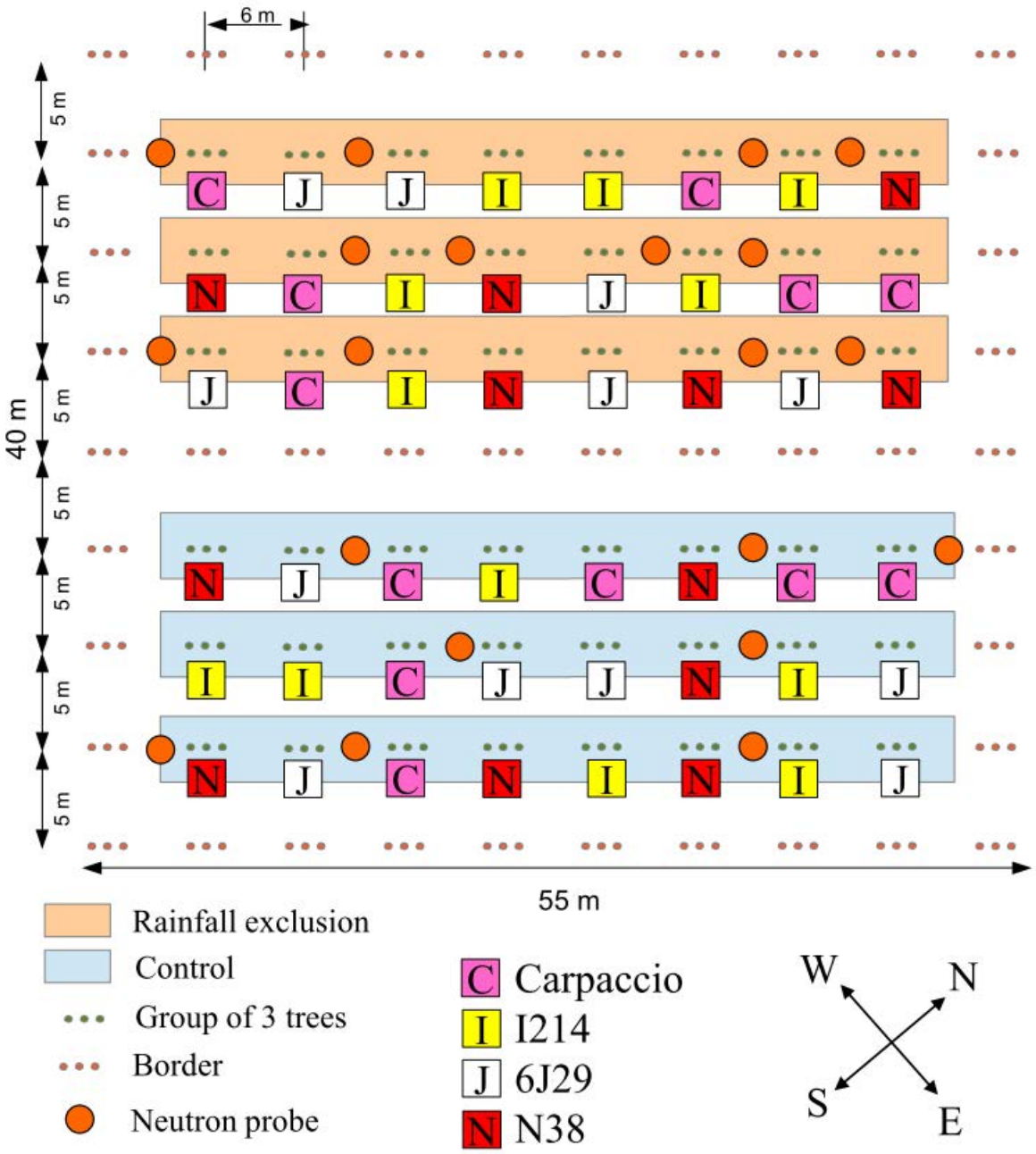

Figure S1. Experimental design for the poplar plantation in the field.

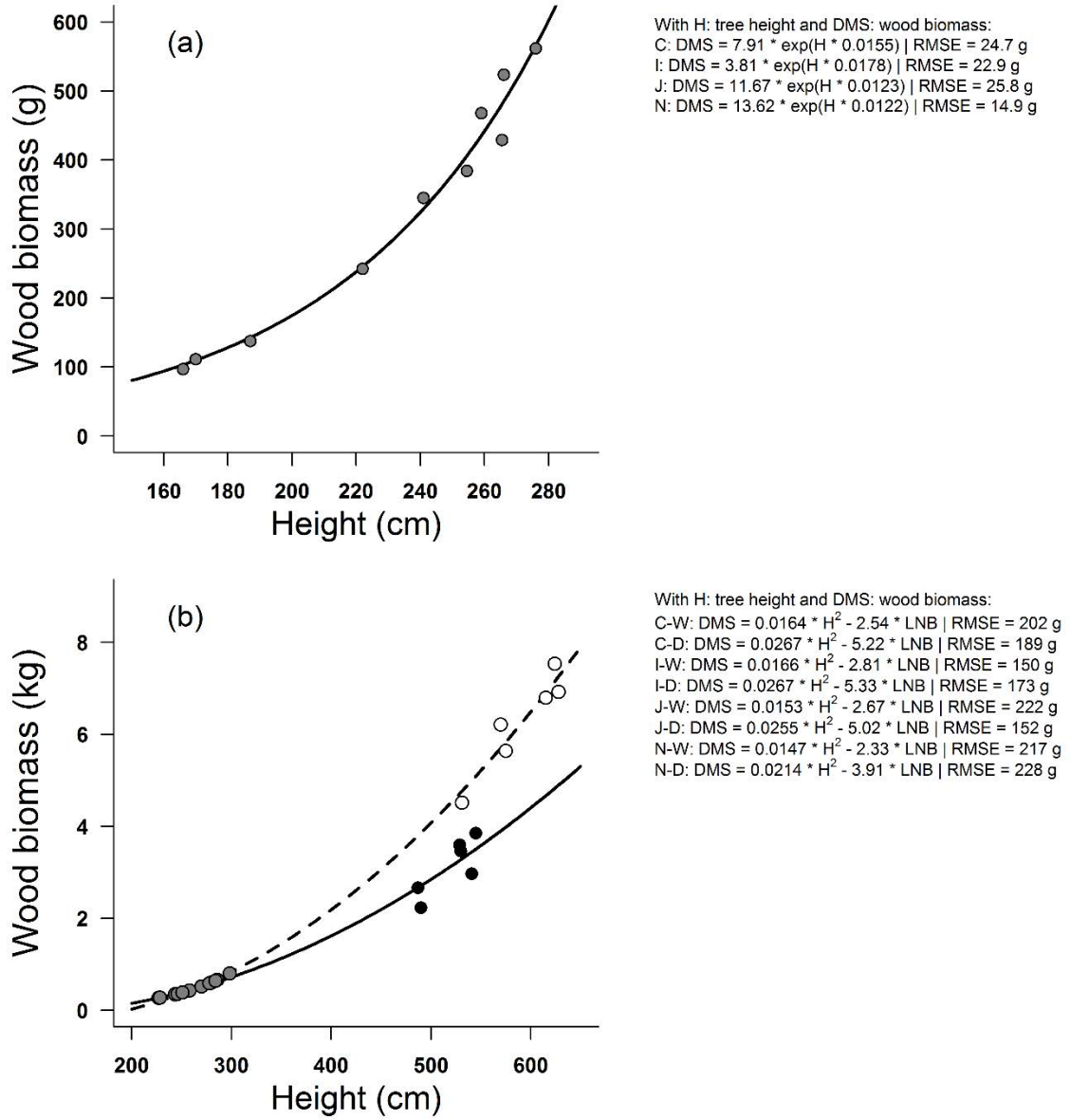

Figure S2. Allometries for wood biomass estimation in irrigated or rainfall exclusion Carpaccio trees (Populus deltoides × nigra) in the field. a) Allometry between plant height and wood biomass on 48 harvested trees in April 2016. b) Allometry between plant height and wood biomass on 48 harvested trees in September 2017. Black and white circles are of irrigated and rainfall exclusion trees respectively. Gray circles are for the April 2016 biomass and height of the harvested trees, either measured in April 2016 (a) or calculated in September 2017 (b). Continuous and dashed lines are the predicted values of the relationship for irrigated and rainfall exclusion trees respectively. Equations for each combination of genotype (C, I, J and N is for Carpaccio, I214, 6J29 and N38 respectively) and water treatment (W and D is for irrigated and rainfall exclusion trees respectively) is given along with their residual mean squared error (RMSE).

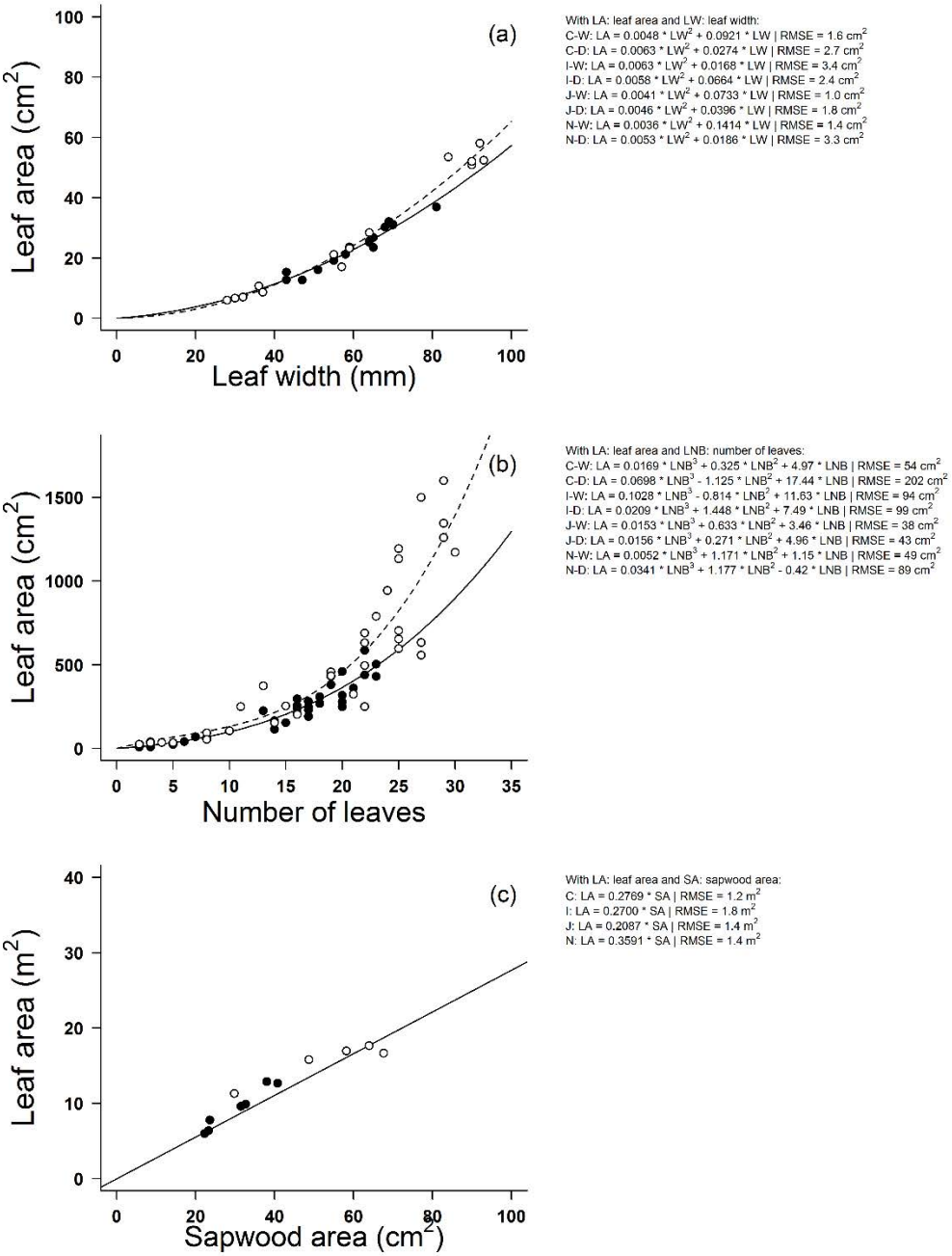

Figure S3. Allometries for total leaf area estimation in irrigated or rainfall exclusion Carpaccio trees (Populus deltoides × nigra) in the field. a) Allometries between leaf width and leaf area. b) Allometries between the number of leaves on a branch and the total leaf area of that branch. c) Allometries between the sapwood area of the main stem and the total leaf area of a tree. Black and white circles are of irrigated and rainfall exclusion trees respectively. Continuous and dashed lines are the predicted values of the relationship for irrigated and rainfall exclusion trees respectively. Equations for each combination of genotype (C, I, J and N is for Carpaccio, I214, 6J29 and N38 respectively) and water treatment (W and D is for irrigated and rainfall exclusion trees respectively) is given along with their residual mean squared error (RMSE).

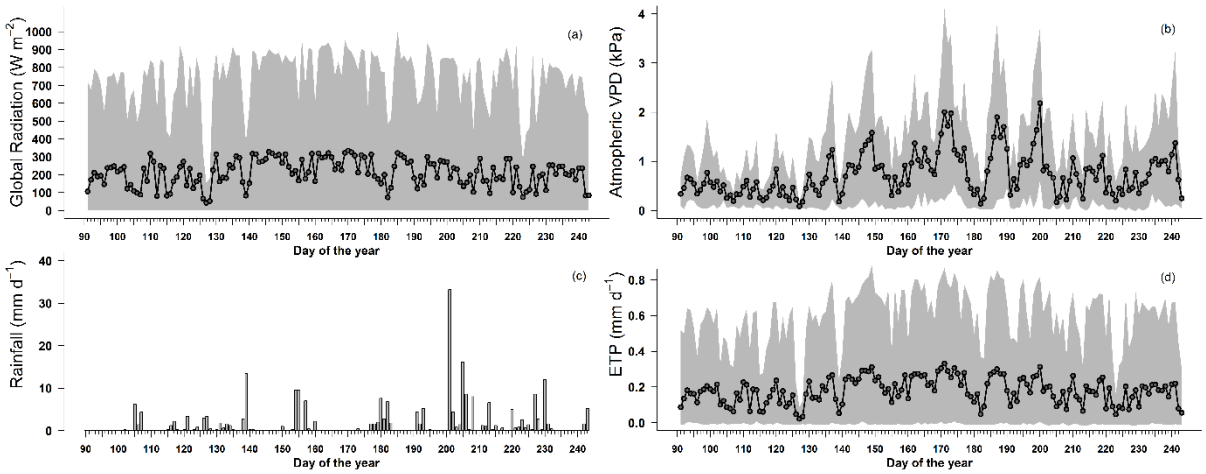

Figure S4. Weather data during the 2017 growth season, from April 1st (91st day) to August 31st (243th day) 2017. a) global radiation b) atmospheric vapour pressure deficit (VPD) c) rainfall and d) potential evapotranspiration (ETP) calculated from the Penman equation. Gray circles show the daily means and the gray area show the range as the difference between maximum and minimum daily values.

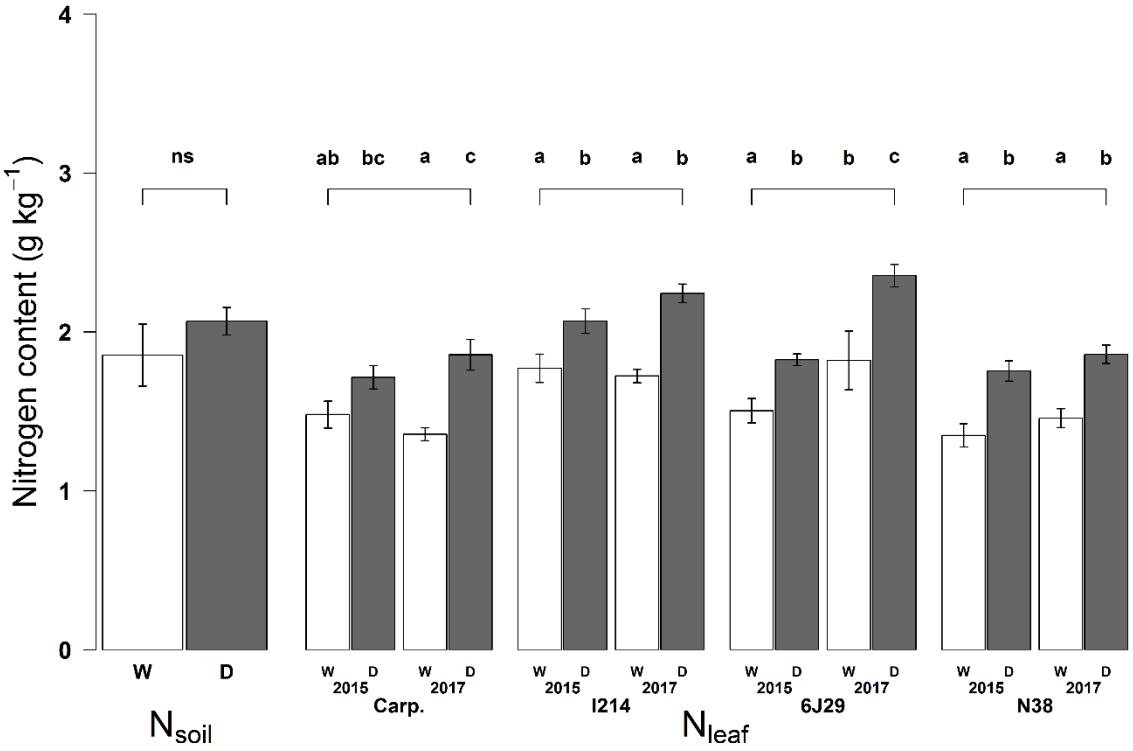

Figure S5. Soil and leaf nitrogen content, N_{soil} and N_{leaf} respectively in the field on two *Populus deltoides* × *nigra* (Carpaccio and I214) and two *Populus nigra* (6J29 and N38) genotypes. Soil nitrogen content was measured in October 2017. Leaf nitrogen content was measured in September 2015 and 2017. W and D (white and gray bars respectively) are for the irrigated and rainfall exclusion plots or trees. Values reported are means ± standard error (n = 6). Letters show significant differences among year and water treatment for each genotype by *post-hoc* contrast analysis. ns: not significant.

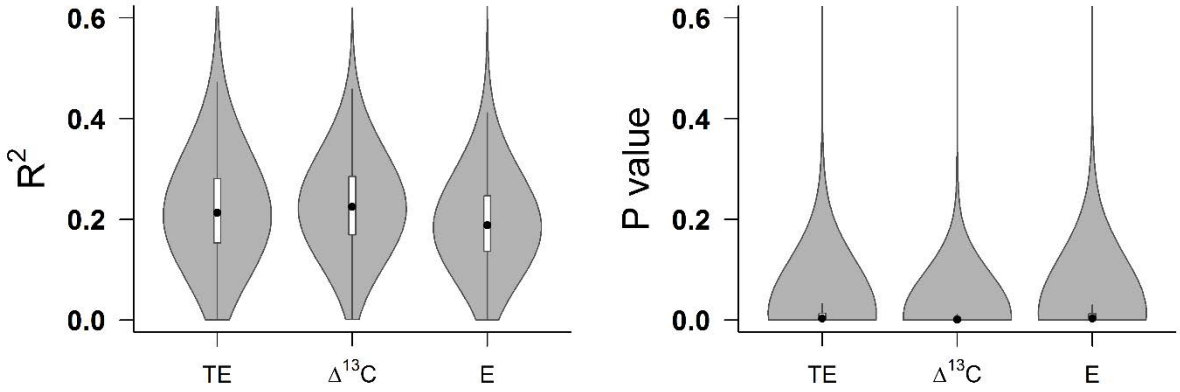

Figure S6. Distribution of R^2 (a) and *P* values (b) from linear regression between glasshouse and field values of TE, Δ and E randomly paired for each genotype and water regime. Boxes show the 25th and 75th percentiles, lines show the 10th, 90th percentiles and the point the median. The outer curved lines show the density distribution of either R^2 or *P* values from 1,000,000 random samplings.

Transition

Au cours de ce chapitre nous avons pu mettre en évidence des similitudes assez fortes de l'efficience d'utilisation de l'eau entre le niveau foliaire et le niveau de la plante entière pour chacune des deux conditions environnementales. Egalement, le classement des génotypes était généralement maintenu au niveau foliaire et au niveau de la plante entière entre conditions environnementales, mais pas entre régimes hydriques. Nous avons pu voir qu'en dépit de ces résultats, à l'échelle de la plante entière les variations de l'efficience de transpiration entre génotypes étaient dues à différents trait sous-jacents en serre et en pépinière.

Il est connu que la densité stomatique peut être modifiée chez les peupliers en fonction des conditions du milieu (Bobich et al., 2010; Di Baccio et al., 2010). Ces différences pourraient également entrainer des variations de la taille des stomates, puisque ces deux variables semblent corrélées entre elles à travers une multitude d'espèces (Hetherington & Woodward, 2003. Si c'est le cas, ces différences pourraient induire des variations de la dynamique stomatique, agissant également au niveau de la transpiration de la plante entière (voir Chapitre I).

CHAPITRE III

Impact des conditions de croissance sur la dynamique stomatique induite par des changements de l'irradiance ou du VPD.

CHAPITRE III :
Impact des conditions de croissance sur la dynamique stomatique induite par des changements de l'irradiance ou du VPD.

Présentation synthétique de l'article

Contexte

Les stomates sont responsables de la majorité des flux d'eau et de CO_2 sortant et entrant de la feuille, respectivement. Composés de deux cellules de garde, ils sont capables de modifier leur ouverture et se faisant, peuvent favoriser ou limiter les échanges gazeux avec l'atmosphère. Ces mouvements sont relativement lents (> 20 min) et peuvent entrainer un découplage entre les conditions environnementales et la vitesse des flux d'H_2O et de CO_2. Ainsi la dynamique temporelle des mouvements stomatiques impose des limitations sur le suivi des conditions extérieures par les stomates, ce qui pourrait induire sur le long terme une plus forte consommation en eau et/ou un « manque à gagner » en termes d'assimilation du carbone. De plus, il a été montré expérimentalement que non seulement l'intensité mais également les fluctuations d'irradiance pendant la croissance impactent la dynamique temporelle des mouvements stomatiques (Matthews *et al.*, 2018). Ces mesures sont bien souvent réalisées sur des plants élevés en conditions contrôlées. Pourtant il existe de nombreuses conditions environnementales, d'intensité et ayant des fluctuations différentes en conditions contrôlées et naturelles (vitesse du vent, irradiance, VPD et températures). Chacune de ces variables, qui participent à l'acclimatation de la plante, pourraient intervenir dans la plasticité génotypique des dynamiques stomatiques.

Objectifs

Nous avons réalisé des mesures de la dynamique temporelle des stomates en réponse à des changements d'irradiance et de VPD sur des peupliers plantés en conditions naturelles sous différents régimes hydriques. Ces données ont été comparées à un jeu de données similaire, publié précédemment (Chapitre I), sur les mêmes génotypes de peupliers élevés en conditions contrôlées (serre) également sous différents régimes hydriques. Ce travail permettra (1) de déterminer si les différences génotypiques et entre régimes hydriques observés en serre sont maintenue en conditions naturelles, et (2) d'établir si les corrélations entre la dynamique

stomatique et la morphologie des stomates, ainsi qu'avec les pertes en eau à l'échelle de la plante entière sont retrouvées, indépendamment des conditions de croissance.

Stratégie

Deux génotypes de peupliers euraméricains (Carpaccio et I214) et deux génotypes de peupliers noirs (6J29 et N38) ont été utilisés au cours des deux expériences. La mise en place de l'expérimentation en serre et en pépinière a été détaillée au cours du chapitre I et II, respectivement. La dynamique stomatique peut être quantifiée à l'aide de systèmes d'échanges gazeux, qui permettent de réguler et de stabiliser les conditions environnementales. La variation de l'irradiance et du VPD (dans le cadre d'expériences séparées) induisent des mouvements stomatiques, enregistrés et ajustés avec un modèle de la dynamique temporelle stomatique. Ce modèle est composé de paramètres décrivant la réponse stomatique et sont comparables entre expériences. Les paramètres dynamiques des plantes en pépinière ont été mesurés et comparés à ceux de la serre (voir Chapitre I).

Résultats et conclusions

Nous avons observé un faible effet génotypique et du régime hydrique sur la dynamique stomatique en conditions naturelles. Ceci contraste avec la variabilité génotypique et entre traitements hydriques observés en serre. Cependant I214 et 6J29, respectivement le génotype le plus rapide et le plus lent en réponse à l'irradiance et au VPD pendant l'expérimentation en serre, le sont également en conditions naturelles. Ce qui suggère que les dynamiques temporelles stomatiques seraient liées à des facteurs endogènes et environnementaux. Le cas échéant, il est possible qu'une réponse stomatique plus lente puisse avoir des avantages dans certaines conditions, notamment en limitant le coût énergétique des mouvements stomatiques qu'un suivi parfait des conditions extérieures aurait.

En conditions naturelles les stomates étaient plus lents, plus nombreux et plus petits qu'en conditions contrôlées. L'irradiance étant bien plus forte en conditions naturelles, ces résultats sont en accord avec l'augmentation généralement observée de la densité stomatique avec l'intensité de l'irradiance lumineuse. Cependant ce résultat est également contradictoire avec l'hypothèse proposant que des stomates plus petits soient plus rapides. Quelques faibles corrélations ont néanmoins été détectées avec la morphologie stomatique. Ces résultats suggèrent que la contribution de la morphologie stomatique à la dynamique stomatique dépend des conditions environnementales de culture.

Article: Impacts of growing conditions on the stability of stomatal dynamics induced by changes in irradiance and vapour-pressure deficit.

En préparation

MAXIME DURAND[1] • OLIVER BRENDEL[1] • CYRIL BURÉ[1] • DIDIER LE THIEC[1]

[1] *Inra, Université de Lorraine, AgroParisTech, SILVA, F-54280 Champenoux, France*

Correspondance:

Didier Le Thiec

Email: didier.lethiec@inra.fr

Telephone: (+33) 3 83 39 40 98

ABSTRACT

• Recent investigations showed how acclimation of plants to diverse patterns of light intensity modified the dynamic response of stomata. Therefore if plants are grown in controlled conditions or in the field, it may have an impact on the stomatal dynamics.

• We analyzed stomatal dynamics on two *Populus euramericana* (Moench.) and two *Populus nigra* (L.) genotypes grown in the field under contrasting water availability. By comparing this dataset with stomatal dynamics of the same genotypes grown in a glasshouse, we were able to examine if the differences between growing conditions would have an impact on genotypic differences in stomatal dynamics and their response to a soil water deficit.

• We found stomatal dynamics were much slower in the field than in the glasshouse, despite higher stomatal density and smaller stomatal size. Overall, differences among genotypes and their response to a soil water deficit were much less pronounced in the field compared to the glasshouse.

• These results suggest that stomatal dynamics are regulated by both endogenous and environmental factors. Moreover, having slower stomata may be advantageous under certain conditions. While stomatal dynamics were linked with whole-plant transpiration in both experiments, the contribution of stomatal morphology seems to depend on environmental conditions.

KEYWORDS

drought, kinetics of stomatal responses, light, *Populus*, stomatal conductance, VPD, growing conditions

INTRODUCTION

The majority of gas exchange between the leaf sub-stomatal cavities and the atmosphere are controlled by stomata. Thus they play a pivotal role in regulating the inward flow of CO_2 for photosynthesis and the outward flow of water by transpiration. They are composed of two guard cells able to change in volume so that the central aperture can be increased or reduced. The size of the stomatal aperture together with the number of stomata on an area basis (*i.e*. stomatal density) shape the resistance to diffusion between the leaf and the surrounding air. This stomatal resistance in usually expressed as its inverse, a stomatal conductance (g_s). A number of endogenous and external factors can cause an adjustment of g_s, such as circadian rythms (de Dios, 2017), irradiance (Shimazaki *et al.*, 2007), vapor pressure deficit (Mc Adam & Brodribb, 2015) and soil water availability (Monclus *et al.*, 2006), among others. Cowan & Farquhar (1977) proposed that g_s is regulated so that the CO_2 intake is at a maximum with regards to the water transpired. This key process at the interface between the plant and environment can become of critical importance when soil water conditions are limiting.

An increasing proportion of Earth's surface is subject to soil water deficits since 1950 (Dai, 2011), and current global climate models predict for the coming years a reduction of soil moisture and more frequent drought events of increased intensity and duration (Sheffield & Wood, 2008; Dai, 2012; IPCC, 2014). Not only will they cause severe and durable consequences on society and economies (Touma *et al.*, 2015), droughts are a central concern of global change research for their effect on forests, given the tight relation between forests and climate (Bonan, 2008). Reductions of productivity are an expected outcome of a decline in soil moisture, especially in species with a large water use such as poplars and eucalypts (Monclus *et al.*, 2006; Coopman *et al.*, 2008). Since the growth of poplars is closely linked to water availability, they are naturally distributed along riparian habitats (Tschaplinski & Blake, 1989). However, their cultivation extends to mesophyte habitats where soil water deficits are more frequent. This foreseen decline of productivity is to be contrasted with the rising demand for wood products driven by governmental policies, demography and economic growth (FAO, 2018). In order to mitigate the impact of these diverging trends, a possible solution is to improve the whole plant water-use efficiency (Condon *et al.*, 2004), the amount of biomass produced with regards to the quantity of water used over a defined period of time (transpiration efficiency, TE).

At the leaf-level, water-use efficiency (WUE) can be defined intrinsically as the net CO_2 assimilation (A) over g_s (W_i). Yet, the relation between A and g_s is asymptotic (Wong *et al.*, 1979), which means there is a range of high g_s for which A does not improve further. Moreover, diurnal changes of A are several orders of magnitude faster than those of g_s, resulting in a decoupling between the two, immediately following an environmental change (Kaiser & Kappen, 2000) and inducing larges changes of W_i. In natural conditions the environment is changing frequently, thus g_s may rarely reach a steady-state (Rayment *et al.*, 2000; Vialet-Chabrand *et al.*, 2013), which is nonetheless the way g_s is modeled in the wide majority of models (Damour *et al.*, 2010).

Several studies have shown a wide diversity of stomatal dynamics across and among species (Vico *et al.*, 2011; Mc Ausland *et al.*, 2016; Males & Griffiths, 2017; Durand *et al.*, 2019) as well as between environmental drivers (Dumont *et al.*, 2013; Gérardin *et al.*, 2018; Haworth *et al.*, 2018). Further, recent studies showed the impact of different light environments during growth on stomatal dynamics (Gérardin *et al.*, 2018; Matthews *et al.*, 2018). The latter study on *Arabidopsis thaliana* (L.), showed that not only the intensity but also fluctuations of irradiance modified significantly the speed of g_s response to irradiance. These stomatal dynamics measurements, for the most part conducted in controlled conditions, might not be similar to stomatal dynamics of plants grown in the field. Indeed, a number of environmental parameters are particularly different between controlled and natural conditions (*e.g.* wind speed, air humidity, temperature and irradiance).

The drivers of these observed differences in stomatal dynamics are still unclear. Largee and less stomata may be slower than smaller and more numerous stomata because of their lower surface-to-volume ratio (Drake *et al.*, 2013; Raven, 2014). This hypothesis was discussed and tested but no consensus has been found yet (Elliott-Kingston *et al.*, 2016; Mc Ausland *et al.*, 2016; Kardiman & Ræbild, 2018; Durand *et al.*, 2019; Lawson & Vialet-Chabrand, 2019). Other suspected factors which could impact stomatal dynamics involve the number and activity of transporters and pumps on the guard cells plasma membrane, but to our knowledge this hypothesis has not been tested yet.

We performed measurements of stomatal dynamics, stomatal morphology and transpiration efficiency based on above-ground biomass and stem water flow on poplar trees planted in a comparative field plantation in order to answer the following questions: (1) are the differences among genotypes and water regimes that had been previously observed in controlled conditions maintained when poplars are planted in the field? (2) are differences in stomatal dynamics

observed among genotypes related to differences in stomatal morphology? (3) likewise, are differences in stomatal dynamics observed among genotypes related to whole-plant transpiration?

MATERIAL & METHOD

Plant material and growth conditions

Every measurement performed and reported here were part of the rainfall exclusion experimental poplar plantation described elsewhere. The controlled conditions data which we compare here with the field data is from a glasshouse drought experiment described in Durand *et al*. (2019). In both experiment, two hybrid poplar genotypes (Carpaccio and I214, *Populus deltoides* × *nigra* Moench.) and two black poplar genotypes (6J29 and N38, *Populus nigra* L.) were used, chosen for their diversity of drought tolerance with I214 and 6J29 being usually found to be more drought-sensitive (Chen *et al.*, 1997; Giovannelli *et al.*, 2007; Muller & Lambs, 2009; Viger *et al.*, 2016). Concerning the field experiment, briefly 144 shoot cuttings were planted in June 2nd 2014 in a nursery located in the INRA-Grand-Est site (48°45′09.3″N, 6°20′27.6″E; Champenoux, France). The soil was characterized by a deep homogenous swelling heavy clay soil (52% silt, 40% clay, 8% sand), with a pH of 7.1, an organic matter content of 33.3 g kg^{-1} and a total nitrogen content of 1.66 g kg^{-1}. The planting was conducted by groups of three poplars, planted in lines along six parallel rows spaced 5 meters apart. Plants were separated by 1 and 4 meters within and between groups in each row, respectively. The plot was separated in four blocs containing 12 groups each, from which genotypes were arranged randomly, however a single genotype was selected for each plant of the group. One tree of each group of three (n = 48) was harvested for their biomass on the 18th of April 2016 and another one on the 4th of September 2017. Whole-plant transpiration was calculated from sapflow measurements, using the thermal dissipation technique. 48 probes 20 millimeters-long were installed 20 cm above ground from July 11th to September 3rd 2017 (55 days) following Granier (1985; 1987). Whole-plant water use was calculated by scaling sap flux density from transversal cross-section at sensor height since harvests revealed the absence of heartwood, which is common in young trees. Whole-plant transpiration was computed by dividing whole-plant water use by total leaf area, measured at the start and the end of the sapflow experiment and interpolated for each day.

Half the experimental design was used to set up a treatment with lower water availability. Covers 1.5 meters-wide were placed on the ground on each side of the three rows, covering 85% of the ground area on this side of the plot. Since the land exhibited a 6° slope southeastward, this design enabled us to guide water runoffs with gutters toward the lower side of the plot. Covers were two-fold, one was impermeable to liquids but not to gases preventing

rainfall to reach the ground but not soil evaporation to escape into the atmosphere (Berner France, Saint-Julien-du-Sault, France). The other, on top, was green to mirror soil optical properties and to limit the rise of temperatures under the covers (green canvas mulch, Triangle-outillage, Ennevelin, France). Waterings by a water-dripping system equipped on each tree (50 l day^{-1} $tree^{-1}$) was stopped at the end of May 2015 on the rainfall exclusion plot. It should be noted that the covers not only reduced water availability, but also probably increased nitrogen assimilation, thus increasing biomass production in the rainfall excusion plot compared to the irrigated trees.

Leaf sampling and stomatal morphology

Two leaves per tree were collected on the 23rd of August 2017 (*i.e.* 96 leaves) and immediately submerged in liquid nitrogen. The rest of the protocol for stomatal density and stomatal size measurements was detailed in Durand *et al.* (2019). Leaves were freeze-dried and two discs of 78.54 mm^2 were sampled to study each side separately. Discs were tungsten-coated and then placed under a scanning electron microscope coupled with a backscattered secondary electron detector (ΣIGMA-VP, Carl Zeiss, Oberkochen, Germany). A set of 16 pictures covering an area of 3.44 mm^2 were taken (*i.e.* 3072 pictures). 20 stomata were randomly chosen for each sample (*i.e.* 3840 stomata). Stomatal density and size measurements were performed manually with the ImageJ software following (de Boer *et al.*, 2016). AGC (area of the guard cells) was computed by subtracting the area of the stomatal aperture (A_p, μm^2) from the area of the stomata, both calculated as an ellipse by measuring its length and width. An index of the area of the guard cells per leaf area was calculated as the product of AGC and SD summed over both sides (SAI, μm^2 mm^{-2}), similar to the stomatal pore index of Sack *et al.* (2003) excepted for the use of AGC instead of the guard cell length squared.

Gas exchange measurements

Stomatal dynamic measurements were conducted with four intercalibrated Li-6400XT portable photosynthesis systems (LiCor, Lincoln, NE, USA), following Durand *et al.* (2019) unless specified otherwise. Briefly, sun leaves facing toward the South-Est and 1.5 meters high in the canopy were placed in the gas exchange cuvette and left to acclimate until CO_2 assimilation and stomatal conductance were stable (steady-state, less than 5% variation in 5 min). Unless mentioned otherwise, vapour-pressure deficit (VPD) is the leaf-to-air VPD. Environment inside the leaf cuvette was maintained stable throughout the measurement (photosynthetically active radiation (PAR): 1200 µmol m^{-2} s^{-1}, CO_2 concentration: 400 ppm, leaf temperature: 25°C, VPD: 1.5 kPa and flow: 500 µmol s^{-1}). Irradiance-induced stomatal dynamics were performed as such:

when g_s reached a steady-state after the acclimation (SS_0), irradiance was reduced to 100 µmol m^{-2} s^{-1} until a new steady-state was reached (SS_1). At that moment, irradiance was switched back to 1200 µmol m^{-2} s^{-1} until the final steady-state was reached (SS_2). The same protocol was used for VPD-induced stomatal dynamics by changing the VPD from 1.5 to 3 and back to 1.5 kPa, for SS_0, SS_1 and SS_2, respectively. Irradiance and VPD levels were somewhat different than those used in Durand *et al.* (2019) where irradiance was changed from 1000 to 100 µmol m^{-2} s^{-1} and VPD from 1 to 3 kPa. VPD control on the gas exchange system was limited in natural summer conditions compared to the controlled glasshouse environment. Moreover, irradiance is usually higher outside than in the glasshouse, so they were adjusted to assure good repeatability and g_s response.

Stomatal dynamics modeling

Stomatal dynamics to irradiance and VPD were fitted with an empirical descriptive sigmoidal model (Vialet-Chabrand *et al.*, 2013), such that:

$$g_s = g_0 + (G - g_0)e^{-e^{(\frac{\lambda - t}{\tau})}} \quad (1)$$

with g0 et G the steady-state values of g_s at the start and end of the curve, respectively (mol m^{-2} s^{-1}). τ is a response time constant (s), λ is the stomatal response delay (s), « t » is the time (s) and « e » is Euler's number (≈ 2.718). From these parameters we can compute an estimator of the speed of the stomatal response, the maximum speed at the inflection point (SL_{max}):

$$SL_{max} = \frac{G - g_0}{\tau \times e} \quad (2)$$

More information on the model and its parameters are available in the literature (Vialet-Chabrand *et al.*, 2013; Gérardin *et al.*, 2018; Durand *et al.*, 2019).

Synchronous modelling of stomatal aperture and conductance change

We used the equation linking the area of the stomatal aperture (A_p) and SD with g_s (Franks & Farquhar, 2001), of the form:

$$\widehat{g_s} = \frac{SD \times A_p \times {}^{D}/_{V}}{d_p + {}^{\pi}/_{2}\sqrt{{}^{A_p}/_{\pi}}} \quad (3)$$

with D the diffusivity of water in air (2.82×10^{-5} m^2 s^{-1}), V the molar volume of air (0.0244 m^3 mol^{-1}) and d_p the pore depth, assumed to be equal to half of one guard cell width (de Boer *et al.*, 2016). By applying equation (1) to simulate changes of A_p instead of g_s and estimating g_s with equation (3) we were able to compare synchronously the dynamics of A_p and g_s and the

interplay with SD. Furthermore, for a given sigmoidal change of g_s, plants with different SD will require different starting and ending A_p. For example, a plant with lower SD will require a larger reduction in their A_p than a plant with higher SD would for the same change of g_s. Thus, we can compute values of τ so that, different plants with different SD will show a similar speed of A_p change by applying equation (2) to aperture changes. For a given sigmoidal change of g_s, the speed of aperture change between two plants will be equal if:

$$SL_{\max, A_p} = \frac{A_{ref} - a_{ref}}{\tau_{ref}.e} = \frac{A-a}{\tau.e} \quad (5)$$

With "A" and "a" the steady-state values of A_p at the start and end of the curve, respectively (μm^2). The subscript "ref" describes the values of "A", "a" and τ of a reference plant. We can then compute the τ necessary so that the two plants will show a similar speed of A_p change (τ_{crit}), by re-arranging equation (5):

$$\tau_{crit} = \frac{\tau_{ref}(A-a)}{A_{ref} - a_{ref}} \quad (6)$$

Thus, for a given reference SD, τ and Δg_s, we can find sets of τ and SD needed so that another plant will show the same speed of A_p change. Every set of parameters τ and SD differing from those values will result in one of four possibilities. Either both the speed of A_p and g_s change will be slower or quicker than the reference plant, or the speed of A_p change will be quicker but the speed of g_s change will be slower, or the speed of A_p change will be slower but the speed of g_s change will be quicker than the reference plant. A graphical representation and their impact on the speed of A_p and g_s is shown in Fig. S1. If we consider the same change of g_s (*i.e.* same Δg_s), two plants will have the same g_s speed if and only if they have equal τ, regardless of SD. This is represented by the horizontal line in Fig. 7 and S1, where $\tau - \tau_{ref} = 0$.

Statistics

Statistics were done using R 3.5.2 (R Core Team, 2019). A type two factorial ANOVA was used to detect significant differences among the four genotypes, the two water regime and the two growing conditions using both the data from the field and the glasshouse experiment. Normality and homoscedasticity were checked respectively by a Shapiro-Wilk normality test and a Levene test. Post-hoc contrast analyses were performed to test differences between modalities for each factor. Correlations were computed by performing ANCOVAs with stomatal dynamics parameters as dependent variables, water regime as categorical independent variable and either stomatal morphology or whole plant water use efficiency and its components

as continuous independent variables (n = 24). Partial R^2 for the continuous independent variables were computed and *P* values were adjusted to control for the false discovery rate. Significant differences were considered significant at $P < 0.05$ for all tests.

RESULTS

Stomatal morphology in the field

Differences of stomatal morphology between leaf sides

Guard cell length (GCL) range across genotypes, water regime and leaf sides was quite narrow, from 20.5 µm on the abaxial side of Carpaccio rainfall exclusion trees to 25.3 µm on the adaxial side of 6J29 control trees (Table 1). On the other hand, the guard cell area (AGC) ranged from 175.8 μm^2 to 292.5 μm^2 on the abaxial side of rainfall exclusion Carpaccio and the abaxial side of 6J29 control trees, respectively. Only 6J29 showed GCL and AGC significantly higher on the adaxial side than on the abaxial side of the leaf ($P < 0.02$ and $P < 0.001$ for GCL and AGC respectively). For AGC, similar trends were found in Carpaccio and N38 while I214 trees showed the reverse (not significant). By contrast, stomatal density (SD) was always significantly lower on the adaxial side by 46, 43, 57 an 64% for Carpaccio, I214, 6J29 and N38 respectively ($P < 0.001$).

Genotype and rainfall exclusion on stomatal morphology

We found an overall significant water regime effect for both GCL and AGC. They tended to decrease when trees were water limited. For GCL specifically, we were only able to find a significant reduction of GCL under rainfall exclusion on the adaxial side of Carpaccio trees by *post-hoc* comparisons ($P < 0.02$). However in Carpaccio and N38, both sides of the leaf showed a reduced AGC (by 13% on average) in the rainfall exclusion trees as compared to the control trees ($P < 0.03$). The AGC on the adaxial side of 6J29 trees was also reduced by 11% under rainfall exclusion whereas I214 did not show any significant change of GCL or AGC under rainfall exclusion in either side of the leaf ($P > 0.74$). The water regime impacted SD on both sides of the leaf differently depending on genotype (interaction: $P = 0.001$). In general, SD was similar under rainfall exclusion and control conditions in hybrid poplars on both leaf sides but decreased under rainfall exclusion in black poplars (Table 1). SAI followed the same pattern of decrease under rainfall exclusion in the black poplars ($P < 0.005$) and was the highest in I214. We found a significant negative correlation between SD and AGC (not shown), no matter if we controlled for the genotype, for the water regime, for the leaf side effect or for all of them (in every case, $P < 0.001$ and $R^2 = 0.17$). This showed that overall, a higher stomatal density was associated with smaller stomata independently of the effect driving the variation.

Genotype and rainfall exclusion effect on irradiance-induced stomatal dynamics in the field

Steady-state A, g_s and W_i during irradiance-induced stomatal dynamics

We found only a small genotype effect on the steady-state CO_2 assimilation (A) during irradiance-induced stomatal dynamics ($P < 0.04$, Table 2). 6J29 tended to have the highest A and N38 the lowest. CO_2 assimilation did not show any significant difference between water regimes during SS_0 and SS_1 but tended to be lower in the rainfall exclusion trees during SS_2, by 10% on average (not significant by *post-hoc* comparisons but overall $P < 0.05$). g_s was significantly lower in the rainfall exclusion trees during all three steady-states (by 48, 17, 35 an 49% on average for Carpaccio, I214, 6J29 and N38, respectively, $P < 0.001$) which led to a significant increase of W_i in the rainfall exclusion trees as compared to the control ones in SS_0, SS_1 and SS_2. Differences of A, g_s and W_i between SS_0 and SS_2 were almost never significant, except for A in N38 rainfall exclusion trees and g_s in Carpaccio and I214 control trees where they were reduced in SS_2.

Magnitude and speed of irradiance-induced stomatal dynamics

The amplitude of variation in A (ΔA) was significantly lower in N38 than in 6J29 for stomatal closing and opening (Fig. 1**a-b**, $P < 0.03$ and $P = 0.001$, respectively) while no genotypic differences of the amplitude of g_s (Δg_s) was found neither during stomatal closing nor opening (Fig. 1**c-d**).

In general, we found only a weak genotype effect on parameters of stomatal dynamics as a response to irradiance in the field. Only the response time (τ) during stomatal opening was significantly higher in Carpaccio than in I214 and N38 (Fig. 3, $P < 0.003$) by 80 and 82%, respectively. Moreover, Carpaccio was the only genotype showing a τ twice as high during stomatal opening in the control as compared to the rainfall exclusion trees. The lag time (λ) tended to be higher in the hybrid poplars than in the black poplars during stomatal closing, depending on the water regime, with λ being 2.7 times higher in the Carpaccio rainfall exclusion trees as well (Fig. 3**c**, $P < 0.001$). λ during stomatal opening was higher in 6J29 than in I214 and N38 and no significant effect of the water regime was found. For SL_{max}, we were able to show it was twice as high in I214 during stomatal opening as it was in the other three genotypes (Fig. 3**f**, $P < 0.02$). There was no effect of the genotype during stomatal opening and neither genotype nor water regime effect during stomatal closing on SL_{max}.

Genotype and rainfall exclusion effect on VPD-induced stomatal dynamics in the field

Steady-state A, g_s and W_i during VPD-induced stomatal dynamics

As for the VPD response, CO_2 assimilation was again the highest in 6J29 but the lowest in Carpaccio in all three steady-states (Table 2). During SS_1 and SS_2, A tended to be higher in the control trees than in the rainfall exclusion. g_s showed a similar increase in the control trees as compared to the rainfall exclusion trees in all three steady-states (by 38, 61 and 48% during SS_0, SS_1 and SS_2 when averaged by genotype). This led again to significant increases of W_i in the rainfall exclusion plot. Unlike the response to irradiance, the decrease of A in SS_1 was solely driven by the concurrent decrease in g_s. Thus, W_i was increased in SS_1 as compared to SS_0 and SS_2. No difference of A, g_s or W_i were found between SS_0 and SS_2 for the VPD response.

Magnitude and speed of VPD-induced stomatal dynamics

As for the magnitude of the VPD-induced stomatal dynamics, ΔA was lower in Carpaccio than in I214, 6J29 and N38 (by 40, 45 and 52%, respectively, Fig. 2**a-c**) during stomatal closing. A similar but not significant trend was found for Δg_s. There was no significant genotype effect on either ΔA or Δg_s during stomatal opening. Trees under rainfall exclusion showed a higher ΔA and a lower Δg_s than control trees, both during stomatal closing and opening, with no interaction with the genotype. ΔA decreased by 3.8 and 10.5 µmol m^{-2} s^{-1} and increased by 2 and 5.3 µmol m^{-2} s^{-1} in the control and rainfall exclusion trees respectively during stomatal closing and opening. On the contrary, Δg_s decreased by 0.26 and 0.2 mol m^{-2} s^{-1} and increased by 0.13 and 0.09 mol m^{-2} s^{-1} in the control and rainfall exclusion trees respectively during stomatal closing and opening.

Regarding the stomatal dynamics parameters for the VPD response, τ showed a weak genotype effect in the field, with 6J29 being the highest during stomatal closing. We found a significant decrease of τ in the N38 and 6J29 rainfall exclusion trees as compared to the control trees during stomatal closing and opening, respectively ($P < 0.02$ and $P < 0.005$, respectively, Fig. 4**a-b**). For λ, the water regime effect depended on the genotype during stomatal closing, with I214 and 6J29 showing no effect while Carpaccio and N38 showed a lag time 52 and 62% shorter in the rainfall exclusion trees than in the control ($P < 0.001$). During stomatal opening there was no genotype effect on λ, but it tended to decrease and increase in the hybrid and black poplars, respectively (only significant in N38, $P < 0.02$). As for SL_{max}, even though there is a trend of lower SL_{max} in the trees under rainfall exclusion (Fig. 4**e-f**), we could not find any significant difference of genotype or water regime, either during stomatal closing or opening.

Comparisons of stomatal dynamics between natural and controlled conditions

Irradiance-induced stomatal dynamics between natural and controlled conditions

Stomatal dynamics between controlled and natural conditions were quite different (Table 3). When considering the irradiance response, ΔA was higher in the field than in the glasshouse by 64 and 47% in Carpaccio, by 34 and 24% in I214 and 27 and 25% in 6J29 during the closing and opening, respectively (Fig. 1**a-b**). On the contrary, ΔA in N38 tended to be lower in the field than in the glasshouse (only significant during stomatal opening, $P < 0.03$). Δg_s was lower in the field by 43% on average during stomatal closing (Fig. 1**c-d**). The same trend was found during stomatal opening in I214, 6J29 and N38, but not in Carpaccio ($P > 0.65$). Furthermore, τ for closing was increased from 7.5 min in the glasshouse to 16.2 min on average in the field ($P < 0.001$, Fig. 3**a**). We found a similar trend of increased τ for opening in the field, significant only in Carpaccio (from 7.6 to 16.3 min, $P < 0.001$) and 6J29 (from 6.6 to 12.3 min, $P < 0.02$). Overall, λ also tended to increase in the field as compared to the glasshouse, to various magnitudes depending on genotype and water regime. This trend was more explicit during stomatal opening where it was significant in every genotype ($P < 0.05$), with λ in the field being 1.7 times higher than in the glasshouse in I214 and N38, 2.9 times higher in Carpaccio and 4.4 times higher in 6J29 trees. Finally, SL_{max} was overall reduced by 72 and 71% in the field as compared to the glasshouse during stomatal closing and opening, respectively (Fig. 3**e-f**). During stomatal closing, this decrease was stronger in hybrid poplars than in black poplars. Overall, irradiance-induced stomatal dynamics in the field was more than twice as slow as they were in controlled conditions, regardless of the water regime.

VPD-induced stomatal dynamics between natural and controlled conditions

Concerning the VPD response, ΔA was lower in the field than in the glasshouse specifically in control trees but not in the rainfall exclusion trees (Fig. 2**a-b**). This was true in every genotype during stomatal closing (53% reduction, overall) but only in I214 and N38 during stomatal opening (by 60 and 61%, respectively). Similarly, Δg_s was also lower in I214 and N38 during stomatal opening (by 43 and 33%, respectively) while it tended to be lower during stomatal closing in black poplars only ($P = 0.07$ and $P = 0.03$ for 6J29 and N38, respectively). As for the response time τ during stomatal closing, it increased in the field as compared to the glasshouse in both hybrid poplars from 6.6 to 19.0 min in Carpaccio ($P < 0.001$) and from 4.6 to 17.3 min in I214 ($P < 0.001$) whereas it decreased in black poplars from 30.1 to 23.2 min in 6J29 ($P < 0.008$) and from 22.2 to 15.0 min in N38 ($P < 0.008$, Fig. 4). A similar but less pronounced trend was found during stomatal opening. λ was significantly modified in the field,

but differently depending on genotype and treatment. Overall, λ was increased in the field, as compared to the glasshouse, more strongly in the hybrid poplars than in the black poplars during stomatal closing. During stomatal opening, λ was similar between growing conditions in the hybrid poplars but decreased in the black poplars. Finally, SL_{max} tended to be smaller in the field than in the glasshouse for all genotypes and water regimes both during stomatal closing and opening, but was significant only in the hybrid poplars, which showed the highest SL_{max} in the glasshouse (Fig. 4**e-f**). SL_{max} was on average 4.9 and 5.2 times smaller in the field than in the glasshouse in Carpaccio trees, and on average 11 and 4.6 times smaller in I214, for stomatal closing and opening respectively.

Correlation analyses in the field

Correlations between stomatal dynamics and stomatal morphology

Correlation analyses between parameters of the stomatal dynamics performed in the field (τ, λ and SL_{max}) either during stomatal closing or opening and stomatal morphology (GCL, AGC and SD) either on the abaxial or the adaxial side of the leaf were generally not significant. More precisely, no correlation was found to be significant between stomatal dynamics parameters as a response to irradiance or VPD and stomatal morphology on the abaxial side ($P > 0.06$ in every case). λ during stomatal closing as a response to VPD was positively correlated with GCL on the adaxial side. τ during stomatal closing as a response to VPD was also positively correlated with GCL and with AGC as well on the adaxial side (Fig. 5, $P < 0.03$, partial $R^2 = 0.37$ and 0.29, respectively). Neither SL_{max} nor SD showed any significant correlation with stomatal morphology and dynamic parameters, respectively.

Correlation between stomatal dynamics and whole-plant productivity and water use

Correlation analyses between parameters of the stomatal dynamics performed in the field and whole-plant productivity and water use were also generally not significant. We did not find any significant correlation between stomatal dynamics and neither dry matter, height nor leaf area increments. The cumulated water use and the transpiration efficiency was not correlated to stomatal dynamics either. This was true for stomatal dynamics as a response to irradiance and VPD. The only significant correlations we found were positives and involved the average daily whole plant transpiration per unit leaf area and either the response time τ during stomatal closing as a response to VPD or the lag time λ during stomatal opening as a response to irradiance (Fig. 6, $P < 0.006$, partial $R^2 = 0.42$ and 0.30, respectively)

DISCUSSION

In this study we assessed stomatal dynamics in response to changes of irradiance and VPD on poplar genotypes under contrasting water regimes, and planted in the field. Our objective was also to investigate stomatal dynamics when plants were planted in controlled and natural conditions to determine if stomatal dynamics analyses would hold across growing conditions. Modeling plant gas exchange with the environment has been done using dynamics models (Vialet-Chabrand *et al.*, 2016), and when compared, they showed a better match between computed and observed data than steady-states models (Vialet-Chabrand *et al.*, 2013). However there is some evidence that estimating dynamic parameters on a relatively small sample of plants grown in the same conditions might not inform us about genotype or species-specific dynamics (Matthews *et al.*, 2018). Whether stomatal dynamics show a phenotypic plasticity or not is up for debate, but if dynamic models are to be improved, understanding how dynamics parameters may vary with the environment is a central concern that needs to be addressed.

Differences of stomatal dynamics between genotypes and water regimes are dependent on growing conditions

Overall our data suggests genotypic and water regime differences were often not significant in the field, whereas Durand *et al.* (2019) found strong genotypic differences in the same poplar genotypes grown in a glasshouse experiment. They found the genotype I214 to be always the faster to close its stomata in response to a decrease of irradiance or an increase of VPD. 6J29 tended to be the slowest and in response to VPD, both black poplars were several times slower than hybrid poplars. In our field experiment, I214 also tended to exhibit the lowest τ, λ and the highest SL_{max} while 6J29 was among the slowest (Fig. 3-4), in agreement with the glasshouse study. These similarities suggest both endogenous and environmental determinisms of stomatal dynamics in poplars, since there were large differences of stomatal dynamics between the glasshouse and the field experiment.

If stomatal dynamics show a plasticity between conditions, there may be advantages of both slow and fast stomatal responses depending on external conditions, assuming they are actively regulated by the plant. It has been proposed that having faster stomata may enable better tracking of external conditions, taking advantage of sunflecks but limiting water losses quickly when the environment becomes unfavorable, and improving instant water use efficiency, so that soil water content may be depleted more slowly (Vialet-Chabrand *et al.*, 2013; Mc Ausland *et al.*, 2016; Lawson & Vialet-Chabrand, 2019). However far fewer studies suggested benefits

to have slower stomata. A good stomatal tracking is possible only when external fluctuations are slower than the stomatal response, and under certain conditions even the fastest stomata are not able to perfectly track the environment. Gregory & Pearse (1937), studying stomatal resistance to fluctuations of irradiance found that under alternating periods of light, stomata tend to reach an equilibrium dependent on the light duration. Moreover, stomata of *Vicia faba* (L.) adapted to a continuous light only tracked the irradiance for a few days, when put in dynamic light conditions, before losing sensitivity to it and reverting to their behavior under constant light (Kaiser & Kappen, 1997). With a modeling approach Vico *et al.* (2011) concluded that under low light, faster stomatal dynamics would help harvest the limited supply of light. However, under high light availability or rapid fluctuations, a slower stomatal response would reduce the metabolic cost of stomatal movement and generally allow for a higher carbon gain. We could therefore hypothesize that rapid environmental changes, too fast for stomata to track, would lead to g_s being far from optimal at all time, while averaging g_s may yield less carbon gains and more water losses but more steadily and in a more predictable manner. Thus, averaging environmental changes instead of tracking might be more advantageous in some conditions. Not always the fastsest stomatal dynamics are necessarily the most optimal, depending on the environment. Further investigations are needed to determine if inherent physical and biochemical limitations are the only causes explaining why some plants have slower stomata.

Overall, correlation analyses between stomatal dynamics and either stomatal morphology or components of the transpiration efficiency showed very few significant results in the field whereas we found several during the glasshouse experiment (Durand *et al.*, 2019). Still, it is interesting that each of the four correlations with either whole-plant transpiration or stomatal size found (Fig. 5 and 6) in the field were among the strongest we found in the glasshouse and involved the lag and response time. This suggests stomatal density and size do play a role in determining stomatal movement speed in poplar genotypes. However, the extent to which it contributes to stomatal dynamics seem to vary strongly with environnemental conditions. Moreover, such correlations may not have been found without the use of the dynamic model. Furthermore, we found again a correlation between stomatal dynamics and whole plant transpiration per unit leaf area not not whole-plant water of TE, adding further evidence that even if stomatal dynamics impact the whole-plant transpiration, the whole-plant water use is substantially driven by the total leaf area.

Slower stomatal dynamics in the field

In the field experiment, stomatal dynamics were much slower than in the glasshouse experiment, regardless of genotype or water availability (Fig. 3 and 4, Durand *et al.*, 2019). Magnitude of irradiance and VPD change were 300 µmol m^{-2} s^{-1} higher and 0.5 kPa lower in the field than in the glasshouse experiment, respectively. Despite this, Δg_s during the irradiance response was almost always twice smaller as in the glasshouse, while Δg_s during the VPD response was sometimes, but not always, reduced correspondingly to the smaller magnitude of VPD change. Thus, we can conclude that the different irradiance and VPD level did not systematically impact the steady-states levels in controlled and natural conditions.

When considering the same decrease of g_s, we can compare the stomatal dynamics in the field in reference to the ones in the glasshouse by representing the average difference of τ and SD for each genotype and water regime (Fig. 7). Whether plants have lower or higher SD and lower or higher response time will influence their relative speed of g_s and A_p to one another. This enables us to clearly determine whether the speed of g_s does reflect the speed of aperture change or not. In almost all cases, there was both a slower g_s and A_p response in the field compared to the glasshouse. Only the stomatal opening to a decreased VPD in 6J29 control trees showed a faster g_s and A_p response. More interestingly, the speed of stomatal closing and opening in control and drought-stressed 6J29, respectively, show a slower g_s but a faster A_p response in the field than in the glasshouse. This suggests an uncoupled response of A_p and g_s when comparing plants with different stomatal density (Durand *et al.*, 2019). Here we have shown experimentally for the first time how they interact. Caution should be exercised when attempting to link guard cell specific traits, such as stomatal morphology, with g_s dynamics. However this method, by enabling the modeling of guard cell opening speeds, allows us to test more thoroughly the underlying traits driving the diversity of stomatal dynamics.

Stomatal morphology was also quite distinct between the field and the glasshouse experiment, with a decrease of GCL and AGC of 20 and 25% respectively in the field whereas SD increased by 20 and 10% on the abaxial and adaxial side, respectively (Durand *et al.*, 2019). A trade-off of SD and AGC is in line with the inverse relationship the two variables share across species (Hetherington & Woodward, 2003). Usually, stomatal density tends to increase under more intense irradiation (Brownlee, 2001), which can also be observed in the upper canopy where leaves are subjected to higher irradiance (Al Afas *et al.*, 2006). This is consistent with the irradiance being three times as high in the field as it was in the glasshouse (Table S1). However, these findings are not in agreement with the hypothesis that smaller, more numerous stomata

may have faster dynamics than larger, more sparsely displayed stomata (Hetherington & Woodward, 2003; Drake *et al.*, 2013; Raven, 2014). Taken together with the wide difference in significativity in the glasshouse and field experiment correlation analyses, this evidence suggests that stomatal sizes are far from being the main driver of variations in stomatal dynamics in poplars. Interestingly, black poplars but not hybrid poplars showed a reduction of the stomatal area index under rainfall exclusion conditions. This is independent of the observed trade-off between SD and AGC and highlights that under reduced water availability black poplars are reducing their overall stomatal area per leaf area while the hybrid poplars are not.

Very few studies have investigated the impact of different growing conditions on stomatal dynamics. In *Nicotiana tabacum* (L.), plants growing under shade exhibited lower SD and slower stomatal dynamics, especially during closing (Gérardin *et al.*, 2018). Testing different rainforest species, Kardiman & Ræbild (2018) found both faster and slower stomatal opening under shade, unrelated with SD. In *Arabidopsis thaliana* (L.), plants grown under fluctuating irradiance showed faster opening but slower closing of the stomata (Matthews *et al.*, 2018), consistent with the idea that light-use efficiency may be improved under those conditions by maintaining stomata open (Ooba & Takahashi, 2003). Moreover, different dynamics were reported for different light intensities, depending on the light fluctuations during their growth (Matthews *et al.*, 2018). There does not appear to be a consensus on the effect of irradiance during growth, consequently we can only speculate that part of the reason why stomatal dynamics were slower in the field was because of the higher overall irradiance. Other factors may also have played a role, as distinct stomatal dynamics were found for plant subjected to different VPD levels (Tinoco-Ojanguren & Pearcy, 1993) and leaf water potentials (Davies & Kozlowski, 1975; Barradas *et al.*, 1994). VPD in the field was on average half as high as in the glasshouse due to differences of both humidity and temperature (Table S1). Hydraulic functioning may also have been different considering differences in soil water content, soil characteristics and age of the trees between the two growing conditions.

In conclusion, our study points to both endogenous and environmental drivers of stomatal speed, depending on the growing conditions. Stomatal dynamics in the field were much slower than in the glasshouse, despite smaller and more numerous stomata, indicating that stomatal morphology is far from the main factor controlling stomatal speed, even though we were able to detect significant correlations. Other authors proposed that the amount and activity of channels and transporters on the guard cell membrane may induce faster water movements and lead to faster stomatal dynamics (Lawson & Blatt, 2014; Raven, 2014). Going forward, there is

a number of suggestions, we think may help future studies to improve our understanding of stomatal dynamics. First, the multiple procedures and methodologies used to characterize stomatal dynamics are, in some cases, preventing us to compare results between studies. We suggest at the very least future investigations into stomatal dynamics consider reporting all parameters defining the time, magnitude and rate of g_s change because they are three closely related components of the full g_s response. Focusing on a single parameter may lead to inaccurate conclusions. Secondly, wherever possible the rate of g_s and aperture change should be examined, especially when hypotheses on stomatal dynamics relate more to one than the other. Thirdly, this study has shown we need to further explore the diversity of stomatal dynamics inside a single genotype or species and the determinisms driving that diversity (*e.g.* light, VPD, temperatures) before we can fully understand more complex responses, such as drought stresses.

ACKNOWLEDGEMENTS

This work was conducted in the frame of the WATBIO (Development of improved perennial biomass crops for water-stressed environments), a collaborative research project funded from the European Union's Seventh Programme for research, technological development and demonstration under grant agreement No. 311929. The research received funding from the French National Research Agency through the Laboratory of Excellence ARBRE (ANR-12-LABXARBRE-01). M.D. received a Ph.D. scholarship from the Lorraine Région and EFPA (INRA research department). We thank the nursery of Guéméné Penfao for providing the euramerican poplar cuttings. The authors acknowledge Marc Villar and Catherine Bastien from the UR0588-INRA Unit for access to the referenced Populus nigra clones 6J29 and N38 as well as Joseph Levillain, David Cohen and Irène Hummel for their technical help.

CONFLICT OF INTEREST

The authors declare that the research was conducted in the absence of any commercial or financial relationships that could be construed as a potential conflict of interest.

AUTHOR CONTRIBUTION

M.D., C.B. and D.L.T. contributed to the data collection. M.D., O.B. and D.L.T. contributed to the experimental design, data analysis and interpretation as well as the writing of the manuscript.

REFERENCES

Al Afas N, Marron N, Ceulemans R. 2006. Clonal variation in stomatal characteristics related to biomass production of 12 poplar (Populus) clones in a short rotation coppice culture. *Environmental and Experimental Botany* **58**(1-3): 279-286.

Barradas VL, Jones HG, Clark JA. 1994. Stomatal responses to changing irradiance in Phaseolus vulgaris L. *Journal of Experimental Botany* **45**(7): 931-936.

Bonan GB. 2008. Forests and climate change: forcings, feedbacks, and the climate benefits of forests. *Science* **320**(5882): 1444-1449.

Brownlee C. 2001. The long and the short of stomatal density signals. *Trends in Plant Science* **6**(10): 441-442.

Chen SL, Wang SS, Altman A, Huttermann A. 1997. Genotypic variation in drought tolerance of poplar in relation to abscisic acid. *Tree Physiology* **17**(12): 797-803.

Condon AG, Richards RA, Rebetzke GJ, Farquhar GD. 2004. Breeding for high water-use efficiency. *Journal of Experimental Botany* **55**(407): 2447-2460.

Coopman RE, Jara JC, Bravo LA, Sáez KL, Mella GR, Escobar R. 2008. Changes in morpho-physiological attributes of Eucalyptus globulus plants in response to different drought hardening treatments. *Electronic Journal of Biotechnology* **11**(2): 30-39.

Cowan IR, Farquhar GD. 1977. Stomatal function in relation to leaf metabolism and environment. *Symposia of the Society for Experimental Biology* **31**: 471-505.

Dai A. 2012. Increasing drought under global warming in observations and models. *Nature Climate Change* **3**: 52.

Dai AG. 2011. Drought under global warming: a review. *Wiley Interdisciplinary Reviews-Climate Change* **2**(1): 45-65.

Damour G, Simonneau T, Cochard H, Urban L. 2010. An overview of models of stomatal conductance at the leaf level. *Plant Cell and Environment* **33**(9): 1419-1438.

Davies WJ, Kozlowski TT. 1975. Stomatal responses to changes in light intensity as influenced by plant water stress. *Forest Science* **21**(2): 129-133.

de Boer HJ, Price CA, Wagner-Cremer F, Dekker SC, Franks PJ, Veneklaas EJ. 2016. Optimal allocation of leaf epidermal area for gas exchange. *New Phytologist* **210**(4): 1219-1228.

de Dios VR. 2017. Circadian regulation and diurnal variation in gas exchange. *Plant Physiology* **175**(1): 3-4.

Drake PL, Froend RH, Franks PJ. 2013. Smaller, faster stomata: scaling of stomatal size, rate of response, and stomatal conductance. *Journal of Experimental Botany* **64**(2): 495-505.

Dumont J, Spicher F, Montpied P, Dizengremel P, Jolivet Y, Le Thiec D. 2013. Effects of ozone on stomatal responses to environmental parameters (blue light, red light, CO2 and vapour pressure deficit) in three Populus deltoides x Populus nigra genotypes. *Environmental Pollution* **173**: 85-96.

Durand M, Brendel O, Buré C, Le Thiec D. 2019. Altered stomatal dynamics induced by changes in irradiance and vapour-pressure deficit under drought: impact on the whole plant transpiration efficiency of poplar genotypes. *New Phytologist* **222**: 1789-1802.

Elliott-Kingston C, Haworth M, Yearsley JM, Batke SP, Lawson T, McElwain JC. 2016. Does size matter? Atmospheric CO2 may be a stronger driver of stomatal closing rate than stomatal size in taxa that diversified under low CO2. *Frontiers in Plant Science* **7**.

FAO. 2018. Muller E, Kushlin A, Linhares-Juvenal T, Muchoney D, Wertz-Kanounnikoff S, Henderson-Howat D, eds. *The state of the world's forests*. Rome, Italy.

Franks PJ, Farquhar GD. 2001. The effect of exogenous abscisic acid on stomatal development, stomatal mechanics, and leaf gas exchange in Tradescantia virginiana. *Plant Physiology* **125**(2): 935-942.

Gérardin T, Douthe C, Flexas J, Brendel O. 2018. Shade and drought growth conditions strongly impact dynamic responses of stomata to variations in irradiance in Nicotiana tabacum. *Environmental and Experimental Botany* **153**: 188-197.

Giovannelli A, Deslauriers A, Fragnelli G, Scaletti L, Castro G, Rossi S, Crivellaro A. 2007. Evaluation of drought response of two poplar clones (Populus x canadensis Monch 'I-214' and P-deltoides Marsh. 'Dvina') through high resolution analysis of stem growth. *Journal of Experimental Botany* **58**(10): 2673-2683.

Granier A. 1985. A new method of sapflow measurement in tree stems. *Annales Des Sciences Forestieres* **42**(2): 193-200.

Granier A. 1987. Evaluation of transpiration in a Douglas-fir stand by means of sapflow measurements. *Tree Physiology* **3**(4): 309-319.

Gregory FG, Pearse HL. 1937. The effect on the behaviour of stomata of alternating periods of light and darkness of short duration. *Annals of Botany* **1**(1): 3-10.

Haworth M, Marino G, Cosentino SL, Brunetti C, De Carlo A, Avola G, Riggi E, Loreto F, Centritto M. 2018. Increased free abscisic acid during drought enhances stomatal sensitivity and modifies stomatal behaviour in fast growing giant reed (Arundo donax L.). *Environmental and Experimental Botany* **147**: 116-124.

Hetherington AM, Woodward FI. 2003. The role of stomata in sensing and driving environmental change. *Nature* **424**(6951): 901-908.

IPCC. 2014. Meyer L, Brinkman S, van Kesteren L, Leprince-Ringuet N, van Boxmeer F, eds. *Climate change 2014: Synthesis report. Contribution of working groups I, II and III to the fifth assessment report of the intergovernmental panel on climate change*. Geneva, Switzerland: Cambridge University Press.

Kaiser H, Kappen L. 1997. In situ observations of stomatal movements in different light-dark regimes: the influence of endogenous rhythmicity and long-term adjustments. *Journal of Experimental Botany* **48**(8): 1583-1589.

Kaiser H, Kappen L. 2000. In situ observation of stomatal movements and gas exchange of Aegopodium podagraria L. in the understorey. *Journal of Experimental Botany* **51**(351): 1741-1749.

Kardiman R, Ræbild A. 2018. Relationship between stomatal density, size and speed of opening in Sumatran rainforest species. *Tree Physiology* **38**(5): 696-705.

Lawson T, Blatt MR. 2014. Stomatal size, speed, and responsiveness impact on photosynthesis and water use efficiency. *Plant Physiology* **164**(4): 1556-1570.

Lawson T, Vialet-Chabrand S. 2019. Speedy stomata, photosynthesis and plant water use efficiency. *New Phytologist* **221**(1): 93-98.

Males J, Griffiths H. 2017. Specialized stomatal humidity responses underpin ecological diversity in C3 bromeliads. *Plant Cell and Environment* **40**(12): 2931-2945.

Matthews JSA, Vialet-Chabrand S, Lawson T. 2018. Acclimation to fluctuating light impacts the rapidity of response and diurnal rhythm of stomatal conductance. *Plant Physiology* **176**(3): 1939-1951.

Mc Adam SAM, Brodribb TJ. 2015. The evolution of mechanisms driving the stomatal response to vapor pressure deficit. *Plant Physiology* **167**(3): 833-843.

Mc Ausland L, Vialet-Chabrand S, Davey P, Baker NR, Brendel O, Lawson T. 2016. Effects of kinetics of light-induced stomatal responses on photosynthesis and water-use efficiency. *New Phytologist* **211**(4): 1209-1220.

Monclus R, Dreyer E, Villar M, Delmotte FM, Delay D, Petit JM, Barbaroux C, Le Thiec D, Brechet C, Brignolas F. 2006. Impact of drought on productivity and water use

efficiency in 29 genotypes of Populus deltoides x Populus nigra. *New Phytologist* **169**(4): 765-777.

Muller E, Lambs L. 2009. Daily variations of water use with vapor pressure deficit in a plantation of I214 poplars. *Water* **1**(1): 32.

Ooba M, Takahashi H. 2003. Effect of asymmetric stomatal response on gas-exchange dynamics. *Ecological Modelling* **164**(1): 65-82.

Raven JA. 2014. Speedy small stomata? *Journal of Experimental Botany* **65**(6): 1415-1424.

Rayment MB, Loustau D, Jarvis PG. 2000. Measuring and modeling conductances of black spruce at three organizational scales: shoot, branch and canopy. *Tree Physiology* **20**(11): 713-723.

Sack L, Cowan PD, Jaikumar N, Holbrook NM. 2003. The 'hydrology' of leaves: co-ordination of structure and function in temperate woody species. *Plant, Cell & Environment* **26**(8): 1343-1356.

Sheffield J, Wood EF. 2008. Projected changes in drought occurrence under future global warming from multi-model, multi-scenario, IPCC AR4 simulations. *Climate Dynamics* **31**(1): 79-105.

Shimazaki K-i, Doi M, Assmann SM, Kinoshita T 2007. Light regulation of stomatal movement. *Annual Review of Plant Biology*, 219-247.

Tinoco-Ojanguren C, Pearcy RW. 1993. Stomatal dynamics and its importance to carbon gain in two rainforest Piper species. *Oecologia* **94**(3): 395-402.

Touma D, Ashfaq M, Nayak MA, Kao S-C, Diffenbaugh NS. 2015. A multi-model and multi-index evaluation of drought characteristics in the 21st century. *Journal of Hydrology* **526**: 196-207.

Tschaplinski TJ, Blake TJ. 1989. Water relations, photosynthetic capacity, and root shoot partitioning of photosynthates as determinants of productivity in hybrid poplar. *Canadian Journal of Botany-Revue Canadienne De Botanique* **67**(6): 1689-1697.

Vialet-Chabrand S, Dreyer E, Brendel O. 2013. Performance of a new dynamic model for predicting diurnal time courses of stomatal conductance at the leaf level. *Plant Cell and Environment* **36**(8): 1529-1546.

Vialet-Chabrand S, Matthews JSA, Brendel O, Blatt MR, Wang Y, Hills A, Griffiths H, Rogers S, Lawson T. 2016. Modelling water use efficiency in a dynamic environment: An example using Arabidopsis thaliana. *Plant Science* **251**: 65-74.

Vico G, Manzoni S, Palmroth S, Katul G. 2011. Effects of stomatal delays on the economics of leaf gas exchange under intermittent light regimes. *New Phytologist* **192**(3): 640-652.

Viger M, Smith HK, Cohen D, Dewoody J, Trewin H, Steenackers M, Bastien C, Taylor G. 2016. Adaptive mechanisms and genomic plasticity for drought tolerance identified in European black poplar (Populus nigra L.). *Tree Physiology* **36**(7): 909-928.

Wong SC, Cowan IR, Farquhar GD. 1979. Stomatal conductance correlates with photosynthetic capacity. *Nature* **282**(5737): 424-426.

TABLES

Table 1. Stomatal morphology of four poplar genotypes (Carpaccio, I214, 6J29 and N38) for each water regime and leaf side. Values shown are means ± standard deviation. ANOVA factors are considered significant at $P < 0.05$. Letters show the significant differences by *post-hoc* comparisons between the 16 groups (4 genotypes and 2 water regimes and 2 leaf sides).

Genotype	Water regime	Face	GCL (µm)	AGC (µm²)	SD (mm⁻²)	SAI (µm² mm⁻²)
Carpaccio	control	Abaxial	21.8 ± 0.9 abcde	203.7 ± 11.8 bcd	169.5 ± 9.5 e	$53.7\times10^3 \pm 3.4\times10^3$ a
		Adaxial	23.2 ± 1.4 cdef	210.1 ± 10.8 cd	91.6 ± 7.4 bc	
	Rainfall exclusion	Abaxial	20.5 ± 1.5 a	175.8 ± 16.3 a	188.8 ± 9.3 f	$52.2\times10^3 \pm 4.8\times10^3$ a
		Adaxial	20.8 ± 1.7 ab	183.7 ± 8.7 ab	103.5 ± 10.4 c	
I214	control	Abaxial	21.3 ± 0.8 abc	199.4 ± 12.9 bcd	217.5 ± 16.7 g	$67.0\times10^3 \pm 4.3\times10^3$ cd
		Adaxial	20.9 ± 1.1 ab	195.9 ± 15.9 abcd	122 ± 15.9 d	
	Rainfall exclusion	Abaxial	21.3 ± 1.3 abc	202.8 ± 22.8 bcd	221.5 ± 25.5 g	$67.7\times10^3 \pm 3.9\times10^3$ d
		Adaxial	21 ± 2.5 ab	187.1 ± 12 abc	125 ± 14.2 d	
6J29	control	Abaxial	22.5 ± 0.8 bcdef	200.8 ± 18 bcd	208.1 ± 16.1 g	$66.9\times10^3 \pm 5.1\times10^3$ cd
		Adaxial	25.3 ± 1.4 g	292.5 ± 22.6 f	86.5 ± 10.1 b	
	Rainfall exclusion	Abaxial	21.6 ± 0.6 abcd	194.8 ± 15.2 abcd	184.9 ± 10.9 ef	$56.7\times10^3 \pm 4.1\times10^3$ ab
		Adaxial	24 ± 0.8 fg	260.3 ± 17.8 e	79.5 ± 8.9 ab	
N38	control	Abaxial	23.4 ± 2.1 defg	238.7 ± 18.8 e	190 ± 14.3 f	$61.4\times10^3 \pm 3.7\times10^3$ bc
		Adaxial	23.7 ± 1 efg	237.6 ± 16.5 e	68.1 ± 7.7 a	
	Rainfall exclusion	Abaxial	22.3 ± 0.9 abcdef	202.8 ± 23.9 bcd	187.5 ± 12.3 f	$52.7\times10^3 \pm 6.9\times10^3$ a
		Adaxial	22.2 ± 1.4 abcdef	211.5 ± 29.2 d	69.2 ± 5.5 a	
P	Genotype (G)		**<0.001**	**<0.001**	**<0.001**	**<0.001**
	Water regime (T)		**<0.001**	**<0.001**	ns	**0.001**
	Face (S)		**0.006**	**<0.001**	**<0.001**	
	Interaction G:T		ns	**0.038**	**0.001**	**0.014**
	Interaction G:S		**0.002**	**<0.001**	**<0.001**	
	Interaction T:S		ns	ns	ns	
	Interaction G:T:S		ns	ns	ns	

GCL: Guard cell length, AGC: Area of the guard cells, SD: Stomatal density, SAI: Stomatal area index, ns: not significant.

Table 2. Steady-state values of the temporal dynamics of gas exchange as a response to a change in irradiance or VPD on four poplar genotypes (Carpaccio, I214, 6J29 and N38). Values shown are means ± standard deviation before the irradiance change (SS_0), after a decrease of irradiance (SS_1) and after an increase of irradiance (SS_2). ΔSS show the significant differences between SS_0 and SS_2 by *post-hoc* comparisons of a linear model the include the genotype, water regime and the steady-state effect. ANOVA factors are considered significant at $P < 0.05$. Letters show the significant differences by *post-hoc* comparisons between the eight groups (4 genotypes and 2 water regimes).

			A (µmol m^{-2} s^{-1})				**g_s (mol m^{-2} s^{-1})**				**W_i (µmol mol^{-1})**			
	Genotype	**Water regime**	SS0	SS1	SS2	ΔSS	SS0	SS1	SS2	ΔSS	SS0	SS1	SS2	ΔSS
Irradiance	Carp.	control	18.3 ± 1.2 a	4.1 ± 1.4 a	18.1 ± 2.5 abc	ns	0.45 ± 0.11 b	0.23 ± 0.11 d	0.35 ± 0.04 c	**0.046**	43.6 ± 13.2 a	22.1 ± 12.4 a	51.3 ± 8.2 a	ns
		Rainfall exclusion	19.3 ± 3.9 a	4.4 ± 0.5 a	16.5 ± 3.2 ab	ns	0.23 ± 0.08 a	0.1 ± 0.05 abc	0.21 ± 0.06 b	ns	91.3 ± 27.9 bc	53.2 ± 26.5 bcd	83.1 ± 16.9 bc	ns
	I214	control	20.2 ± 4.7 a	4.2 ± 0.9 a	17.3 ± 4.8 abc	ns	0.29 ± 0.08 a	0.08 ± 0.04 ab	0.2 ± 0.05 ab	**0.037**	71.4 ± 16.4 ab	57.5 ± 19.4 bcd	87.2 ± 12.7 bcd	ns
		Rainfall exclusion	19.2 ± 2.5 a	4.6 ± 0.8 a	18.5 ± 1.2 abc	ns	0.21 ± 0.03 a	0.07 ± 0.02 a	0.18 ± 0.02 ab	ns	90.7 ± 15.3 bc	69.7 ± 16.9 d	102.2 ± 11.5 cde	ns
	6J29	control	21.5 ± 4.4 a	5.4 ± 0.2 a	21.9 ± 3.8 c	ns	0.27 ± 0.06 a	0.16 ± 0.01 bcd	0.3 ± 0.06 c	ns	79 ± 5.3 abc	32.7 ± 1.1 abc	74.3 ± 11.3 ab	ns
		Rainfall exclusion	20.7 ± 3.6 a	4.8 ± 0.4 a	19 ± 3.5 bc	ns	0.22 ± 0.12 a	0.09 ± 0.06 abc	0.17 ± 0.08 ab	ns	112.3 ± 39.3 c	61.4 ± 34.9 cd	123.7 ± 31.9 e	ns
	N38	control	17.8 ± 3 a	4.4 ± 0.4 a	17.9 ± 1.5 abc	ns	0.29 ± 0.09 a	0.15 ± 0.05 c	0.32 ± 0.05 c	ns	67.5 ± 22.2 ab	32.4 ± 13 ab	50.4 ± 17.1 a	ns
		Rainfall exclusion	17 ± 2.2 a	4.5 ± 0.4 a	13.5 ± 2.6 a	**0.049**	0.19 ± 0.07 a	0.07 ± 0.03 a	0.13 ± 0.05 a	ns	93.6 ± 23.7 bc	67.3 ± 27.2 d	109.4 ± 22.7 de	ns
	P	Genotype	**0.039**	ns	**0.006**		**0.016**	**0.002**	**0.008**		**0.041**	**0.035**	**0.001**	
		Water regime	ns	ns	**0.041**		**<0.001**	**<0.001**	**<0.001**		**<0.001**	**<0.001**	**<0.001**	
		Interaction	ns	ns	ns		ns	ns	**0.004**		ns	ns	**0.034**	
VPD	Carp.	control	14.4 ± 1.6 a	12.5 ± 2 bcd	13.4 ± 2 ab	ns	0.37 ± 0.08 bc	0.17 ± 0.05 cd	0.23 ± 0.07 bc	ns	39.5 ± 6.5 a	78 ± 9.7 a	62.9 ± 14.7 a	ns
		Rainfall exclusion	17.6 ± 2 ab	9.7 ± 2.5 abc	14.3 ± 4.4 ab	ns	0.21 ± 0.04 a	0.08 ± 0.02 a	0.13 ± 0.06 a	ns	83.6 ± 11.7 b	129.3 ± 9.7 b	117 ± 18.1 b	ns
	I214	control	19.5 ± 3 bc	16.6 ± 4 de	18.3 ± 3.3 b	ns	0.44 ± 0.06 cd	0.21 ± 0.05 cd	0.26 ± 0.03 c	ns	45.4 ± 9.3 a	79.4 ± 4.1 a	69.4 ± 8 a	ns
		Rainfall exclusion	19.3 ± 1.9 bc	8.1 ± 2.7 ab	14.5 ± 3.8 ab	ns	0.24 ± 0.04 a	0.06 ± 0.03 a	0.14 ± 0.05 a	ns	80.3 ± 13.6 b	145.3 ± 23.5 b	112 ± 21.7 b	ns
	6J29	control	22.8 ± 4 cd	18.1 ± 3.8 e	19.1 ± 2.8 b	ns	0.52 ± 0.1 d	0.22 ± 0.06 d	0.27 ± 0.07 c	ns	44.7 ± 9.8 a	83 ± 13.2 a	74.1 ± 21.4 a	ns
		Rainfall exclusion	24.1 ± 4.4 d	12.1 ± 5.5 bcd	17.2 ± 4.7 b	ns	0.37 ± 0.1 bc	0.09 ± 0.07 ab	0.16 ± 0.07 ab	ns	67.9 ± 16.6 b	153.6 ± 43.8 b	119.1 ± 30.4 b	ns
	N38	control	19.6 ± 1.5 bc	13.9 ± 1.8 cde	17 ± 1.8 b	ns	0.43 ± 0.09 cd	0.15 ± 0.04 bc	0.23 ± 0.08 bc	ns	47.1 ± 8 a	97.6 ± 17.4 a	77.4 ± 17.6 a	ns
		Rainfall exclusion	18.1 ± 3.3 ab	7.3 ± 3.9 a	10.1 ± 5 a	ns	0.28 ± 0.11 ab	0.06 ± 0.04 a	0.09 ± 0.06 a	ns	71.7 ± 20.8 b	129 ± 26.4 b	118 ± 22.4 b	ns
	P	Genotype	**<0.001**	**0.012**	**0.017**		**0.001**	**0.049**	ns		ns	ns	ns	
		Water regime	ns	**<0.001**	**0.012**		**<0.001**	**<0.001**	**<0.001**		**<0.001**	**<0.001**	**<0.001**	
		Interaction	ns	ns	ns		ns	ns	ns		ns	ns	ns	

Carp.: Carpaccio; A, Net CO_2 assimilation; g_s, stomatal conductance to water vapour; W_i, intrinsic water use efficiency; ns, not significant.

Table 3. Summary of factorial analyses of variance results of a linear model which includes the genotype (G), the water regime (T) and the growing conditions (Z) effect using both the data from the field and the glasshouse experiement. *P*-values are shown. ΔA and Δgs are the magnitude of net CO_2 assimilation and stomatal conductance change following either a change of irradiance or VPD. τ, λ and SLmax are parameters of the dynamic model. Subscripts "cl" and "op" are for stomatal closing and opening respectively. ANOVA factors are considered significant at $P < 0.05$. ns: not significant.

	Factor	ΔA_{cl}	ΔA_{op}	Δgs_{cl}	Δgs_{op}	τ_{cl}	τ_{op}	λ_{cl}	λ_{op}	$SL_{max\ cl}$	$SL_{max\ op}$
irradiance	**Genotype (G)**	ns	**0.015**	ns	**0.002**	ns	ns	**0.028**	ns	**<0.001**	**0.012**
	Water regime (T)	ns	**0.002**	ns	**0.005**	ns	**<0.001**	ns	ns	**0.003**	ns
	Growing conditions (Z)	**<0.001**	**0.005**	**<0.001**	**<0.001**	**<0.001**	**<0.001**	**<0.001**	**<0.001**	**<0.001**	**<0.001**
	G:T	ns	ns	ns	ns	ns	**0.025**	**0.003**	ns	ns	ns
	G:Z	**<0.001**	**<0.001**	ns	**<0.001**	ns	**0.043**	**0.029**	**0.005**	**<0.001**	ns
	T:Z	ns	ns	ns	ns	ns	ns	ns	ns	**0.008**	ns
	G:T:Z	ns	ns	ns	**0.007**	ns	ns	**0.042**	ns	ns	ns
VPD	**Genotype (G)**	**<0.001**	**<0.001**	**<0.001**	**0.002**	**<0.001**	**<0.001**	**<0.001**	**<0.001**	**<0.001**	**<0.001**
	Water regime (T)	**<0.001**	**0.001**	**<0.001**	**0.017**	ns	**0.044**	**<0.001**	ns	**<0.001**	ns
	Growing conditions (Z)	ns	**<0.001**	ns	**0.002**	**0.045**	ns	**<0.001**	0.022	**<0.001**	**<0.001**
	G:T	ns	ns	ns	ns	**0.002**	**0.002**	**<0.001**	**<0.001**	**<0.001**	ns
	G:Z	ns	**0.001**	**0.041**	**0.012**	**<0.001**	**0.001**	**0.002**	**0.001**	**<0.001**	**<0.001**
	T:Z	**<0.001**	**0.008**	ns	ns	ns	ns	**0.022**	**0.003**	**0.006**	ns
	G:T:Z	ns	ns	ns	ns	ns	ns	**<0.001**	ns	**0.002**	ns

FIGURES

Figure 1. Magnitude of variation in CO_2 assimilation (ΔA, **a-b**) and stomatal conductance (Δg_s, **c-d**) during a decrease (**a-c**) or an increase (**b-d**) of irradiance in four poplar genotypes (Carpaccio, I214, 6J29 and N38). Data were collected on poplars grown in a glasshouse (Gh) or in the field (F), well-watered (T) or under reduced water availability (DS). Values shown are means ± standard errors. Dark and light blue, yellow and orange are for Carpaccio, I214, 6J29 and N38, respectively. Letters show significant differences by *post-hoc* comparisons. ANOVA results are given for main effects (G: genotype, T: water treatment, Z: growth conditions) and interactions (n = 4-6). When the second order interaction was significant (G-T-Z), letters are shown independently for each genotype.

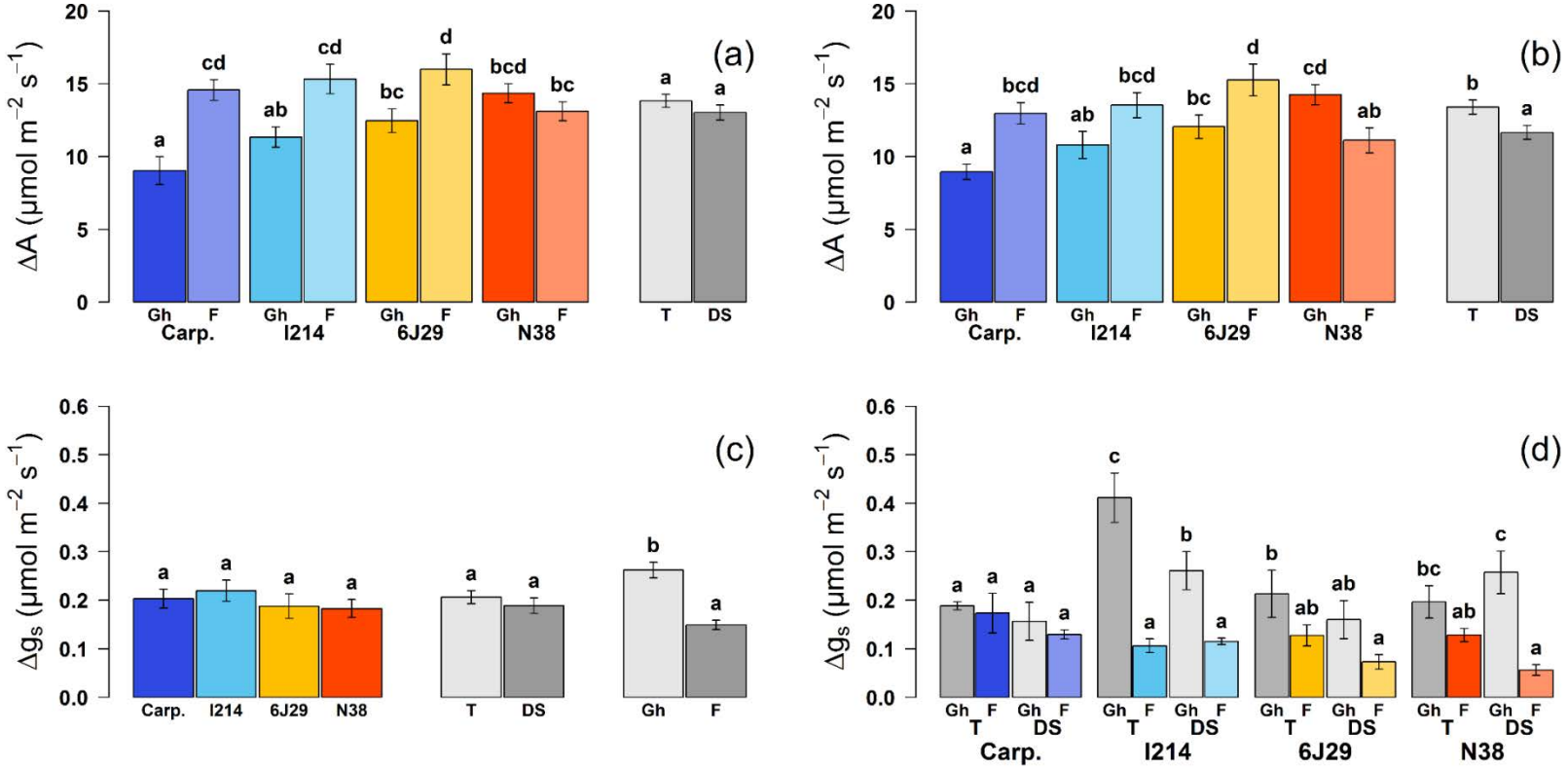

Figure 2. Magnitude of variation in CO_2 assimilation (ΔA, **a-b**) and stomatal conductance (Δg_s, **c-d**) during an increase (**a-c**) or a decrease (**b-d**) of VPD in four poplar genotypes (Carpaccio, I214, 6J29 and N38). Data were collected on poplars grown in a glasshouse (Gh) or in the field (F), well-watered (T) or under reduced water availability (DS). Values shown are means ± standard errors. Dark and light blue, yellow and orange are for Carpaccio, I214, 6J29 and N38, respectively. Letters show significant differences by *post-hoc* comparisons. ANOVA results are given for main effects (G: genotype, T: water treatment, Z: growth conditions) and interactions (n = 4-6). When the second order interaction was significant (G-T-Z), letters are shown independently for each genotype.

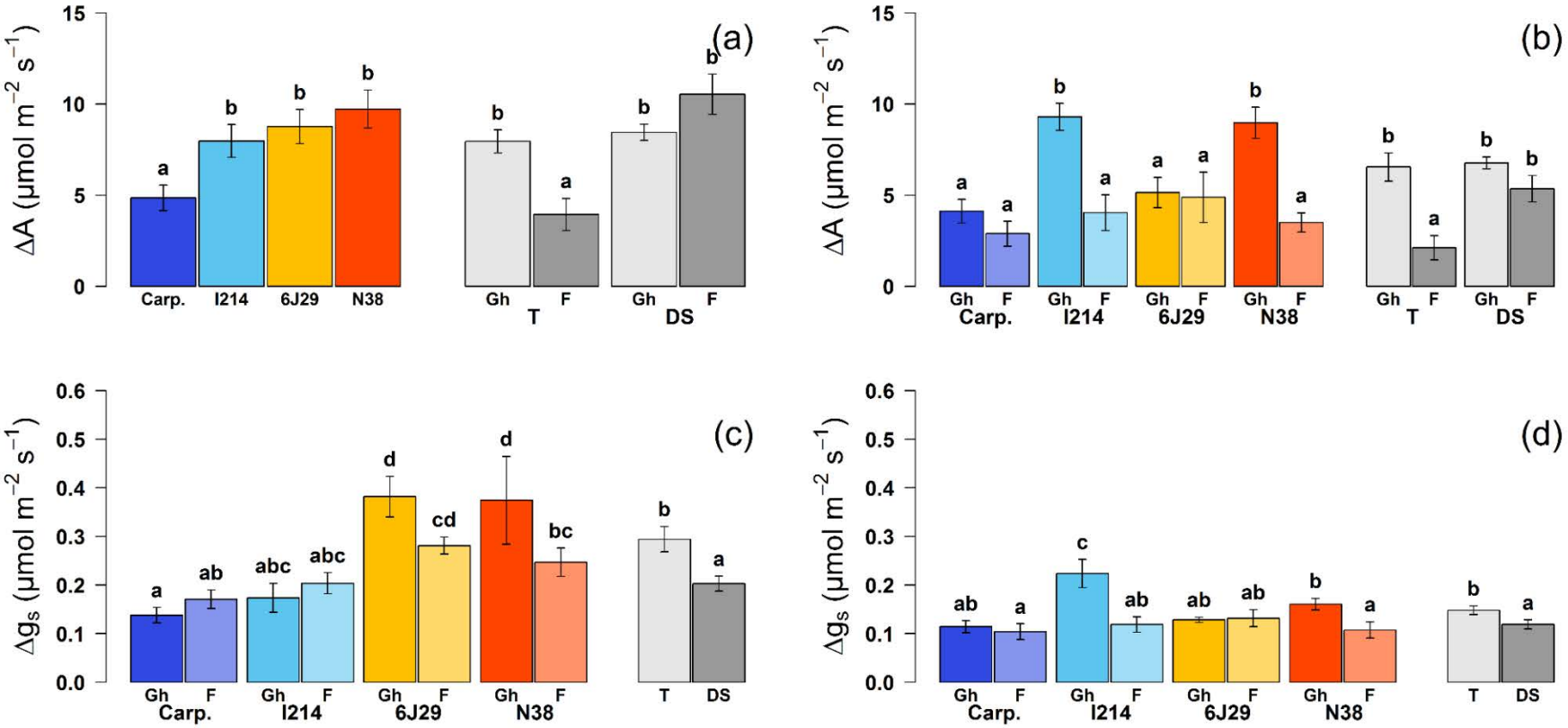

Figure 3. Stomatal dynamics parameters of the g_s response to a decrease (**a-c-e**) or an increase (**b-d-f**) of irradiance in four poplar genotypes (Carpaccio, I214, 6J29 and N38). Data were collected on poplars grown in a glasshouse (Gh) or in the field (F), well-watered (T) or under reduced water availability (DS). Values shown are means ± standard errors. Dark and light blue, yellow and orange are for Carpaccio, I214, 6J29 and N38, respectively. Letters show significant differences by *post-hoc* comparisons. ANOVA results are given for main effects (G: genotype, T: water treatment, Z: growth conditions) and interactions (n = 4-6). When the second order interaction was significant (G-T-Z), letters are shown independently for each genotype.

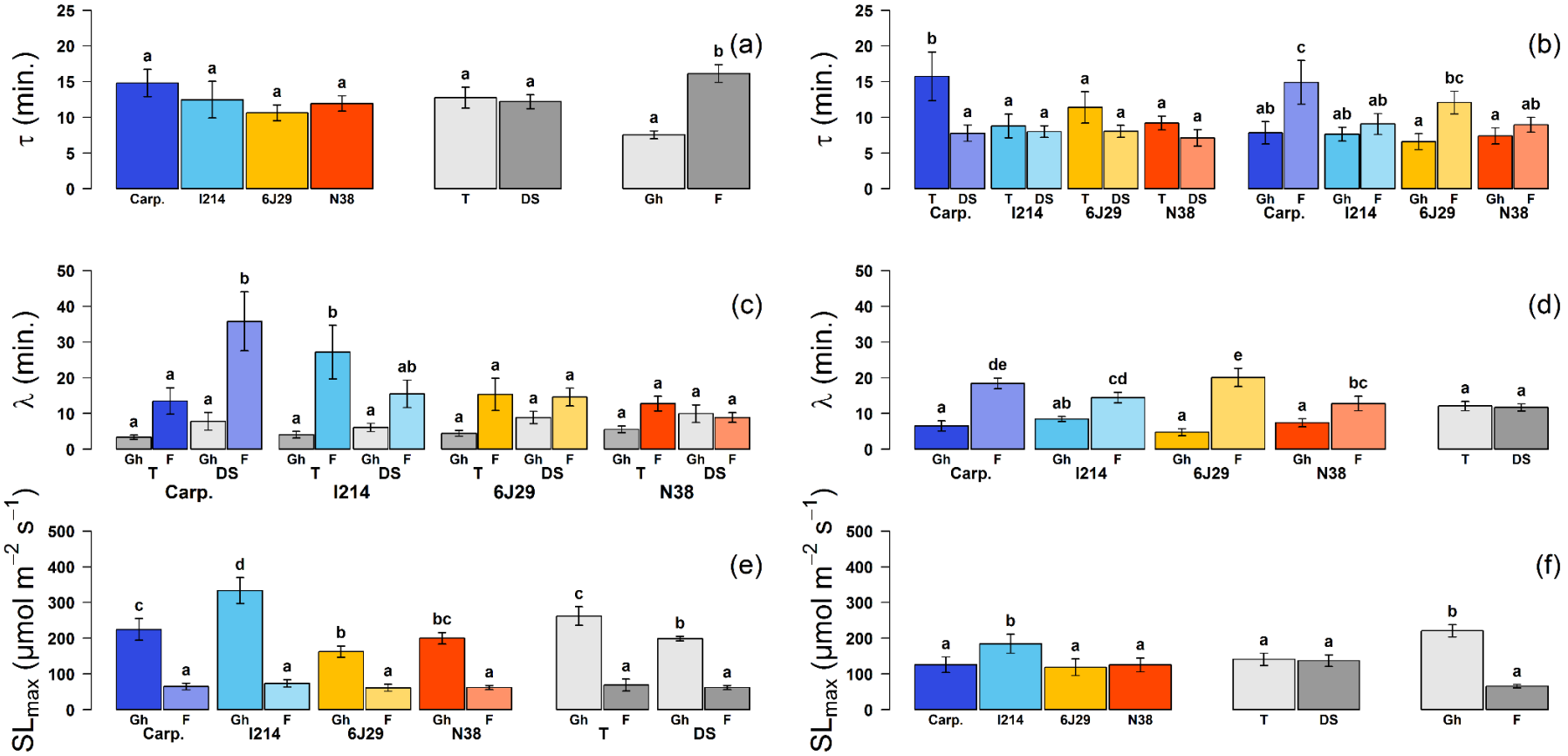

Figure 4. Stomatal dynamics parameters of the g_s response to an increase (**a-c-e**) or a decrease (**b-d-f**) of VPD in four poplar genotypes (Carpaccio, I214, 6J29 and N38). Data were collected on poplars grown in a glasshouse (Gh) or in the field (F), well-watered (T) or under reduced water availability (DS). Values shown are means ± standard errors. Dark and light blue, yellow and orange are for Carpaccio, I214, 6J29 and N38, respectively. Letters show significant differences by *post-hoc* comparisons. ANOVA results are given for main effects (G: genotype, T: water treatment, Z: growth conditions) and interactions (n = 4-6). When the second order interaction was significant (G-T-Z), letters are shown independently for each genotype.

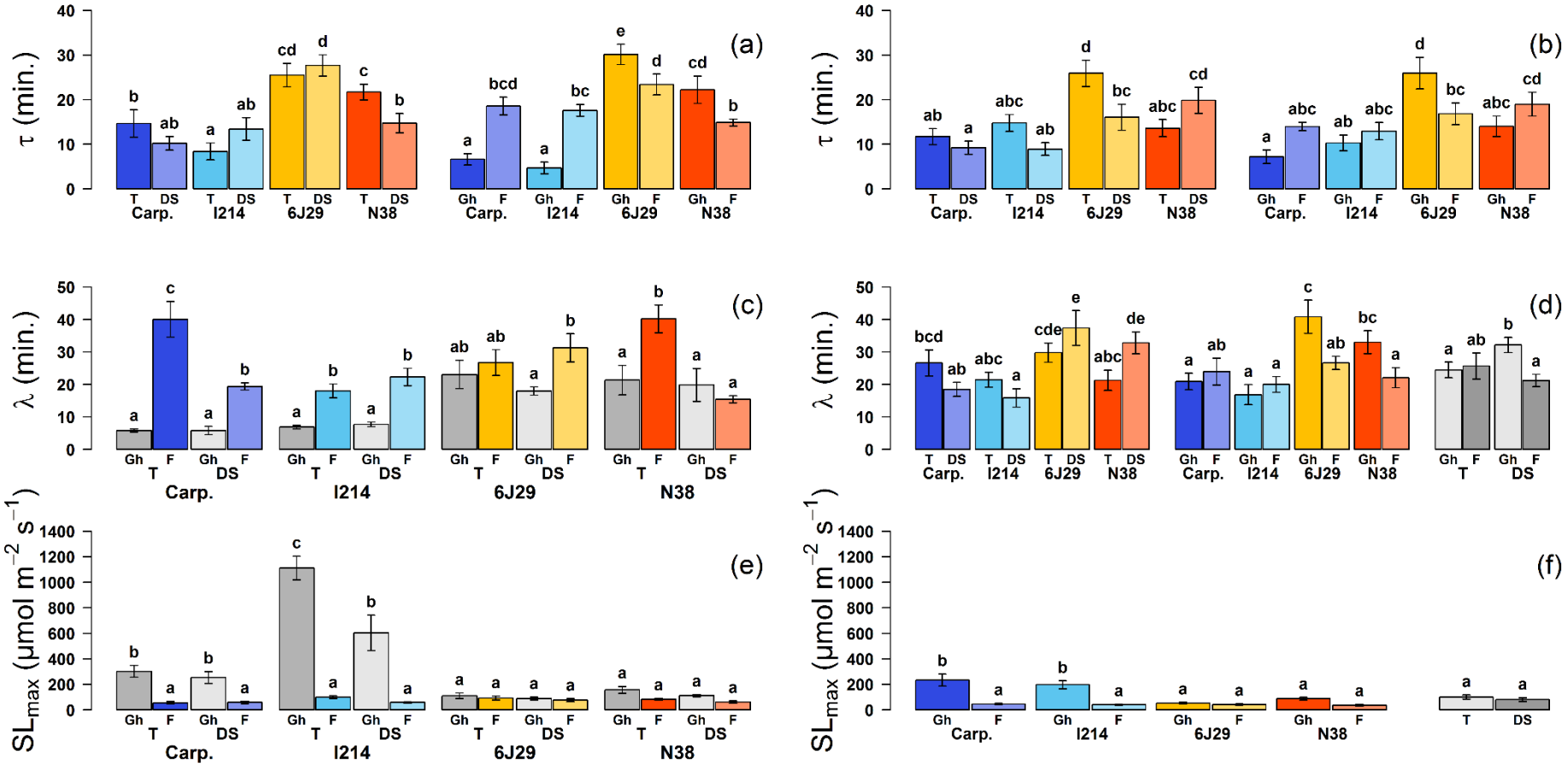

Figure 5. Correlations between the response time τ during stomatal closing response to a change of VPD and guard cell length (**a**) or guard cell area (**b**) on the adaxial side of the leaf. Partial R^2 and *P* value after controlling for the water regime effect are reported (n = 24). The black line in the regression line. Dark and light blue, yellow and orange are for Carpaccio, I214, 6J29 and N38, respectively.

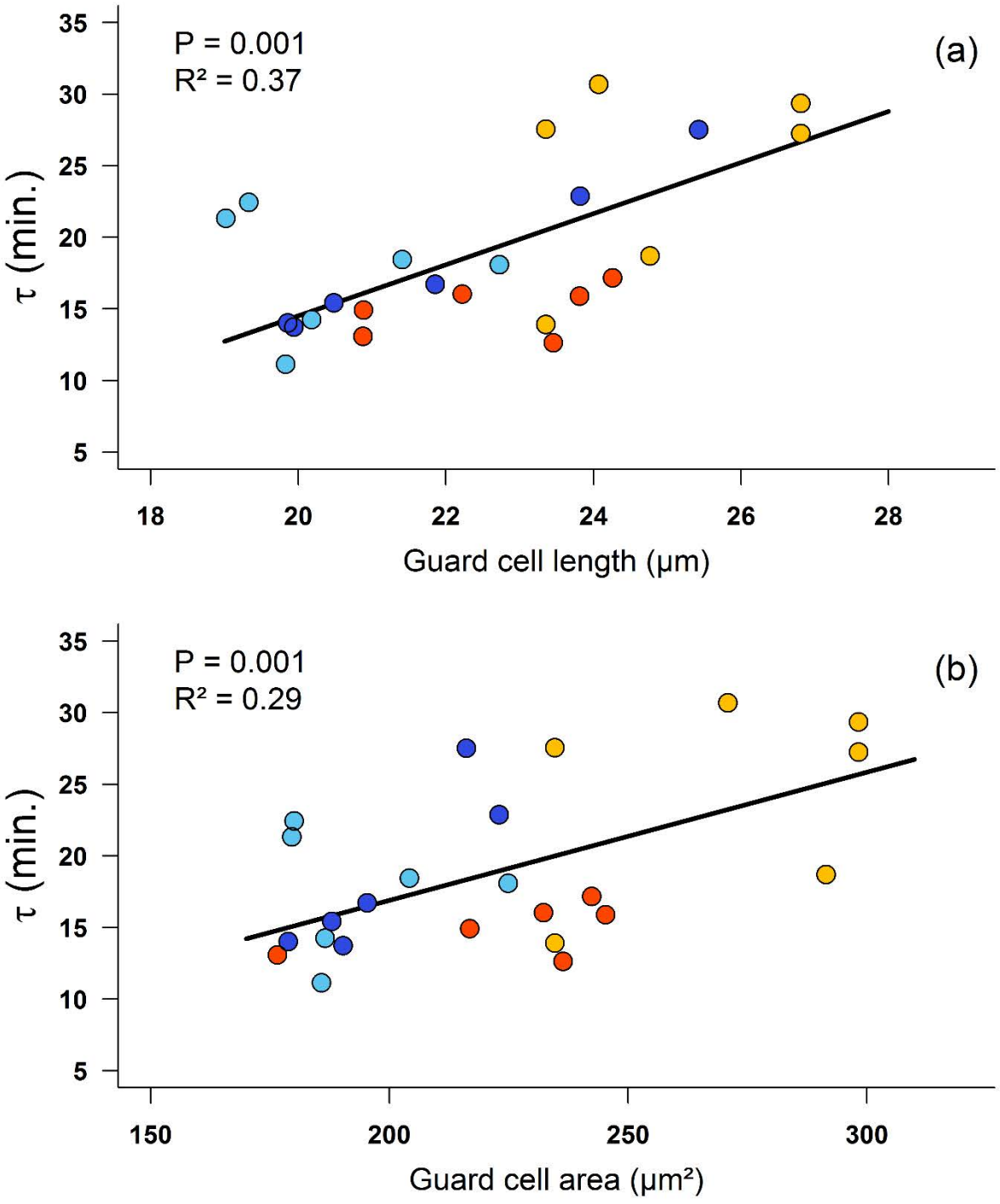

Figure 6. Correlations between the average daily transpiration per unit leaf area and either the response time τ for stomata closing as a response to VPD (**a**) or the lag time λ for stomatal opening as a response to irradiance (**b**). Partial R^2 and *P* value after controlling for the water regime effect are reported (n = 24). The black line in the regression line. Dark and light blue, yellow and orange are for Carpaccio, I214, 6J29 and N38, respectively.

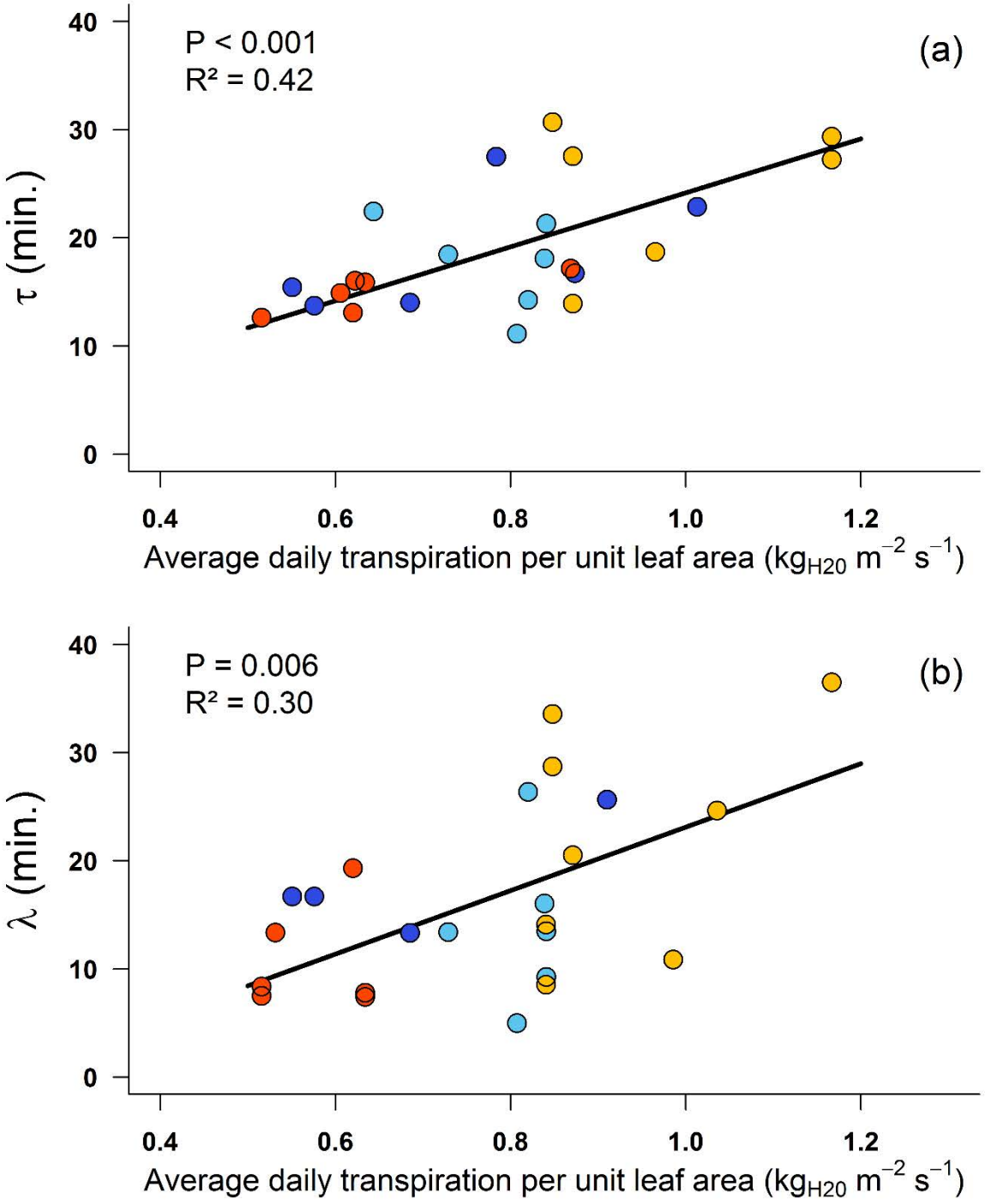

Figure 7. Combined comparison of stomatal morphology and stomatal dynamics of poplars planted in the field in reference to poplars planted in a glasshouse. Values shown are mean response time (τ) and mean stomatal density (SD) of four poplar genotypes (Carpaccio, I214, 6J29 and N38) under two water regimes and grown in a glasshouse (τ_{ref} and SD_{ref}) subtracted from mean τ and SD of the same genotypes under contrasting water regimes grown in the field. The black curve shows all the sets of τ and SD required so that the speed of A_p is the same as the reference plant for a change of g_s from 0.8 to 0.5 mol m^{-2} s^{-1}. For each point, cross and plus signs are for the irradiance and VPD response, respectively. Dark and light blue, yellow and orange are for Carpaccio, I214, 6J29 and N38, respectively. Colored areas show four spaces, highlighting the relationship between the speed of guard cell aperture change (A_p) and the speed of stomatal conductance change (g_s). The blue area represents parameters values where both the speed of A_p and g_s are slower than the reference and the red area is when both the speed of A_p and g_s are quicker than the reference. The yellow area represents parameters values where the speed of A_p is quicker than the reference but the speed of g_s is slower than the reference while the green zone shows the reverse.

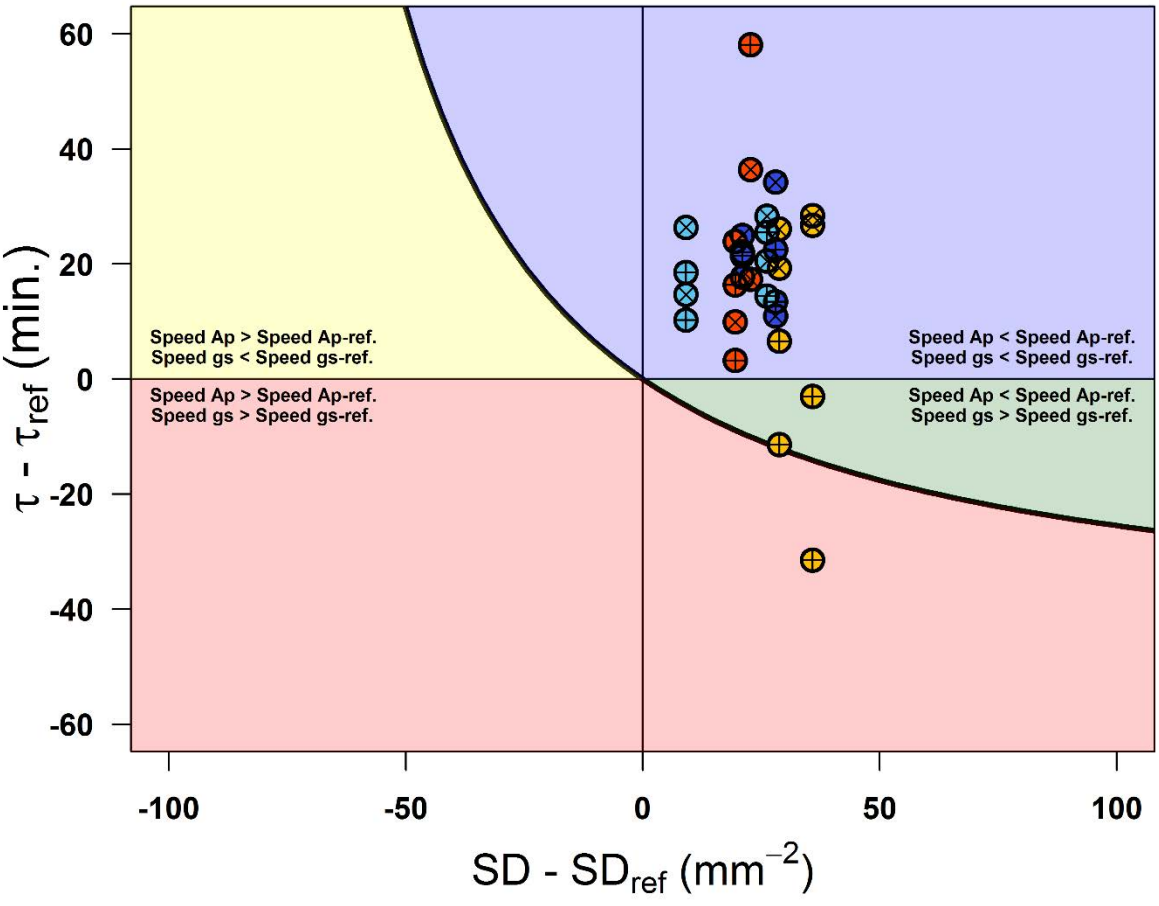

DONNEES SUPPLEMENTAIRES

Table S1. Summary of meteorological data during the growth period (April 1st to October 1st) of four poplar genotypes (Carpaccio, I214, 6J29 and N38) grown in a glasshouse between March 31st and June 22nd 2016 and in the field between June 2nd 2014 and September 4th 2017. Field data is either shown as the mean from 2014 to 2017 or for 2017 only. Values are means ± standard deviation of daily data.

	Relative humidity (%)			**Temperature (°C)**			**VPD (kPa)**	**Global radiation (W m^{-2})**	**Wind speed (m s^{-1})**
	mean	min	max	mean	min	max			
Glasshouse (2016)	61.8 ± 9.8	42.5 ± 11.3	70.4 ± 8.5	21.0 ± 1.5	16.6 ± 1.8	25.7 ± 1.3	1.0 ± 0.2	73.6 ± 28.5	< 0.2
Field (2014 to 2017)	74.9 ± 11.8	46.8 ± 14.9	97.0 ± 5.2	15.9 ± 4.8	10.4 ± 4.7	22 ± 5.7	0.5 ± 0.3	204.9 ± 77.1	1.2 ± 0.5
Field (2017)	74.2 ± 10.8	45.9 ± 13.7	97.2 ± 3.5	16.3 ± 5.4	10.4 ± 5.3	22.5 ± 6.1	0.5 ± 0.4	221.9 ± 78	1.2 ± 0.4

Figure S1. Example of the combined effect of stomatal morphology and stomatal dynamics on the speed of aperture (A_p) change and the speed on stomatal conductance (g_s) change when comparing two plants. The black and red curves show the A_p (**b-e-h-k**) and g_s (**c-f-i-l**) dynamics for the reference plant and the plant of interest, respectively. Dashed lines show the maximum speed at the inflexion point (SL_{max}). The black curve (**a-d-g-j**) show all the sets of τ and SD required so that the speed of A_p is the same as the reference plant for a change of g_s from 1.063 to 0.495 mol m^{-2} s^{-1}. Colored areas (**a-d-g-j**) show four spaces, highlighting the relationship between the speed of guard cell aperture change (A_p) and the speed of stomatal conductance change (g_s). The blue area represents parameters values where both the speed of A_p and g_s are slower than the reference and the red area is when both the speed of A_p and g_s are quicker than the reference. The yellow area represents parameters values where the speed of A_p is quicker than the reference but the speed of g_s is slower than the reference while the green zone shows the reverse.

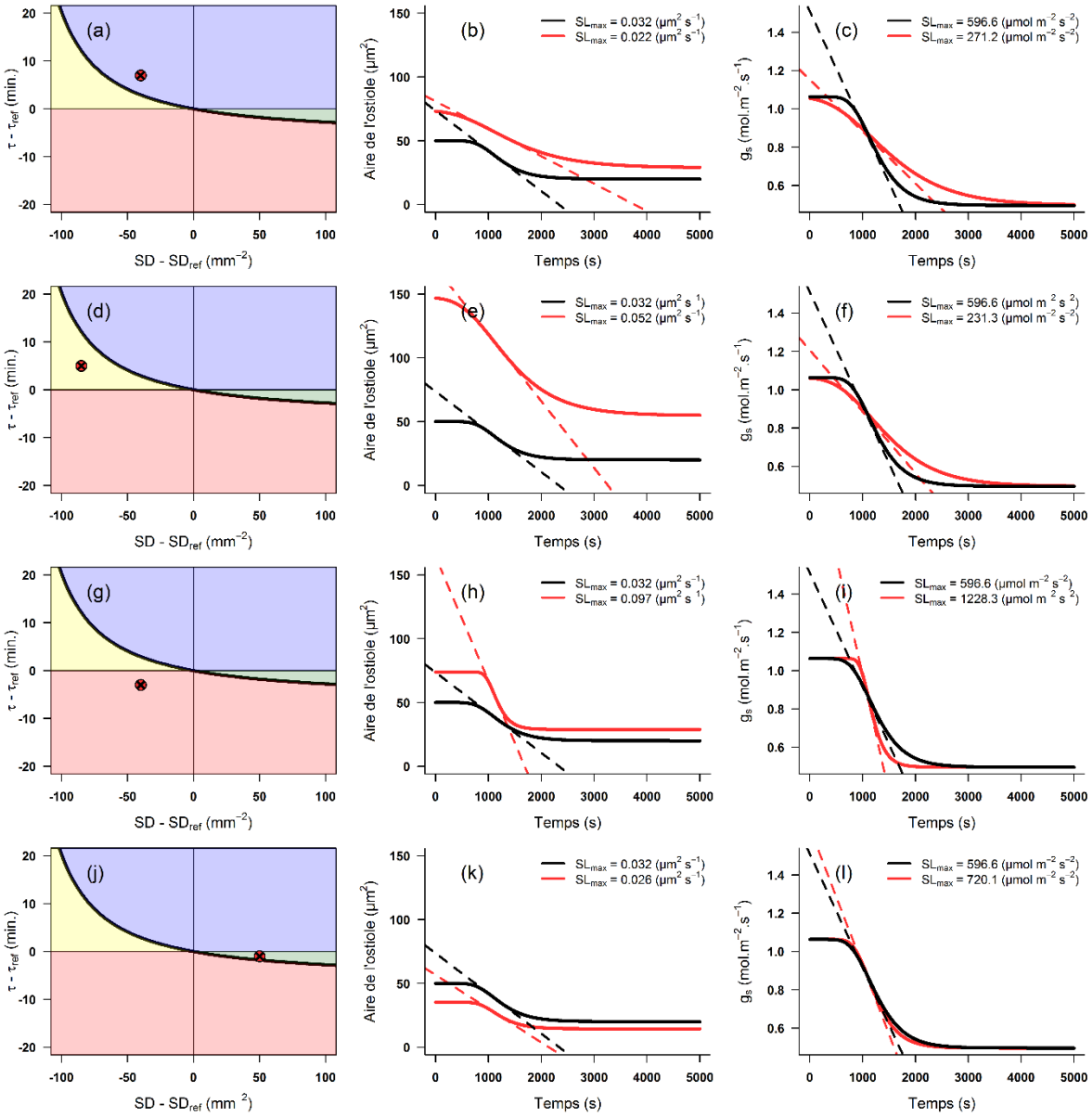

Figure S2. Correlation matrixes between stomatal dynamics as a response to irradiance and VPD and either stomatal morphology (**a**) or whole-plant productivity and water use (**b**). A linear model which included the water regime effect as well as the dependent variable was used. Colors show significant positive correlations and non-significant correlations in orange and white, respectively. All *P*-values were corrected to control for the "false discovery rate". Values shown are partial R^2. τ, λ and SL_{max} are parameters of the dynamic model. GCL, AGC, SD and SAI are the guard cell length and area, the stomatal density and the stomatal area index, respectively. Subscripts "cl" and "op" are for stomatal closing and opening and subscripts "ab" and "ad" are for the abaxial and the adaxial side of the leaf, respectively.

(a)

GCL_{ab}	AGC_{ab}	SD_{ab}	GCL_{ad}	AGC_{ad}	SD_{ad}	SAI		
0.07	0.03	0.01	0.2	0.17	0.15	0.07	τ_{cl}	Irradiance
0.02	0.02	0.04	0.01	0.02	0	0.02	τ_{op}	
0.14	0.07	0	0.27	0.15	0.19	0.02	λ_{cl}	
0.05	0.12	0.04	0.08	0.11	0	0.07	λ_{op}	
0	0.01	0.02	0.02	0.01	0.01	0.02	$SL_{max\ cl}$	
0.05	0.01	0.13	0.21	0.17	0.14	0	$SL_{max\ op}$	
0.01	0.05	0	0.37	0.29	0.01	0.21	τ_{cl}	VPD
0	0	0	0.01	0.06	0.03	0.04	τ_{op}	
0.02	0	0.17	0.23	0.1	0.11	0	λ_{cl}	
0.04	0.09	0.02	0.03	0.01	0	0	λ_{op}	
0.01	0	0.02	0.07	0.02	0.06	0.03	$SL_{max\ cl}$	
0	0	0.02	0	0	0.03	0	$SL_{max\ op}$	

(b)

DMT	H	TLA	WU	E	TE		
0.06	0	0.02	0.08	0	0.01	τ_{cl}	Irradiance
0.02	0.11	0.03	0.06	0.14	0	τ_{op}	
0.1	0.08	0.17	0.04	0.01	0.04	λ_{cl}	
0	0	0.01	0.01	0.3	0.04	λ_{op}	
0	0.01	0	0	0.02	0.01	$SL_{max\ cl}$	
0.18	0.09	0.2	0.08	0.05	0.06	$SL_{max\ op}$	
0.02	0.01	0	0.04	0.42	0.02	τ_{cl}	VPD
0.05	0.01	0.07	0.03	0.01	0	τ_{op}	
0	0.07	0	0	0.04	0.01	λ_{cl}	
0.02	0.02	0.01	0	0.13	0.01	λ_{op}	
0	0.01	0.03	0	0.01	0.08	$SL_{max\ cl}$	
0.03	0.04	0.1	0.01	0	0.02	$SL_{max\ op}$	

Transition

A travers ce chapitre, nous avons vu que les vitesses des mouvements stomatiques était liées à la fois à des facteurs endogènes et environnementaux. De plus, la morphologie stomatique semble impacter différemment la dynamique stomatique selon les conditions extérieures. Ainsi, il ne semble pas être le facteur déterminant responsable des variations de la dynamique stomatique. Ces résultats suggèrent que d'autres facteurs pourraient être impliqués dans la régulation de la conductance stomatique et de sa dynamique temporelle. Les mouvements stomatiques sont déterminés par des flux d'eau à travers les parois des cellules de garde, eux-mêmes induits par des changements de concentration en ions entre le cytoplasme et l'apoplasme (Schroeder *et al.*, 1984). Par conséquent, des variations de l'expression de gènes impliqués dans les mouvements stomatiques, tel que SLAC1 (Geiger *et al.*, 2009) ou KAT1 (Sato *et al.*, 2009) pourraient conduire à une modification de l'activité des canaux ioniques, déterminant la conductance stomatique et peut-être également la vitesse de la dynamique stomatique. Le chapitre suivant est le résultat de prélèvements foliaires associés à des mesures de g_s sur chaque face de la feuille séparément, et à deux moments de la journée (matin et après-midi). Ces prélèvements ont été opérés pendant l'expérimentation de sécheresse en serre. Ils sont destinés à l'étude du contenu en éléments minéraux au sein des cellules de garde et de l'expression de gènes impliqués dans les mouvements stomatiques.

CHAPITRE IV

Le contenu en élément et l'expression de gènes d'intérêt dans les cellules de garde sont connectés aux variations spatiotemporelles de la conductance stomatique.

CHAPITRE IV :

Le contenu en élément et l'expression de gènes d'intérêt dans les cellules de garde sont connectés aux variations spatiotemporelles de la conductance stomatique.

Présentation synthétique de l'article

Contexte

Les stomates sont composés de deux cellules de garde capable de modifier leur ouverture, contrôlant la majorité des échanges gazeux de la plante. Ces mouvements stomatiques font intervenir des mouvements d'eau à travers les parois des cellules de garde, induit par des transferts d'ions entre le cytoplasme et l'apoplasme à l'aide de canaux ioniques. Bien que ces processus soit relativement bien connus chez des plantes modèles, les mécanismes de perception des variations environnementales sont encore largement inconnus. De plus la conductance stomatique pourrait être régulée indépendamment sur chacune des faces de la feuille, et être sujette à des rythmes circadiens spécifiques par rapport au reste du mésophylle. L'étude de ces mécanismes physiologiques et moléculaires au niveau des cellules de garde, indépendamment du reste de la feuille, n'est pas triviale. Cependant, le rôle central des stomates dans les échanges gazeux chez les végétaux, et leurs impacts jusqu'au niveau de l'écosystème, nous incite à améliorer notre compréhension de ces phénomènes.

Objectifs

A partir d'une expérience de sécheresse en serre sur quatre génotypes de peupliers, nous avons mesuré la conductance stomatique de chaque face de la feuille, à deux moments de la journée, selon deux régimes hydriques et pour quatre génotypes de peupliers. Ces mesures ont été associées à la détermination, spécifiquement dans les cellules de garde, du contenu en éléments minéraux et de l'expression de gènes candidats impliqués dans les mouvements stomatiques. Nous avons voulu mettre en évidence : (1) des différences génotypiques constitutives du contenu en éléments et de l'expression de gènes candidats dans les cellules de garde, (2) l'effet du régime hydrique, du moment de la journée et de la face de la feuille sur la réponse des stomates en lien avec a) la conductance stomatique, b) le contenu en éléments et, c) l'expression de gènes candidats dans les cellules de garde.

Stratégie

La croissance et le dispositif de sécheresse appliquée à deux génotypes de peupliers euraméricains (Carpaccio et I214) et deux génotypes de peupliers noirs (6J29 et N38) ont été

décrits dans un article précédemment publié (Chapitre I). Des mesures de la conductance stomatique ont été réalisées immédiatement avant le prélèvement des feuilles. Ces échantillons ont servi d'une part à la mesure du contenu en éléments minéraux des cellules de garde par microanalyse X, et d'autre part à l'étude de l'expression de gènes candidats après microdissection des cellules de garde, extraction d'ARN et RT-qPCR.

Résultats

La conductance stomatique était variable entre génotypes. Les peupliers noirs présentaient une conductance en général plus forte que les peupliers euraméricains, mais le génotype n'était pas le facteur de variabilité principal. La majeure partie des variations pouvait être attribuée aux variations entre les faces des feuilles, aux moments de la journée, et aux régimes hydriques, par ordre d'importance. Au contraire de la conductance stomatique, les six éléments analysés, ainsi que 26 des 27 gènes dont l'expression a été déterminée, montraient une variabilité d'abord due au génotype avant n'importe quel autre facteur. Par exemple le contenu en chlore était 4.6 fois plus élevé chez les peupliers noirs tandis que les aquaporines étaient sous-exprimées chez I214 comparé aux trois autres génotypes. Le régime hydrique était le facteur montrant le moins de variabilité, à la fois sur le contenu en éléments minéraux et sur l'expression génique. En normalisant les données par l'effet génotype, nous avons pu mettre en évidence des motifs de contenu en éléments minéraux et d'expression liés à la face de la feuille et au moment de la journée, similaires entre génotypes. De manière générale, le contenu en éléments était plus élevé le matin, sur la face abaxiale lorsque la conductance était maximale alors que l'expression des gènes impliqués dans les mouvements stomatiques était plus forte l'après-midi, sur la face adaxiale.

Conclusions

Les fortes différences génotypiques observées d'expression génique et de contenu en éléments minéraux mettent en évidence la diversité physiologique des cellules de garde au service des mouvements stomatiques. Ceci suggère également que de telles différences pourraient contribuer à différents mécanismes de régulation et peut-être de dynamique stomatique entre génotypes. Le faible impact de la sécheresse peut s'expliquer par le prélèvement foliaire, réalisé 21 jours après le début d'une sécheresse délibérément modérée, sur des feuilles déjà matures avant le début de la sécheresse. L'effet de déficit hydrique était également faible sur la conductance stomatique, impliquant que la régulation au sein des cellules de garde était faible. Enfin, les motifs d'expression génique et de contenu en éléments minéraux, semblables entre

génotypes, mettent en lumière la régulation spécifique et différentielle de chaque face de la feuille mais de façon similaire au cours de la journée.

Article: Element content and expression of genes of interest in guard cells are connected to spatiotemporal variations in stomatal conductance.

Publié dans Plant, Cell and Environment (2019)

MAXIME DURAND[1] • DAVID COHEN[1] • NATHALIE AUBRY[1] • CYRIL BURÉ[1] • IVANA TOMÁŠKOVÁ[2] • IRÈNE HUMMEL[1] • OLIVER BRENDEL[1] • DIDIER LE THIEC[1]

[1] *Inra, Université de Lorraine, AgroParisTech, SILVA, F-54280 Champenoux, France*

[2] *Department of Genetics and Physiology of Forest Trees, Faculty of Forestry and Wood Sciences, Czech University of Life Sciences Prague, Prague, Czech Republic*

Corresponding author:

Didier Le Thiec

Email: didier.lethiec@inra.fr

Telephone: (+33) 3 83 39 40 98

Accepté le 18 Août 2019

DOI : 10.111/pce.13644

Received: 24 April 2019 | Accepted: 11 August 2019
DOI: 10.1111/pce.13644

ORIGINAL ARTICLE

WILEY Plant, Cell & Environment

Element content and expression of genes of interest in guard cells are connected to spatiotemporal variations in stomatal conductance

Maxime Durand[1] | David Cohen[1] | Nathalie Aubry[1] | Cyril Buré[1] | Ivana Tomášková[2] | Irène Hummel[1] | Oliver Brendel[1] | Didier Le Thiec[1]

[1] Inra, Université de Lorraine, AgroParisTech, SILVA, F-54280 Champenoux, France

[2] Department of Genetics and Physiology of Forest Trees, Faculty of Forestry and Wood Sciences, Czech University of Life Sciences Prague, Prague 165 00, Czech Republic

Correspondence
D. Le Thiec, Inra, Université de Lorraine, AgroParisTech, SILVA, F-54280 Champenoux, France.
Email: didier.lethiec@inra.fr

Funding information
FP7 Food, Agriculture and Fisheries, Biotechnology, Grant/Award Number: Watbio / 311929; Institut National de la Recherche Agronomique, Grant/Award Number: Dpt EFPA; Lorraine region; French National Research Agency, Grant/Award Number: ANR-12-LABXARBRE-01; European Union's Seventh Programme, Grant/Award Number: 311929

Abstract

Element content and expression of genes of interest on single cell types, such as stomata, provide valuable insights into their specific physiology, improving our understanding of leaf gas exchange regulation. We investigated how far differences in stomatal conductance (g_s) can be ascribed to changes in guard cells functioning in amphistomateous leaves. g_s was measured during the day on both leaf sides, on well-watered and drought-stressed trees (two *Populus euramericana* Moench and two *Populus nigra* L. genotypes). In parallel, guard cells were dissected for element content and gene expressions analyses. Both were strongly arranged according to genotype, and drought had the lowest impact overall. Normalizing the data by genotype highlighted a structure on the basis of leaf sides and time of day both for element content and gene expression. Guard cells magnesium, phosphorus, and chlorine were the most abundant on the abaxial side in the morning, where g_s was at the highest. In contrast, genes encoding H^+-ATPase and aquaporins were usually more abundant in the afternoon, whereas genes encoding Ca^{2+}-vacuolar antiporters, K^+ channels, and ABA-related genes were in general more abundant on the adaxial side. Our work highlights the unique physiology of each leaf side and their analogous rhythmicity through the day.

KEYWORDS

abaxial and adaxial surfaces, droughts, elements, gene expression, plant stomata, Populus, stomatal conductance

1 | INTRODUCTION

Stomata are small pores on the surface of the leaf responsible for almost all gas exchange between the leaf internal environment and the surrounding air. They are composed of two guard cells that modify their volume, adjusting the central aperture and controlling the flow of gases in and out of the leaf. These adjustments are regulated by a variety of internal and external factors, including but not limited to water availability (Monclus et al., 2006), irradiance (Shimazaki, Doi, Assmann, & Kinoshita, 2007), and circadian rhythms (de Dios, 2017). Regulation of stomatal aperture is considered a key phenomenon, maximizing CO_2 uptake for photosynthesis with regard to water loss by transpiration (Cowan & Farquhar, 1977), whose importance increases as internal and environmental conditions become more limiting.

Poplars are dicots, model trees for molecular studies (Jansson & Douglas, 2007; Tuskan et al., 2006), with amphistomateous leaves. As such, despite being in the same environment, each leaf side experiences a different magnitude of irradiance and temperature (Clum,

1926; Sheriff, 1979). Literature evidence suggests that guard cell sensitivity to irradiance (Kassam, 1973), vapour-pressure deficit (Pallardy & Kozlowski, 1979), leaf water potential (Kanemasu & Tanner, 1969), and ozone (Dumont et al., 2014) differs between leaf sides. Moreover, some species showed independent stomatal regulation between surfaces (Mott, 2007; Richardson, Brodribb, & Jordan, 2017), consistent with an optimal stomatal behaviour of each leaf side. This suggests that, in poplars, stomatal movements under drought and along the day may depend on the side of the leaf.

As a consequence of global climate change, droughts are expected to be more intense and frequent in the future (Dai, 2012; Intergovernmental Panel on Climate Change, 2014). A prolonged reduction in water availability will induce a wide variety of severe and long-lasting humanitarian, economic, and environmental impacts on ecosystems and societies (Touma, Ashfaq, Nayak, Kao, & Diffenbaugh, 2015). Among them, the impact of drought on forests is a central concern in global climate change research given the interrelation between forests and climate (Bonan, 2008). Poplars are commonly distributed along riparian ecosystems due to their high water requirements (Tschaplinski & Blake, 1989). Their cultivation however usually extend to mesophyte habitats where they are more frequently subjected to soil water deficit. Plant response to drought is complex, but stomatal closure and a reduction in plant productivity is generally observed (Ciais et al., 2005; Coopman et al., 2008; Monclus et al., 2006).

For soil water deficit and high vapor pressure deficit (VPD) conditions, it remains unresolved whether hydraulic or hormonal mechanisms are responsible for stomatal closure (Merilo et al., 2018; Rodriguez-Dominguez et al., 2016). One hypothesis states that a decrease in stomatal conductance (g_s) during drought is mostly driven by hormonal signals such as abscisic acid (ABA), which are generated independently of leaf water status (Davies & Zhang, 1991; Dodd, 2005; Tardieu & Simonneau, 1998). However, the complex regulation of stomatal functioning can involve a number of actors, from phytohormones to strigolactones (Acharya & Assmann, 2009; Lv et al., 2018). It has alternatively been proposed that stomatal closure during edaphic droughts is caused by an actively mediated negative feedback response of stomata to reduced leaf turgor (Brodribb & Cochard, 2009; Buckley, 2005; Sperry, Hacke, Oren, & Comstock, 2002). ABA is a central plant hormone responsible for promoting stomatal closure and inhibiting opening under drought (Chaves, Maroco, & Pereira, 2003; Huang, Wu, Abrams, & Cutler, 2008). In recent years, evidence has accumulated showing that guard cells possess the full ABA biosynthesis pathway (Bauer et al., 2013) and the early ABA signal transduction (Zhang et al., 2015). ABA binds and inhibits PP2C-type phosphatases by binding to the PYR/PYLs family of proteins (Merilo et al., 2013), including ABI1 (Park et al., 2009; Yoshida et al., 2006). This in turns relieves the repression on OST1, which inactivates the KAT1 inward-rectifying potassium channel (Sato et al., 2009) and activates the S-type anion channel SLAC1 (Geiger et al., 2009). These channels, among others, induce a reduction of osmotic potential inside the guard cells leading to a flow of water outward, which results in stomatal closure (Schroeder & Hedrich, 1989; Schroeder, Raschke, & Neher, 1987).

In addition, circadian rhythms in transcript accumulation (Wilkins, Waldron, Nahal, Provart, & Campbell, 2009) and gas exchange (de Dios, 2017) are limiting our ability to fully understand the molecular signals involved in stomatal movements. A number of genes involved in the regulation of stomatal movements were found to be gated by the circadian clock, including ABA biosynthesis and signalling pathways (for a complete review, see Seung, Risopatron, Jones, & Marc, 2012) and *TIPs* and *PIPs* (aquaporins) mRNA levels (Chaumont & Tyerman, 2014). Circadian rhythms appear to be cell-specific as stomata were shown to have a distinct rhythmicity compared with surrounding mesophyll cells in *Arabidopsis thaliana* (Hassidim et al., 2017; Yakir et al., 2011). Given the importance of stomata in regulating gas exchange and thus the productivity of plantations, there is a need to better understand the regulation of g_s during the day and under different water availabilities.

Specifically studying stomata independently from the surrounding mesophyll cells is not trivial (Leonhardt et al., 2004). Hence, not much is known about the physiological and molecular processes in guard cells driving stomatal conductance in trees species such as poplars. To increase our understanding of the differences in such cellular processes among genotypes, between leaf sides, during the day and plastic responses related to soil water deficit, there is a need for studies targeting a specific cell type.

To test well-established processes exerted by the guard cells, quantification of their element content and their expression of 27 genes of interest were monitored separately on both leaf sides from leaves harvested in the morning and the afternoon. We used two *Populus nigra* × *Populus deltoides* (*Populus euramericana*, Moench) and two *P. nigra* (L.) genotypes grown in parallel under control and soil water deficit conditions. Given this experimental set-up, we aimed to answer the following questions: (a) Is there a constitutive difference among genotypes of element content and gene expression in poplar guard cells? (b) Do factors such as water regime, time of the day, and leaf side induce a plastic response in terms of guard cells (i) element content and (ii) gene expression?

2 | MATERIAL AND METHOD

2.1 | Plant material and growth conditions

Woody cuttings of four poplar genotypes belonging to different species or commercial hybrids (Carpaccio and I214: *P. deltoides* × *P. nigra*, Moench, 6J29 and N38: *P. nigra*, L.) were grown in a fully automated glasshouse under natural light with a free range for air temperature between 15°C and 25°C at INRA-Grand-Est (48°45′09.3″N, 6°20′27.6″E; Champenoux, France), as described previously (Durand, Brendel, Buré, & Le Thiec, 2019). Genotypes were chosen based on their contrasting drought response: I214 and 6J29 are generally found to be sensitive to drought (Chen, Wang, Altman, & Huttermann, 1997; Giovannelli et al., 2007; Muller & Lambs, 2009; Viger et al., 2016). Sixteen cuttings per genotype were planted in 9.5 kg (±1.5%) of a sand/peat mixture (1/1, v/v), complemented with fertilizer (1 g L^{-1} of

CaMg $(CO_3)_2$ and 20 g of Nutricote T100, 13:13:13 NPK and micronutrients, FERTIL S.A.S., Boulogne-Billancourt, France). Each 10-L pot was covered with 1.4 kg of white marble gravel (8–12 mm). Pots were weighed and watered to 27.9% volumetric soil water content (SWC; 85% of field capacity) at least three times a day with a robot (Durand et al., 2019). After 60 days of precultivation, watering was stopped for half the individuals (randomly chosen) until an SWC of 18.3% was reached. This controlled soil water deficit was maintained constant for 25 days using a pot-specific linear regression between SWC measured by time domain reflectometry (HD2, IMKO, Ettlingen, Germany) and pot mass (R^2 > .8). Reference masses were adjusted each week to take the plant growth into account. Growth, transpiration, and meteorological data are available in Durand et al. (2019).

2.2 | Leaf gas exchange and leaf sampling

Leaf gas exchange and leaf sampling were performed sequentially in order to accurately capture stomatal conductance at the time of sampling. The first fully expanded leaf (selected before the drought) and the one immediately below were sampled 21 days after the start of the drought experiment at 10:30 a.m. and 3:00 p.m. local time, respectively. At the time, the natural daytime lasted 16 hr (starting at 4:30), global radiation was 297.2 ± 47.8 and 145.6 ± 45.1 W m^{-2}, air temperature was 24.9 ± 0.2 and 24.8 ± 0.2°C, and vapour-pressure deficit was 1.31 ± 0.02 and 1.20 ± 0.07 kPa for the two sampling events, respectively. From previous g_s time-course measurements, stomata were likely fully open in the morning and in a closing phase in the afternoon (Durand et al., 2019). The last watering event was completed 2 hr before each sampling. A leaf porometer was used in order to measure g_s separately on the abaxial and adaxial surfaces of the leaves (SC-1 porometer; Decagon Devices, Inc., Pullman, WA, USA). Stomata being on the leaf surfaces, sampled leaves were flash frozen in liquid nitrogen immediately after measurements, to guarantee both RNA integrity and that diffusive elements remained in guard cells (Amsellem et al., 1983; Jaiprakash et al., 2003).

2.3 | X-ray microanalysis

Sample preparation and microanalyses were performed following Dumont et al. (2014), except for the use of a tungsten coating on the samples and a probe intensity of 1 nA, in order to allow analyses in stomata specifically. Although the analysed X-rays originate from a lower layer in the sample than electrons (Amsellem et al., 1983), the electron beam diameter and depth of penetration is lower than 2 µm and has been simulated in a Monte Carlo procedure (Pouchou & Pichoir, 1991); 20 guard cells, each belonging to different stomata of freeze-dried leaves, were specifically targeted and analysed for each of the two leaf sides, the two times of day, the two water treatments, and the four genotypes with six replicates in each condition. Microanalyses were corrected by measuring the content of beech leaves powder of known mass fraction (CRM 100, BCR® certified reference material, Commission of the European Communities, Brussels, Belgium) for sodium (Na), magnesium (Mg), phosphorus (P), chlorine (Cl), potassium (K), and calcium (Ca). All forms were measured, both organic and inorganic. We also computed a ratio of anions over cations for each guard cell (i.e., P and Cl over Na, Mg, K, and Ca later referred to as *An/Cat*). Values were converted from percent to "per mille" (or mg g^{-1}) of dry mass.

2.4 | Guard cell microdissection, RNA extraction and cDNA amplification

Guard cells microdissection, RNA isolation, RNA reverse-transcription, and cDNA amplification were performed following Dumont et al. (2014). A brief description of the methods is given hereinafter. If not otherwise specified, protocols were performed following the manufacturer's instructions; 1,000 stomata per sample were microdissected using the PALM MicroBeam system (Carl Zeiss MicroImaging GmbH, Jena, Germany). Total RNA was extracted using Qiagen RNeasy Plus Micro Kit (Qiagen, Courtaboeuf, France). Previous tests in our lab and in the literature show that the process of freeze-drying and preparing microscopic slide does not impact the RNA integrity (Damsteegt, McHugh, & Lokman, 2016; Dumont et al., 2014; García-Baldenegro et al., 2015; Heinen et al., 2014; Jaiprakash et al., 2003). Transplex® Whole Transcriptome Amplification Kit (MERCK, Saint-Quentin Fallavier, France) was used for RNA reverse transcription and cDNA amplification (100 µl twice by sample). The latter was purified by Gene Elute PCR (SIGMA, Saint-Quentin Fallavier, France). cDNA purity and concentration were measured (Nanodrop 1000; Thermo Scientific, Illkirch, France). All cDNA samples exhibited a good purity level ($1.6 < A_{260}/A_{280} < 2.0$ and $1.3 < A_{260}/A_{230} < 1.9$), and each sample was diluted to get 2.5 ng μl^{-1}. Absence of genomic DNA was confirmed by PCR with intron-flanking primers.

2.5 | Expression of genes of interest and real-time PCR

The genes of interest were retrieved on the Populus genome v3.0 (Phytozome, RRID:SCR_006507, https://phytozome.jgi.doe.gov/pz/portal.html; Tuskan et al., 2006). The genes of interest were selected for their putative role in encoding ionic pumps, aquaporins, transporters involved in stomatal movements, and phototropins, β-carbonic anhydrases, and genes linked to ABA biosynthesis and signalling. Genes were selected in regard to previous studies (Cohen et al., 2010; Dumont et al., 2014; Heinen et al., 2014) on the basis of a high expression level in poplar guard cells (when available, and in leaves otherwise), their differential expression among genotypes, between leaf sides, water availability, and time of day. The design of primers, with adequate specificity for all four genotypes, was also a limiting step for gene selection. Only primers with a reduced risk of primer dimer formation or nonspecific amplification were selected. Because the expression of gene of interest approach is not exhaustive by definition, we chose to investigate genes with different roles, instead of a whole family of genes. Thus, our interpretation is not limited to a

single family of transporters but benefits from a more exhaustive assessment of guard cell processes linked with stomatal regulation. The targeted genes and their description are provided in Table 1 (additional information is given in Table S1).

Real-time PCR was performed in a 96-well Mx3005P thermocycler (Agilent, Waghaeusel-Wiesental, Germany) using the recommended cycling programme: 5 min at 95°C, 40 cycles of 5 s at 95°C, and 20 s at 58°C or 60°C depending on primers, followed by melting cycle to ensure a single amplicon (Dumont et al., 2014). The mix contained 10 ng of cDNA, the reference dye (ROX, Agilent technologies), gene-specific primers, and the Brilliant III UltraFast SYBR GREEN qPCR Master Mix (Agilent, Santa Clara, CA). No-template control reactions were prepared for each gene. The plate set-up included all samples from two genotypes and the negative controls. The Ct values were determined with the same threshold. For each targeted gene-genotype group, efficiency was calculated from standard curves over seven dilutions. Efficiencies varied from 65% to 102% ($R^2 \geq .985$) and were taken into account in all subsequent calculations (Bizet et al., 2015). Among the studied genes, *UBQ11* (Brunner, Yakovlev, & Strauss, 2004), *QUAC1* (Dumont et al., 2014), and *BAM1* were the most stable and used as references, together with an external control (GENORM v3.5, RRID:SCR_006763, https://genorm.cmgg.be/; Mestdagh et al., 2009; Vandesompele et al., 2002). The fluorescent threshold being set constant, the nonnormalized expression level was computed as $RQ = 1/(Ta \cdot E^{Ct})$, Ta being the amplicon length in bp and E the efficiency (Bizet et al., 2015; Gutierrez et al., 2008).

TABLE 1 Description of the genes studied and their localization

Genes	Description
NCED3.1	Key enzyme in ABA biosynthesis (9-cis-epoxycarotenoid dioxygenase).
NCED3.2	Key enzyme in ABA biosynthesis (9-cis-epoxycarotenoid dioxygenase).
ABI1	Protein phosphatases type 2C (PP2Cs), negative regulator of ABA promotion of stomatal closure.
OST1	SNF1-related protein kinase, involved in ABA-induced stomatal closure by activating of S-type anion channels and inhibiting inward rectifying potassium channel.
PYL2	PYR/PYL/RCAR family of protein, inhibits the activity of group-A protein phosphatases type 2C (PP2Cs) when activated by ABA.
PYL4	PYR/PYL/RCAR family of protein, inhibits the activity of group-A protein phosphatases type 2C (PP2Cs) when activated by ABA.
PYL8	PYR/PYL/RCAR family of protein, inhibits the activity of group-A protein phosphatases type 2C (PP2Cs) when activated by ABA.
CA1	Beta-carbonic anhydrase, involved in CO_2-mediated stomatal closure (chloroplast).
CA4	Beta-carbonic anhydrase, involved in CO_2-mediated stomatal closure (PM).
PHOT1	Blue light photoreceptors, mediate blue light-dependent activation of the plasma membrane H^+-ATPases
PHOT2	Blue light photoreceptors, mediate blue light-dependent activation of the plasma membrane H^+-ATPases
AKT2	Inward rectifying potassium channel (PM), responsible for the Ca^{2+} sensitivity of the K^+ uptake channel.
KAT1.2	Inward rectifying potassium channel (PM), responsible for the Ca^{2+} sensitivity of the K^+ uptake channel.
KAT3	Inward rectifying potassium channel (PM), responsible for the Ca^{2+} sensitivity of the K^+ uptake channel. Involved in down-regulating AKT1 and KAT1 channel activity by forming heteromers.
OST2	Proton ATPases (PM)
AHA11	Proton ATPases (PM)
SLAC1	Slow anion channel (PM), involved in stomatal closure in response to a variety of signals including elevated CO_2, ozone, ABA, darkness, and humidity.
CAX1	Calcium antiporter (V)
CAX1.6	Calcium antiporter (V)
NHX1.13	Potassium, sodium/proton antiporter (V) involved in salt tolerance and ion homeostasis
PIP1.2	Aquaporin: plasma membrane intrinsic protein (PM)
PIP2.1	Aquaporin: plasma membrane intrinsic protein (PM)
PIP2.5	Aquaporin: plasma membrane intrinsic protein (PM)
TIP1.3	Aquaporin: tonoplast intrinsic protein (V)
TIP1.4	Aquaporin: tonoplast intrinsic protein (V)
TIP2.1	Aquaporin: tonoplast intrinsic protein (V)
TIP2.2	Aquaporin: tonoplast intrinsic protein (V)

[a]Abbreviations: PM, plasma membrane; V: vacuole.

The normalized expression of targeted genes were computed by dividing their RQ by the geometric average of the reference gene's RQ (Bizet et al., 2015).

2.6 | Statistics

Statistics were performed using R 3.5.1 (R Project for Statistical Computing, RRID:SCR_001905, https://cran.r-project.org/, all data used are available in Table S2). We used a type 2 factorial analysis of variance design to study the variation of g_s (n = 6), element content (n = 6), and normalized mRNA levels (n = 4) by genotype, water regime, time of day, and leaf side and their first-order interaction. Given the complexity of the design, we decided to focus our interpretation of the dataset on the significant main factors and their first-order interactions, instead of computing all pairwise comparisons between our 32 groups. This enabled us to explore the major trends with a larger sample size and a higher statistical power than if we specifically addressed each pairwise comparison. Normalized transcript levels were transformed with a logarithmic function of base 2 in order to achieve a normal distribution of the data. Post hoc contrast analyses were performed to test differences between specific modalities of the studied factors depending their significance, and P values were adjusted to control for the false discovery rate. The partial R^2 was calculated to compare the contribution with the explained variable of each of the four dependent variables. We performed a principal component analysis (PCA) on the six elements studied and the ratio *An/Cat* on one hand and on the expression data of 27 genes of interest on the other hand. We fitted to every variable a linear model that included the highly significant genotype effect as a dependent factor. The residuals of these models were used as the data for the two PCA in order to emphasize the other main effects (water regime, time of day, and leaf side). Stomatal conductance data were fitted with a similar model, and the residuals were added as a supplementary variable.

3 | RESULTS

3.1 | Stomatal conductance

Testing for genotypic, water availability, time of day, and leaf side effects on g_s measured immediately before sampling the leaves, we found all four to be significant (Table 2, P < .002 in all cases). Drought-stressed poplars had an overall 20% lower g_s than well-watered trees. Because there was no interaction with the water treatment, we showed the average g_s of both treatments (Figure 1). The significant interaction between genotype and time of day (P = .023) showed that the afternoon decrease of g_s tended to be stronger in both hybrid poplars than in the black poplars (Figure 1). Black poplars exhibited in general a higher g_s than the hybrid poplars, and g_s was overall higher on the abaxial side. Essentially, the highest g_s tended to be observed on the abaxial side, in the morning and on well-watered trees for all genotypes, whereas the adaxial side, in the afternoon on drought-stressed trees, showed the lowest g_s.

3.2 | Genotypic diversity of element content and gene expression within guard cells

In this study, element content was measured as the whole guard cell average. We found significant genotypic diversity in all measured elements (Figure S1, Table 2, in all cases P < .001). The genotype effect was always the factor explaining the total variance of element content the most (Table S3). To highlight these genotypic differences, we decided to show the genotype means for each element in Figure 2. Partial R^2 for genotype ranged from.16 for the P content to.7 for the Cl content (Na: .57, Mg: .49, P: .16, Cl: .70, K: 0.33, Ca: 0.21). The main elements in the guard cells were K and Ca. Na content was the highest in the guard cells of the hybrid poplars, and especially in Carpaccio were it was 3.1, 5.3, and 3.8 times higher than I214, 6J29, and N38 respectively. Additionally, Mg content was 1.7 times higher in Carpaccio than in the other three genotypes, but K content was 1.6 times higher in I214 than in the other three genotypes. On the other hand, Cl content was 4.6 times lower in both hybrid poplars than in the two black poplar genotypes. This effect was passed on in our calculation of *An/Cat*, which was 2.2 times lower in the two hybrid poplars than in the *P. nigra* genotypes. Moreover the guard cells of 6J29 showed a P and Ca content, respectively, 17% and 24% lower than in the other three genotypes on average.

The expression of genes of interest in the guard cells was also structured according to genotype. Figures 3 and S2 show the back-transformed mean of normalized mRNA levels by genotype, that is, by applying a base 2 exponential to the means of the log2-transformed data, to be consistent with statistical analyses. For all measured transcripts (in all cases P < .001) except for *CAX1* (P = .34), the genotype effect was always the factor explaining the total variance of normalized mRNA levels the most (Table S3). Partial R^2 for the genotype effect ranged from 0.13 to 0.98 for *AKT2* encoding a K^+ channel and *PYL2*, encoding an ABA receptor, respectively, with an average of 0.57. Overall, the normalized expression of *NCEDs*, encoding 9-cis-epoxycarotenoid dioxygenases involved in ABA biosynthesis, were the highest in black poplars. Specifically, N38 and 6J29 exhibited the highest accumulation of transcripts for *NCED3.1* and *NCED3.2*, respectively (Figure S2a,b). Conversely, ABA signalling pathway-related transcripts appeared more expressed in I214 guard cells, and especially the genes encoding the ABA receptor *PYL2* and *PYL8* (Figure S2e,g). Carpaccio was consistently among the genotypes with the lowest accumulation of transcripts related to both ABA biosynthesis and signalling pathways. Regarding ß-carbonic anhydrases, N38 exhibited equivalent levels of *CA1* and *CA4* mRNA, whereas for the other genotypes, *CA1* transcripts were accumulated up to 100 times more than *CA4*. Hence, *CA1* normalized transcript levels were the highest in the guard cells of Carpaccio and 6J29, but *CA4* levels were the highest in the guard cells of N38 (Figure S2h,i). The transcript accumulation of genes encoding phototropins *PHOT1* and *PHOT2* were significantly different across all genotypes. Concerning ion channels, I214 was often the genotype with the lowest level of transcripts for inward-rectifying K^+ channels (*AKT2* and *KAT3*) and proton H^+-ATPase (*OST2* and *AHA11*). Among black poplars guard cells, these

TABLE 2 Summary of the genotype, water treatment, time of day, and leaf side effect on stomatal conductance (n = 6), guard cell element content (n = 6), and expression of genes of interest (n = 4)

	Genotype (G)	Water treatment (T)	Time of day (D)	Leaf side (S)	Interaction G:T	Interaction G:D	Interaction G:S	Interaction T:D	Interaction T:S	Interaction D:S
g_s	<.001	.002	<.001	<.001	ns	.023	ns	ns	ns	ns
Na content	<.001	ns	ns	<.001	ns	ns	<.001	ns	ns	ns
Mg content	<.001	ns	.043	ns	ns	ns	ns	ns	ns	ns
P content	<.001	ns	.003	<.001	.032	ns	ns	ns	ns	ns
Cl content	<.001	.003	.009	<.001	ns	ns	<.001	ns	ns	ns
K content	<.001	ns	ns	.001	ns	ns	.015	ns	ns	ns
Ca content	<.001	ns	ns	<.001	.008	ns	ns	ns	ns	ns
An/Cat	<.001	ns	.001	.003	ns	ns	ns	ns	ns	ns
ABI1	<.001	ns	ns	.002	.004	ns	ns	ns	ns	.03
AHA11	<.001	ns	<.001	ns	.027	ns	ns	ns	ns	ns
AKT2	<.001	ns	ns	<.001	.004	.018	.001	ns	ns	ns
CA1	<.001	ns	ns	.002	.025	ns	ns	ns	ns	ns
CA4	<.001	ns	ns	<.001	ns	ns	ns	.024	ns	ns
CAX1	ns	ns	ns	<.001	ns	ns	ns	.029	ns	ns
CAX1.6	<.001	ns	ns	<.001	.042	ns	ns	ns	ns	ns
KAT1.2	<.001	ns	.031	<.001	<.001	ns	.007	ns	ns	ns
KAT3	<.001	.005	<.001	ns	ns	ns	ns	ns	ns	ns
NCED3.1	<.001	ns	.023	<.001	ns	ns	ns	ns	ns	ns
NCED3.2	<.001	ns	.049	.013	.022	ns	ns	ns	ns	ns
NHX1.13	<.001	ns	ns	ns	ns	.015	.004	ns	ns	ns
OST1	<.001	.034	.001	<.001	.01	ns	<.001	ns	ns	ns
OST2	<.001	ns	.014	ns	ns	ns	ns	ns	ns	ns
PHOT1	<.001	ns	ns	.016	ns	ns	ns	ns	ns	ns
PHOT2	<.001	ns	.011	ns	ns	ns	ns	ns	ns	ns
PIP1.2	<.001	ns	<.001	<.001	.005	ns	<.001	ns	ns	ns
PIP2.1	<.001	<0.001	.022	ns	ns	ns	ns	ns	ns	ns
PIP2.5	<.001	ns	.009	ns	ns	ns	.003	ns	ns	ns
PYL2	<.001	ns	ns	ns	ns	.048	ns	ns	ns	ns
PYL4	<.001	0.008	ns	ns	.037	ns	ns	ns	ns	ns
PYL8	<.001	ns	.032	<.001	.015	ns	.003	ns	ns	ns
SLAC1	<.001	0.018	ns	.016	.039	ns	.008	ns	ns	ns
TIP1.3	<.001	ns	.001	ns	.02	ns	ns	ns	ns	ns
TIP1.4	<.001	ns	ns	ns	.004	ns	.009	ns	ns	ns
TIP2.1	<.001	ns	.005	.049	ns	.001	ns	ns	ns	ns
TIP2.2	<.001	ns	ns	ns	ns	ns	ns	ns	ns	ns

[a]*Note*. A type two factorial analysis of variance design with first-order interactions was used. Normalized transcript levels were transformed with a logarithm function of base 2 in order to achieve a normal distribution of the data.

[b]Abbreviations: g_s, stomatal conductance to water vapour; An/Cat, ratio of anions over cations (i.e., P and Cl over Na, Mg, K, and Ca); ns, not significant. $^*P < .05$. $^{**}P < .01$. $^{***}P < .001$.

genes were either similarly or more expressed in 6J29 than in N38 (*AKT2*, *OST2*, and *SLAC1*). As to vacuolar Ca^{2+} antiporters, although transcripts accumulation for *CAX1* did not show any significant genotype effect, *CAX1.6* was on average 161 times more accumulated in the guard cells of hybrid poplars than in the black poplars. The same pattern was found for the vacuolar Na^+/H^+ antiporter *NHX1.13*. Its mRNA levels were also high in Carpaccio, compared with I214. Interestingly, *NHX1.13* expression correlated to the Na content in guard cells (Figure 4, $P < .001$, $R^2 = .35$). Targeted aquaporins (*PIPs* and *TIPs*) mRNA were consistently expressed at the lowest levels in I214, with

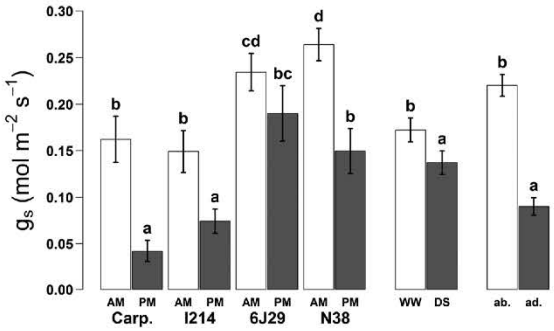

FIGURE 1 Stomatal conductance of four poplar genotypes under contrasting water availability. Each leaf side has been measured separately once in the morning and once in the afternoon (10:30 a.m. and 3:00 p.m.). Carpaccio and I214 are *Populus deltoides* × *Populus nigra*, whereas 6J29 and N38 are *P. nigra* genotypes. White and grey coloured bars show the contrasts used for statistical design. Letters show significant differences among groups for the genotype-time of day interaction, the water treatment and the leaf side ($P < .05$)

the notable exception of *TIP2.1*, which was expressed at the highest level in I214 guard cells (Figure S2u–aa).

3.3 | Impact of water availability on element content and transcript accumulation in guard cells

Cl was the only element whose content in the guard cells was significantly 13% higher in the drought-stressed trees across all genotypes (Figure S1d, $P = .003$). Moreover, the guard cells Cl content was positively correlated with g_s when controlling for genotype and water treatment differences (Figure 5, partial $R^2 = .15$, $P < .001$). Other modifications of element content in response to water regime were genotype specific. The guard cells of I214 had a P content 11% lower under drought (for well-watered and drought-stressed trees, respectively: 1.92 and 1.71 mg g^{-1}, $P = .011$, Figure S1c). Among black poplars, 6J29 and N38 exhibited an increased guard cells Ca content, respectively, 15% and 13% higher in the drought-stressed than in the well-watered trees (for control and drought-stressed, respectively, 6J29: 4.92 and 5.78 mg g^{-1}, $P = .028$; N38: 6.60 and 7.55 mg g^{-1}, $P = .015$, Figure S1f). Neither K nor any other element in guard cells were under a significant effect of the water regime, either as a main effect or as part of an interaction ($P > .075$, Table 2).

With respect to the normalized transcript accumulation, the water regime was highly genotype specific as 14 of 27 genes showed a significant interaction between the two factors (Table 2, Figure S2). Only *KAT3* and *PIP2.1* mRNA levels were significantly lower and higher, respectively, in the drought-stressed trees than in the control, in all genotypes ($P < .006$, Figure S2n–v). Concerning the hybrid poplars, the expression of three genes was down-regulated in response to water stress in the guard cells of Carpaccio (*KAT1.2*, *SLAC1*, and *TIP1.4*) but only two in the guard cells of I214 (*AHA11* and *TIP1.3*). For 6J29, the expression of *PYL8*, *CA1*, and *PIP1.2* was up-regulated in response to water stress. N38 showed the widest responsiveness to water stress. The expression of *PYL4* and *TIP1.3* was significantly down-regulated, whereas the expression of *ABI1*, *OST1*, *AKT2*, *KAT1.2*, and *PIP1.2* was up-regulated under water stress.

3.4 | Diurnal and leaf side differences of element content in guard cells

The PCA highlighted four groups consisting of every paired modality of the time of day and leaf side (Figure 6). The first and second axis explained 36.1% and 24.7% of the total variance with the third

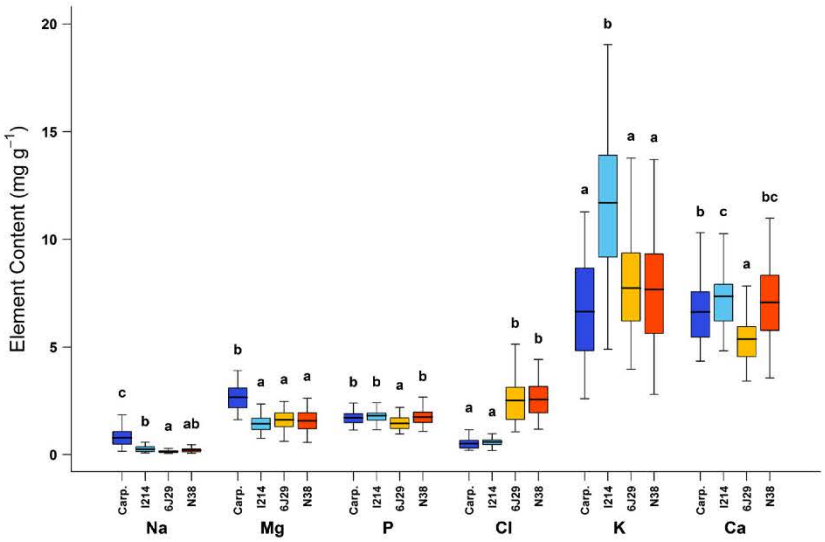

FIGURE 2 Guard cell element content of four poplar genotypes. Carpaccio and I214 are *Populus deltoides* × *Populus nigra*, whereas 6J29 and N38 are *P. nigra* genotypes (in dark and light blue, yellow and orange, respectively). Values inside each box are the genotypic mean expressed as "per mille" of dry mass, or mg g^{-1} ($n = 42–48$). Boxes and bars show the 10th, 25th, 75th, and 90th percentiles. Letters show significant differences by post hoc contrast among the four genotypes for each element [Colour figure can be viewed at wileyonlinelibrary.com]

Carp.	I214	6J29	N38	
0.00019 a	0.0001 a	0.00018 a	0.0025 b	*NCED3.1*
0.000007 a	0.0000051 a	0.0003 b	0.000002 a	*NCED3.2*
0.37 a	1 b	1.3 b	0.47 a	*ABI1*
0.13 a	0.24 b	0.61 c	0.22 b	*OST1*
0.19 a	18 d	0.93 b	8.9 c	*PYL2*
0.028 a	0.058 b	0.02 a	0.061 b	*PYL4*
0.14 a	2.3 b	0.19 a	0.26 a	*PYL8*
2.8 b	0.88 a	8 c	0.83 a	*CA1*
0.071 b	0.04 a	0.077 b	0.21 c	*CA4*
0.24 c	0.035 a	0.17 b	0.75 d	*PHOT1*
0.91 c	0.29 b	0.074 a	4.3 d	*PHOT2*
0.0036 b	0.00059 a	0.0085 b	0.00098 a	*AKT2*
0.016 a	0.019 a	0.031 b	0.034 b	*KAT1.2*
0.16 c	0.013 a	0.035 b	0.036 b	*KAT3*
0.052 d	0.0017 a	0.033 c	0.0059 b	*OST2*
0.017 b	0.0063 a	0.042 c	0.038 c	*AHA11*
0.000079 b	0.000052 ab	0.016 c	0.000015 a	*SLAC1*
0.00013 a	0.00047 a	0.0001 a	0.00017 a	*CAX1*
0.0062 b	0.0025 b	0.000033 a	0.000021 a	*CAX1.6*
0.019 d	0.0068 c	0.00039 a	0.0021 b	*NHX1.13*
0.4 d	0.023 a	0.2 c	0.071 b	*PIP1.2*
0.056 b	0.0002 a	0.46 d	0.25 c	*PIP2.1*
0.0018 b	0.0007 a	0.026 d	0.011 c	*PIP2.5*
2.2 b	0.043 a	2.7 c	4.6 d	*TIP1.3*
0.0049 b	0.0012 a	0.0021 a	0.031 c	*TIP1.4*
0.00062 ab	0.0065 c	0.0028 bc	0.00033 a	*TIP2.1*
0.000012 b	0.00000077 a	0.0000016 a	0.046 c	*TIP2.2*

FIGURE 3 Guard cell transcript accumulation heatmap of four poplar genotypes. Carpaccio and I214 are *Populus deltoides* × *Populus nigra*, whereas 6J29 and N38 are *P. nigra* genotypes. Values inside each box are back-transformed means by genotype of normalized transcript accumulation (n = 2–4). Colors range from white to orange to dark red to show the lowest, middling, and highest overall normalized expression values. Letters show significant differences by post hoc contrast among the four genotypes for each gene [Colour figure can be viewed at wileyonlinelibrary.com]

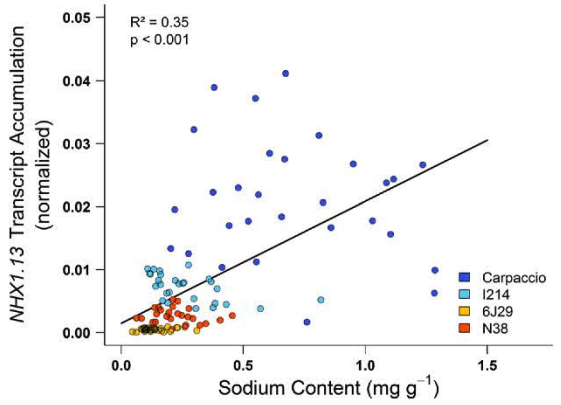

FIGURE 4 Correlation between NHX1.13 normalized transcript accumulation and sodium content (as "per mille" of dry mass) inside the guard cells of four poplar genotypes. Carpaccio and I214 are *Populus deltoides* × *Populus nigra*, whereas 6J29 and N38 are *P. nigra* genotypes (in dark and light blue, yellow and orange, respectively; n = 115) [Colour figure can be viewed at wileyonlinelibrary.com]

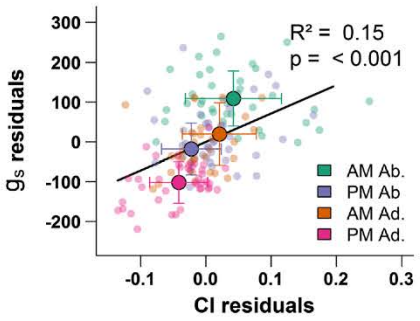

FIGURE 5 Correlation between the stomatal conductance and the chlorine content inside the guard cells once the genotype and water treatment effect is taken into account. Data used are residuals of a linear model with genotype and water treatment as main effect, chlorine content as independent variable, and stomatal conductance as dependent variable (n = 10–22) [Colour figure can be viewed at wileyonlinelibrary.com]

accounting for less than 14% (not shown). P and Ca content in the guard cells contributed the most to the first axis, whereas the *An/Cat* ratio, Cl, and K content contributed the most to the second axis.

Focusing on the first two axis, the four groups formed a diagonal line parallel to the Cl and Mg content and to the supplementary variable g_s. The group associated with the abaxial side in the morning was positively related to these variables, whereas the group formed

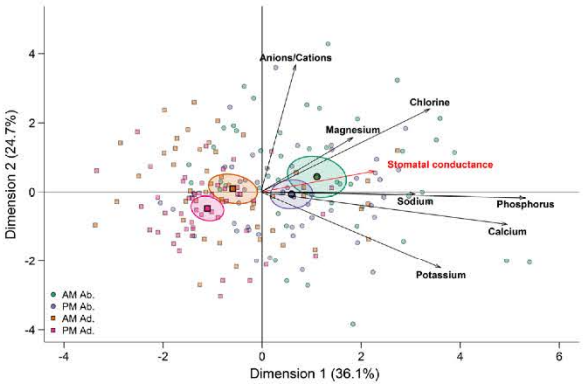

FIGURE 6 Principal component analysis of guard cell element content for each leaf side and time of day. Data used are residuals of linear models with genotype as main effect and each element content as dependent variable (n = 48). Stomatal conductance was added as a supplementary variable (in red). Mean points and confidence ellipse are shown. Circles and squares are for the abaxial and adaxial side respectively. Green and orange are for the morning and blue and pink are for the afternoon [Colour figure can be viewed at wileyonlinelibrary.com]

by the data associated to the adaxial side in the afternoon was negatively related to them. The leaf sampled in the morning showed overall a higher Mg, P, and Cl content in the guard cells and a higher *An/Cat* ratio than in the leaf sampled in the afternoon (Figure S1b,c, d,g; P = .043, P = .003, P = .009, and P < .001, respectively). The afternoon decrease ranged from 7% for P to 13% for Cl. Moreover, a higher amount of element was found in the guard cells on the abaxial side than on the adaxial side, with a noticeable exception of the Mg content (P = .07). P, Ca, and the ratio *An/Cat* were, respectively, 15%, 17%, and 10% more abundant on the abaxial side (P < .003). Cl and K were also significantly higher on the abaxial side of black poplars (Figure S1d,e). Similar trends, however not significant, were observed in hybrid poplars, as well as a 98% higher Na content in the abaxial guard cells of Carpaccio, compared with the adaxial side (Figure S1a, P < .001).

3.5 | Diurnal and leaf side differences of guard cells transcript accumulation in guard cells

Because the PCA on the guard cells element content revealed a strong structuration of sampling modalities (Figure 6), we performed a similar analysis on the gene expression for the 27 studied genes (Figure 7). The first three axis explained 21.3%, 13.1%, and 7.6% of the total variance. Among the genes contributing the most to the first axis, we found genes involved in the ABA biosynthesis and signalling pathways (*NCED3.1*, *NCED3.2*, *ABI1*, *OST1*, and *PYL8*), K^+ channels (*AKT2* and *KAT1.2*), and some of the aquaporins (*PIP1.2*, *PIP2.5*, *TIP1.4*, and *TIP2.1*). The genes contributing highly to the second axis were those encoding H^+-ATPase (*AHA11* and *OST2*), Ca^{2+} vacuolar antiporters (*CAX1* and *CAX1.6*), K^+ channels (*KAT1.2* and *KAT3*), and *NHX1.13*. Similar to the PCA on guard cells element content (Figure 6), the four modalities composed by the crossed factors leaf sides and time of day were even more clearly separated by the first two axis, compared with the element content. Morning and afternoon measures were separated on the upward diagonal, whereas leaf sides were separated on the downward diagonal. Overall, the differences between time of day were related to the expression levels of gene encoding H^+-ATPase and aquaporins, whereas the differences of leaf sides could be ascribed to genes associated mostly with the ABA response, Ca^{2+} vacuolar antiporters, and K^+ channels.

Out of the 27 genes we tested, 20 showed some degree of differential expression in the guard cells between the morning and the afternoon (Table 2, Figure S2). Only three genes were overall less expressed in the afternoon (*OST1*, *KAT1.2*, and *KAT3*) than in the morning by 16%, 17%, and 22%, respectively (Figure S2d,m,n). The remaining 17 genes were expressed at the highest level in the afternoon. This included both *NCEDs* (*NCED3.1* and *NCED3.2*), both H^+-

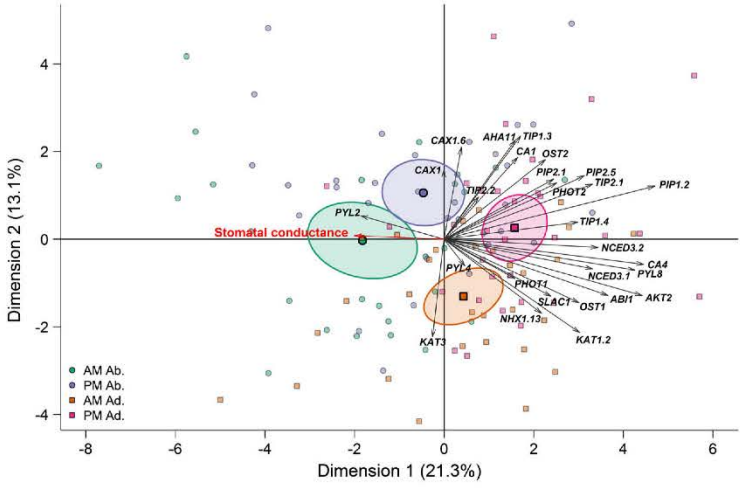

FIGURE 7 Principal component analysis of guard cell normalized transcript accumulation for each leaf side and time of day. Data used are residuals of linear models with genotype as main effect and each transcript as dependent variable (n = 30–31). Stomatal conductance was added as a supplementary variable (in red). Mean points and confidence ellipse are shown. Circles and squares are for the abaxial and adaxial side, respectively. Green and orange are for the morning and blue and pink are for the afternoon [Colour figure can be viewed at wileyonlinelibrary.com]

ATPase (*OST2* and *AHA11*), the three tested *PIPs* (*PIP1.2*, *PIP2.1*, and *PIP2.5*) as well as *PYL8*, *PHOT2*, and *TIP1.3*. *ABI1* normalized mRNA levels were higher in the afternoon but only in the guard cells on the abaxial side (Figure S2c, $P = .004$). Few significant interactions occurred between genotype and times of day. Both *NHX1.13* and *TIP2.1* transcripts levels were higher in the afternoon, but in the guard cells of hybrid poplars ($P < .05$) or of black poplars ($P < .002$), respectively (Figure S2t,z). Both *AKT2* and *PYL2* genes were more expressed in the afternoon but only in the guard cells of I214 and N38 ($P < .04$), respectively (Figure S2e,l).

With respect to the transcripts levels between leaf sides, 18 of the 27 tested genes exhibited a differential expression. In general, we observed the highest expression in the guard cells on the adaxial side of the leaf. Solely, *CAX1* and *CAX1.6* genes were, respectively, 12.6 and 10.1 times more expressed in the guard cells on the abaxial side than on the adaxial side (Figure S2r,s, $P < .001$). The same pattern was found for *TIP1.3* and for *PIP2.5* but only in I214 (Figure S2w,x). The tested *NCEDs* transcripts levels were 13.5 and 6.8 times more abundant on the adaxial side ($P < .01$). Similarly, the two ß-carbonic anhydrases (*CA1* and *CA4*), *PHOT1* and *ABI1* were also overall more expressed on the adaxial side, the accumulation of ABI1 transcripts being only significant in the morning (Figure S2c, $P = .002$). A number of genes showed a genotype-specific differential expression between leaf sides. *OST1*, *PYL8*, *AKT2*, and *KAT1.2* genes were more expressed in the adaxial guard cells only in Carpaccio and N38. *TIP1.4* mRNA level was higher in the guard cells on the adaxial side in Carpaccio. *SLAC1*, *NHX1.13*, *PIP1.2*, and *PIP2.5* genes exhibited the same pattern in N38 only. *PYL8* was also 3.3 times more expressed in the guard cells on the adaxial side than on the abaxial side of 6J29 ($P = .013$).

4 | DISCUSSION

4.1 | Genotypic diversity of element content and gene expression in the guard cells

Our study focused on the relationships between guard cell element content, expression of genes of interest, and stomatal conductance. By modulating the water regime, leaf sides, and times of day on four poplar genotypes, we intended to gain insight into the molecular drivers of gas exchange regulation and the unique physiology of guard cells.

We found a tremendous diversity for both element content and gene expression in the guard cells of four poplar genotypes. This adds to previous investigations highlighting the considerable diversity of transcript accumulation and responses to environmental factors in distinct organs of poplars (Bizet et al., 2015; Cohen et al., 2013; Dumont et al., 2014; Wilkins et al., 2009). Interestingly, Carpaccio exhibited the lowest expression of genes related to ABA biosynthesis and signalling pathways, especially compared with I214. This was not associated with a lower plasticity of stomatal closure under drought, as previous studies found a lack of stomatal response under various water deficits in I214 but not in Carpaccio (Durand et al., 2019; Muller & Lambs, 2009). Instead, exogenous supply of ABA to the I214 clone induced leaf abscission (Chen et al., 1997), which may be part of its drought response (Giovannelli et al., 2007). Additionally, we found a lower expression for the genes encoding K^+ channels, H^+-ATPase, and aquaporins in I214. These differences could in theory contribute to a reduced stomatal control by limiting the exchange of solutes and water across the plasma membrane. However, of the four genotypes studied, I214 showed the highest stomatal density and the smallest stomata (Durand et al., 2019). As such, one could expect that not only less water is required to modify the guard cell turgescence but a smaller change in aperture added over the whole leaf could result in a massive change in stomatal conductance. Durand et al. (2019) also showed that I214 had the fastest stomatal closing speed; here we found that it may not be due to an increased expression of genes encoding transporters on the guard cell plasma membrane.

Along with differences in transcript accumulation, we found evidence of a genotypic diversity of elements contributing to stomatal movements. Little is known on this topic in poplars as the majority of studies focus only on three species (Assmann, 1993), namely, *A. thaliana* (L.), *Commelina communis* (L.), and *Vicia faba* (L.). *NHX1.13* encodes a vacuolar Na^+ and K^+ transporter that has been shown to regulate cell turgor and stomatal function in *A. thaliana* (Barragan et al., 2012). The higher amount of Na in the guard cells of hybrid poplars, linked with higher *NHX1.13* mRNA levels, highlights the importance of this element for stomatal control in these genotypes. Because K^+ channels and some aquaporins may be permeable to Na^+ as well (Byrt et al., 2017; Jezek & Blatt, 2017), one could speculate that these transporters have an increased permeability for Na^+ compared with black poplars. In contrast, the higher Cl content in black poplars emphasize its role in stomatal function in these genotypes. Both malate and Cl^- act as counter-ions to balance the uptake of K^+ into the guard cells in various proportions depending on species, Cl availability, and starch metabolism (Raschke & Schnabl, 1978; Santelia & Lawson, 2016).

4.2 | Impact of water availability

A relatively weak effect of the water regime occurred on element content and normalized mRNA levels, especially as compared with the other tested factors (Table S3). This might be related to the leaf sampling, which occurred 21 days after the start of a mild drought, when short-term gene expression responses were replaced by acclimation of physiological processes. Similarly in *Populus tremula*, few changes in the expression of genes of interest were found in leaves sampled more than 20 days after the start of the drought (Possen et al., 2011). The drought response at the transcript level was highly genotype specific, in agreement with transcriptomic studies on poplar genotypes, showing divergent expression profiles under drought even when the physiological response was similar (Cohen et al., 2010; Wilkins et al., 2009). *PIP2.1* was the only up-regulated gene in all four genotypes under drought. Despite not always being the case, similar results were found on various hybrid poplars (Almeida-Rodriguez,

Cooke, Yeh, & Zwiazek, 2010; Cohen et al., 2013). *AtPIP2.1* and *ZmPIP2.1* increased water permeability when expressed in *Xenopus* oocytes and protoplasts of *Lilium longifolium* pollen (Lopez et al., 2003; Sommer et al., 2008). Moreover, *AtPIP2.1* was related to ABA-induced stomatal closure, mediated by *OST1* by increasing guard cell permeability for water enabling its efflux (Grondin et al., 2015; Maurel, Verdoucq, & Rodrigues, 2016). Increasing *PIP2.1* expression under drought may allow for a faster stomatal closure.

Under drought, there was an increased Ca content in black poplars together with a higher Cl content for all genotypes. During stomatal closure, free Ca^{2+} entering the cytosolic spaces of guard cells is known to be responsible for the inactivation of inward-rectifying K^+ channels in *V. faba* (Grabov & Blatt, 1999; Schroeder & Hagiwara, 1989) and the activation of anion channels, such as SLAC1 when expressed in *Xenopus laevis* oocytes (Geiger et al., 2010). However, Ca^{2+} elevation in the cytosol has been found to be mostly due to influx from the vacuole and the endoplasmic reticulum as opposed to entry from the apoplast (Chen et al., 2012). Unfortunately, we are not able to localize specific subcellular compartments. Concurrently to the increased Ca content, the Cl content increased as well under drought. This suggests that an increased solute concentration in guard cells may be in part a response to a decline in leaf water content in poplars under drought (Guo, Zhang, & Huang, 2010; Marron et al., 2003).

4.3 | Leaf side and time of day shape guard cell element content and transcript accumulation

Gene expression and element content in the guard cells followed opposite patterns over the leaf and along the day. Although stomatal conductance and element content reached a maximum on the abaxial side in the morning, transcript levels was overall at the lowest. The same pattern occurred, but reversed on the adaxial side in the afternoon.

There was no significant change of K content in guard cells of various apertures despite the overall element content being higher in more opened stomata, particularly with the increased Cl content (Figure 6). These results were checked by X-ray microanalyses under cryogenic conditions (−145°C). Both techniques (cryo and freeze-dried samples) showed no difference of K content inside the guard cells between leaves with markedly different stomatal conductance. The lack of decrease in K concentration in stomatal guard cells with lower stomatal aperture was quite unexpected as K is known to be of primary importance for stomatal movements. A previous study on hybrid poplar genotypes found an increased K content in guard cells under ozone while having lower g_s (Dumont et al., 2014). Langer et al. (2004) found only a 25% decrease in guard cell K content between *P. tremula* × *Populus tremuloides* leaves grown under CO_2-free environment and leaves in the dark subjected to 100-μM ABA, resulting in an 80% g_s decrease.

In our study, stomatal conductance was impacted by the different water regimes, leaf sides, and times of day. Because the difference in g_s between well-watered and drought-stressed poplars was relatively small, differences of K content would most likely also be relatively small. Consequently, such small changes may not be identified using this technique, especially when considering the many roles K has in multiple processes, from homeostasis to enzymes activation (Clarkson & Hanson, 1980). Despite a significantly lower K content on the adaxial side of the leaf, differences in g_s between leaf sides may be predominantly attributed to differences of stomatal density rather than apertures (Durand et al., 2019). Hence, differences of g_s between times of day were our best candidate to find corresponding differences in guard cell K content. However, unlike stomatal opening, it has been proposed that stomatal closure in the afternoon may be more related to sucrose than K (Amodeo, Talbott, & Zeiger, 1996; Granot & Kelly, 2019; Kottapalli et al., 2018; Talbott & Zeiger, 1996). When the rate of sucrose production is higher than its loading into the phloem, excess sucrose accumulate in the apoplast and may enter guard cells (Ewert, Jr, Zhang, Aghoram, & Riddle, 2000; Kang, Outlaw, Andersen, & Fiore, 2007), inducing stomatal closure mediated by hexokinases (Kelly et al., 2013). Clearly, more research is needed to decipher changes of element content in poplar guard cells related to stomatal movements, which will necessitate the input of multiple techniques.

Diurnal rhythms in transcript accumulation were reported by previous studies for the expression of aquaporin-encoding genes and genes involved in ABA regulation. In contrast to our findings, whole leaves and roots generally have an increased accumulation of aquaporin transcripts in the morning, or in the few hours following an increase of light (Hachez, Heinen, Draye, & Chaumont, 2008; Henzler et al., 1999; Lopez et al., 2003; Lopez et al., 2013; Vandeleur et al., 2009). On the other hand, even if leaf ABA concentrations tend to increase at the end of the day (Novakova et al., 2005), the genes involved in the ABA-related pathways seem to present a diversity of diurnal rhythms in leaves (Seung et al., 2012). Despite their close proximity to mesophyll cells, stomata have specific circadian rhythms (Hassidim et al., 2017; Yakir et al., 2011). Given their relatively low proportion in the leaf compared with other cell types, the different expression profile along the day in guard cells compared with whole leaves could result from the cellular complexity of the organ that hides cell-type specific regulations (Nourbakhsh-Rey & Libault, 2016). In addition to the changes in element content, guard cells are also subjected to pH variations during stomatal movement. In general, stomatal closure induces cytosolic and vacuolar alkalinization (Irving, Gehring, & Parish, 1992; Zhang, Dong, Gao, & Song, 2001), whereas stomatal opening induces acidification (Huang, She, Zhang, & Zhao, 2013), linked with H_2O_2 and Ca^{2+} signalling during both ABA and dark-induced stomatal responses (Agurla & Raghavendra, 2016; Ma & Niu, 2017). Moreover, external pH changes strongly altered transcript levels, which was linked to ABA-responsive element motifs in the promoter region of pH-responsive genes (Lager et al., 2010). Little is known about the effect of intracellular pH on transcript accumulation, and whether or not guard cell movements affect its own expression pattern remains to be established.

Potential differences in the physiology of guard cells between leaf sides is seldom investigated, and even fewer studies compare the

patterns of transcript accumulation and/or element content. We reported here an overall stronger expression of genes of interest on the adaxial side for a number of genes, including *NCEDs* and ß-carbonic anhydrases. However, the higher expression of vacuolar Ca^{2+} antiporters on the abaxial side was associated with a higher Ca content on this side, in agreement with Dumont et al. (2014). It has been hypothesized that guard cells on each side may have different pathways for Ca^{2+}-mediated signal transduction (Wang, Wu, & Assmann, 1998). There is evidence of an independent control of gas exchange between leaf sides (Mott, Cardon, & Berry, 1993; Richardson et al., 2017). Such control would allow amphistomatal leaves to regulate more efficiently in response to the environmental conditions specific to each side. Previously reported thermal and irradiance gradients between leaf surfaces of a few degrees (Buckley, John, Scoffoni, & Sack, 2015; Clum, 1926; Sheriff, 1979) could result in different perceived environmental conditions between leaf sides (e.g., light, VPD, and temperature), prompting different stomatal control, as was found on poplar clones in response to a change in light and VPD (Ceulemans, Hinckley, & Impens, 1989; Pallardy & Kozlowski, 1979). Differences in the intensity and nature of perceived stresses, such as evaporative demand, light, and heat (Urban, Ingwers, McGuire, & Teskey, 2017) may induce a distinct conjugation of stress between sides, which may affect the synergic or antagonistic response to environmental cues (Bigot et al., 2018). This would result in a different perception and signalization between sides; for example, stomata of *Gossypium barbadense* (L.) have distinct sensitivity to light between sides linked with different pigment contents (Lu, Quiñones, & Zeiger, 1993). A different sensitivity between sides would lead to a diversity of gene expression (see Bigot et al., 2018), and element content in the guard cells, which may be a part of what we observed. A stronger gene expression on the adaxial side might be seen as the result of a more extreme condition on the side facing the light source.

In conclusion, even though we found a strong genotypic diversity, our data show how changes in stomatal conductance between leaf sides and time of day are linked to guard cell element content and transcript accumulation profiles in a similar way across the four studied genotypes (Figures 6 and 7). Future technical developments such as cryogenic electron microscopy will allow for an easier element cellular compartmentation. Because stomata are responsible for optimizing carbon gain with regard to water loss, their functions affect not only the plant but the ecosystem as well (Berry, Beerling, & Franks, 2010). Understanding the specificities of guard cells functioning will further expand our current knowledge of stomatal physiology and their global consequences.

ACKNOWLEDGMENTS

This work was conducted in the frame of the WATBIO (Development of improved perennial biomass crops for water-stressed environments), a collaborative research project funded from the European Union's Seventh Programme for research, technological development and demonstration under grant agreement 311929. The research received funding from the French National Research Agency through the Laboratory of Excellence ARBRE (ANR-12-LABXARBRE-01). M. D. received a PhD scholarship from the Lorraine Région and EFPA (INRA research department). We thank the nursery of Guéméné Penfao for providing the Euramerican poplar cuttings. The authors acknowledge Marc Villar and Catherine Bastien from the UR0588-INRA Unit for access to the referenced *P. nigra* clones 6J29 and N38 as well as SILVATECH from UMR 1434 SILVA, 1136 IAM, 1138 BEF, and 4370 EA LERMAB EEF research centre INRA Grand-Est for its contribution to X-ray microanalyses. SILVATECH facility is supported by the French National Research Agency through the Laboratory of Excellence ARBRE.

CONFLICT OF INTEREST

The authors declare that the research was conducted in the absence of any commercial or financial relationships that could be construed as a potential conflict of interest.

AUTHOR CONTRIBUTION

D. L. T., O. B., C. B., M. D., and D. C. developed the experimental design. C. B. carried out the experimental drought set-up. D. L. T. collected leaf porometer data; D. L. T., D. C., I. H., and N. A. sampled the leaves; M. D. performed X-ray microanalysis; M. D., D. C., and I. T. microdissected the stomata and extracted the RNA. N. A. performed cDNA amplification, RT-PCR, and data standardization. M. D., D. L. T., D. C., and I. H. performed data analysis. All contributors were involved in the writing and reviewing of the manuscript.

ORCID

Didier Le Thiec https://orcid.org/0000-0002-4204-551X

REFERENCES

Acharya, B. R., & Assmann, S. M. (2009). Hormone interactions in stomatal function. *Plant Molecular Biology*, *69*(4), 451–462. https://doi.org/10.1007/s11103-008-9427-0

Agurla, S., & Raghavendra, A. S. (2016). Convergence and divergence of signaling events in guard cells during stomatal closure by plant hormones or microbial elicitors. *Frontiers in Plant Science*, *7*(1332). https://doi.org/10.3389/fpls.2016.01332

Almeida-Rodriguez, A. M., Cooke, J. E. K., Yeh, F., & Zwiazek, J. J. (2010). Functional characterization of drought-responsive aquaporins in *Populus balsamifera* and *Populus simonii* × *balsamifera* clones with different drought resistance strategies. *Physiologia Plantarum*, *140*(4), 321–333. https://doi.org/10.1111/j.1399-3054.2010.01405.x

Amodeo, G., Talbott, L. D., & Zeiger, E. (1996). Use of potassium and sucrose by onion guard cells during a daily cycle of osmoregulation. *Plant and Cell Physiology*, *37*(5), 575–579. https://doi.org/10.1093/oxfordjournals.pcp.a028983

Amsellem, J., Nicaise, G., Blaineau, S., Quintana, C., Escaig, J., Roinel, N., … Vicario, E. (1983). *Microanalyse × en biologie*. Société Française de Microscopie Electronique, Paris.

Assmann, S. M. (1993). Signal transduction in guard cells. *Annual Review of Cell Biology*, *9*(1), 345–375. https://doi.org/10.1146/annurev.cb.09.110193.002021

Barragan, V., Leidi, E. O., Andres, Z., Rubio, L., De Luca, A., Fernandez, J. A., … Pardo, J. M. (2012). Ion exchangers NHX1 and NHX2 mediate active

potassium uptake into vacuoles to regulate cell turgor and stomatal function in Arabidopsis. *Plant Cell*, *24*(3), 1127–1142. https://doi.org/10.1105/tpc.111.095273

Bauer, H., Ache, P., Lautner, S., Fromm, J., Hartung, W., Al-Rasheid, K. A. S., … Hedrich, R. (2013). The stomatal response to reduced relative humidity requires guard cell-autonomous ABA synthesis. *Current Biology*, *23*(1), 53–57. https://doi.org/10.1016/j.cub.2012.11.022

Berry, J. A., Beerling, D. J., & Franks, P. J. (2010). Stomata: Key players in the earth system, past and present. *Current Opinion in Plant Biology*, *13*(3), 232–239. https://doi.org/10.1016/j.pbi.2010.04.013

Bigot, S., Buges, J., Gilly, L., Jacques, C., Boulch, P. L., Berger, M., … Couée, I. (2018). Pivotal roles of environmental sensing and signaling mechanisms in plant responses to climate change. *Global Change Biology*, *24*(12), 5573–5589. https://doi.org/10.1111/gcb.14433

Bizet, F., Bogeat-Triboulot, M. B., Montpied, P., Christophe, A., Ningre, N., Cohen, D., & Hummel, I. (2015). Phenotypic plasticity toward water regime: Response of leaf growth and underlying candidate genes in Populus. *Physiologia Plantarum*, *154*(1), 39–53. https://doi.org/10.1111/ppl.12271

Bonan, G. B. (2008). Forests and climate change: Forcings, feedbacks, and the climate benefits of forests. *Science*, *320*(5882), 1444–1449. https://doi.org/10.1126/science.1155121

Brodribb, T. J., & Cochard, H. (2009). Hydraulic failure defines the recovery and point of death in water-stressed conifers. *Plant Physiology*, *149*(1), 575–584. https://doi.org/10.1104/pp.108.129783

Brunner, A. M., Yakovlev, I. A., & Strauss, S. H. (2004). Validating internal controls for quantitative plant gene expression studies. *BMC Plant Biology*, *4*(1), 14. https://doi.org/10.1186/1471-2229-4-14

Buckley, T. N. (2005). The control of stomata by water balance. *New Phytologist*, *168*(2), 275–291. https://doi.org/10.1111/j.1469-8137.2005.01543.x

Buckley, T. N., John, G. P., Scoffoni, C., & Sack, L. (2015). How does leaf anatomy influence water transport outside the xylem? *Plant Physiology*, *168*(4), 1616–1635. https://doi.org/10.1104/pp.15.00731

Byrt, C. S., Zhao, M., Kourghi, M., Bose, J., Henderson, S. W., Qiu, J., … Tyerman, S. (2017). Non-selective cation channel activity of aquaporin AtPIP2;1 regulated by Ca2+ and pH. *Plant, Cell & Environment*, *40*(6), 802–815. https://doi.org/10.1111/pce.12832

Ceulemans, R., Hinckley, T. M., & Impens, I. (1989). Stomatal response of hybrid poplar to incident light, sudden darkening and leaf excision. *Physiologia Plantarum*, *75*(2), 174–182. https://doi.org/10.1111/j.1399-3054.1989.tb06165.x

Chaumont, F., & Tyerman, S. D. (2014). Aquaporins: Highly regulated channels controlling plant water relations. *Plant Physiology*, *164*(4), 1600–1618. https://doi.org/10.1104/pp.113.233791

Chaves, M. M., Maroco, J. P., & Pereira, J. S. (2003). Understanding plant responses to drought — from genes to the whole plant. *Functional Plant Biology*, *30*(3), 239–264. https://doi.org/10.1071/FP02076

Chen, S. L., Wang, S. S., Altman, A., & Huttermann, A. (1997). Genotypic variation in drought tolerance of poplar in relation to abscisic acid. *Tree Physiology*, *17*(12), 797–803. https://doi.org/10.1093/treephys/17.12.797

Chen, Z.-H., Hills, A., Bätz, U., Amtmann, A., Lew, V. L., & Blatt, M. R. (2012). Systems dynamic modeling of the stomatal guard cell predicts emergent behaviors in transport, signaling, and volume control. *Plant Physiology*, *159*(3), 1235–1251. https://doi.org/10.1104/pp.112.197350

Ciais, P., Reichstein, M., Viovy, N., Granier, A., Ogee, J., Allard, V., … Valentini, R. (2005). Europe-wide reduction in primary productivity caused by the heat and drought in 2003. *Nature*, *437*(7058), 529–533. https://doi.org/10.1038/nature03972

Clarkson, D. T., & Hanson, J. B. (1980). The mineral nutrition of higher plants. *Annual Review of Plant Physiology and Plant Molecular Biology*, *31*, 239–298. https://doi.org/10.1146/annurev.pp.31.060180.001323

Clum, H. H. (1926). The effect of transpiration and environmental factors on leaf temperatures II. Light intensity and the relation of transpiration to the thermal death point. *American Journal of Botany*, *13*(4), 217–230. https://doi.org/10.1002/j.1537-2197.1926.tb05879.x

Cohen, D., Bogeat-Triboulot, M. B., Tisserant, E., Balzergue, S., Martin-Magniette, M. L., Lelandais, G., … Hummel, I. (2010). Comparative transcriptomics of drought responses in Populus: A meta-analysis of genome-wide expression profiling in mature leaves and root apices across two genotypes. *BMC Genomics*, *11*, 21.

Cohen, D., Bogeat-Triboulot, M. B., Vialet-Chabrand, S., Merret, R., Courty, P. E., Moretti, S., … Hummel, I. (2013). Developmental and environmental regulation of aquaporin gene expression across Populus species: Divergence or redundancy? *PLoS ONE*, *8*(2), 12.

Coopman, R. E., Jara, J. C., Bravo, L. A., Sáez, K. L., Mella, G. R., & Escobar, R. (2008). Changes in morpho-physiological attributes of *Eucalyptus globulus* plants in response to different drought hardening treatments. *Electronic Journal of Biotechnology*, *11*(2), 30–39.

Cowan, I. R., & Farquhar, G. D. (1977). Stomatal function in relation to leaf metabolism and environment. *Symposia of the Society for Experimental Biology*, *31*, 471–505.

Dai, A. (2012). Increasing drought under global warming in observations and models. *Nature Climate Change*, *3*, 52.

Damsteegt, E. L., McHugh, N., & Lokman, P. M. (2016). Storage by lyophilization—Resulting RNA quality is tissue dependent. *Analytical Biochemistry*, *511*, 92–96.

Davies, W. J., & Zhang, J. H. (1991). Root signals and the regulation of growth and development of plants in drying soil. *Annual Review of Plant Physiology and Plant Molecular Biology*, *42*, 55–76. https://doi.org/10.1146/annurev.pp.42.060191.000415

de Dios, V. R. (2017). Circadian regulation and diurnal variation in gas exchange. *Plant Physiology*, *175*(1), 3–4. https://doi.org/10.1104/pp.17.00984

Dodd, I. C. (2005). Root-to-shoot signalling: Assessing the roles of 'up' in the up and down world of long-distance signalling in planta. *Plant and Soil*, *274*(1-2), 251–270. https://doi.org/10.1007/s11104-004-0966-0

Dumont, J., Cohen, D., Gerard, J., Jolivet, Y., Dizengremel, P., & Le Thiec, D. (2014). Distinct responses to ozone of abaxial and adaxial stomata in three Euramerican poplar genotypes. *Plant, Cell and Environment*, *37*(9), 2064–2076. https://doi.org/10.1111/pce.12293

Durand, M., Brendel, O., Buré, C., & Le Thiec, D. (2019). Altered stomatal dynamics induced by changes in irradiance and vapour-pressure deficit under drought: Impact on the whole plant transpiration efficiency of poplar genotypes. *New Phytologist*, *222*, 1789–1802. https://doi.org/10.1111/nph.15710

Ewert, M. S., Jr, W. H. O., Zhang, S., Aghoram, K., & Riddle, K. A. (2000). Accumulation of an apoplastic solute in the guard-cell wall is sufficient to exert a significant effect on transpiration in *Vicia faba* leaflets. *Plant, Cell & Environment*, *23*(2), 195–203. https://doi.org/10.1046/j.1365-3040.2000.00539.x

García-Baldenegro, C. V., Vargas-Arispuro, I., Islas-Osuna, M., Rivera-Domínguez, M., Aispuro-Hernández, E., & Martínez-Téllez, M. Á. (2015). Total RNA quality of lyophilized and cryopreserved dormant grapevine buds. *Electronic Journal of Biotechnology*, *18*(2), 134–137. https://doi.org/10.1016/j.ejbt.2015.01.002

Geiger, D., Scherzer, S., Mumm, P., Marten, I., Ache, P., Matschi, S., … Hedrich, R. (2010). Guard cell anion channel SLAC1 is regulated by CDPK protein kinases with distinct Ca2+ affinities. *Proceedings of the National Academy of Sciences of the United States of America*, *107*(17), 8023–8028. https://doi.org/10.1073/pnas.0912030107

Geiger, D., Scherzer, S., Mumm, P., Stange, A., Marten, I., Bauer, H., … Hedrich, R. (2009). Activity of guard cell anion channel SLAC1 is controlled by drought-stress signaling kinase-phosphatase pair. *Proceedings of the National Academy of Sciences*, *106*(50), 21425–21430. https://doi.org/10.1073/pnas.0912021106

Giovannelli, A., Deslauriers, A., Fragnelli, G., Scaletti, L., Castro, G., Rossi, S., & Crivellaro, A. (2007). Evaluation of drought response of two poplar clones (Populus×canadensis Mönch 'I-214' and P. deltoides Marsh. 'Dvina') through high resolution analysis of stem growth. *Journal of Experimental Botany*, *58*(10), 2673–2683. https://doi.org/10.1093/jxb/erm117

Grabov, A., & Blatt, M. R. (1999). A steep dependence of inward-rectifying potassium channels on cytosolic free calcium concentration increase evoked by hyperpolarization in guard cells. *Plant Physiology*, *119*(1), 277–288. https://doi.org/10.1104/pp.119.1.277

Granot, D., & Kelly, G. (2019). Evolution of guard-cell theories: The story of sugars. *Trends in Plant Science*, *24*(6), 507–518. https://doi.org/10.1016/j.tplants.2019.02.009

Grondin, A., Rodrigues, O., Verdoucq, L., Merlot, S., Leonhardt, N., & Maurel, C. (2015). Aquaporins contribute to ABA-triggered stomatal closure through OST1-mediated phosphorylation. *The Plant Cell*, *27*(7), 1945–1954. https://doi.org/10.1105/tpc.15.00421

Guo, X. Y., Zhang, X. S., & Huang, Z. Y. (2010). Drought tolerance in three hybrid poplar clones submitted to different watering regimes. *Journal of Plant Ecology*, *3*(2), 79–87. https://doi.org/10.1093/jpe/rtq007

Gutierrez, L., Mauriat, M., Guenin, S., Pelloux, J., Lefebvre, J. F., Louvet, R., … Van Wuytswinkel, O. (2008). The lack of a systematic validation of reference genes: A serious pitfall undervalued in reverse transcription-polymerase chain reaction (RT-PCR) analysis in plants. *Plant Biotechnology Journal*, *6*(6), 609–618. https://doi.org/10.1111/j.1467-7652.2008.00346.x

Hachez, C., Heinen, R. B., Draye, X., & Chaumont, F. (2008). The expression pattern of plasma membrane aquaporins in maize leaf highlights their role in hydraulic regulation. *Plant Molecular Biology*, *68*(4-5), 337–353. https://doi.org/10.1007/s11103-008-9373-x

Hassidim, M., Dakhiya, Y., Turjeman, A., Hussien, D., Shor, E., Anidjar, A., … Green, R. M. (2017). CIRCADIAN CLOCK ASSOCIATED1 (CCA1) and the circadian control of stomatal aperture. *Plant Physiology*, *175*(4), 1864–1877. https://doi.org/10.1104/pp.17.01214

Heinen, R. B., Bienert, G. P., Cohen, D., Chevalier, A. S., Uehlein, N., Hachez, C., … Chaumont, F. (2014). Expression and characterization of plasma membrane aquaporins in stomatal complexes of Zea mays. *Plant Molecular Biology*, *86*(3), 335–350. https://doi.org/10.1007/s11103-014-0232-7

Henzler, T., Waterhouse, R. N., Smyth, A. J., Carvajal, M., Cooke, D. T., Schaffner, A. R., … Clarkson, D. T. (1999). Diurnal variations in hydraulic conductivity and root pressure can be correlated with the expression of putative aquaporins in the roots of *Lotus japonicus*. *Planta*, *210*(1), 50–60. https://doi.org/10.1007/s004250050653

Huang, A. X., She, X. P., Zhang, Y. Y., & Zhao, J. L. (2013). Cytosolic acidification precedes nitric oxide removal during inhibition of ABA-induced stomatal closure by fusicoccin. *Russian Journal of Plant Physiology*, *60*(1), 60–68. https://doi.org/10.1134/S1021443712060076

Huang, D., Wu, W., Abrams, S. R., & Cutler, A. J. (2008). The relationship of drought-related gene expression in *Arabidopsis thaliana* to hormonal and environmental factors. *Journal of Experimental Botany*, *59*(11), 2991–3007. https://doi.org/10.1093/jxb/ern155

Intergovernmental Panel on Climate Change (2014). *Climate change 2014: Synthesis report. Contribution of working groups I, II and III to the fifth assessment report of the intergovernmental panel on climate change*. Geneva, Switzerland: Cambridge University Press. https://doi.org/10.1017/CBO9781107415416

Irving, H. R., Gehring, C. A., & Parish, R. W. (1992). Changes in cytosolic pH and calcium of guard-cells precede stomatal movements. *Proceedings of the National Academy of Sciences of the United States of America*, *89*(5), 1790–1794. https://doi.org/10.1073/pnas.89.5.1790

Jaiprakash, M. R., Pillai, B., Venkatesh, P., Subramanian, N., Sinkar, V. P., & Sadhale, P. P. (2003). RNA isolation from high-phenolic freeze-dried tea (*Camellia sinensis*) leaves. *Plant Molecular Biology Reporter*, *21*(4), 465–466. https://doi.org/10.1007/BF02772599

Jansson, S., & Douglas, C. J. (2007). Populus: A model system for plant biology. *Annual Review of Plant Biology*, *58*, 435–458. https://doi.org/10.1146/annurev.arplant.58.032806.103956

Jezek, M., & Blatt, M. R. (2017). The membrane transport system of the guard cell and its integration for stomatal dynamics. *Plant Physiology*, *174*(2), 487–519. https://doi.org/10.1104/pp.16.01949

Kanemasu, E. T., & Tanner, C. B. (1969). Stomatal diffusion resistance of snap beans I. Influence of leaf-water potential. *Plant Physiology*, *44*(11), 1547–1552. https://doi.org/10.1104/pp.44.11.1547

Kang, Y. U. N., Outlaw, W. H., Andersen, P. C., & Fiore, G. B. (2007). Guard-cell apoplastic sucrose concentration ? a link between leaf photosynthesis and stomatal aperture size in the apoplastic phloem loader Vicia faba L. *Plant, Cell & Environment*, *30*(5), 551–558. https://doi.org/10.1111/j.1365-3040.2007.01635.x

Kassam, A. H. (1973). Influence of light and water deficit upon diffusive resistance of leaves of Vicia faba L. *New Phytologist*, *72*(3), 557–570. https://doi.org/10.1111/j.1469-8137.1973.tb04407.x

Kelly, G., Moshelion, M., David-Schwartz, R., Halperin, O., Wallach, R., Attia, Z., … Granot, D. (2013). Hexokinase mediates stomatal closure. *The Plant Journal*, *75*(6), 977–988. https://doi.org/10.1111/tpj.12258

Kottapalli, J., David-Schwartz, R., Khamaisi, B., Brandsma, D., Lugassi, N., Egbaria, A., … Granot, D. (2018). Sucrose-induced stomatal closure is conserved across evolution. *PLoS ONE*, *13*(10), e0205359. https://doi.org/10.1371/journal.pone.0205359

Lager, I., Andreasson, O., Dunbar, T. L., Andreasson, E., Escobar, M. A., & Rasmusson, A. G. (2010). Changes in external pH rapidly alter plant gene expression and modulate auxin and elicitor responses. *Plant, Cell and Environment*, *33*(9), 1513–1528.

Langer, K., Levchenko, V., Fromm, J., Geiger, D., Steinmeyer, R., Lautner, S., … Hedrich, R. (2004). The poplar K+ channel KPT1 is associated with K + uptake during stomatal opening and bud development. *The Plant Journal*, *37*(6), 828–838. https://doi.org/10.1111/j.0960-7412.2003.02008.x

Leonhardt, N., Kwak, J. M., Robert, N., Waner, D., Leonhardt, G., & Schroeder, J. I. (2004). Microarray expression analyses of Arabidopsis guard cells and isolation of a recessive abscisic acid hypersensitive protein phosphatase 2C mutant. *Plant Cell*, *16*(3), 596–615. https://doi.org/10.1105/tpc.019000

Lopez, D., Venisse, J. S., Fumanal, B., Chaumont, F., Guillot, E., Daniels, M. J., … Gousset-Dupont, A. (2013). Aquaporins and leaf hydraulics: poplar sheds new light. *Plant and Cell Physiology*, *54*(12), 1963–1975. https://doi.org/10.1093/pcp/pct135

Lopez, M., Bousser, A. S., Sissoeff, I., Gaspar, M., Lachaise, B., Hoarau, J., & Mahe, A. (2003). Diurnal regulation of water transport and aquaporin gene expression in maize roots: Contribution of PIP2 proteins. *Plant*

and Cell Physiology, *44*(12), 1384–1395. https://doi.org/10.1093/pcp/pcg168

Lu, Z., Quiñones, M. A., & Zeiger, E. (1993). Abaxial and adaxial stomata from Pima cotton (*Gossypium barbadense* L.) differ in their pigment content and sensitivity to light quality. *Plant, Cell & Environment*, *16*(7), 851–858. https://doi.org/10.1111/j.1365-3040.1993.tb00507.x

Lv, S., Zhang, Y., Li, C., Liu, Z., Yang, N., Pan, L., … Wang, G. (2018). Strigolactone-triggered stomatal closure requires hydrogen peroxide synthesis and nitric oxide production in an abscisic acid-independent manner. *New Phytologist*, *217*(1), 290–304. https://doi.org/10.1111/nph.14813

Ma, Y., & Niu, J. (2017). The role of phytosphingosine-1-phosphate (Phyto-S1P) and its relationships with cytosolic pH and hydrogen peroxide (H_2O_2) during stomatal closure by darkness in broad bean. *South African Journal of Botany*, *108*, 237–242. https://doi.org/10.1016/j.sajb.2016.11.002

Marron, N., Dreyer, E., Boudouresque, E., Delay, D., Petit, J. M., Delmotte, F. M., & Brignolas, F. (2003). Impact of successive drought and re-watering cycles on growth and specific leaf area of two *Populus* × *canadensis* (Moench) clones, 'Dorskamp' and 'Luisa_Avanzo'. *Tree Physiology*, *23*(18), 1225–1235. https://doi.org/10.1093/treephys/23.18.1225

Maurel, C., Verdoucq, L., & Rodrigues, O. (2016). Aquaporins and plant transpiration. *Plant, Cell and Environment*, *39*(11), 2580–2587. https://doi.org/10.1111/pce.12814

Merilo, E., Laanemets, K., Hu, H., Xue, S., Jakobson, L., Tulva, I., … Kollist, H. (2013). PYR/RCAR receptors contribute to ozone, reduced air humidity, darkness, and CO_2-induced stomatal regulation. *Plant Physiology*, *162*(3), 1652–1668. https://doi.org/10.1104/pp.113.220608

Merilo, E., Yarmolinsky, D., Jalakas, P., Parik, H., Tulva, I., Rasulov, B., … Kollist, H. (2018). Stomatal VPD response: There is more to the story than ABA. *Plant Physiology*, *176*(1), 851–864. https://doi.org/10.1104/pp.17.00912

Mestdagh, P., Van Vlierberghe, P., De Weer, A., Muth, D., Westermann, F., Speleman, F., & Vandesompele, J. (2009). A novel and universal method for microRNA RT-qPCR data normalization. *Genome Biology*, *10*(6), 10.

Monclus, R., Dreyer, E., Villar, M., Delmotte, F. M., Delay, D., Petit, J. M., … Brignolas, F. (2006). Impact of drought on productivity and water use efficiency in 29 genotypes of *Populus deltoides* × *Populus nigra*. *New Phytologist*, *169*(4), 765–777. https://doi.org/10.1111/j.1469-8137.2005.01630.x

Mott, K. A. (2007). Leaf hydraulic conductivity and stomatal responses to humidity in amphistomatous leaves. *Plant, Cell and Environment*, *30*(11), 1444–1449. https://doi.org/10.1111/j.1365-3040.2007.01720.x

Mott, K. A., Cardon, Z. G., & Berry, J. A. (1993). Asymmetric patchy stomatal closure for the 2 surfaces of *Xanthium strumarium* leaves at low humidity. *Plant, Cell and Environment*, *16*(1), 25–34. https://doi.org/10.1111/j.1365-3040.1993.tb00841.x

Muller, E., & Lambs, L. (2009). Daily variations of water use with vapor pressure deficit in a plantation of I214 poplars. *Water*, *1*(1), 32–42. https://doi.org/10.3390/w1010032

Nourbakhsh-Rey, M., & Libault, M. (2016). Decipher the molecular response of plant single cell types to environmental stresses. *BioMed Research International*, *2016*, 1–8. https://doi.org/10.1155/2016/4182071

Novakova, M., Motyka, V., Dobrev, P. I., Malbeck, J., Gaudinova, A., & Vankova, R. (2005). Diurnal variation of cytokinin, auxin and abscisic acid levels in tobacco leaves. *Journal of Experimental Botany*, *56*(421), 2877–2883. https://doi.org/10.1093/jxb/eri282

Pallardy, S. G., & Kozlowski, T. T. (1979). Stomatal response of populus clones to light intensity and vapor pressure deficit. *Plant Physiology*, *64*(1), 112–114. https://doi.org/10.1104/pp.64.1.112

Park, S.-Y., Fung, P., Nishimura, N., Jensen, D. R., Fujii, H., Zhao, Y., … Cutler, S. R. (2009). Abscisic acid inhibits PP2Cs via the PYR/PYL family of ABA-binding START proteins. *Science (New York, N.Y.)*, *324*(5930), 1068–1071.

Possen, B. J. H. M., Oksanen, E., Rousi, M., Ruhanen, H., Ahonen, V., Tervahauta, A., … Vapaavuori, E. (2011). Adaptability of birch (*Betula pendula* Roth) and aspen (*Populus tremula* L.) genotypes to different soil moisture conditions. *Forest Ecology and Management*, *262*(8), 1387–1399. https://doi.org/10.1016/j.foreco.2011.06.035

Pouchou, J.-L., & Pichoir, F. (1991). Quantitative analysis of homogeneous or stratified microvolumes applying the model "PAP". In K. F. J. Heinrich, & D. E. Newbury (Eds.), *Electron Probe Quantitation* (pp. 31–75). Boston, MA: Springer US.

Raschke, K., & Schnabl, H. (1978). Availability of chloride affects balance between potassium-chloride and potassium malate in guard cells of *Vicia faba* L. *Plant Physiology*, *62*(1), 84–87. https://doi.org/10.1104/pp.62.1.84

Richardson, F., Brodribb, T. J., & Jordan, G. J. (2017). Amphistomatic leaf surfaces independently regulate gas exchange in response to variations in evaporative demand. *Tree Physiology*, *37*(7), 869–878. https://doi.org/10.1093/treephys/tpx073

Rodriguez-Dominguez, C. M., Buckley, T. N., Egea, G., de Cires, A., Hernandez-Santana, V., Martorell, S., & Diaz-Espejo, A. (2016). Most stomatal closure in woody species under moderate drought can be explained by stomatal responses to leaf turgor. *Plant, Cell and Environment*, *39*(9), 2014–2026. https://doi.org/10.1111/pce.12774

Santelia, D., & Lawson, T. (2016). Rethinking guard cell metabolism. *Plant Physiology*, *172*(3), 1371–1392.

Sato, A., Sato, Y., Fukao, Y., Fujiwara, M., Umezawa, T., Shinozaki, K., … Uozumi, N. (2009). Threonine at position 306 of the KAT1 potassium channel is essential for channel activity and is a target site for ABA-activated SnRK2/OST1/SnRK2.6 protein kinase. *Biochemical Journal*, *424*, 439–448. https://doi.org/10.1042/BJ20091221

Schroeder, J. I., & Hagiwara, S. (1989). Cytosolic calcium regulates ion channels in the plasma membrane of *Vicia faba* guard cells. *Nature*, *338*, 427–430. https://doi.org/10.1038/338427a0

Schroeder, J. I., & Hedrich, R. (1989). Involvement of ion channels and active transport in osmoregulation and signaling of higher plant cells. *Trends in Biochemical Sciences*, *14*(5), 187–192. https://doi.org/10.1016/0968-0004(89)90272-7

Schroeder, J. I., Raschke, K., & Neher, E. (1987). Voltage dependence of K+ channels in guard-cell protoplasts. *Proceedings of the National Academy of Sciences*, *84*(12), 4108–4112. https://doi.org/10.1073/pnas.84.12.4108

Seung, D., Risopatron, J. P. M., Jones, B. J., & Marc, J. (2012). Circadian clock-dependent gating in ABA signalling networks. *Protoplasma*, *249*(3), 445–457. https://doi.org/10.1007/s00709-011-0304-3

Sheriff, D. W. (1979). Water-vapor and heat-transfer in leaves. *Annals of Botany*, *43*(2), 157–171. https://doi.org/10.1093/oxfordjournals.aob.a085620

Shimazaki, K.-i., Doi, M., Assmann, S. M., & Kinoshita, T. (2007). Light regulation of stomatal movement. *Annual Review of Plant Biology*, *58*, 219–247.

Sommer, A., Geist, B., Da Ines, O., Gehwolf, R., Schäffner, A. R., & Obermeyer, G. (2008). Ectopic expression of *Arabidopsis thaliana* plasma membrane intrinsic protein 2 aquaporins in lily pollen increases the plasma membrane water permeability of grain but not of tube

protoplasts. *New Phytologist*, *180*(4), 787–797. https://doi.org/10.1111/j.1469-8137.2008.02607.x

Sperry, J. S., Hacke, U. G., Oren, R., & Comstock, J. P. (2002). Water deficits and hydraulic limits to leaf water supply. *Plant, Cell and Environment*, *25*(2), 251–263. https://doi.org/10.1046/j.0016-8025.2001.00799.x

Talbott, L. D., & Zeiger, E. (1996). Central roles for potassium and sucrose in guard-cell osmoregulation. *Plant Physiology*, *111*(4), 1051–1057. https://doi.org/10.1104/pp.111.4.1051

Tardieu, F., & Simonneau, T. (1998). Variability among species of stomatal control under fluctuating soil water status and evaporative demand: Modelling isohydric and anisohydric behaviours. *Journal of Experimental Botany*, *49*, 419–432. https://doi.org/10.1093/jxb/49.Special_Issue.419

Touma, D., Ashfaq, M., Nayak, M. A., Kao, S.-C., & Diffenbaugh, N. S. (2015). A multi-model and multi-index evaluation of drought characteristics in the 21st century. *Journal of Hydrology*, *526*, 196–207. https://doi.org/10.1016/j.jhydrol.2014.12.011

Tschaplinski, T. J., & Blake, T. J. (1989). Water relations, photosynthetic capacity, and root shoot partitioning of photosynthates as determinants of productivity in hybrid poplar. *Canadian Journal of Botany-Revue Canadienne De Botanique*, *67*(6), 1689–1697.

Tuskan, G. A., DiFazio, S., Jansson, S., Bohlmann, J., Grigoriev, I., Hellsten, U., … Rokhsar, D. (2006). The genome of black cottonwood, *Populus trichocarpa* (Torr. and Gray). *Science*, *313*(5793), 1596–1604. https://doi.org/10.1126/science.1128691

Urban, J., Ingwers, M., McGuire, M. A., & Teskey, R. O. (2017). Stomatal conductance increases with rising temperature. *Plant Signaling & Behavior*, *12*(8), 3.

Vandeleur, R. K., Mayo, G., Shelden, M. C., Gilliham, M., Kaiser, B. N., & Tyerman, S. D. (2009). The role of plasma membrane intrinsic protein aquaporins in water transport through roots: diurnal and drought stress responses reveal different strategies between isohydric and anisohydric cultivars of grapevine. *Plant Physiology*, *149*(1), 445–460. https://doi.org/10.1104/pp.108.128645

Vandesompele, J., De Preter, K., Pattyn, F., Poppe, B., Van Roy, N., De Paepe, A., & Speleman, F. (2002). Accurate normalization of real-time quantitative RT-PCR data by geometric averaging of multiple internal control genes. *Genome Biology*, *3*(7), research0034.1. https://doi.org/10.1186/gb-2002-3-7-research0034

Viger, M., Smith, H. K., Cohen, D., Dewoody, J., Trewin, H., Steenackers, M., … Taylor, G. (2016). Adaptive mechanisms and genomic plasticity for drought tolerance identified in European black poplar (*Populus nigra* L.). *Tree Physiology*, *36*(7), 909–928. https://doi.org/10.1093/treephys/tpw017

Wang, X.-Q., Wu, W.-H., & Assmann, S. M. (1998). Differential responses of abaxial and adaxial guard cells of broad bean to abscisic acid and calcium. *Plant Physiology*, *118*(4), 1421–1429. https://doi.org/10.1104/pp.118.4.1421

Wilkins, O., Waldron, L., Nahal, H., Provart, N. J., & Campbell, M. M. (2009). Genotype and time of day shape the *Populus* drought response. *Plant Journal*, *60*(4), 703–715. https://doi.org/10.1111/j.1365-313X.2009.03993.x

Yakir, E., Hassidim, M., Melamed-Book, N., Hilman, D., Kron, I., & Green, R. M. (2011). Cell autonomous and cell-type specific circadian rhythms in Arabidopsis. *Plant Journal*, *68*(3), 520–531. https://doi.org/10.1111/j.1365-313X.2011.04707.x

Yoshida, R., Umezawa, T., Mizoguchi, T., Takahashi, S., Takahashi, F., & Shinozaki, K. (2006). The regulatory domain of SRK2E/OST1/SnRK2.6 interacts with ABI1 and integrates abscisic acid (ABA) and osmotic stress signals controlling stomatal closure in Arabidopsis. *Journal of Biological Chemistry*, *281*(8), 5310–5318. https://doi.org/10.1074/jbc.M509820200

Zhang, X., Dong, F. C., Gao, J. F., & Song, C. P. (2001). Hydrogen peroxide-induced changes in intracellular pH of guard cells precede stomatal closure. *Cell Research*, *11*(1), 37–43. https://doi.org/10.1038/sj.cr.7290064

Zhang, X. L., Jiang, L., Xin, Q., Liu, Y., Tan, J. X., & Chen, Z. Z. (2015). Structural basis and functions of abscisic acid receptors PYLs. *Frontiers in Plant Science*, *6*. https://doi.org/10.3389/fpls.2015.00088

SUPPORTING INFORMATION

Additional supporting information may be found online in the Supporting Information section at the end of the article.

Table S1 List of gene studied with their specific primers.

Table S2 Dataset used for statistical analysis (see separate Excel file).

Table S3 Summary of the genotype, water treatment, time of day and leaf side partial R^2 of stomatal conductance, guard cell element content and expression of genes of interest.

Figure S1 Guard cell element content of four poplar genotypes under contrasting water availability with each leaf side measured separately once in the morning and once in the afternoon (10:30 and 15:00).

Figure S2 Normalized guard cell transcript accumulation of four poplar genotypes under contrasting water availability with each leaf side measured separately once in the morning and once in the afternoon (10:30 and 15:00).

Data S2: Supplementary Information

How to cite this article: Durand M, Cohen D, Aubry N, et al. Element content and expression of genes of interest in guard cells are connected to spatiotemporal variations in stomatal conductance. *Plant Cell Environ*. 2019;1–16. https://doi.org/10.1111/pce.13644

DONNEES SUPPLEMENTAIRES

Table S1. List of gene studied with their specific primers.

Gene name	Phytozome v8.0 name	Primers sens	Primers antisens	Symbol used in
ABI1	Potri.006G224600.2	ATTTGCCTCACCAGACTGCT	TCTCCTCGGACAAAGCTGAA	
AHA11	Potri.012G071600	TAATCATCGTGGCAGCCAAT	GGCAACAGATGACATGAAAC	(a)
AKT2	Potri.003G018800	GGTGTGAAGGGGAACAAGAA	GATCAATCTCCCAGCTTCCA	(a)
BAM1	Potri.010G062900.1	ACAGAAACAGCAGCCCAAGT	TTCACAGCCCCTTCTCAACT	
CA1	Potri.001G348900	AGACTAAGTACGCTGGAGTT	CCATCATAAGGGAAGGACAT	(a)
CA4	Potri.010G041100	GAAGGAGGCTGTTAATGTGT	GTTCCCTTGACAAAGTCGTA	(a)
CAX1	Potri.016G115500	TGTTATTGGGGCGTGCTTTT	AAGCTGCAATGACTGATCCA	(a)
CAX1.6	Potri.006G099900	TCCCTTCAAAGCTGAAATGC	TGCCATATGCCACCTTCTAT	(a)
KAT1.2	Potri.004G132200	TCACTATCCACATGCAGCTT	GGCAATTCTGAGCAACTCTT	(b, c)
KAT3	Potri.018G035500	CATTCCATCATCAGCCTACA	CATGTATTTCCCTCCCTTGT	(a)
NCED3.1	Potri.001G393800	AAGACCCGGTTCGCTTACTT	CTCCGTAAGTGTGCTTGTGT	(d)
NCED3.2	Potri.011G112400	GAAAATCCCGGTTTGCTTACT	ACAAAGGCTCTCCACCGAAT	(d)
NHX1.13	Potri.013G031700	AAGCCCTGCTACATCTTTGA	GCTAACATACATCGCAAAGC	(a)
OST1	Potri.009G106900.2	TGCCACCGTGACTTGAAACT	TTTCGGTTGTGAGTGCAGCA	
OST2	Potri.018G090300	CTAGATAGGGGAGAAAATGG	CTGTGTAACCAGGTGGCATT	(a)
PHOT1	Potri.001G342000	TCCATTCTTCAAGGGTGTCA	TGTCTGTAGATCCTGCATTC	(a)
PHOT2	Potri.004G209700	GGATCAAAAGCTGGTGCTAA	GCCTTCGGATCTTTTCCAAT	(a)
PIP1.2	Potri.008G065600	CGAGTTGCATAATGGTGGTG	TGGCATCAGTTGCAGAGAAG	(c, e)
PIP2.1	Potri.009G136600	CTTCCAATTGGGTTTGCTGT	CAATGATCATCCCAGGCTTT	(e)
PIP2.5	Potri.006G128000	TAGTCCAAAAGGGCTTGGAA	CAAGTGCCCAATACGCGTAC	(e)
PYL2	Potri.018G054400.1	TTCTTCCCCTTGCATGCTGT	TGTTGGGTGCTGGCTCAAAT	
PYL4	Potri.016G125400	GTTGTTGGTGGGGACCATA	ACCGCGTAAGACTCCATGA	(b)
PYL8	Potri.012G000800.1	GCTGGAAAGAGTCGGCATTT	TCCTGCCATTCCCCATGTTA	
QUAC1	Potri.001G144300	TTTAAACCCGGAGATGAGGT	GTATAGCCCGATATCCATAG	(a)
SLAC1	Potri.001G114300	AATGTCCCTGGTGTTCTAAG	CCAAACAAAAGCGTGCAGAA	(a)
TIP1.3	Potri.010G209900	CATGCATTCGCACTCTTTGT	CCAATAAGTGCACCGAAGGT	(e)
TIP1.4	Potri.008G050700	AATCCTGCTGTGACCTTTGG	GAAGCAAGCAAGCAACAACA	(e)
TIP2.1	Potri.001G186700	TGATGCAGCTCTTGATCCTG	AAGAGCCAAGCCAAAAGTGA	(e)
TIP2.2	Potri.003G050900	ATTTTCTGGTGGGTCCATGA	TAAGTCCAGCTAGCCCTCCA	(e)
UBQ11	Potri.001G418500	GTTGATTTTTGCTGGGAAGC	GATCTTGGCCTTCACGTTGT	(a, c, f)

(a): **Dumont J, Cohen D, Gerard J, Jolivet Y, Dizengremel P, Le Thiec D.** 2014. Distinct responses to ozone of abaxial and adaxial stomata in three Euramerican poplar genotypes. *Plant Cell and Environment* 37(9): 2064-2076.

(b): **Cohen D, Bogeat-Triboulot MB, Tisserant E, Balzergue S, Martin-Magniette ML, Lelandais G, Ningre N, Renou JP, Tamby JP, Le Thiec D, et al.** 2010. Comparative transcriptomics of drought responses in Populus: a meta-analysis of genome-wide

expression profiling in mature leaves and root apices across two genotypes. *Bmc Genomics* 11: 21.

(c): **Bizet F, Bogeat-Triboulot MB, Montpied P, Christophe A, Ningre N, Cohen D, Hummel I.** 2015. Phenotypic plasticity toward water regime: response of leaf growth and underlying candidate genes in Populus. *Physiologia Plantarum* 154(1): 39-53.

(d): **Royer M, Cohen D, Aubry N, Vendramin V, Scalabrin S, Cattonaro F, Bogeat-Triboulot MB, Hummel I.** 2016. The build-up of osmotic stress responses within the growing root apex using kinematics and RNA-sequencing. *Journal of Experimental Botany* 67(21): 5961-5973.

(e): **Cohen D, Bogeat-Triboulot MB, Vialet-Chabrand S, Merret R, Courty PE, Moretti S, Bizet F, Guilliot A, Hummel I.** 2013. Developmental and environmental regulation of aquaporin gene expression across populus species: divergence or redundancy? *Plos One* 8(2): 12.

(f): **Brunner AM, Yakovlev IA, Strauss SH.** 2004. Validating internal controls for quantitative plant gene expression studies. *BMC Plant Biology* 4(1): 14.

Table S2. Summary of the genotype, water treatment, time of day and leaf side partial R^2 of stomatal conductance (n = 6), guard cell element content (n = 6) and candidate gene expression (n = 4). A type two factorial ANOVA design with first order interactions was used. Normalized transcript levels were transformed with a logarithm function of base 2 in order to achieve a normal distribution of the data.

	Genotype (G)	Water treatment (T)	Time of day (D)	Leaf side (S)	Interaction G:T	Interaction G:D	Interaction G:S	Interaction T:D	Interaction T:S	Interaction D:S
g_s	0.189	0.020	0.138	0.317	0.006	0.020	0.008	0.002	0.004	< 0.001
Na content	0.568	0.005	0.000	0.063	0.004	0.010	0.092	0.002	0.001	0.002
Mg content	0.487	< 0.001	0.012	0.009	0.008	0.005	0.007	0.002	< 0.001	0.001
P content	0.156	0.001	0.032	0.144	0.031	0.024	0.017	< 0.001	< 0.001	0.001
Cl content	0.697	0.010	0.007	0.070	0.006	0.007	0.024	0.004	0.002	< 0.001
K content	0.326	< 0.001	< 0.001	0.035	0.006	0.020	0.037	0.001	0.007	< 0.001
Ca content	0.214	0.006	0.009	0.144	0.040	0.023	0.007	0.001	0.002	0.003
An/Cat	0.686	0.001	0.018	0.013	0.001	0.011	0.008	< 0.001	0.003	< 0.001
ABI1	0.268	0.005	0.020	0.051	0.073	0.002	0.022	0.001	< 0.001	0.025
AHA11	0.709	0.004	0.028	< 0.001	0.020	0.015	0.009	0.001	0.004	0.001
AKT2	0.127	0.002	0.017	0.117	0.071	0.054	0.094	0.002	0.001	0.001
CA1	0.889	0.001	0.002	0.009	0.008	0.005	0.002	< 0.001	< 0.001	< 0.001
CA4	0.652	< 0.001	0.007	0.080	0.007	0.008	0.016	0.011	< 0.001	0.007
CAX1	0.023	< 0.001	0.007	0.129	0.037	0.036	0.025	0.033	0.005	0.016
CAX1.6	0.388	< 0.001	0.006	0.079	0.037	0.015	0.007	0.003	0.015	0.001
KAT1.2	0.296	< 0.001	0.020	0.097	0.091	0.018	0.052	< 0.001	0.010	0.001
KAT3	0.839	0.010	0.018	< 0.001	0.002	0.008	0.001	< 0.001	0.001	< 0.001
NCED3.1	0.138	0.004	0.032	0.133	0.013	0.002	0.021	0.017	< 0.001	0.010
NCED3.2	0.161	0.006	0.024	0.040	0.063	0.041	0.010	0.001	0.001	0.019
NHX1.13	0.849	< 0.001	0.001	0.003	0.007	0.012	0.015	0.001	< 0.001	0.001
OST1	0.745	0.006	0.015	0.026	0.016	0.002	0.052	< 0.001	0.002	0.001
OST2	0.699	0.009	0.015	0.002	0.003	0.015	0.005	0.004	< 0.001	0.001
PHOT1	0.881	< 0.001	0.001	0.006	0.001	0.003	0.003	0.002	0.003	< 0.001
PHOT2	0.865	< 0.001	0.008	0.003	0.001	0.004	0.003	< 0.001	< 0.001	< 0.001
PIP1.2	0.719	0.005	0.040	0.020	0.020	0.011	0.031	0.001	0.004	< 0.001
PIP2.1	0.940	0.007	0.002	< 0.001	0.001	0.002	0.002	< 0.001	< 0.001	< 0.001
PIP2.5	0.888	< 0.001	0.006	< 0.001	0.003	0.006	0.012	0.001	0.001	0.002
PYL2	0.980	0.001	< 0.001	0.001	< 0.001	0.001	< 0.001	< 0.001	< 0.001	< 0.001
PYL4	0.222	0.044	0.001	0.006	0.053	0.017	0.025	0.015	0.001	0.002
PYL8	0.295	0.003	0.018	0.153	0.043	0.007	0.060	< 0.001	0.010	0.010
SLAC1	0.385	0.025	0.009	0.025	0.037	0.033	0.052	0.003	< 0.001	< 0.001
TIP1.3	0.946	0.001	0.005	< 0.001	0.004	0.001	0.001	< 0.001	< 0.001	< 0.001
TIP1.4	0.443	0.012	0.003	0.003	0.055	0.030	0.048	< 0.001	< 0.001	< 0.001
TIP2.1	0.132	< 0.001	0.049	0.024	0.032	0.102	0.033	0.001	0.007	0.003
TIP2.2	0.785	0.002	0.005	0.002	0.006	0.011	0.008	< 0.001	0.001	< 0.001

g_s: stomatal conductance to water vapor; An/Cat: ratio of anions over cations (*i.e.* P and Cl over Na, Mg, K, and Ca)

Figure S1. Guard cell element content of four poplar genotypes under contrasting water availability with each leaf side measured separately once in the morning and once in the afternoon (10:30 and 15:00). From **(a)** to **(f)**: sodium, magnesium, phosphorus, chlorine, potassium, calcium content. **(g)**: ratio of anions over cations. Carpaccio and I214 are *Populus deltoides* × *nigra* while 6J29 and N38 are *Populus nigra* genotypes. White and gray colored bars show the contrasts used for statistical design. Each factor (*i.e.* genotype, water treatment, time of day and leaf side) is either shown alone or with another factor when the interaction between them was significant. Letters show significant differences among these groups ($P < 0.05$). Values are means ± standard errors (expressed as "per mille" of dry mass, or mg g^{-1}).

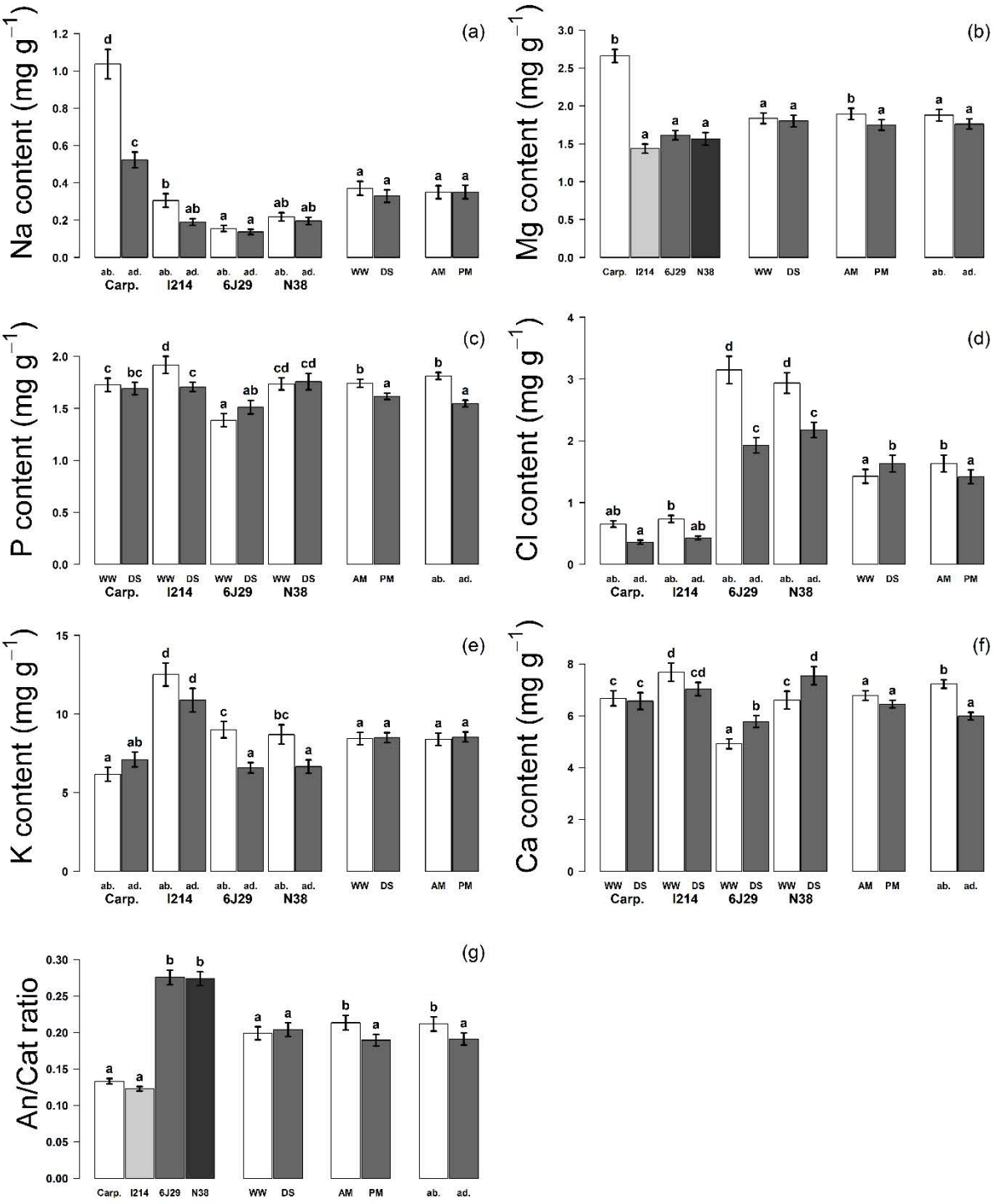
(a)
Na content (mg g^{-1})
(b)
Mg content (mg g^{-1})
(c)
P content (mg g^{-1})
(d)
Cl content (mg g^{-1})
(e)
K content (mg g^{-1})
(f)
Ca content (mg g^{-1})
(g)
An/Cat ratio
Carp.
I214
6J29
N38
WW
DS
AM
PM
ab.
ad.

Figure S2. Normalized guard cell transcript accumulation of four poplar genotypes under contrasting water availability with each leaf side measured separately once in the morning and once in the afternoon (10:30 and 15:00). From **(a)** to **(aa)**: *NCED3.1*, *NCED3.2*, *ABI1*, *OST1*, *PYL2*, *PYL4*, *PYL8*, *CA1*, *CA4*, *PHOT1*, *PHOT2*, *AKT2*, *KAT1.2*, *KAT3*, *OST2*, *AHA11*, *SLAC1*, *CAX1*, *CAX1.6*, *NHX1.13*, *PIP1.2*, *PIP2.1*, *PIP2.5*, *TIP1.3*, *TIP1.4*, *TIP2.1* and *TIP2.2*. Carpaccio and I214 are *Populus deltoides* × *nigra* while 6J29 and N38 are *Populus nigra* genotypes. White and gray colored bars show the contrasts used for statistical design. Each factor (*i.e.* genotype, water treatment, time of day and leaf side) is either shown alone or with another factor when the interaction between them was significant. Letters show significant differences among these groups ($P < 0.05$). Values are back-transformed means ± standard errors normalized mRNA levels on a logarithmic scale.

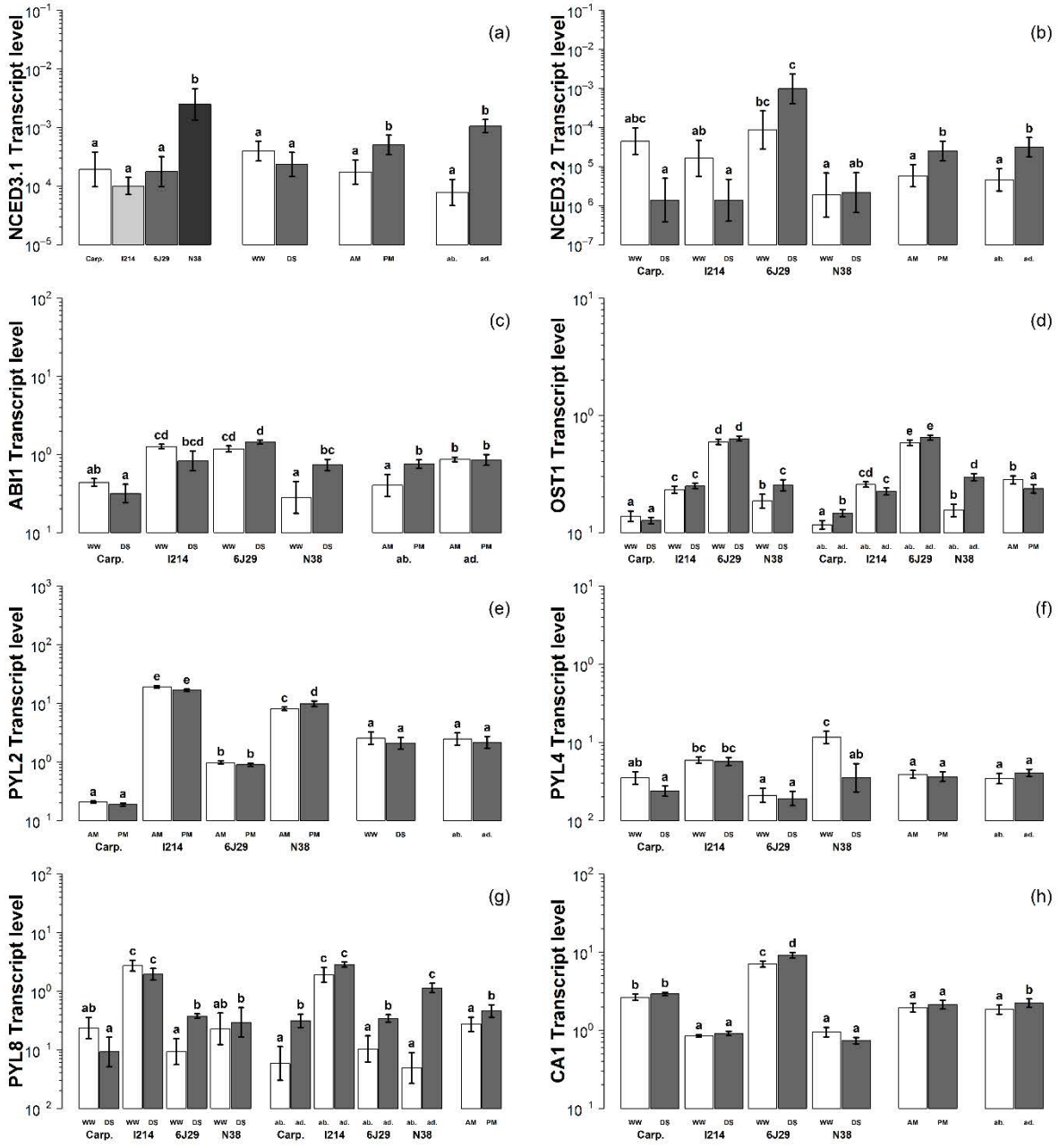
(a)
NCED3.1 Transcript level
(b)
NCED3.2 Transcript level
(c)
ABI1 Transcript level
(d)
OST1 Transcript level
(e)
PYL2 Transcript level
(f)
PYL4 Transcript level
(g)
PYL8 Transcript level
(h)
CA1 Transcript level
Carp.
I214
6J29
N38
WW
DS
AM
PM
ab.
ad.

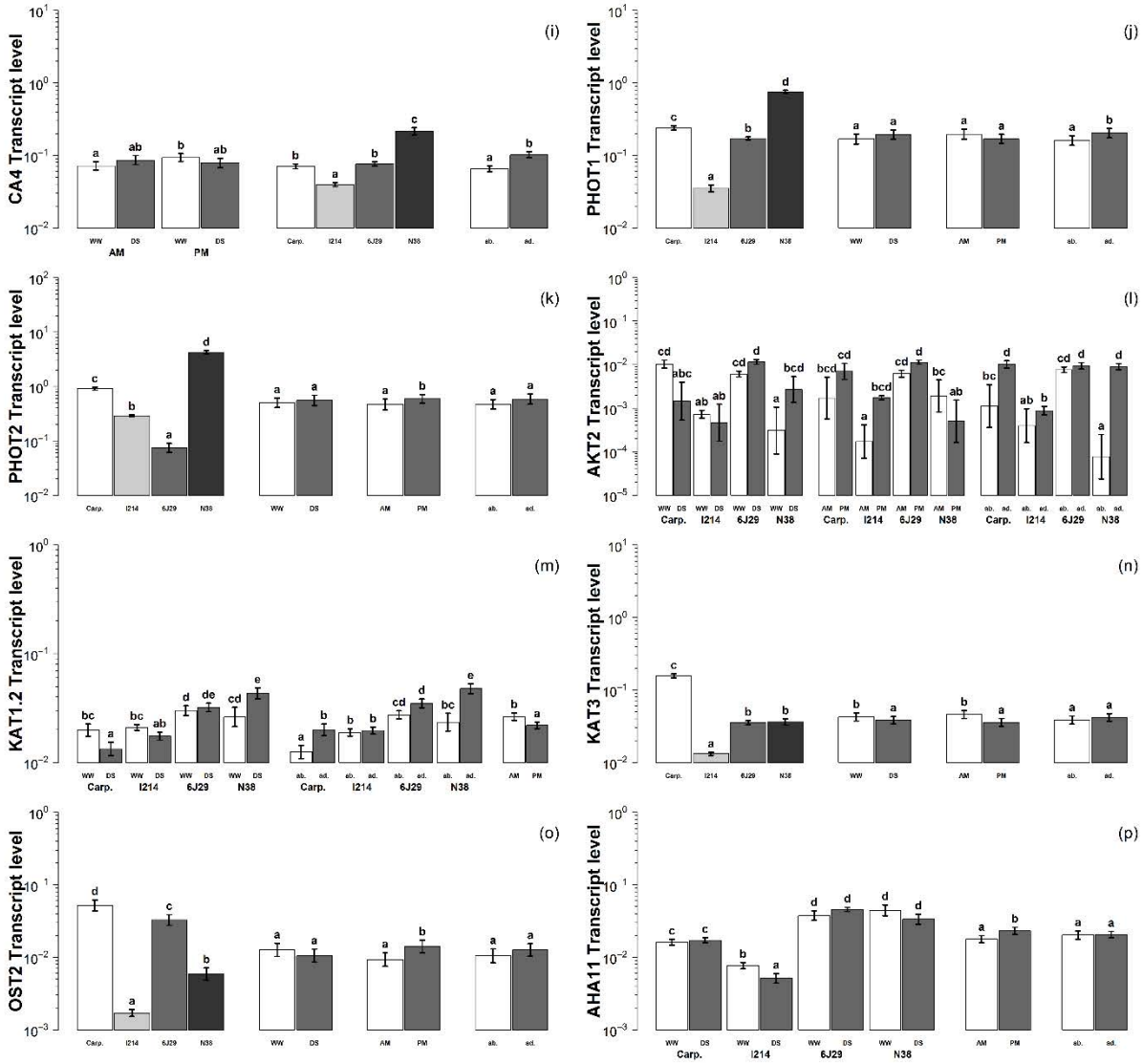
(i)
CA4 Transcript level
(j)
PHOT1 Transcript level
(k)
PHOT2 Transcript level
(l)
AKT2 Transcript level
(m)
KAT1.2 Transcript level
(n)
KAT3 Transcript level
(o)
OST2 Transcript level
(p)
AHA11 Transcript level
WW
DS
AM
PM
Carp.
I214
6J29
N38
ab.
ad.

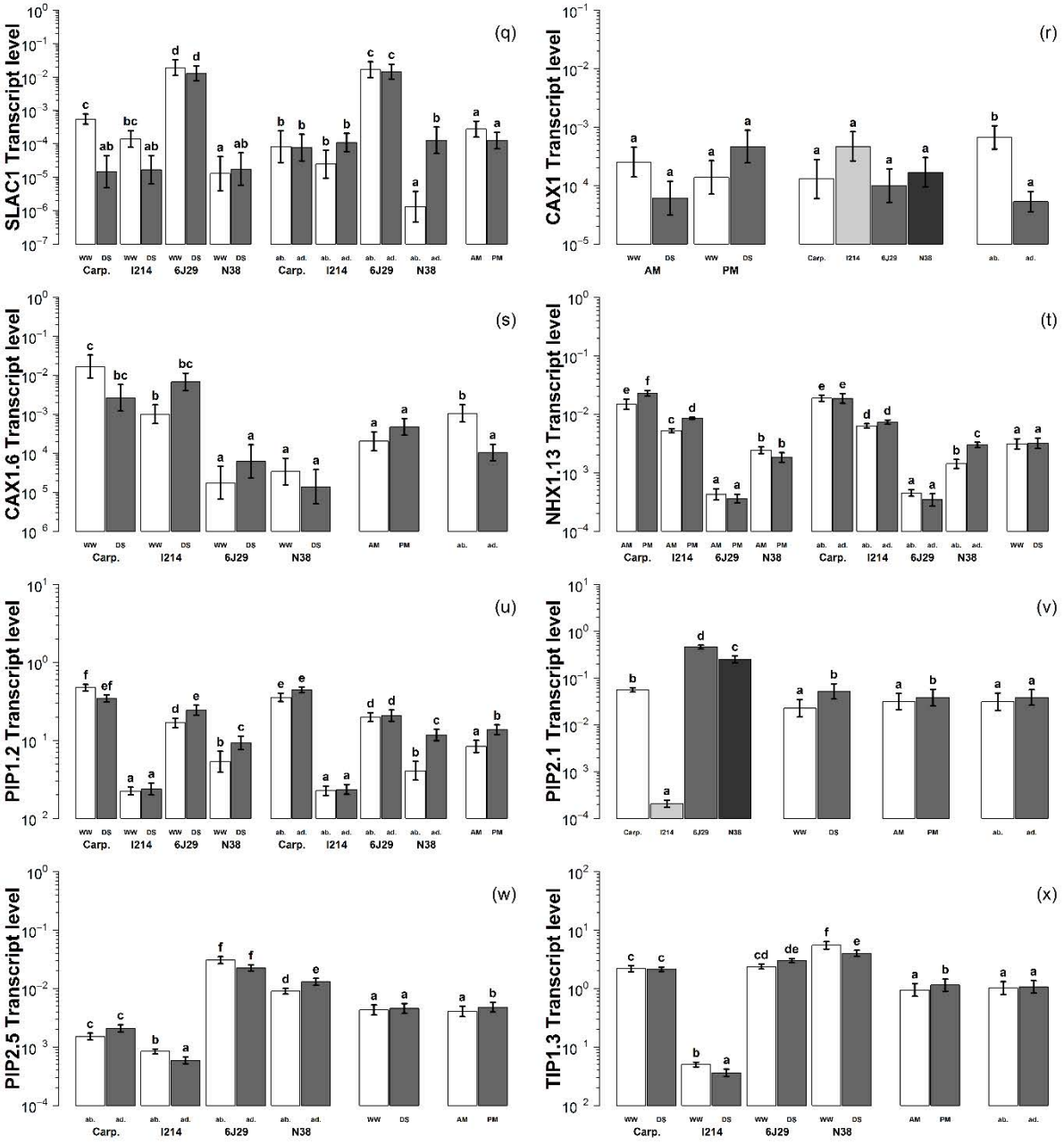
(q)
SLAC1 Transcript level
(r)
CAX1 Transcript level
(s)
CAX1.6 Transcript level
(t)
NHX1.13 Transcript level
(u)
PIP1.2 Transcript level
(v)
PIP2.1 Transcript level
(w)
PIP2.5 Transcript level
(x)
TIP1.3 Transcript level
WW DS
AM PM
ab. ad.
Carp. I214 6J29 N38

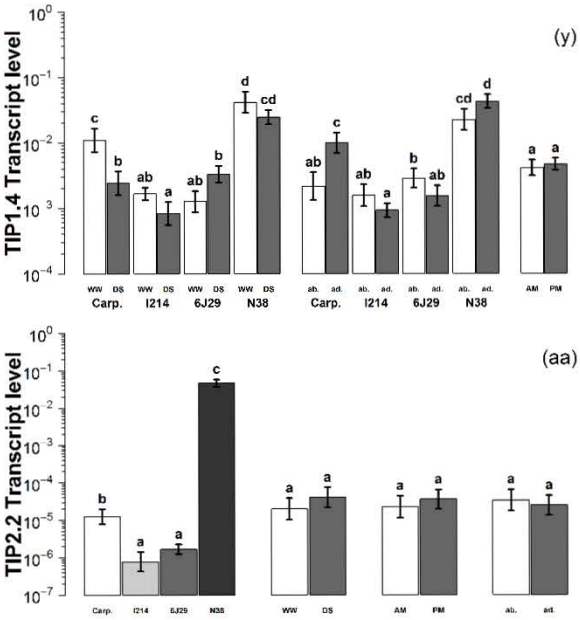
(y)
TIP1.4 Transcript level
WW DS
Carp. I214 6J29 N38
ab. ad.
AM PM

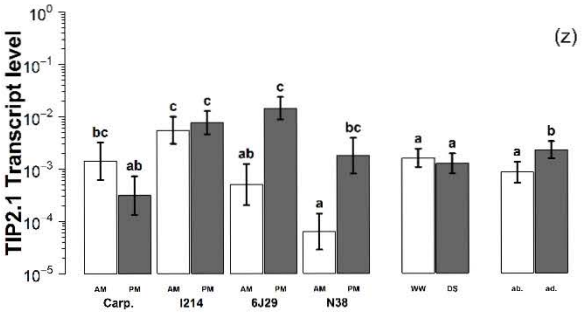
(z)
TIP2.1 Transcript level
AM PM
Carp. I214 6J29 N38
WW DS
ab. ad.

(aa)
TIP2.2 Transcript level
Carp. I214 6J29 N38
WW DS
AM PM
ab. ad.

DISCUSSION GENERALE

DISCUSSION GENERALE

1. Dynamiques temporelles de la conductance stomatique

1.1. Vers une modélisation dynamique à l'échelle globale ?

Il nous faut souligner que l'étude des dynamiques temporelles de la conductance stomatique est relativement récente. Les premières études datent des années 1970 (Davies & Kozlowski, 1975), mais ce n'est qu'à partir des années 1990 que cette thématique est réellement étudiée (Fig. 1). Elle connait depuis un essor exponentiel. Les problèmes rencontrés sont donc, en partie, inhérents à une nouvelle thématique : pas ou peu de méthodologie commune, comparaisons difficiles et un appui de la littérature limité.

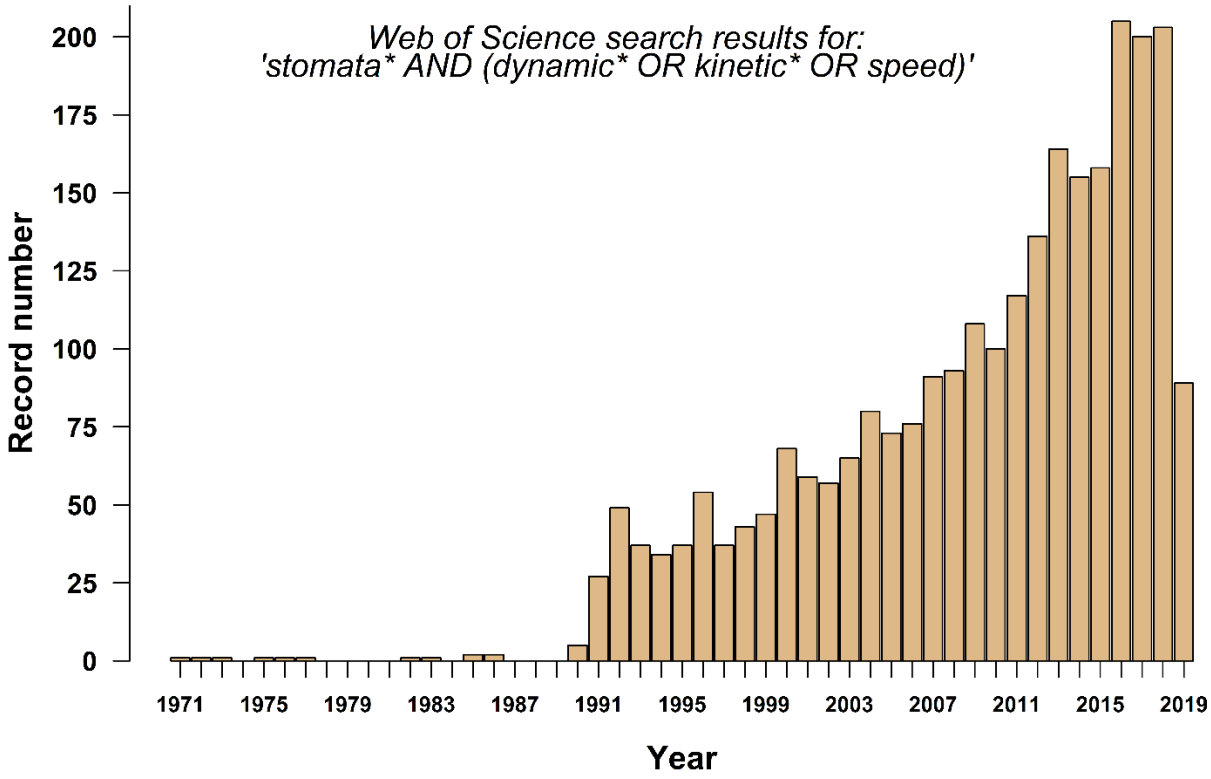

Figure 1. Nombre de publications associées aux dynamiques stomatiques de 1971 à 2019. Graphique produit à partir de la base de données « Web of Science ». La phrase recherchée est « stomata* AND (dynamic* OR kinetic* OR speed) ».

A travers ces travaux de thèse nous avons pu mettre en évidence une très large diversité des dynamiques temporelles de la conductance stomatique. Cette diversité peut être liée à des facteurs environnementaux comme l'irradiance, le VPD, le déficit hydrique et les conditions de croissance, mais aussi à des facteurs endogènes liés au fonctionnement spécifique du génotype ou de l'espèce. De manière générale nous avons pu observer à travers l'expérimentation en

serre (Chapitre I) que les mouvements stomatiques en réponse au VPD étaient plus lents qu'en réponse à un changement d'irradiance. En conditions naturelles (Chapitre III) les mouvements stomatiques étaient plus lents qu'en conditions contrôlées, mais la réponse à la lumière était également plus rapide que la réponse au VPD. De plus, la dynamique stomatique était généralement plus rapide chez les peupliers hybrides que chez les peupliers noirs, à la fois en serre et en pépinière. Ces résultats suggèrent un contrôle génétique mais également une plasticité phénotypique des dynamiques stomatiques, puisque malgré des conditions environnementales largement différentes induisant des changements de la dynamique stomatique, les différences génotypiques étaient maintenues.

La réponse plus lente des stomates au VPD par rapport à l'irradiance implique des mécanismes de perception et de signalisation différents, qui pourraient être liés aux variations couramment plus lentes du VPD atmosphérique (lié aux dynamiques de l'humidité de l'air et de la température) par rapport aux variations de l'irradiance (ombrage par des feuilles proches, passage d'un nuage, percée de lumière). Bien que notre méthodologie se soit focalisée sur l'étude d'une variable environnementale à la fois, en conditions naturelles les stomates répondent simultanément à un ensemble de variables environnementales, parfois contradictoires. Il a été proposé qu'un ordre de priorités des variables microclimatiques régisse la réponse des stomates (Aasamaa & Sober, 2011), toutefois elles pourraient également avoir un caractère synergique ou antagoniste. Des signaux contratictoires (par exemple augmentation de la lumière et du VPD) pourraient ralentir la réponse stomatique alors que plusieurs signaux concordants pourraient les accélérer.

Pendant l'expérience en serre, la sécheresse a induit un ralentissement de la vitesse des mouvements stomatiques, en particulier pendant la fermeture. Cependant en conditions naturelles cet effet n'était pas clairement visible. Il est difficile de comparer le déficit hydrique mis en place en serre et en pépinière puisque la durée, l'intensité, et la mise en place de la sécheresse étaient différents, s'ajoutant à un âge de la plantation et un type de sol également contrasté. Néanmoins, ces résultats suggèrent que les modalités de l'établissement de la sécheresse induisent un ajustement spécifique des dynamiques stomatiques dépendant du génotype. Ces résultats s'ajoutent à la diversité des dynamiques stomatiques observée en réponse au CO_2 (Haworth *et al.*, 2018), au potentiel hydrique foliaire (Davies & Kozlowski, 1975), et même à la période de la journée (Matthews *et al.*, 2017) ou à l'ozone (Dumont *et al.*, 2013). Même si l'effet de ces facteurs sur la dynamique stomatique est encore mal connu, nous pouvons soupçonner que d'autres facteurs peuvent influencer ces dynamiques (température,

vent, fertilité du sol). Une diversité si considérable des dynamiques stomatiques observées nous permet de poser deux hypothèses très générales.

D'une part nous pourrions considérer que des stomates plus ou moins rapides n'engendreraient pas ou peu de bénéfices ou d'inconvénients sur la plante entière. Dans ce paradigme, les vitesses des mouvements stomatiques seraient définies comme la résultante circonstancielle d'autres traits, ayant eux un fort impact sur la plante (densité stomatique, nombre et activité des transporteurs sur la membrane des cellules de garde). D'autre part, la forte plasticité phénotypique des dynamiques stomatiques observées serait liée à une régulation active permettant de répondre de manière spécifique à une large gamme de facteurs à la fois à court et long terme. Cette question est difficile à trancher d'après nos connaissances actuelles. Néanmoins, les corrélations négatives observées en serre et en champs entre les vitesses stomatiques et la transpiration foliaire par unité de surface impliquent que des stomates plus lents induisent une plus grande transpiration foliaire. Ceci aurait potentiellement de fortes conséquences sur l'efficience d'utilisation de l'eau de l'individu. Au niveau foliaire, Δ semble être sous contrôle génétique (Brendel *et al.*, 2008) suggérant que le WUE de la plante entière pourrait l'être également, ce qui nous fait considérer la deuxième hypothèse comme la plus probable.

Les modèles climatiques globaux calculent fréquemment la conductance stomatique en regroupant les végétaux en types fonctionnels (Krinner *et al.*, 2005; Franks *et al.*, 2018). Ainsi, prédire une conductance stomatique moyenne (et en régime permanent) sur une zone géographique donnée qui intègre temporellement la diversité et l'abondance spécifique est à la fois complexe et est un élément critique de ces modèles (Franks *et al.*, 2018). Pendant ma visite à l'institut Hawkesbury pour l'environnement (Western Sydney University, Australie), j'ai pu travailler avec le Dr. Remko Duursma sur le modèle de conductance stomatique se basant sur la théorie d'optimisation des mouvements stomatiques (Cowan & Farquhar, 1977; Medlyn *et al.*, 2011) de type :

$$g_s = g_0 + 1.6\left(1 + \frac{g_1}{VPD^{g_k}}\right)\frac{A}{CO_2} \quad (1)$$

Où g_0, g_1 et g_k sont des paramètres empiriques. Ce modèle est notamment intégré dans des modèles climatiques globaux (Franks *et al.*, 2018). En ajustant ce modèle sur les cinétiques journalières de la conductance stomatique en serre nous avons pu observer, pour tous les génotypes et les deux régimes hydriques, un décalage en fin de journée entre les valeurs de g_s observées et prédites par le modèle. (Fig. 2a). Ce décalage serait en partie dû au fait que l'effet

du VPD sur la conductance stomatique n'est pas identique à tout moment de la journée (Fig. 2b). Compte-tenu des vitesses lentes des mouvements stomatiques en réponse au VPD observées en serre, nous avons posé l'hypothèse que ce décalage est en fait induit par la dynamique temporelle du VPD en augmentation de 0.7 à 2.0 kPa de 3h45 à 13h20 (temps universel) puis en décroissance jusque 1.2 kPa à 16h15. Cette diminution du VPD en fin de journée n'est pas accompagnée d'une stabilisation ou d'une augmentation de g_s, qui continue de décroître à la même vitesse depuis 7h50. Un tel décalage entre les mesures observées et prédites pourrait avoir un impact considérable dans un modèle global intégrant plusieurs types fonctionnels de végétaux sur une vaste période de temps.

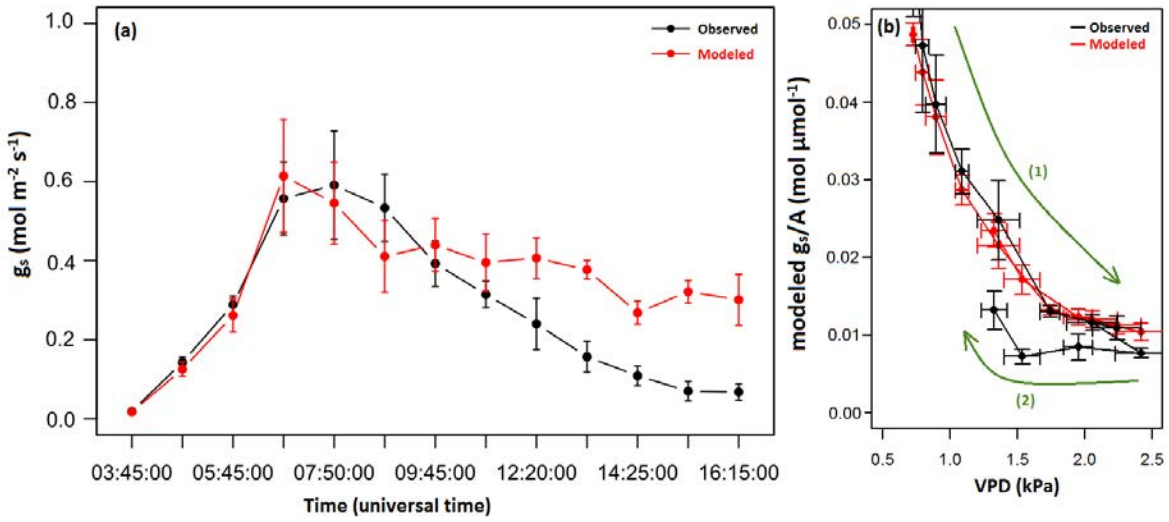

Figure 2. (**a**) : Ajustement d'une cinétique journalière de Carpaccio mesurée en serre (9 juin 2016) à l'aide du modèle « optimal » en régime permanent (proche de Ball et Berry, Medlyn, 2011). (**b**) Relation entre le VPD et l'efficience d'utilisation de l'eau (représentée comme g_s/A puisque calculée ainsi par le modèle) observée et ajusté. Les lignes, et les flèches vertes, représentent le sens de la dynamique journalière. Les couleurs noires et rouges représentent les données observées et ajustées, respectivement. Les points et les barres horizontales montrent la moyenne et l'erreur standard.

La prise en compte de la dynamique stomatique dans la modélisation de la conductance stomatique permet d'accorder les données observées et calculées avec une meilleure précision (Vialet-Chabrand *et al.*, 2013; Vialet-Chabrand *et al.*, 2016). Ce modèle dynamique calcule une conductance « cible » à partir de l'irradiance, puis du VPD :

$$G_{PPFD} = g_{min} + \frac{[\alpha_g \, PPFD \, (g_{max} - g_{min})]}{\sqrt{(g_{max} - g_{min})^2 + (\alpha_g \, PPFD)^2}} \quad (2)$$

$$G_{VPD} = \frac{G_{PPFD} - \theta \frac{VPD}{e_{sat}}}{1 + Z * VPD} \quad (3)$$

avec G_{PPFD} et G_{VPD} les conductances cibles pour l'irradiance et le VPD, respectivement, g_{min} et g_{max} étant la conductance stomatique minimale et maximale, α_g la pente initiale de la réponse de g_s à l'irradiance, PPFD la densité de flux de photons photosynthétiques, e_{sat} la fraction molaire de vapeur d'eau à saturation dans l'air et Z et θ sont des paramètres empiriques définis par Peak & Mott (2011). La conductance stomatique est ensuite calculée :

$$\frac{dg_s}{dt} = \frac{1}{\tau}(G_{VPD} - g_s) \quad (4)$$

où g_s est la valeur de la conductance stomatique à l'instant « t », G_{VPD} la conductance cible et τ une constante de temps pour les mouvements stomatiques. Un τ différent est utilisé pour l'ouverture et la fermeture stomatique.

Il est possible de comparer le modèle « dynamique » (équation 2 à 4) et le modèle « optimal », tous les deux basés sur des processus physiologiques contraignant l'ajustement des paramètres, à un modèle statistique par séparateurs à vaste marge (SVM; Cortes & Vapnik, 1995; Drucker *et al.*, 1997). Une telle méthodologie permet d'obtenir un point de repère pour évaluer la performance de modèles mécanistes (par exemple : Abramowitz, 2005). Le modèle SVM établit une régression entre un jeu de variables d'entrée (ici la concentration atmosphérique en CO_2, la température foliaire, le VPD et l'irradiance) et une variable de sortie. Ce modèle n'est absolument pas contraint par des processus biophysiques et physiologiques mais permet une estimation du meilleur modèle mécaniste qu'il serait possible de formuler à partir des variables d'entrée. Le principe des SVM est l'utilisation d'algorithmes d'apprentissage supervisé et a pour origine un problème de classification, qui a été plus tard généralisé à des problèmes de régression, à l'image du modèle linéaire (capable de réaliser des analyses de variance et des régressions). Intuitivement, les SVM recherchent l'hyperplan (un plan généralisé à plus de 3 dimensions) ayant la marge optimale, c'est-à-dire la séparation la plus éloigné des groupes à classifier (Fig. 3a-b). Dans la plupart des cas, une séparation linéaire n'est pas possible et une transformation est opérée permettant de redéfinir l'espace des données pour trouver une séparation (Fig. 3c-d).

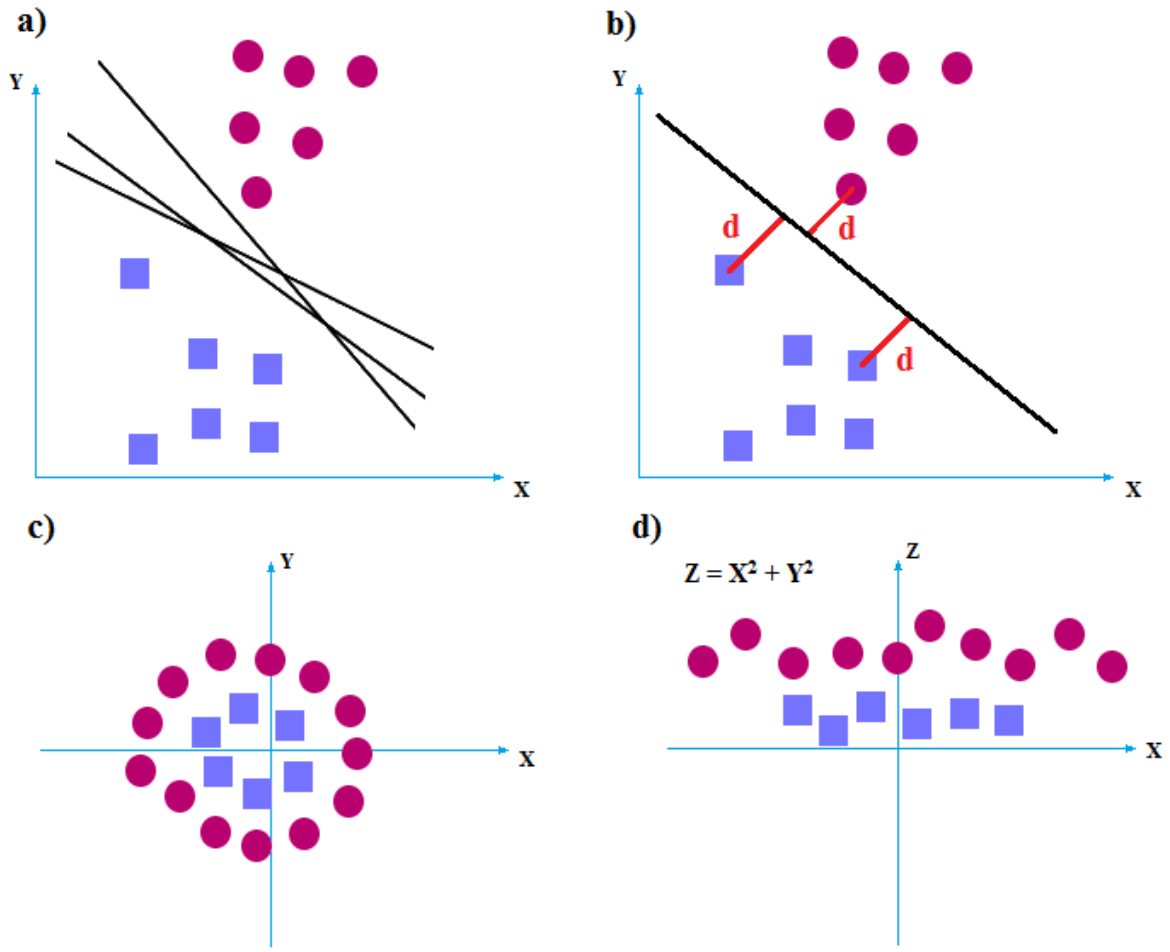

Figure 3. Principe du fonctionnement du modèle par séparateurs à vastes marges. (**a**) : Le problème de classification cherche à séparer linéairement les carrées et les cercles et plusieurs possibilités existent. (**b**) : Le modèle recherche le plan offrant la marge « d » maximale. (**c**) : Pour des problèmes plus complexes, une solution linéaire n'est pas possible. Il est nécessaire de transformer l'espace en ajoutant la variable Z tel que $Z = X^2 + Y^2$. L'espace passe donc de deux à trois dimensions. (**d**) : La transformation a permis de trouver une solution linéaire.

La figure 4 montre la comparaison du modèle « optimal » (équation 1), « dynamique » (équations 2 à 4) à un modèle ajusté par séparateurs à vastes marges. Le modèle « dynamique » s'ajuste clairement mieux aux données observées que le modèle « optimal » (le RMSE est 33% plus faible, Fig. 4b) mais il est également apparent d'après le modèle SVM que de fortes améliorations sont encore possibles. Par exemple, la paramétrisation du modèle dynamique requiert actuellement la définition simultanée (par inférence bayésienne ou à l'aide d'algorithmes génétiques) d'au moins quatre paramètres qui sont les constantes de temps τ pour l'ouverture et la fermeture stomatique, g_{min} et g_{max}. τ a par ailleurs une valeur unique quels que soient le ou les changements environnementaux.

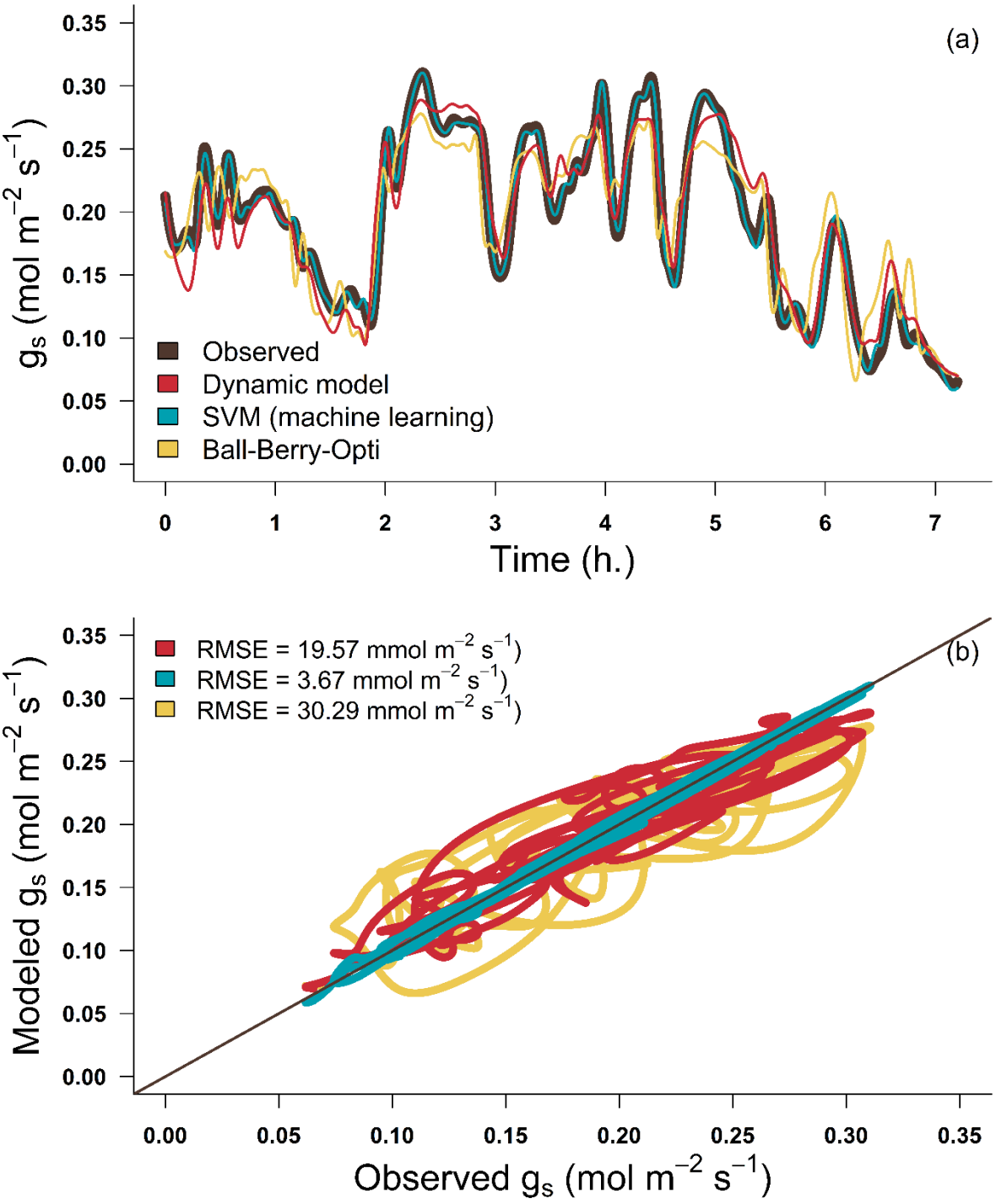

Figure 4. Ajustement de trois modèles de conductance stomatique sur une cinétique journalière de la conductance stomatique chez le chêne sessile (**a**, données collectées par Silvère Vialet-Chabrand) et comparaisons entre données observées et prédites par les modèles (**b**). Les couleurs noires, rouges, bleues et jaunes représentent la conductance stomatique observée, calculée par le modèle dynamique (Vialet-Chabrand, 2013), calculé par « Séparateurs à Vastes Marges » (SVM, apprentissage supervisé à partir des concentrations en CO_2, de la température foliaire, du VPD et de la quantité de PAR) et par le modèle « optimal » en régime permanent (proche de Ball et Berry, Medlyn, 2011). L'erreur quadratique moyenne pour chaque modèle est affichée.

Au vu des fortes différences observées pendant ces travaux de la dynamique stomatique en réponse à l'irradiance et au VPD nous pouvons supposer qu'un τ unique ne permet pas de définir précisément le champ des dynamiques possibles au sein d'un individu. Des premiers tests à partir d'une version modifiée du modèle dynamique semblent encourageants (Fig. 5). Dans cette version, l'équation (3) n'est pas systématiquement utilisée. A la place, nous définissons une valeur de VPD, ajustée par le modèle. Pour des VPD en dessous de cette valeur, G_{PPFD} est utilisé à la place de G_{VPD} dans l'équation (4), sinon les équations (2), (3) et (4) sont prises en compte. Cela permet de prendre en compte un jeu de paramètres τ différent pour l'irradiance et le VPD selon si la conductance cible est calculée à partir de l'équation (2) uniquement, ou de l'équation (2) et (3). De plus amples recherches sont nécessaires pour mieux comprendre comment les stomates conjuguent leur réponse à différentes variations environnementales, afin de formuler par un modèle un effet qui pourrait être synergique, antagoniste, pondéré, avec un seuil défini et/ou un ordre de priorités (Aasamaa & Sober, 2011; Haworth *et al.*, 2018).

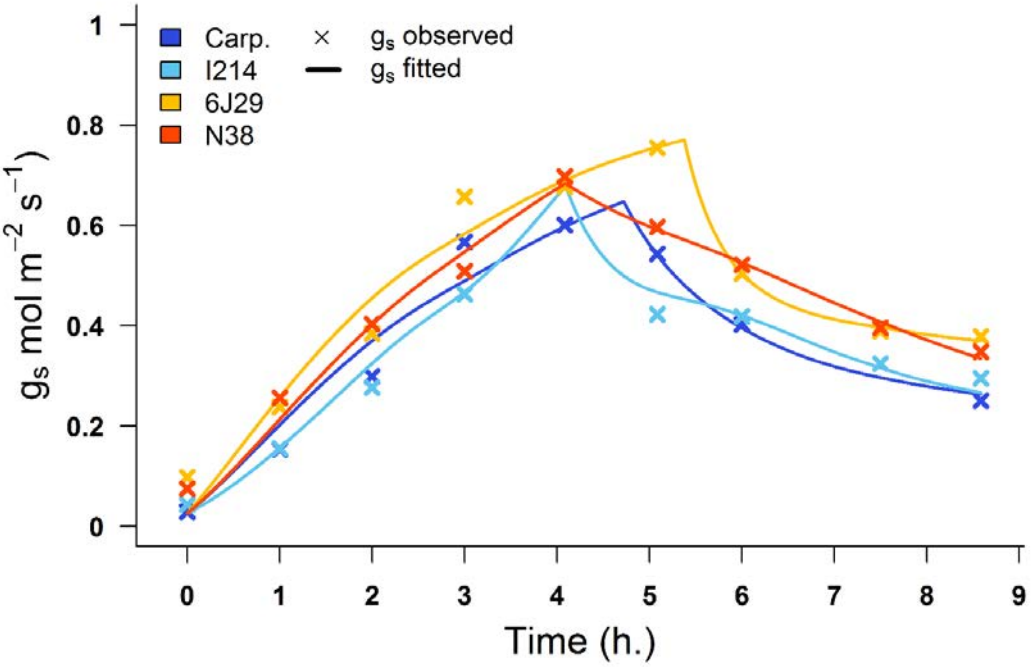

Figure 5. Ajustement des cinétiques journalières mesurées en serre (9 juin 2016) sur des peupliers témoins. Les données observées sont représentées par des croix et l'ajustement à partir d'une version modifiée du modèle dynamique est représenté à l'aide de lignes. Les couleurs représentent les quatre génotypes : Carpaccio, I214, 6J29 et N38. La modification du modèle dynamique permet de prendre en compte deux jeux de paramètres τ, un pour la réponse à l'irradiance et un pour la réponse au VPD. Cette dernière s'activant à partir d'une valeur de VPD critique (la brisure apparente de la ligne continue) ajusté par le modèle. Si la conductance n'atteint pas cette valeur, la conductance cible n'est définie qu'à partir des variations de l'irradiance et les paramètres τ adéquats sont utilisés. Au contraire, lorsque cette valeur est atteinte, les paramètres τ pour la réponse au VPD sont activés et la conductance cible est définie à partir de l'irradiance et du VPD.

Cependant, intégrer cette dynamique stomatique dans des modèles plus globaux utilisant des mesures de flux à grande échelle comme FLUXNET (Baldocchi *et al.*, 2001) est encore loin d'être à notre portée. D'abord, la modélisation dynamique de la conductance stomatique nécessite un suivi continu, de l'ordre de plusieurs secondes à une minute. Un suivi par des mesures plus ponctuelles, qui peuvent ensuite être interpolées, aura une précision diminuée proportionnellement à la longueur du pas de temps. Si la perte de précision est raisonnable pour des pas de temps de 30 secondes à une minute, des moyennes semi-horaires sont souvent utilisés pour modéliser les les flux à grande échelle (Baldocchi *et al.*, 2001; Dufrêne *et al.*, 2005). Enfin, la modélisation dynamique de la conductance stomatique se fait par la résolution d'une ou plusieurs équations différentielles qui, lorsque la quantité de données est importante, pose des contraintes supplémentaires : un temps d'analyse long et la nécessité d'avoir une forte puissance de calcul.

Ces travaux de thèse ont également permis d'examiner plusieurs hypothèses quant aux déterminants des dynamiques stomatiques. La morphologie des stomates apparaissait être une piste prometteuse, puisque reposant sur des concepts physiques, et elle était fortement liée à la dynamique stomatique en réponse au VPD en serre (chapitre I). Pourtant nous avons mis en évidence par une étude similaire en pépinière (chapitre III) que son effet n'est probablement pas déterminant, ou pour le moins elle aurait un effet dépendant des conditions environnementales et de croissance. D'autres paramètres morphologiques, comme la taille et le nombre de cellules épidermiques entourant les cellules de garde (Dow *et al.*, 2014) ou l'agencement des microfibrilles dans les cellules de garde (Galatis *et al.*, 1983) pourraient participer à la diversité de la vitesse des mouvements stomatiques observés. Toutefois la physiologie des cellules de garde nous semble être l'élément décisif permettant d'expliquer une telle diversité. En effet, des régulations actives du nombre et de l'activité des transporteurs d'éléments responsables des mouvements stomatiques (K^+, Cl^-, Ca^{2+}, $malate^{2-}$) permettraient une modification dynamique et réversible des vitesses stomatiques selon les conditions environnementales. Une telle régulation des mouvements stomatiques par des caractères morphologiques, et donc fixes après la maturation des feuilles, est plus difficilement envisageable.

A ce propos, les expressions géniques mesurées en serre et présentées au Chapitre IV ont été mises en relation avec les paramètres de la dynamique stomatique présentée au Chapitre I (Fig. 6). Toutes les corrélations significatives détectées sont portées par les différences génotypiques de l'expression génique. Lorsque nous contrôlons cet effet, aucune corrélation n'apparait

significative. Carpaccio et I214, présentant constitutivement une plus grande quantité de transcrits de NHX1.13, CAX1.6 et une plus faible quantité de PIP2.1, PIP2.5, TIP1.3 et AHA11, ont tendance à avoir des stomates plus rapides (Fig. 6a). Ces transcrits codent pour des transporteurs, aquaporines et pompes à protons impliqués dans les mouvements d'eau responsables des mouvements stomatiques. Ces tendances pourraient avoir une explication physiologique. Si c'est le cas, ce type de caractères pourrait être utilisé pour sélectionner des génotypes ayant des mouvements stomatiques plus rapides. Cependant, il existe une grande séparation organisationnelle entre la transcription d'un gène codant pour un canal ionique et l'activité dudit canal sur la membrane des cellules de garde. Les variations génotypiques de l'expression génique pourraient simplement refléter des divergences intrinsèques du fonctionnement du génome, sans pour autant provoquer une diversité phénotypique. Ces éléments, lorsqu'ils sont ajoutés à l'absence de corrélation similaire au niveau individuel (Fig. 6b), nous contraignent à interpréter ces corrélations avec la plus grande prudence (exemple : pourquoi une plus forte expression d'aquaporines serait liée à des mouvements stomatiques plus lents ?), d'autant plus que plusieurs jours ont séparé les mesures de dynamique stomatique et le prélèvement des feuilles pour l'expression génique.

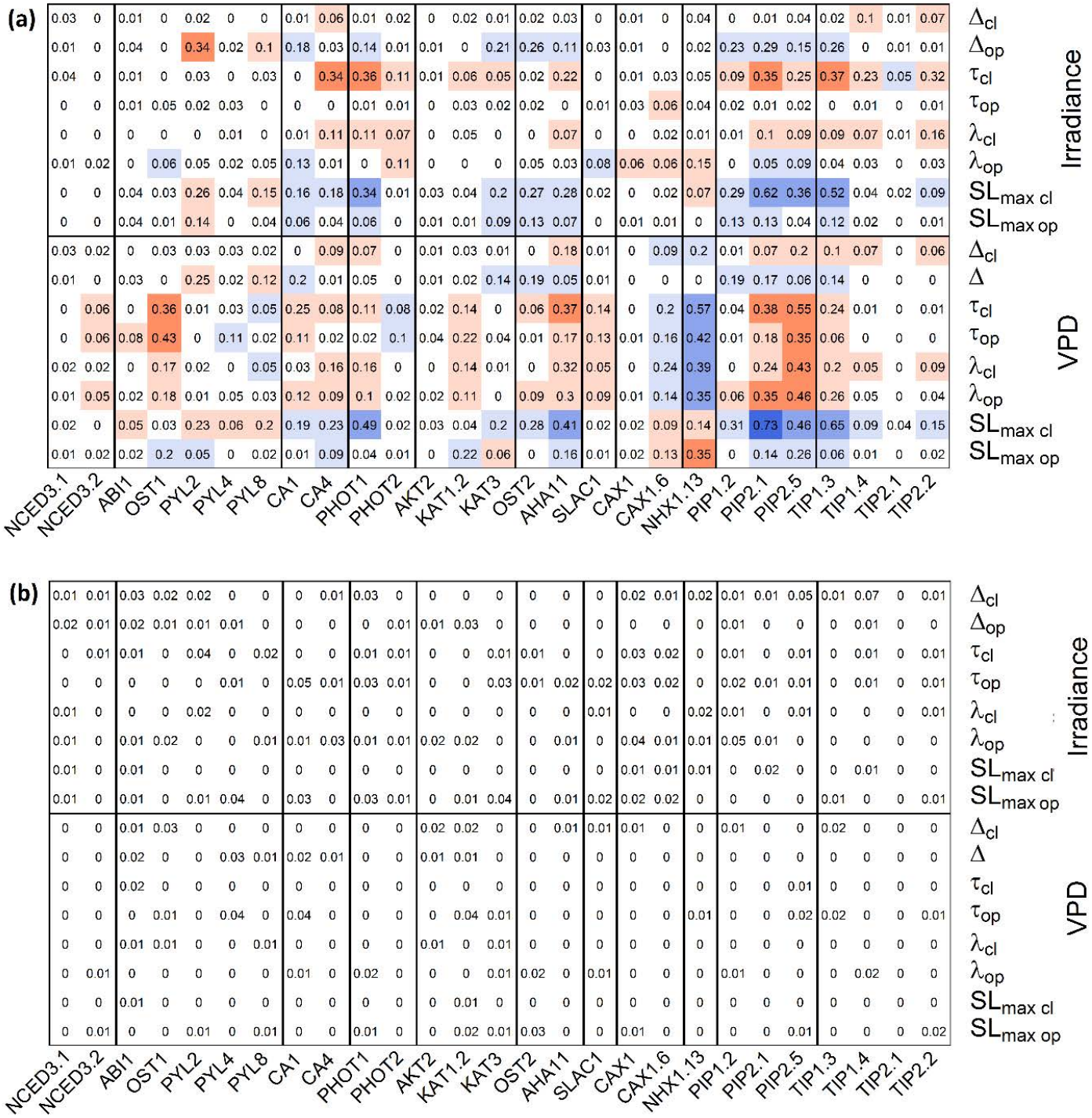

Figure 6. Matrice des corrélations entre la dynamique stomatique en réponse à l'irradiance et au VPD et l'expression de 27 gènes dans les cellules de garde. Un modèle linéaire simple (**a**) ou prenant en compte l'effet du génotype (**b**) a été utilisé. Les couleurs orange et bleues montrent les corrélations significativement positives et négatives, respectivement. La couleur blanche représente les corrélations non-significatives après correction post-hoc du « false discovery rate ». Les valeurs représentées sont les R^2 partiels. Δ : amplitude de la conductance stomatique, τ et λ : des paramètres du modèle dynamique et SL_{max}, la pente maximum de la sigmoïde au point d'inflexion.

1.2. Critiques

Notre méthodologie pour décrire la dynamique temporelle des stomates n'est pas parfaite. Par définition le modèle dynamique nécessite une description *a priori* de la forme de la dynamique pour définir l'utilisation du modèle dynamique exponentiel (non présenté ici) ou sigmoïde :

$$g_s = g_0 + (G - g_0)e^{-e^{(\frac{\lambda - t}{\tau})}} \quad (5)$$

De plus la sigmoïde est doublement asymptotique (à g_0 et G, les valeurs de g_s initiale et finale) et présente une asymétrie fixe, avec une pente maximum au point d'inflexion fixée à 37% de la conductance stomatique initiale. En effet, en prenant la forme simple de la courbe : y = exp(-exp(x)), nous obtenons une sigmoïde qui tend vers 1 et 0 entre $-\infty$ et $+\infty$ (respectivement) et qui, pour x = 0 produit y = 1/exp(1) soit ≈ 0.3678 (pour une représentation interactive : www.google.com/search?q=y+%3D+exp(-exp(x))). Bien que cette fixité permette de limiter l'ajout de paramètres empiriques à déterminer, elle limite aussi notre capacité à améliorer l'ajustement de la dynamique des stomates. Par exemple, le caractère doublement asymptotique implique que la conductance stomatique soit toujours inférieure à sa valeur initiale au moment du changement environnemental : à t = 0 pour une diminution de g_s de 1 à 0 mol m^{-2} s^{-1} nous avons $g_s = 1 + (0 - 1) * \exp(-\exp((\lambda-0)/\tau))$ soit $g_s = 1 + (-\exp(-\exp(\lambda/\tau)))$. Ainsi à t = 0 la conductance calculée est égale à la conductance initiale, auquel est soustrait $(-\exp(-\exp(\lambda/\tau))$. Ce dernier problème peut être résolu au prix d'une complexification significative du modèle (Vialet-Chabrand & Lawson, 2019).

Au-delà des considérations purement mathématiques, la forte variabilité individuelle observée nécessite un grand nombre de réplicas afin d'obtenir une puissance statistique suffisante, en dépit de la complexité et de la longueur de ces mesures. Techniquement, la dynamique stomatique enregistrée sur une feuille n'est parfois pas indépendante du reste de l'arbre. Une augmentation expérimentale de l'irradiance dans la chambre du système d'échanges gazeux (pour induire une ouverture stomatique) peut être influencée par l'effet sur la plante entière du passage d'un nuage. De plus, les systèmes d'échanges gazeux utilisés ne contrôlent pas le VPD de manière optimale. Le flux d'air entrant et sortant de la chambre de mesure est suffisamment lent pour assurer une mesure adéquate, mais il présente l'inconvénient que l'humidité de l'air perçue par la feuille peut être influencée par la transpiration même de la feuille, et ainsi découpler la feuille de l'atmosphère. Les évolutions instrumentales récentes améliorant le contrôle de l'humidité de l'air et la vitesse du flux nécessaire pour obtenir une mesure adéquate permettent en grande partie de résoudre ce problème. Enfin, le peuplier présente des stomates

sur les deux faces, de densités et de tailles différentes (Chapitre I et III) et soumises à des variations microclimatiques différentes (Sheriff, 1979). Ceci impliquerait une régulation indépendante de chaque face (Mott *et al.*, 1993; Richardson *et al.*, 2017). D'après cette hypothèse, les dynamiques stomatiques pourraient être différentes selon la face considérée et devraient donc être étudiées indépendamment.

1.3. Perspectives

Il est clair que nous n'avons fait qu'effleurer les possibilités et les questions de recherche centrées sur les dynamiques stomatiques. De manière générale, des progrès dans la détermination des mécanismes de perception et de signalisation en réponse aux changements environnementaux (VPD, température, CO_2, potentiel hydrique) permettront de formuler des hypothèses plus précises sur les déterminants de la dynamique stomatique. De plus, mieux comprendre la variabilité des vitesses stomatiques nécessite une connaissance approfondie des mécanismes de réponse des stomates. Cette dernière aidera au calcul des coûts énergétiques de l'ouverture stomatique, et donc du coût du suivi environnemental des stomates. En parallèle, des avancements de modélisation théorique seront requis pour, à la fois résoudre les contraintes inhérentes au modèle dynamique actuel, mais également pour intégrer la diversité observée des réponses stomatiques.

Plus spécifiquement, il existe un décalage entre les hypothèses concernant les dynamiques stomatiques, souvent formulées au niveau de l'ouverture de l'ostiole, et les mesures de la conductance stomatique intégrant non seulement l'ouverture stomatique mais également leur morphologie et densité. Par exemple, l'hypothèse que des stomates de plus grande taille seraient également plus lents implique seulement la morphologie et la vitesse des cellules de garde, alors que la plupart des études testant cette hypothèse se concentrent sur la vitesse de la conductance stomatique (Elliott-Kingston *et al.*, 2016; Mc Ausland *et al.*, 2016; Kardiman & Ræbild, 2018). D'après les comparaisons des vitesses de la conductance stomatique et de l'ouverture de l'ostiole aux chapitres I et III, il est clair que se placer uniquement au niveau de la conductance stomatique ne permet pas de tester cette hypothèse.

Afin de résoudre cette discordance, nous proposons de se placer à l'échelle de l'ouverture de l'ostiole. Par des techniques de microscopie, couplées à un dispositif permettant un contrôle environnemental, il est possible d'étudier directement les mouvements des cellules de garde et de l'ouverture de l'ostiole à la suite d'un changement environnemental (Oxborough & Baker, 1997; Lawson *et al.*, 2002). Une telle étude requiert la prise de photographie en séries, ou

l'enregistrement de vidéos et pourrait fournir sur une simple feuille une grande quantité de d'informations.

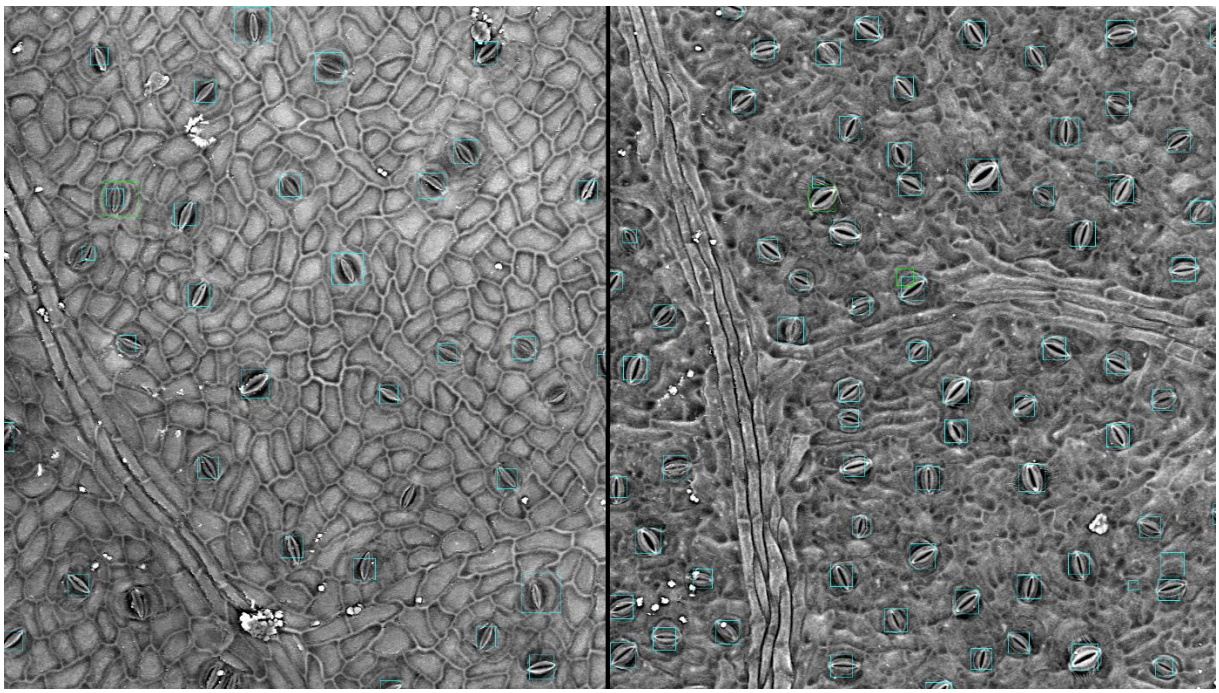

Figure 7. Exemple de la reconnaissance automatisée de stomates par la méthode de Viola & Jones (2004) à l'aide du module OpenCV de Python 3.0 (face adaxiale à gauche, face abaxiale à droite). Les stomates reconnus par l'algorithme sont représentés par des carrées turquoises et verts. Les carrés verts ont été supprimés du comptage *a posteriori* en supprimant les zones se recouvrant, ainsi un stomate ne peut être détecté qu'une fois.

Au cours des mesures de densité et de taille des stomates, il est apparu évident que la principale limitation à l'analyse de ces données était les mesures morphologiques manuelles (le comptage des stomates et les mesures de la taille des cellules de garde). En effet, le prélèvement foliaire, la lyophilisation, la métallisation puis la photographie de la surface foliaire peuvent s'opérer relativement rapidement. De nombreuses améliorations ont pu être développées pour rendre ce traitement pratiquement automatisé. Une fois les échantillons placés sous le microscope électronique à balayage, un programme permet de se déplacer automatiquement sur les différents échantillons et régler les paramètres voulus (brillance, contraste, grandissement). De plus, nous pouvons réaliser des photographies avec un certain pourcentage de recouvrement et fusionner ces différentes photographies pour augmenter substantiellement la zone analysée. En revanche, compter et mesurer individuellement chaque stomate photographié requiert un temps considérable. Cependant, par des techniques d'intelligence artificielle, nous pouvons réaliser une analyse d'image par des techniques de « vision par ordinateur ». Parmi elles, la méthode de Viola & Jones (2004), a pu être utilisée dans de nombreuses applications (reconnaissance

faciale ou de plaques d'immatriculation). A partir de la bibliothèque OpenCV disponible sous Python 3.0, il est possible d'utiliser ce genre de techniques pour la reconnaissance de stomates. J'ai eu l'occasion de mettre en place une telle technique dans l'optique d'accélérer les mesures de densités et de morphologie stomatique (Fig. 7), à partir de travaux similaires chez le chêne (Vialet-Chabrand & Brendel, 2014). La paramétrisation de l'algorithme n'est pas aisée et est hautement spécifique à l'objet reconnu. Néanmoins le traitement de l'information automatique offre une opportunité considérable, et de bons résultats peuvent être obtenus rapidement. La figure 8 montre la précision obtenue après un premier essai de paramétrisation d'une seule semaine de travail, et démontre la faisabilité d'un tel projet.

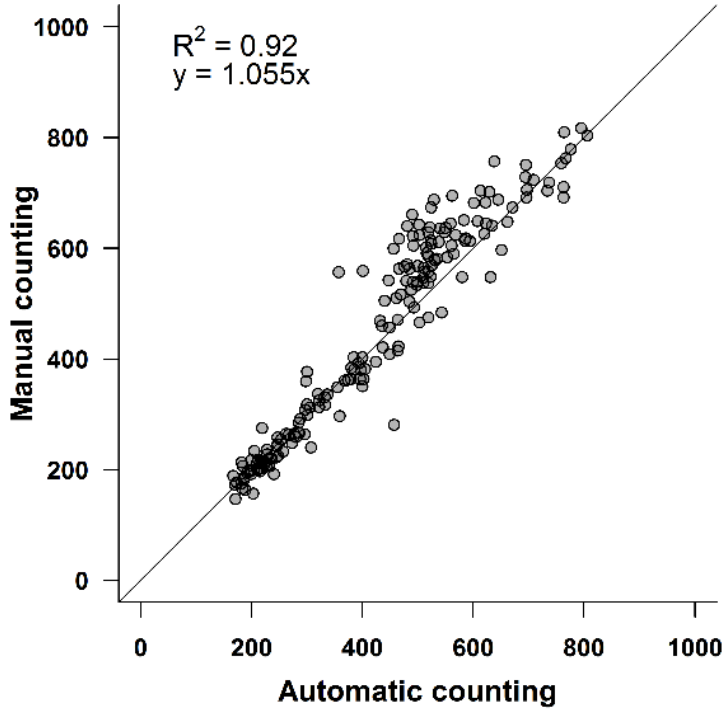

Figure 8. Précision obtenue à partir d'un premier essai de la technique de reconnaissance automatisée de stomates par la méthode de Viola & Jones (2004). 192 photographies composées de faces abaxiales et adaxiales de feuilles de quatre génotypes de peuplier ont été utilisés. Le coefficient de détermination et l'équation de la droite sont montrés. La ligne représente la droite 1:1.

A partir de ces mesures morphologiques, il serait alors possible de suivre l'évolution du volume des cellules de garde (Franks *et al.*, 2001), et donc des quantités d'eau entrant et sortant des cellules de garde. Ces mesures morphologiques pourraient alors être reliées à la dynamique du stomate. Toutefois elles devraient également inclure une quantification de la profondeur du pore stomatique pour modéliser précisément la conductance. Malgré le peu d'informations disponibles, la profondeur du pore stomatique est trop souvent supposée comme proportionnelle à la taille des stomates (Franks & Beerling, 2009; Fanourakis *et al.*, 2014; de

Boer *et al.*, 2016), ce qui n'est pas toujours le cas (Roth-Nebelsick *et al.*, 2012), et devrait plutôt représenter la longueur du chemin de diffusion de la surface foliaire jusqu'aux cavités sous-stomatiques.

En parallèle, le développement des techniques de microanalyses, par exemple par cryogénie, permettrait d'étudier spécifiquement les contenus en éléments dans chaque compartiment cellulaire. L'ensemble de ces données pourraient être utilisées dans un modèle de type « bottom-up » tel que OnGuard (Hills *et al.*, 2012) pour associer la quantification des mouvements d'eau, du contenu en élément dans les compartiments cellulaires stomatiques, du nombre et de l'activité des transporteurs ioniques et des vitesses d'ouverture de l'ostiole. Les applications avec les techniques actuelles sont nombreuses, et les développements futurs permettront un meilleur accord entre notre compréhension des mécanismes stomatiques au niveau cellulaire et foliaire.

2. *Efficience d'utilisation de l'eau*

2.1. Vers des critères de sélection basés sur l'efficience ?

Les objectifs 3 et 4 de la thèse consistaient à comparer l'efficience d'utilisation de l'eau et ses déterminants au niveau foliaire et de la plante entière, à la fois en conditions contrôlées et naturelles. En ce qui concerne la comparaison entre niveaux d'organisation (feuille, plante entière), nous avons pu mettre en évidence une certaine stabilité de l'efficience d'utilisation de l'eau en conditions contrôlées que nous avons confirmé en conditions naturelles. Ces résultats impliquent que les processus non pris en compte dans le WUE foliaire (photosynthèse des tiges, transpiration de nuit) ne modifient pas significativement les conclusions tirées au niveau de la plante entière. Une étude sur les génotypes de peupliers noirs utilisés dans ces travaux a pu calculer la proportion de l'eau transpirée de nuit par rapport à celle transpirée de jour, variant de 1 à 4% selon le génotype (Bogeat-Triboulot *et al.*, 2019). Ce ratio correspond également à la proportion de l'efficience de transpiration modifiée lorsque cet élément est inclus dans le calcul de TE, montrant ainsi la faible contribution de ce phénomène à TE. En ce qui concerne l'assimilation photosynthétique des tiges, la contribution de la photosynthèse corticale à la biomasse des tiges nues (où l'écorce s'est détachée) était de 11% chez l'eucalyptus (*Eucalyptus minata*, Cunn.), connu pour son écorce décidueuse (Cernusak & Hutley, 2011). D'après les auteurs, cette proportion calculée est très sensible aux valeurs théoriques choisies de la composition isotopique de ^{18}O de l'eau absorbée par les racines. La surface des tiges peut être estimée en serre par le calcul de la surface d'un cône (puisque la grande majorité des plants ne présentaient pas de sylleptiques) soit $S = \pi*r*(r^2+h^2)^{0.5}$ avec r et h le rayon et la hauteur du

cône, respectivement. Ainsi, la surface des tiges en serre était de 30 à 60 cm^2, et représentait environ 1% de la surface foliaire totale. Sur un arbre composé de plusieurs branches insérées les unes sur les autres ce ratio pourrait être modifié mais l'ordre de grandeur serait vraisemblablement similaire parce que la lignification des tiges les plus anciennes ne permet pas la photosynthèse corticale. De plus la capacité photosynthétique des tiges est probablement plus faible que celle des feuilles puisque dépourvues de stomates, malgré la présence courante de lenticelles (Isebrands & Richardson, 2014).

En conditions contrôlées et naturelles, l'efficience d'utilisation de l'eau était relativement stable même si ses déterminants étaient différents. Une WUE aussi similaire entre des conditions environnementales aussi diverses suggère un contrôle génétique de l'efficience chez les peupliers, ce qui est en accord avec l'identification de QTLs liés à WUE chez le peuplier (Viger *et al.*, 2013) et plusieurs espèces arborées (Brendel *et al.*, 2002; Casasoli *et al.*, 2004; Marguerit *et al.*, 2014). Par contre, la sécheresse est un facteur susceptible d'influencer les stratégies de sélection de génotype de peupliers pour leur forte WUE. Nous avons pu voir que le déficit hydrique modifie plus fortement le classement génotypique que les différentes conditions de croissance, ce qui implique des modifications physiologiques spécifiques au génotype sous sécheresse et suggère ainsi une plasticité phénotypique lié à l'intéraction entre le génotype et l'environnement. WUE observée est alors dépendante de la réponse à la sécheresse du génotype considéré, ainsi il semblerait que le coût hydrique du gain en carbone (λ au sens Cowan & Farquhar, 1977) est modifié lorsque la disponibilité en eau diminue. En se plaçant dans un contexte de sélection génotypique, des génotypes considérés comme fortement efficients puisque sélectionnés sur des critères de WUE sous une disponibilité en eau non-limitante pourraient être très peu efficients sous sécheresse et balayer l'intérêt de les avoir sélectionné.

Les prédictions climatiques pour les années à venir prévoient des sécheresses plus fréquentes et plus intenses (IPCC, 2014), et sont dès à présent perçues par les collectivités, les acteurs économiques et les citoyens (Ministère de l'agriculture et de l'alimentation, 2019). Lorsqu'une sécheresse intervient, des restrictions peuvent se mettre en place allant de l'interdiction d'irriguer pendant certaines heures à une interdiction absolue pendant plusieurs jours ou semaines. Ces restrictions sont définies sur la base de seuils au niveau local par la préfecture (Ministère de la transition écologique et solidaire, 2016), ce qui peut entrainer une perte de production. Certains agriculteurs sont soumis à des restrictions d'irrigation dès avril, très tôt dans la saison de croissance, lorsqu'une période de sécheresse se succède à un hiver sec, ne permettant pas de recharger suffisamment les réserves hydrologiques. Comme nous avons pu

le voir, bien que des génotypes plus efficients puissent permettre de limiter l'épuisement des réserves en eau du sol, cela n'implique pas forcement une meilleure tolérance à la sécheresse. Ainsi les pistes envisagées et discutées actuellement font rarement mention de l'utilisation de plants plus efficients. Il est conseillé aux agriculteurs de travailler des cultures consommant moins d'eau, intégrant à la fois un changement de l'espèce cultivée (légumineuse à la place du maïs) et un changement de génotype (Ministère de la transition écologique et solidaire, 2016). Certaines propositions envisagent la création et l'utilisation de retenues d'eau collinaires artificielles, l'extension des réseaux d'irrigation existants ou un changement de stratégie d'irrigation. Cette dernière implique d'irriguer moins mais au bon moment, de limiter le ruissèlement et l'évaporation ou de se passer de systèmes d'irrigation gravitaire (où la distribution de l'eau se fait entièrement à l'air libre par simple écoulement à la surface du sol) pour introduire des systèmes de microirrigation alimentant le végétal au sol, selon ses exigences. De manière générale, il est ainsi plutôt proposé actuellement d'optimiser l'efficience d'irrigation plutôt que l'efficience d'utilisation de l'eau.

En France, les génotypes de peupliers autorisés à la vente sont inscrits au registre national des matériels de base des essences forestières. L'inscription requiert d'abord l'identification de la provenance, la définition des critères de sélection utilisés et enfin la démonstration de la supériorité du matériel de base par rapport à des témoins déjà inscrits au registre sur la base de critères définis. Les essais comparatifs peuvent être différents selon l'usage recherché (pour le bois d'œuvre ou la biomasse) mais se concentrent principalement sur la sensibilité aux bioagresseurs, la vigueur et la productivité selon des protocoles définis. Pour le peuplier, la sensibilité à la rouille foliaire (M*elampsora larici-populina*), à la brunissure des feuilles (*Marssonina brunnea*), au chancre bactérien (*Xanthomonas populi*) et au puceron lanigère (*Phloeomyzus passerinii*) est testée souvent *in vitro* et en pépinière. Il faut noter qu'une résistance complète à un bioagresseur disqualifie le matériel de base. En effet, une résistance partielle entrainant une faible réduction de la productivité est privilégiée puisqu'elle réduit la pression de sélection et ainsi l'apparition de nouvelles virulences contournant cette résistance. Les caractères testés liés à la productivité et à la vigueur du matériel incluent différents paramètres de croissance (hauteur, diamètre), phénologique (date de débourrement et d'arrêt de croissance) et de mortalité. Ils doivent également être répliqués dans des conditions environnementales variées. En définitive la tolérance à la sécheresse n'intervient que très peu, et les sélectionneurs ne sont donc pas contraint de l'améliorer, même s'il existe une certaine demande des populiculteurs. Ajouter des critères de sélection basés sur la tolérance à la

sécheresse et l'efficience d'utilisation de l'eau est peut-être encore précoce, avant que les techniques de sélection sur ces paramètres soient bien développées. En contrepartie cela pourrait contraindre les sélectionneurs à considérer ces traits pendant la sélection, et aider le développement de ces techniques.

2.2. Critiques

Tester l'effet de différentes conditions de croissance à travers l'expérimentation en serre et en pépinière n'était pas sans difficultés. Comparer de tels dispositifs intègre un grand nombre de variables différentes (par exemple : âge, type de sol, disponibilité en eau, lumière, vent). Il est donc complexe d'attribuer ou de déterminer avec précision la contribution de chaque facteur. Néanmoins, une telle évaluation permet d'étudier un ensemble de facteurs et leur interaction pour avoir une vision globale. Bien sûr, nous étions loin de nous douter que les peupliers sous le traitement d'exclusion des pluies auraient une telle croissance, malgré la disponibilité en eau réduite. Rétrospectivement l'ajout d'un traitement témoin intermédiaire sur lequel nous aurions posé des bâches vertes identiques à celles posées sur le traitement d'exclusion des pluies nous aurait permis de séparer l'effet des bâches du reste de l'environnement pour l'analyser indépendamment. Définir les caractéristiques du sol et sa variabilité spatiale en amont de la plantation aurait également aidé à définir le design expérimental et l'interprétation des résultats.

Concernant les liens entre l'efficience d'utilisation de l'eau au niveau de la feuille et de la plante entière, nous avons remarqué que finalement peu d'effort se sont concentrés sur la quantification des gains et pertes en carbone et en eau indépendant des feuilles (respiration des tiges et des racines, assimilation photosynthétique et transpiration des tiges). Etudier la proportion de carbone destinée à la croissance en biomasse et à la séquestration, en comparant l'assimilation photosynthétique en carbone à la quantité de carbone dans la biomasse produite pendant une période donnée, aurait permis de préciser le lien entre l'assimilation photosynthétique et la production de biomasse. De plus, il aurait été possible de déconnecter l'intégration temporelle et spatiale de l'efficience de transpiration à l'aide de campagnes de mesures d'échanges gazeux foliaires plus conséquentes (mesures plus régulières, sous différentes conditions météorologiques, sur plusieurs orientations et étages foliaires). Bien que l'objectif fût d'étudier WUE dans une optique de sélection pour la production de bois, estimer la biomasse racinaire et l'interaction avec les micro-organismes auraient pu expliquer les différentes réponses à l'exclusion des pluies. L'exploration du sol par les racines s'est peut-être étendue au-delà du dispositif, cependant puisque l'arbre le plus excentré est situé à une distance de 5 et 6 mètres des bordures, l'analyse du système racinaire au-delà du dispositif aurait

nécessité un très lourd investissement. De plus, de nombreuses contraintes auraient limité l'intérêt d'une telle étude. Les racines fines responsables de la majorité de l'assimilation en eau sont particulièrement difficiles à examiner, et reconnaitre l'appartenance d'une racine fine observée à un arbre du dispositif (et non une espèce herbacée proche ou même un arbre de bordure) serait difficile à déterminer. Enfin, même s'il était possible de déterminer précisément la proportion de racines fines à l'intérieur et à l'extérieur du dispositif d'exclusion des pluies, évaluer leur absorption d'eau respective n'aurait pas été aisé.

2.3. Perspectives

Ces travaux de thèses devaient, à l'origine, aboutir à la modélisation de l'efficience d'utilisation de l'eau au niveau de la plante entière à partir de données d'échanges gazeux foliaires, de structure du houppier et de bilan hydrique à l'aide du modèle MAESPA. Ce modèle est en développement depuis le début des années 1970 (Medlyn, 2004), à l'origine utilisé pour calculer la température foliaire à partir du bilan radiatif et de l'architecture des houppiers afin d'optimiser l'arrangement de chaudières au fioul pour combattre les dommages liés au froid dans des vergers (Welles *et al.*, 1979; Norman & Welles, 1983). Le modèle aujourd'hui est le résultat de dizaines d'années de développement, intégrant à la fois l'interception des radiations solaires par le houppier en définissant individuellement son architecture (Grace *et al.*, 1987), l'assimilation et la transpiration foliaire par un modèle d'échanges gazeux couplé au modèle biochimique de Farquhar de la cinétique de la Rubisco (Farquhar *et al.*, 1980; Medlyn *et al.*, 2011; Duursma & Medlyn, 2012), et le bilan hydrique d'une parcelle à partir de l'intégration du modèle Soil-Plant-Atmosphere (Williams *et al.*, 1996; Williams *et al.*, 2001). Le modèle nécessite un effort soutenu de paramétrisation, dont la plupart ont été réalisé pendant cette thèse en vue de son utilisation, notamment à l'aide de télédétection par laser (lidar) pour définir l'architecture du houppier (par exemple : forme du houppier, orientation des feuilles, distribution de la proportion de surface foliaire en hauteur). Cependant, obtenir des résultats intéressants avec suffisamment de confiance aurait nécessité au minimum plusieurs mois de travail en plus pour paramétrer le modèle, analyser la sensibilité des paramètres, et valider les résultats sur un jeu de données additionnel. L'intérêt d'utiliser un tel modèle réside dans la possibilité d'étudier à chaque instant la variabilité spatiale de l'assimilation de CO_2, de la conductance stomatique et de l'efficience d'utilisation de l'eau intrinsèque foliaire avec les conditions microclimatiques. A partir de ce type de données de nombreuses applications sont possibles. Cela permettrait par exemple de mieux comprendre la variabilité de WUE lié à l'architecture de la plante (par exemple l'orientation et l'étage foliaire) et aux variables

microclimatiques (la quantité de lumière incidente reçue, l'humidité de l'air, la disponibilité de l'eau dans le sol) et comment cette diversité est intégrée dans l'efficience de transpiration à l'échelle de la plante entière (Medrano *et al.*, 2015). Relier WUE intrinsèque au niveau de la plante entière à l'efficience de transpiration pourrait ainsi permettre de déceler des motifs mettant en lumière de nouveaux déterminants liants ces processus. Par ailleurs, soustraire l'efficience intrinsèque foliaire de l'efficience de transpiration de la plante entière pourrait conduire à une estimation de WUE intrinsèque et indépendante des feuilles (c'est-à-dire la respiration des tiges, des racines et des fruits, la photosynthèse et la transpiration des tiges et des fruits) à partir des gains et pertes en carbone et en eau indépendant des feuilles. Ainsi, la mise à l'échelle de l'efficience d'utilisation de l'eau de la feuille à la plante entière ne se résumerait pas à considérer la plante entière comme un peuplement de feuilles.

Nous pourrions envisager également d'introduire un modèle dynamique d'échanges gazeux foliaires au modèle MAESPA, qui utilise actuellement un modèle de type Ball & Berry (Duursma & Medlyn, 2012), puisqu'un modèle dynamique semble produire un meilleur ajustement aux données observées (Fig. 4). Se faisant, il aurait été possible d'étudier non seulement la variabilité spatiale mais également temporelle de l'efficience d'utilisation de l'eau intrinsèque foliaire. Le modèle fonctionne avec une résolution temporelle de la minute au maximum, ce qui est suffisant pour observer le découplage de l'assimilation de CO_2 et de la conductance stomatique à la suite d'un changement environnemental. Par exemple lors du passage d'un nuage, la photosynthèse diminue instantanément alors que g_s est maintenue forte plusieurs minutes au cours de la fermeture stomatique. Inclure cette dynamique au sein du modèle MAESPA permettra de quantifier avec précision l'erreur attribuable à la dynamique stomatique de modèles fonctionnant en régime permanent. Un tel modèle pourrait servir de base à l'estimation, entre autre, des coûts énergétiques de l'ouverture des stomates, et de l'intérêt d'un suivi précis de l'environnement. Enfin, cela permettrait d'étudier la diversité des dynamiques stomatiques au sein du houppier. Tous ces éléments participent au développement des connaissances liés aux dynamiques stomatiques afin de quantifier au plus juste, la conductance stomatique observable en conditions naturelles.

Alternativement, le développement des techniques de télédétection, d'analyse d'images et de phénotypage à haut-débit permettent déjà une détermination de la photosynthèse (Porcar-Castell *et al.*, 2014). Dans certaines conditions, la conductance stomatique peut également être déterminée à partir de l'équation de balance énergétique de Penmann et Monteith (Vialet-Chabrand & Lawson, 2019), en lien fort avec la température foliaire. Une telle technique est

prometteuse et pourrait permettre à l'avenir de collecter rapidement un nombre considérable de données à utiliser en association avec les efforts de modélisation, par exemple comme jeux de données pour le paramétrage ou la validation de modèles.

Afin de mettre en lumière les déterminants des différentes réponses en serre et en pépinière, il serait peut-être judicieux d'établir des conditions intermédiaires, comme des chambres à ciel ouvert ou des plantes en pots élevées en conditions naturelles. Cela permettrait d'étudier plus spécifiquement l'interaction entre un jeu plus réduit de variables (fortes températures et forte irradiance, faible humidité atmosphérique et développement racinaire limité). Puisque la sécheresse est un stress complexe, la réponse physiologique est probablement variable selon la modalité du stress. Ainsi il est nécessaire de répliquer ces comparaisons pour différentes intensités, durées et vitesses d'établissement de la sécheresse. De plus, la répétition à long terme d'épisodes de déficit hydrique pourrait induire une acclimatation spécifique. Tous ces éléments contribueraient à définir des critères permettant de sélectionner des génotypes plus efficients dans leur utilisation de l'eau, à la fois lorsque la disponibilité en eau n'est pas limitante et lors d'épisodes de sécheresse.

RÉFÉRENCES

Aasamaa K, Sober A. 2011. Responses of stomatal conductance to simultaneous changes in two environmental factors. *Tree Physiology* **31**(8): 855-864.

Abramowitz G. 2005. Towards a benchmark for land surface models. *Geophysical Research Letters* **32**(22).

Baldocchi D, Falge E, Gu L, Olson R, Hollinger D, Running S, Anthoni P, Bernhofer C, Davis K, Evans R, et al. 2001. FLUXNET: A new tool to study the temporal and spatial variability of ecosystem-scale carbon dioxide, water vapor, and energy flux densities. *Bulletin of the American Meteorological Society* **82**(11): 2415-2434.

Bogeat-Triboulot MB, Buré C, Gérardin T, Chuste PA, Le Thiec D, Hummel I, Durand M, Wildhagen H, Douthe C, Molins A, et al. 2019. Additive effects of high growth rate and low transpiration rate drive differences in whole plant transpiration efficiency among black poplar genotypes. *Environmental and Experimental Botany* **In press**.

Brendel O, Le Thiec D, Scotti-Saintagne C, Bodenes C, Kremer A, Guehl JM. 2008. Quantitative trait loci controlling water use efficiency and related traits in Quercus robur L. *Tree Genetics & Genomes* **4**(2): 263-278.

Brendel O, Pot D, Plomion C, Rozenberg P, Guehl JM. 2002. Genetic parameters and QTL analysis of delta(13)C and ring width in maritime pine. *Plant Cell and Environment* **25**(8): 945-953.

Casasoli M, Pot D, Plomion C, Monteverdi MC, Barreneche T, Lauteri M, Villani F. 2004. Identification of QTLs affecting adaptive traits in Castanea sativa Mill. *Plant Cell and Environment* **27**(9): 1088-1101.

Cernusak LA, Hutley LB. 2011. Stable isotopes reveal the contribution of corticular photosynthesis to growth in branches of Eucalyptus miniata. *Plant Physiology* **155**(1): 515-523.

Cortes C, Vapnik V. 1995. Support-vector networks. *Machine Learning* **20**(3): 273-297.

Cowan IR, Farquhar GD. 1977. Stomatal function in relation to leaf metabolism and environment. *Symposia of the Society for Experimental Biology* **31**: 471-505.

Davies WJ, Kozlowski TT. 1975. Stomatal responses to changes in light intensity as influenced by plant water stress. *Forest Science* **21**(2): 129-133.

de Boer HJ, Price CA, Wagner-Cremer F, Dekker SC, Franks PJ, Veneklaas EJ. 2016. Optimal allocation of leaf epidermal area for gas exchange. *New Phytologist* **210**(4): 1219-1228.

Dow GJ, Berry JA, Bergmann DC. 2014. The physiological importance of developmental mechanisms that enforce proper stomatal spacing in Arabidopsis thaliana. *New Phytologist* **201**(4): 1205-1217.

Drucker H, J. C C, Kaufman L, Smola A, Vapnik V 1997. Support Vector Regression Machines. In: Mozer M. C., Jordan M. I., Petsche T. eds. *Advances in Neural Information Processing Systems 9*: MIT Press, 155--161.

Dufrêne E, Davi H, François C, Maire Gl, Dantec VL, Granier A. 2005. Modelling carbon and water cycles in a beech forest: Part I: Model description and uncertainty analysis on modelled NEE. *Ecological Modelling* **185**(2): 407-436.

Dumont J, Spicher F, Montpied P, Dizengremel P, Jolivet Y, Le Thiec D. 2013. Effects of ozone on stomatal responses to environmental parameters (blue light, red light, CO2 and vapour pressure deficit) in three Populus deltoides x Populus nigra genotypes. *Environmental Pollution* **173**: 85-96.

Duursma RA, Medlyn BE. 2012. MAESPA: a model to study interactions between water limitation, environmental drivers and vegetation function at tree and stand levels, with

an example application to CO2 x drought interactions. *Geoscientific Model Development* **5**(4): 919-940.

Elliott-Kingston C, Haworth M, Yearsley JM, Batke SP, Lawson T, McElwain JC. 2016. Does size matter? Atmospheric CO2 may be a stronger driver of stomatal closing rate than stomatal size in taxa that diversified under low CO2. *Frontiers in Plant Science* **7**.

Fanourakis D, Giday H, Milla R, Pieruschka R, Kjaer KH, Bolger M, Vasilevski A, Nunes-Nesi A, Fiorani F, Ottosen C-O. 2014. Pore size regulates operating stomatal conductance, while stomatal densities drive the partitioning of conductance between leaf sides. *Annals of Botany* **115**(4): 555-565.

Farquhar GD, Caemmerer SV, Berry JA. 1980. A biochemical model of photosynthetic CO2 assimilation in leaves of C3 species. *Planta* **149**(1): 78-90.

Franks PJ, Beerling DJ. 2009. Maximum leaf conductance driven by CO2 effects on stomatal size and density over geologic time. *Proceedings of the National Academy of Sciences of the United States of America* **106**(25): 10343-10347.

Franks PJ, Bonan GB, Berry JA, Lombardozzi DL, Holbrook NM, Herold N, Oleson KW. 2018. Comparing optimal and empirical stomatal conductance models for application in Earth system models. *Global Change Biology* **24**(12): 5708-5723.

Franks PJ, Buckley TN, Shope JC, Mott KA. 2001. Guard cell volume and pressure measured concurrently by confocal microscopy and the cell pressure probe. *Plant Physiology* **125**(4): 1577-1584.

Galatis B, Apostolakos P, Katsaros C. 1983. Microtubules and their organizing centres in differentiating guard cells of Adiantum capillus veneris. *Protoplasma* **115**(2): 176-192.

Grace JC, Jarvis PG, Norman JM. 1987. Modelling the interception of solar radiant energy in intensively managed stands. *New Zealand Journal of Forestry Science* **17**(2-3): 193-209.

Haworth M, Marino G, Cosentino SL, Brunetti C, De Carlo A, Avola G, Riggi E, Loreto F, Centritto M. 2018. Increased free abscisic acid during drought enhances stomatal sensitivity and modifies stomatal behaviour in fast growing giant reed (Arundo donax L.). *Environmental and Experimental Botany* **147**: 116-124.

Hills A, Chen Z-H, Amtmann A, Blatt MR, Lew VL. 2012. OnGuard, a computational platform for quantitative kinetic modeling of guard cell physiology. *Plant Physiology* **159**(3): 1026-1042.

IPCC. 2014. Meyer L, Brinkman S, van Kesteren L, Leprince-Ringuet N, van Boxmeer F, eds. *Climate change 2014: Synthesis report. Contribution of working groups I, II and III to the fifth assessment report of the intergovernmental panel on climate change*. Geneva, Switzerland: Cambridge University Press.

Isebrands JG, Richardson J. 2014. *Poplars and willows : trees for society and the environment*. Boston, Rome CABI and FAO.

Kardiman R, Ræbild A. 2018. Relationship between stomatal density, size and speed of opening in Sumatran rainforest species. *Tree Physiology* **38**(5): 696-705.

Krinner G, Viovy N, de Noblet-Ducoudré N, Ogée J, Polcher J, Friedlingstein P, Ciais P, Sitch S, Prentice IC. 2005. A dynamic global vegetation model for studies of the coupled atmosphere-biosphere system. *Global Biogeochemical Cycles* **19**(1).

Lawson T, Oxborough K, Morison JIL, Baker NR. 2002. Responses of photosynthetic electron transport in stomatal guard cells and mesophyll cells in intact leaves to light, CO2, and humidity. *Plant Physiology* **128**(1): 52-62.

Marguerit E, Bouffier L, Chancerel E, Costa P, Lagane F, Guehl JM, Plomion C, Brendel O. 2014. The genetics of water-use efficiency and its relation to growth in maritime pine. *Journal of Experimental Botany* **65**(17): 4757-4768.

Matthews JSA, Vialet-Chabrand SRM, Lawson T. 2017. Diurnal variation in gas exchange: the balance between carbon fixation and water loss. *Plant Physiology* **174**(2): 614-623.

Mc Ausland L, Vialet-Chabrand S, Davey P, Baker NR, Brendel O, Lawson T. 2016. Effects of kinetics of light-induced stomatal responses on photosynthesis and water-use efficiency. *New Phytologist* **211**(4): 1209-1220.

Medlyn B. 2004. *A MAESTRO retrospective*.

Medlyn BE, Duursma RA, Eamus D, Ellsworth DS, Prentice IC, Barton CVM, Crous KY, de Angelis P, Freeman M, Wingate L. 2011. Reconciling the optimal and empirical approaches to modelling stomatal conductance. *Global Change Biology* **17**(6): 2134-2144.

Medrano H, Tomas M, Martorell S, Flexas J, Hernandez E, Rossello J, Pou A, Escalona JM, Bota J. 2015. From leaf to whole-plant water use efficiency (WUE) in complex canopies: Limitations of leaf WUE as a selection target. *Crop Journal* **3**(3): 220-228.

Ministère de l'agriculture et de l'alimentation. 2019. Le gouvernement annonce la généralisation des projets de territoire pour la gestion de l'eau. [WWW document] https://agriculture.gouv.fr/le-gouvernement-annonce-la-generalisation-des-projets-de-territoire-pour-la-gestion-de-leau, accessed June 12 2019.

Ministère de la transition écologique et solidaire. 2016. Gérer la sécheresse. [WWW document] https://www.ecologique-solidaire.gouv.fr/gerer-secheresse, Accessed June 6 2019.

Mott KA, Cardon ZG, Berry JA. 1993. Asymmetric patchy stomatal closure for the 2 surfaces of Xanthium strumarium leaves at low humidity. *Plant Cell and Environment* **16**(1): 25-34.

Norman JM, Welles JM. 1983. Radiative-transfert in an array of canopies. *Agronomy Journal* **75**(3): 481-488.

Oxborough K, Baker NR. 1997. An instrument capable of imaging chlorophyll a fluorescence from intact leaves at very low irradiance and at cellular and subcellular levels of organization. *Plant, Cell & Environment* **20**(12): 1473-1483.

Peak D, Mott KA. 2011. A new, vapour-phase mechanism for stomatal responses to humidity and temperature. *Plant Cell and Environment* **34**(1): 162-178.

Porcar-Castell A, Tyystjarvi E, Atherton J, van der Tol C, Flexas J, Pfundel EE, Moreno J, Frankenberg C, Berry JA. 2014. Linking chlorophyll a fluorescence to photosynthesis for remote sensing applications: mechanisms and challenges. *Journal of Experimental Botany* **65**(15): 4065-4095.

Richardson F, Brodribb TJ, Jordan GJ. 2017. Amphistomatic leaf surfaces independently regulate gas exchange in response to variations in evaporative demand. *Tree Physiology* **37**(7): 869-878.

Roth-Nebelsick A, Grein M, Utescher T, Konrad W. 2012. Stomatal pore length change in leaves of Eotrigonobalanus furcinervis (Fagaceae) from the Late Eocene to the Latest Oligocene and its impact on gas exchange and CO2 reconstruction. *Review of Palaeobotany and Palynology* **174**: 106-112.

Sheriff DW. 1979. Water-vapor and heat-transfer in leaves. *Annals of Botany* **43**(2): 157-171.

Vialet-Chabrand S, Brendel O. 2014. Automatic measurement of stomatal density from microphotographs. *Trees-Structure and Function* **28**(6): 1859-1865.

Vialet-Chabrand S, Dreyer E, Brendel O. 2013. Performance of a new dynamic model for predicting diurnal time courses of stomatal conductance at the leaf level. *Plant Cell and Environment* **36**(8): 1529-1546.

Vialet-Chabrand S, Lawson T. 2019. Dynamic leaf energy balance: deriving stomatal conductance from thermal imaging in a dynamic environment. *Journal of Experimental Botany* **70**(10): 2839-2855.

Vialet-Chabrand S, Matthews JSA, Brendel O, Blatt MR, Wang Y, Hills A, Griffiths H, Rogers S, Lawson T. 2016. Modelling water use efficiency in a dynamic environment: An example using Arabidopsis thaliana. *Plant Science* **251**: 65-74.

Viger M, Rodriguez-Acosta M, Rae AM, Morison JIL, Taylor G. 2013. Toward improved drought tolerance in bioenergy crops: QTL for carbon isotope composition and stomatal conductance in Populus. *Food and Energy Security* **2**(3): 220-236.

Viola P, Jones MJ. 2004. Robust real-time face detection. *International Journal of Computer Vision* **57**(2): 137-154.

Welles J, Norman J, Martsolf JD. 1979. Orchard foliage temperature model. *Journal American Society for Horticultural Science* **104:5**.

Williams M, Law BE, Anthoni PM, Unsworth MH. 2001. Use of a simulation model and ecosystem flux data to examine carbon-water interactions in ponderosa pine. *Tree Physiology* **21**(5): 287-298.

Williams M, Rastetter EB, Fernandes DN, Goulden ML, Wofsy SC, Shaver GR, Melillo JM, Munger JW, Fan SM, Nadelhoffer KJ. 1996. Modelling the soil-plant-atmosphere continuum in a Quercus-Acer stand at Harvard forest: The regulation of stomatal conductance by light, nitrogen and soil/plant hydraulic properties. *Plant Cell and Environment* **19**(8): 911-927.

ANNEXES

Annexe 1. Production scientifique et technique réalisée pendant la thèse.

Publications

Durand, M., Brendel, O., Buré, C., & Le Thiec, D. (2019). Altered stomatal dynamics induced by changes in irradiance and vapour-pressure deficit under drought: impact on the whole plant transpiration efficiency of poplar genotypes. *New Phytologist*, 222: 1789-1802. doi:10.1111/nph.15710

Bogeat-Triboulot MB, Buré C, Gerardin T, Chuste PA, Le Thiec D, Hummel I, **Durand M**, Wildhagen H, Douthe C, Molins A, Galmés J, Smith HK, Flexas J, Polle A, Taylor G and Brendel O. (2019). Additive effects of high growth rate and low transpiration rate drive differences in whole plant transpiration efficiency among black poplar genotypes. *Environmental and Experimental Botany*. doi: 10.1016/j.envexpbot.2019.05.021

Durand, M., Cohen, D., Aubry, N., Buré, C., Tomáškova, I., Hummel, I., Brendel, O. & Le Thiec, D. Element content and candidate gene expression in guard cells are connected to spatiotemporal variations in stomatal conductance. *Submitted to Plant, Cell & Environment.*

Durand, M., Brendel, O., Buré, C., Courtois, P., Lily, J.C., Granier, A & Le Thiec, D. Leaf-level and whole-plant water-use efficiency under drought: do results reached in controlled conditions still hold in natural environments? *In preparation for Agricultural and Forest Meteorology.*

Durand, M., Brendel, O., Buré, C., & Le Thiec, D. Impacts of growing conditions on the stability of stomatal dynamics induced by changes in irradiance and vapour-pressure deficit under drought. *In preparation.*

Durand, M., Rose, C., Dupouey, J-L., Legout, A., & Ponton, S. Do tree rings record changes in soil fertility? Results from a *Quercus petraea* fertilization trial. *Submitted to Science of the Total Environment.*

Conférences

Durand M, Brendel O. et Le Thiec D. 2018. Altered stomatal dynamics induced by changes in irradiance and vapour-pressure deficit under drought: impact on the whole plant transpiration efficiency of poplar genotypes. *IUFRO seventh international poplar symposium*. 3 novembre 2018, Buenos Aires, Argentina. Présentation orale en anglais.

Durand M, Brendel O. et Le Thiec D. 2017. Physiological, anatomical and molecular determinisms of water use efficiency linked to drought response in poplars: from leaf level to the whole plant scale. *IUFRO 125th anniversary. Symposium on water use efficiency in forest trees under drought.* 18 septembre 2017, Nancy, France. Présentation orale en anglais.

Le Thiec D, **Durand M.** 2017. Présentation de résultats expérimentals conduits au cours du projet Up-Trans financé par le LabEx ARBRE. *Colloque Annuel du LabEx ARBRE*. 13 décembre 2017, Nancy, France. Présentation orale en français.

Durand M, Brendel O. et Le Thiec D. 2016 et 2017. Physiological, anatomical and molecular determinisms of water use efficiency linked to drought response in poplars: from leaf level to the whole plant scale. Journée des doctorants et post-doctorant de l'UMR « Ecologie et Ecophysiologie forestières ». 5 juillet 2016 et 27 juin 2017, Champenoux. Présentation orale en français.

Posters

Durand M, Brendel O. et Le Thiec D. 2018. Altered dynamics of irradiance and VPD induced stomatal response under drought: variability, causes and impact on the whole plant transpiration efficiency of poplar species. *Séminaire annuel RP2E.* 13 février 2018, Nancy. Poster.

Durand M, Brendel O. et Le Thiec D. 2016. Upscaling morphological, physiological and molecular determinisms of transpiration from the leaf level to water use at the whole plant level in poplar trees. *Plant Environment Physiology Group.* 12-16 septembre 2016, Lisbonne. Poster.

Durand M, Brendel O. et Le Thiec D. 2015. Upscaling morphological, physiological and molecular determinisms of transpiration from the leaf level to water use at the whole plant level in poplar trees. *Colloque Annuel du LabEx ARBRE.* 16-17 novembre 2015, Champenoux. Poster.

Autres communications

Bogeat-Triboulot MB et **Durand M.** 2016. Présentation des robots Castor & Pollux. *Journées porte-ouvertes du centre INRA Champenoux.* 21 mai 2016, Champenoux.

Enseignement

64 heures d'enseignement en vacations pour des licences 2 et 3. (2018) :

- TP Licence 2 : Effet de l'auxine sur la croissance des végétaux (6h).
- TP Licence 2 : Induction de l'α-amylase par l'acide gibbérellique au cours de la germination (6h).
- TP Licence 3 : Reconnaissance d'espèces arborées locales (2h).

88 heures d'enseignement pendant un contrat d'attaché temporaire d'enseignement et de recherche à la fin de mon contrat de thèse pour des licences 1 et 2 et des masters 1 (2018-2019) :

- TD Master 1 : Modèle linéaire - ANOVA à deux facteurs : théorie et application sur R
- TD Licence 2 : Dormance et germination des graines (4h)
- TP Licence 2 : Effet de l'auxine sur la croissance des végétaux (6h).
- TP Licence 2 : Induction de l'α-amylase par l'acide gibbérellique au cours de la germination (6h).
- TP Licence 1 : Structure et fonction des parois, plastes et vacuoles (6h)
- TP et TD Licence 1: Projet professionnel professionalisant (orientation professionnelle, 10h)

Formations

Ecole d'été sur les mesures d'échanges gazeux : Plant Environmental Physiology Group (PEPG) Techniques Workshop, 12-16 septembre 2016, Lisbonne, Portugal.

Résidentiel pour doctorants contractuels chargés d'enseignement : Préparer un cours, l'animer et évaluer les acquis : formation à la pédagogie universitaire, 8-12 janvier 2018, St Dié-des-Vosges, France.

Utilisation avancée de Microsoft Excel et Visual Basic pour la résolution de problèmes scientifiques, 26-28 mars 2018, Nancy, France.

Visite à l'Institut Hawkesbury pour l'Environment dans le cadre de la modélisation des échanges gazeux au niveau de la plante entière, paramétrisation, fonctionnement et limitations du modèle MAESPA, Hawkesbury Institute for the Environment, Université de Sydney Ouest, 16 janvier au 20 février 2017, Richmond, NSW, Australie.

Encadrement

Encadrement de 3 Masters 1 pendant 2 mois :

Emmanuelle Ha (2016) : Suivi de la croissance et des échanges gazeux foliaires de deux génotypes de peupliers noirs et deux génotypes de peupliers euraméricains en pépinière, en réponse à la sécheresse.

Marietou Diouf (2016) : Suivi de la croissance et des échanges gazeux foliaires de deux génotypes de peupliers noirs et de deux génotypes de peupliers euraméricains cultivés en serre, en réponse à la sécheresse.

Fabrice Petel (2017) : Suivi de la croissance et établissement d'allométries de quatre génotypes de peupliers en pépinière en réponse à la sécheresse.

Co-encadrement de contrats courts à durée variable :

CDD : Thibaud Salier (5 mois)

CDD : Lucie Le Thiec (2 semaines)

CDD : Basile Le Thiec (6 semaines)

CDD : Flore Pellegrini (1 mois)

CDD : Antoine Bogeat (1 mois)

CDD : Déborah Thevenin (2 mois)

CDD : Hugo Nègre (2 mois)

Stage L3 : Julien Morville (3 semaines)

Stage L3 : Clément Rieux (3 semaines)

Visite : Dr. Ivana Tomaskova (3 mois)

Développement

- Développement d'un package R pour l'analyse de donnée de flux de sève à partir de sondes de type Granier :

  Durand M. (2016). TDPanalysis: Granier's Sap Flow Sensors (TDP) Analysis. R package version 0.99. URL : https://CRAN.R-project.org/package=TDPanalysis

- Développement d'un algorithme classificateur en cascade d'apprentissage supervisé à partir de caractéristiques de Haar pour la reconnaissance et le comptage automatique de stomates de peupliers.

Annexe 2. Analyse statistique utilisé pendant la thèse.

Toutes les analyses statistiques ont été réalisées à l'aide du logiciel R (R Core Team, 2019). Les analyses de variance de type 2 ont été réalisées à l'aide du packages « car » (fonction Anova) et les tests *post-hoc* à l'aide du package « emmeans » (fonction « CLD(emmeans()) ») en utilisant une correction de type FDR. Les analyses de variance avec un design répété (par example, Chapitre I, Fig. 1 et 2) ont été réalisées à partir de la fonction « aov_ez » du package « afex ». Les analyses de co-variances (par example, Chapitre I, Fig. 5 et 6) ont été réalisées à l'aide de la fonction « lm » du package « stat » de base afin de prendre en compte l'effet traitement (variable catégorielle) avant la variable numérique. Les analyses en composantes principales ont été réalisées à l'aide des packages « FactoMineR » et « factoextra » en utilisant la fonction « PCA ».

RÉFÉRENCES

Aasamaa K, Sober A. 2011. Responses of stomatal conductance to simultaneous changes in two environmental factors. *Tree Physiology* **31**(8): 855-864.

Abramowitz G. 2005. Towards a benchmark for land surface models. *Geophysical Research Letters* **32**(22).

Al Afas N, Marron N, Ceulemans R. 2006. Clonal variation in stomatal characteristics related to biomass production of 12 poplar (Populus) clones in a short rotation coppice culture. *Environmental and Experimental Botany* **58**(1-3): 279-286.

Allen CD, Breshears DD, McDowell NG. 2015. On underestimation of global vulnerability to tree mortality and forest die-off from hotter drought in the Anthropocene. *Ecosphere* **6**(8): 55.

Allen CD, Macalady AK, Chenchouni H, Bachelet D, McDowell N, Vennetier M, Kitzberger T, Rigling A, Breshears DD, Hogg EH, et al. 2010. A global overview of drought and heat-induced tree mortality reveals emerging climate change risks for forests. *Forest Ecology and Management* **259**(4): 660-684.

Anyia AO, Slaski JJ, Nyachiro JM, Archambault DJ, Juskiw P. 2007. Relationship of carbon isotope discrimination to water use efficiency and productivity of barley under field and greenhouse conditions. *Journal of Agronomy and Crop Science* **193**(5): 313-323.

Aphalo PJ, Jarvis PG. 1991. Do stomata respond to relative humidity? *Plant, Cell & Environment* **14**(1): 127-132.

Aphalo PJ, Jarvis PG. 1993a. An analysis of Ball's empirical-model of stomatal conductance. *Annals of Botany* **72**(4): 321-327.

Aphalo PJ, Jarvis PG. 1993b. The boundary-layer and the apparent responses of stomatal conductance to wind-speed and to the mole fractions of CO2 and water-vapor in the air. *Plant Cell and Environment* **16**(7): 771-783.

Assmann SM. 1988. Enhancement of the stomatal response to blue light by red light, reduced intercellular concentrations of CO2, and low vapor pressure differences. *Plant Physiology* **87**(1): 226-231.

Assmann SM, Snyder JA, Lee YRJ. 2000. ABA-deficient (aba1) and ABA-insensitive (abi1-1, abi2-1) mutants of Arabidopsis have a wild-type stomatal response to humidity. *Plant Cell and Environment* **23**(4): 387-395.

Baldocchi D, Falge E, Gu L, Olson R, Hollinger D, Running S, Anthoni P, Bernhofer C, Davis K, Evans R, et al. 2001. FLUXNET: A new tool to study the temporal and spatial variability of ecosystem-scale carbon dioxide, water vapor, and energy flux densities. *Bulletin of the American Meteorological Society* **82**(11): 2415-2434.

Ball JT, Woodrow I, Berry J 1987. A model predicting stomatal conductance and its contribution to the control of photosynthesis under different environmental conditions. In: Biggins J ed. *Progress in Photosynthesis Research*: Springer Netherlands, 221-224.

Barradas VL, Jones HG, Clark JA. 1994. Stomatal responses to changing irradiance in Phaseolus vulgaris L. *Journal of Experimental Botany* **45**(7): 931-936.

Bauer H, Ache P, Lautner S, Fromm J, Hartung W, Al-Rasheid KAS, Sonnewald S, Sonnewald U, Kneitz S, Lachmann N, et al. 2013. The stomatal response to reduced relative humidity requires guard cell-autonomous ABA synthesis. *Current Biology* **23**(1): 53-57.

Berger D, Altmann T. 2000. A subtilisin-like serine protease involved in the regulation of stomatal density and distribution in Arabidopsis thaliana. *Genes & Development* **14**(9): 1119-1131.

Bernacchi CJ, Singsaas EL, Pimentel C, Portis AR, Long SP. 2001. Improved temperature response functions for models of Rubisco-limited photosynthesis. *Plant Cell & Environment* **24**(2): 253-259.

Block RMA, Rees KCJ, Knight JD. 2006. A review of fine root dynamics in Populus plantations. *Agroforestry Systems* **67**(1): 73-84.

Bobich EG, Barron-Gafford GA, Rascher KG, Murthy R. 2010. Effects of drought and changes in vapour pressure deficit on water relations of Populus deltoides growing in ambient and elevated CO2. *Tree Physiology* **30**(7): 866-875.

Bogeat-Triboulot MB, Buré C, Gérardin T, Chuste PA, Le Thiec D, Hummel I, Durand M, Wildhagen H, Douthe C, Molins A, et al. 2019. Additive effects of high growth rate and low transpiration rate drive differences in whole plant transpiration efficiency among black poplar genotypes. *Environmental and Experimental Botany* **In press**.

Bonal D, Ponton S, Le Thiec D, Richard B, Ningre N, Hérault B, Ogée J, Gonzalez S, Pignal M, Sabatier D, et al. 2011. Leaf functional response to increasing atmospheric CO2 concentrations over the last century in two northern Amazonian tree species: a historical δ13C and δ18O approach using herbarium samples. *Plant, Cell & Environment* **34**(8): 1332-1344.

Bonan GB. 2008. Forests and climate change: forcings, feedbacks, and the climate benefits of forests. *Science* **320**(5882): 1444-1449.

Bowling DR, Pataki DE, Randerson JT. 2008. Carbon isotopes in terrestrial ecosystem pools and CO2 fluxes. *New Phytologist* **178**(1): 24-40.

Brendel O, Le Thiec D, Scotti-Saintagne C, Bodenes C, Kremer A, Guehl JM. 2008. Quantitative trait loci controlling water use efficiency and related traits in Quercus robur L. *Tree Genetics & Genomes* **4**(2): 263-278.

Brendel O, Pot D, Plomion C, Rozenberg P, Guehl JM. 2002. Genetic parameters and QTL analysis of delta(13)C and ring width in maritime pine. *Plant Cell and Environment* **25**(8): 945-953.

Brodribb TJ, Cochard H. 2009. Hydraulic failure defines the recovery and point of death in water-stressed conifers. *Plant Physiology* **149**(1): 575-584.

Brown HT, Escombe F. 1900. Static diffusion of gases and liquids in relation to the assimilation of carbon and translocation in plants. *Annals of Botany* **14**(3): 537-542.

Brownlee C. 2001. The long and the short of stomatal density signals. *Trends in Plant Science* **6**(10): 441-442.

Brugnoli E, Farquhar GD 2000. Photosynthetic fractionation of carbon isotopes. In: Leegood RC, Sharkey TD, von Caemmerer S eds. *Photosynthesis: physiology and metabolism.* . Dordrecht: Kluwer Academic Publishers, 399-434.

Brugnoli E, Hubick KT, von Caemmerer S, Wong SC, Farquhar GD. 1988. Correlation between the carbon isotope discrimination in leaf starch and sugars of C3 plants and the ratio of intercellular and atmospheric partial pressures of carbon dioxide. *Plant Physiology* **88**(4): 1418-1424.

Buckley TN. 2005. The control of stomata by water balance. *New Phytologist* **168**(2): 275-291.

Bunce JA. 1988. Nonstomatal inhibition of photosynthesis by water stress. Reduction in photosynthesis at high transpiration rate without stomatal closure in field-grown tomato. *Photosynthesis Research* **18**(3): 357-362.

Campany CE, Tjoelker MG, von Caemmerer S, Duursma RA. 2016. Coupled response of stomatal and mesophyll conductance to light enhances photosynthesis of shade leaves under sunflecks. *Plant Cell & Environment* **39**(12): 2762-2773.

Casasoli M, Pot D, Plomion C, Monteverdi MC, Barreneche T, Lauteri M, Villani F. 2004. Identification of QTLs affecting adaptive traits in Castanea sativa Mill. *Plant Cell and Environment* **27**(9): 1088-1101.

Cernusak LA, Hutley LB. 2011. Stable isotopes reveal the contribution of corticular photosynthesis to growth in branches of Eucalyptus miniata. *Plant Physiology* **155**(1): 515-523.

Cernusak LA, Winter K, Aranda J, Turner BL, Marshall JD. 2007. Transpiration efficiency of a tropical pioneer tree (Ficus insipida) in relation to soil fertility. *Journal of Experimental Botany* **58**(13): 3549-3566.

Ceulemans R, Praet L, Jiang XN. 1995. Effects of CO2 enrichment, leaf position and clone on stomatal index and epidermal cell density in poplar (Populus). *New Phytologist* **131**(1): 99-107.

Chamaillard S. 2011. *Efficience d'utilisation de l'eau chez le peuplier noir (Populus nigra L.) : variabilité et plasticité en réponse aux variations de l'environnement* PhD, Université d'Orléans Orléans.

Chen SL, Wang SS, Altman A, Huttermann A. 1997. Genotypic variation in drought tolerance of poplar in relation to abscisic acid. *Tree Physiology* **17**(12): 797-803.

Chevuturi A, Klingaman NP, Turner AG, Hannah S. 2018. Projected changes in the Asian-Australian monsoon region in 1.5°C and 2.0°C global-warming scenarios. *Earth's Future* **6**(3): 339-358.

Ciais P, Reichstein M, Viovy N, Granier A, Ogee J, Allard V, Aubinet M, Buchmann N, Bernhofer C, Carrara A, et al. 2005. Europe-wide reduction in primary productivity caused by the heat and drought in 2003. *Nature* **437**(7058): 529-533.

Collinson ME. 1992. The early fossil record of the Saliceae. *Proceedings of the Royal Society of Edinburgh* **98B**: 155-167.

Condon AG, Richards RA, Rebetzke GJ, Farquhar GD. 2004. Breeding for high water-use efficiency. *Journal of Experimental Botany* **55**(407): 2447-2460.

Coopman RE, Jara JC, Bravo LA, Sáez KL, Mella GR, Escobar R. 2008. Changes in morpho-physiological attributes of Eucalyptus globulus plants in response to different drought hardening treatments. *Electronic Journal of Biotechnology* **11**(2): 30-39.

Cortes C, Vapnik V. 1995. Support-vector networks. *Machine Learning* **20**(3): 273-297.

Cowan IR, Farquhar GD. 1977. Stomatal function in relation to leaf metabolism and environment. *Symposia of the Society for Experimental Biology* **31**: 471-505.

Cruiziat P, Cochard H, Améglio T. 2002. Hydraulic architecture of trees: main concepts and results. *Ann. For. Sci.* **59**(7): 723-752.

Dai A. 2012. Increasing drought under global warming in observations and models. *Nature Climate Change* **3**: 52.

Dai AG. 2011. Drought under global warming: a review. *Wiley Interdisciplinary Reviews-Climate Change* **2**(1): 45-65.

Damour G, Simonneau T, Cochard H, Urban L. 2010. An overview of models of stomatal conductance at the leaf level. *Plant Cell and Environment* **33**(9): 1419-1438.

Davies WJ, Kozlowski TT. 1975. Stomatal responses to changes in light intensity as influenced by plant water stress. *Forest Science* **21**(2): 129-133.

Davies WJ, Zhang JH. 1991. Root signals and the regulation of growth and development of plants in drying soil. *Annual Review of Plant Physiology and Plant Molecular Biology* **42**: 55-76.

de Boer HJ, Price CA, Wagner-Cremer F, Dekker SC, Franks PJ, Veneklaas EJ. 2016. Optimal allocation of leaf epidermal area for gas exchange. *New Phytologist* **210**(4): 1219-1228.

de Dios VR. 2017. Circadian regulation and diurnal variation in gas exchange. *Plant Physiology* **175**(1): 3-4.

de Rigo D, Enescu C, Houston Durrant T, Caudullo G 2016. Populus nigra in Europe: distribution, habitat, usage and threats. In: San-Miguel-Ayanz J, de Rigo D, Caudullo G, Houston Durrant T, Mauri A eds. *European Atlas of Forest Tree Species*. Luxembourg: Publication Office of the European Union.

Devi MJ, Bhatnagar-Mathur P, Sharma KK, Serraj R, Anwar SY, Vadez V. 2011. Relationships between transpiration efficiency and its surrogate traits in the rd29A:DREB1A transgenic lines of groundnut. *Journal of Agronomy and Crop Science* **197**(4): 272-283.

DeVoto B. 1997. *The journals of Lewis and Clark.* New York: Houghton Mifflin Company.
Di Baccio D, Minnocci A, Sebastiani L. 2010. Leaf structural modifications in Populus × euramericana subjected to Zn excess. *Biologia Plantarum* **54**(3): 502-508.
Dickmann DI. 2006. Silviculture and biology of short-rotation woody crops in temperate regions: then and now. *Biomass and Bioenergy* **30**(696-705).
Dixon HH, Joly J. 1895. On the ascent of sap. *Philosophical Transactions of the Royal Society of London. B* **186**: 563-576.
Dodd IC. 2005. Root-to-shoot signalling: assessing the roles of 'up' in the up and down world of long-distance signalling in planta. *Plant and Soil* **274**(1-2): 251-270.
Dow GJ, Berry JA, Bergmann DC. 2014. The physiological importance of developmental mechanisms that enforce proper stomatal spacing in Arabidopsis thaliana. *New Phytologist* **201**(4): 1205-1217.
Drake PL, Froend RH, Franks PJ. 2013. Smaller, faster stomata: scaling of stomatal size, rate of response, and stomatal conductance. *Journal of Experimental Botany* **64**(2): 495-505.
Drucker H, J. C C, Kaufman L, Smola A, Vapnik V 1997. Support Vector Regression Machines. In: Mozer M. C., Jordan M. I., Petsche T. eds. *Advances in Neural Information Processing Systems 9*: MIT Press, 155--161.
Du Puy S, Derrière N, Wurpillot S. 2017. IGN, ed. *La forêt plantée en France: état des lieux*. La feuille de l'inventaire forestier: Institut natianal de l'information géographique et forestière.
Dufrêne E, Davi H, François C, Maire Gl, Dantec VL, Granier A. 2005. Modelling carbon and water cycles in a beech forest: Part I: Model description and uncertainty analysis on modelled NEE. *Ecological Modelling* **185**(2): 407-436.
Dumont J, Spicher F, Montpied P, Dizengremel P, Jolivet Y, Le Thiec D. 2013. Effects of ozone on stomatal responses to environmental parameters (blue light, red light, CO2 and vapour pressure deficit) in three Populus deltoides x Populus nigra genotypes. *Environmental Pollution* **173**: 85-96.
Durand M, Brendel O, Buré C, Le Thiec D. 2019. Altered stomatal dynamics induced by changes in irradiance and vapour-pressure deficit under drought: impact on the whole plant transpiration efficiency of poplar genotypes. *New Phytologist* **222**: 1789-1802.
Duursma RA. 2015. Plantecophys - An R package for analysing and modelling leaf gas exchange data. *Plos One* **10**(11).
Duursma RA, Medlyn BE. 2012. MAESPA: a model to study interactions between water limitation, environmental drivers and vegetation function at tree and stand levels, with an example application to CO2 x drought interactions. *Geoscientific Model Development* **5**(4): 919-940.
Ehdaie B, Hall AE, Farquhar GD, Nguyen HT, Waines JG. 1991. Water-use efficiency and carbon isotope discrimination in Wheat. *Crop Science* **31**(5): 1282-1288.
Ehdaie B, Waines JG. 1993. Variation in water-use efficiency and its components in Wheat .1. Well-watered pot experiment. *Crop Science* **33**(2): 294-299.
Elliott-Kingston C, Haworth M, Yearsley JM, Batke SP, Lawson T, McElwain JC. 2016. Does size matter? Atmospheric CO2 may be a stronger driver of stomatal closing rate than stomatal size in taxa that diversified under low CO2. *Frontiers in Plant Science* **7**.
Etzold S, Ziemińska K, Rohner B, Bottero A, Bose AK, Ruehr NK, Zingg A, Rigling A. 2019. One century of forest monitoring data in Switzerland reveals species- and site-specific trends of climate-induced tree mortality. *Frontiers in Plant Science* **10**(307).
Fanourakis D, Giday H, Milla R, Pieruschka R, Kjaer KH, Bolger M, Vasilevski A, Nunes-Nesi A, Fiorani F, Ottosen C-O. 2014. Pore size regulates operating stomatal conductance, while stomatal densities drive the partitioning of conductance between leaf sides. *Annals of Botany* **115**(4): 555-565.
FAO. 1958. nations Faaootu, ed. *Poplars in forestry and land use*. Rome.

FAO. 2012. Forest Assessment MaCD, ed. *Improving lives with poplars and willows. Synthesis of country progress reports. 24th session of the international poplar commission, Dehradun, India, 30 Oct-2 Nov 2012. Working Paper IPC/12.* Rome: FAO.

FAO. 2018. Muller E, Kushlin A, Linhares-Juvenal T, Muchoney D, Wertz-Kanounnikoff S, Henderson-Howat D, eds. *The state of the world's forests*. Rome, Italy.

Farquhar GD, Buckley T, Miller J. 2002. Optimal stomatal control in relation to leaf area and nitrogen content. *Silva Fennica* **36**(3).

Farquhar GD, Caemmerer SV, Berry JA. 1980. A biochemical model of photosynthetic CO2 assimilation in leaves of C3 species. *Planta* **149**(1): 78-90.

Farquhar GD, Dubbe DR, Raschke K. 1978. Gain of feedback loop involving carbon dioxide and stomata - Theory and measurement. *Plant Physiology* **62**(3): 406-412.

Farquhar GD, Ehleringer JR, Hubick KT. 1989. Carbon isotope discrimination and photosynthesis. *Annual Review of Plant Physiology and Plant Molecular Biology* **40**: 503-537.

Farquhar GD, O'Leary MHO, Berry J. 1982. On the relationship between carbon isotope discrimination and the intercellular carbon dioxide concentration in leaves. *Australian Journal of Plant Physiology* **9**: 121-137.

Farquhar GD, Richards RA. 1984. Isotopic composition of plant carbon correlates with water-use efficiency of wheat genotypes. *Functional Plant Biology* **11**(6): 539-552.

Fortier J, Truax B, Gagnon D, Lambert F. 2015. Plastic allometry in coarse root biomass of mature hybrid poplar plantations. *Bioenergy Research* **8**(4): 1691-1704.

Frank AB, Barker RE, Berdahl JD. 1987. Water-use efficiency of grasses grown under controlled and field conditions. *Agronomy Journal* **79**.

Franks PJ, Beerling DJ. 2009. Maximum leaf conductance driven by CO2 effects on stomatal size and density over geologic time. *Proceedings of the National Academy of Sciences of the United States of America* **106**(25): 10343-10347.

Franks PJ, Bonan GB, Berry JA, Lombardozzi DL, Holbrook NM, Herold N, Oleson KW. 2018. Comparing optimal and empirical stomatal conductance models for application in Earth system models. *Global Change Biology* **24**(12): 5708-5723.

Franks PJ, Buckley TN, Shope JC, Mott KA. 2001. Guard cell volume and pressure measured concurrently by confocal microscopy and the cell pressure probe. *Plant Physiology* **125**(4): 1577-1584.

Franks PJ, Cowan IR, Farquhar GD. 1998. A study of stomatal mechanics using the cell pressure probe. *Plant, Cell & Environment* **21**(1): 94-100.

Franks PJ, Farquhar GD. 2001. The effect of exogenous abscisic acid on stomatal development, stomatal mechanics, and leaf gas exchange in Tradescantia virginiana. *Plant Physiology* **125**(2): 935-942.

Franks PJ, Farquhar GD. 2007. The mechanical diversity of stomata and its significance in gas-exchange control. *Plant Physiology* **143**(1): 78-87.

Gailing O, Langenfeld-Heyser R, Polle A, Finkeldey R. 2008. Quantitative trait loci affecting stomatal density and growth in a Quercus robur progeny: implications for the adaptation to changing environments. *Global Change Biology* **14**(8): 1934-1946.

Galatis B, Apostolakos P, Katsaros C. 1983. Microtubules and their organizing centres in differentiating guard cells of Adiantum capillus veneris. *Protoplasma* **115**(2): 176-192.

Geiger D, Scherzer S, Mumm P, Marten I, Ache P, Matschi S, Liese A, Wellmann C, Al-Rasheid KAS, Grill E, et al. 2010. Guard cell anion channel SLAC1 is regulated by CDPK protein kinases with distinct Ca2+ affinities. *Proceedings of the National Academy of Sciences of the United States of America* **107**(17): 8023-8028.

Geiger D, Scherzer S, Mumm P, Stange A, Marten I, Bauer H, Ache P, Matschi S, Liese A, Al-Rasheid KAS, et al. 2009. Activity of guard cell anion channel SLAC1 is controlled by drought-stress signaling kinase-phosphatase pair. *Proceedings of the National Academy of Sciences* **106**(50): 21425-21430.

Gérardin T, Douthe C, Flexas J, Brendel O. 2018. Shade and drought growth conditions strongly impact dynamic responses of stomata to variations in irradiance in Nicotiana tabacum. *Environmental and Experimental Botany* **153**: 188-197.

Ghashghaie J, Badeck F-W, Lanigan G, Nogués S, Tcherkez G, Deléens E, Cornic G, Griffiths H. 2003. Carbon isotope fractionation during dark respiration and photorespiration in C3 plants. *Phytochemistry Reviews* **2**(1): 145-161.

Ghashghaie J, Duranceau M, Badeck FW, Cornic G, Adeline MT, Deleens E. 2001. δ13C of CO2 respired in the dark in relation to δ13C of leaf metabolites: comparison between Nicotiana sylvestris and Helianthus annuus under drought. *Plant, Cell & Environment* **24**(5): 505-515.

Gillon JS, Griffiths H. 1997. The influence of (photo)respiration on carbon isotope discrimination in plants. *Plant, Cell & Environment* **20**(10): 1217-1230.

Giovannelli A, Deslauriers A, Fragnelli G, Scaletti L, Castro G, Rossi S, Crivellaro A. 2007. Evaluation of drought response of two poplar clones (Populus x canadensis Monch 'I-214' and P-deltoides Marsh. 'Dvina') through high resolution analysis of stem growth. *Journal of Experimental Botany* **58**(10): 2673-2683.

Gonfiantini R. 1984. I.A.E.A Advisory group meeting on stable isotope reference samples for geochemical and hydrological investigations. *Chemical Geology* **46**(1): 85.

Grace JC, Jarvis PG, Norman JM. 1987. Modelling the interception of solar radiant energy in intensively managed stands. *New Zealand Journal of Forestry Science* **17**(2-3): 193-209.

Granier A. 1985. A new method of sapflow measurement in tree stems. *Annales Des Sciences Forestieres* **42**(2): 193-200.

Granier A. 1987. Evaluation of transpiration in a Douglas-fir stand by means of sapflow measurements. *Tree Physiology* **3**(4): 309-319.

Gregory FG, Pearse HL. 1937. The effect on the behaviour of stomata of alternating periods of light and darkness of short duration. *Annals of Botany* **1**(1): 3-10.

Gruber N, Galloway JN. 2008. An Earth-system perspective of the global nitrogen cycle. *Nature* **451**: 293.

Gutierrez MV, Meinzer FC. 1994. Carbon isotope discrimination and photosynthetic gas exchange in coffee hedgerows during canopy development. *Functional Plant Biology* **21**: 207-219.

Hageneder F. 2005. *The meaning of trees.* San Francisco, CA: Chronicle Books.

Ham JM, Kluitenberg GJ, Lamont WJ. 1993. Optical-properties of plastic mulches affect the field temperature regime. *Journal of the American Society for Horticultural Science* **118**(2): 188-193.

Hamdy A, Ragab R, Scarascia-Mugnozza E. 2003. Coping with water scarcity: water saving and increasing water productivity. *Irrigation and Drainage* **52**(1): 3-20.

Haworth M, Marino G, Cosentino SL, Brunetti C, De Carlo A, Avola G, Riggi E, Loreto F, Centritto M. 2018. Increased free abscisic acid during drought enhances stomatal sensitivity and modifies stomatal behaviour in fast growing giant reed (Arundo donax L.). *Environmental and Experimental Botany* **147**: 116-124.

Henry A. 1914. A new hybrid poplar. . *Gardeners' Chronicle* **Series III**(56): 257-258.

Hetherington AM, Woodward FI. 2003. The role of stomata in sensing and driving environmental change. *Nature* **424**(6951): 901-908.

Hills A, Chen Z-H, Amtmann A, Blatt MR, Lew VL. 2012. OnGuard, a computational platform for quantitative kinetic modeling of guard cell physiology. *Plant Physiology* **159**(3): 1026-1042.

Hoerling M, Schubert S, Mo KC. 2013. *An interpretation of the origins of the 2012 central great plains drought assessment report.*: NOAA Drought Task Force.

Hostetler GL, Merwin I, Brown MG, Padilla-Zakour O. 2007. Influence of geotextile mulches on canopy microclimate, yield, and fruit composition of cabernet franc. *American Journal of Enology and Viticulture* **58**: 431-442.

Hsiang SM, Burke M, Miguel E. 2013. Quantifying the influence of climate on human conflict. *Science* **341**(6151): 1235367.

Hsiao TC. 1973. Plant responses to water stress. *Annual Review of Plant Physiology and Plant Molecular Biology* **24**: 519-570.

Hubbard KE, Nishimura N, Hitomi K, Getzoff ED, Schroeder JI. 2010. Early abscisic acid signal transduction mechanisms: newly discovered components and newly emerging questions. *Genes & Development* **24**(16): 1695-1708.

Hubick KT, Farquhar GD. 1989. Carbon isotope discrimination and the ratio of carbon gained to water lost in Barley cultivars. *Plant Cell & Environment* **12**(8): 795-804.

Hubick KT, Farquhar GD, Shorter R. 1986. Correlation between water-use efficiency and carbon isotope discrimination in diverse peanut (arachis) germplasm. *Australian Journal of Plant Physiology* **13**(6): 803-816.

Humble GD, Raschke K. 1971. Stomatal opening quantitatively related to potassium transport: evidence from electron probe analysis. *Plant Physiology* **48**(4): 447-453.

Ibrahim L, Proe MF, Cameron AD. 1998. Interactive effects of nitrogen and water availabilities on gas exchange and whole-plant carbon allocation in poplar. *Tree Physiology* **18**(7): 481-487.

IPCC. 2014. Meyer L, Brinkman S, van Kesteren L, Leprince-Ringuet N, van Boxmeer F, eds. *Climate change 2014: Synthesis report. Contribution of working groups I, II and III to the fifth assessment report of the intergovernmental panel on climate change*. Geneva, Switzerland: Cambridge University Press.

IPCC. 2018. Masson-Delmotte V, Pörtner HO, Skea J, Panmao Z, Roberts D, Shukla PR, Pirani A, Moufouma-Okia W, Péan C, Pidcock R, Connors S, Mattews JBR, Chen Y, Zhou XH, Gomis MI, Lonnoy E, Mauycock T, Tignor M, Waterfield T, eds. *Global warming of 1.5°C. An IPCC special report on the impacts of global warming of 1.5°C above pre-industrial levels and related global greenhouse gas emission pathways, in the context of strengthening the global response to the threat of climate change, sustainable development, and efforts to eradicate poverty*. Switzerland: Intergovernmental Panel on Climate Change. .

Isebrands JG, Richardson J. 2014. *Poplars and willows : trees for society and the environment*. Boston, Rome CABI and FAO.

Jacometti G 1937. I nuovi pioppi italiani. Atti del convegno di pioppicoltori in Casale Monferrato (11 luglio1937). . *Comitato Nazionale Forestale*. Roma.

Jansson S, Douglas CJ. 2007. Populus: A model system for plant biology. *Annual Review of Plant Biology* **58**: 435-458.

Jarvis PG. 1976. Interpretation of variations in leaf water potential and stomatal conductance found in canopies in field. *Philosophical Transactions of the Royal Society of London Series B-Biological Sciences* **273**(927): 593-610.

Jarvis PG, McNaughton KG 1986. Stomatal control of transpiration: scaling up from leaf to region. In: MacFadyen A, Ford ED eds. *Advances in Ecological Research*: Academic Press, 1-49.

Johnson RC, Bassett LM. 1991. Carbon isotope discrimination and water use efficiency in four cool-season grasses. *Crop Science* **31**.

Jones HG. 2014. *Plants and microclimate: A quantitative approach to environmental plant physiology, 3rd edition*. Cambridge: Cambridge Univ Press.

Kaiser H, Kappen L. 1997. In situ observations of stomatal movements in different light-dark regimes: the influence of endogenous rhythmicity and long-term adjustments. *Journal of Experimental Botany* **48**(8): 1583-1589.

Kaiser H, Kappen L. 2000. In situ observation of stomatal movements and gas exchange of Aegopodium podagraria L. in the understorey. *Journal of Experimental Botany* **51**(351): 1741-1749.

Kardiman R, Ræbild A. 2018. Relationship between stomatal density, size and speed of opening in Sumatran rainforest species. *Tree Physiology* **38**(5): 696-705.

Kearney TH, Shantz HL. 1911. The water economy of dry land crops. . *U.S. Department of Agriculture Yearbook for 1911*: 351-361.

Kim DJ, Lee JS. 2007. Current theories for mechanism of stomatal opening: Influence of blue light, mesophyll cells, and sucrose. *Journal of Plant Biology* **50**(5): 523-526.

Kinoshita T, Doi M, Suetsugu N, Kagawa T, Wada M, Shimazaki K-i. 2001. phot1 and phot2 mediate blue light regulation of stomatal opening. *Nature* **414**(6864): 656-660.

Kinoshita T, Nishimura M, Shimazaki K. 1995. Cytosolic concentration of Ca2+ regulates the plasma membrane H+-ATPase in guard cells of fava bean. *The Plant Cell* **7**(8): 1333-1342.

Kinoshita T, Shimazaki Ki. 1999. Blue light activates the plasma membrane H(+)-ATPase by phosphorylation of the C-terminus in stomatal guard cells. *The EMBO journal* **18**(20): 5548-5558.

Krinner G, Viovy N, de Noblet-Ducoudré N, Ogée J, Polcher J, Friedlingstein P, Ciais P, Sitch S, Prentice IC. 2005. A dynamic global vegetation model for studies of the coupled atmosphere-biosphere system. *Global Biogeochemical Cycles* **19**(1).

Lambrides CJ, Chapman SC, Shorter R. 2004. Genetic variation for carbon isotope discrimination in sunflower: association with transpiration efficiency and evidence for cytoplasmic inheritance. *Crop Science* **44**.

Lawson T, Blatt MR. 2014. Stomatal size, speed, and responsiveness impact on photosynthesis and water use efficiency. *Plant Physiology* **164**(4): 1556-1570.

Lawson T, Oxborough K, Morison JIL, Baker NR. 2002. Responses of photosynthetic electron transport in stomatal guard cells and mesophyll cells in intact leaves to light, CO2, and humidity. *Plant Physiology* **128**(1): 52-62.

Lawson T, Simkin AJ, Kelly G, Granot D. 2014. Mesophyll photosynthesis and guard cell metabolism impacts on stomatal behaviour. *New Phytologist* **203**(4): 1064-1081.

Lawson T, Vialet-Chabrand S. 2019. Speedy stomata, photosynthesis and plant water use efficiency. *New Phytologist* **221**(1): 93-98.

Le Quéré C, Andres RJ, Boden T, Conway T, Houghton RA, House JI, Marland G, Peters GP, van der Werf GR, Ahlström A, et al. 2013. The global carbon budget 1959–2011. *Earth Syst. Sci. Data* **5**(1): 165-185.

Leuning R. 1995. A critical-appraisal of a combined stomatal-photosynthesis model for C3 plants. *Plant Cell and Environment* **18**(4): 339-355.

Liu ZJ, Dickmann DI. 1996. Effects of water and nitrogen interaction on net photosynthesis, stomatal conductance, and water-use efficiency in two hybrid poplar clones. *Physiologia Plantarum* **97**(3): 507-512.

Males J, Griffiths H. 2017. Specialized stomatal humidity responses underpin ecological diversity in C3 bromeliads. *Plant Cell and Environment* **40**(12): 2931-2945.

Marguerit E, Bouffier L, Chancerel E, Costa P, Lagane F, Guehl JM, Plomion C, Brendel O. 2014. The genetics of water-use efficiency and its relation to growth in maritime pine. *Journal of Experimental Botany* **65**(17): 4757-4768.

Marino BD, McElroy MB. 1991. Isotopic composition of atmospheric CO2 inferred from carbon in C4 plant cellulose. *Nature* **349**(6305): 127-131.

Marron N. 2003. *Écophysiologie des peupliers euraméricains en réponse à la sécheresse.* PhD, Université d'Orléans Orléans.

Marron N, Villar M, Dreyer E, Delay D, Boudouresque E, Petit JM, Delmotte FM, Guehl JM, Brignolas F. 2005. Diversity of leaf traits related to productivity in 31 Populus deltoides x Populus nigra clones. *Tree Physiology* **25**(4): 425-435.

Masle J, Gilmore SR, Farquhar GD. 2005. The ERECTA gene regulates plant transpiration efficiency in Arabidopsis. *Nature* **436**(7052): 866-870.

Matthews JSA, Vialet-Chabrand S, Lawson T. 2018. Acclimation to fluctuating light impacts the rapidity of response and diurnal rhythm of stomatal conductance. *Plant Physiology* **176**(3): 1939-1951.

Matthews JSA, Vialet-Chabrand SRM, Lawson T. 2017. Diurnal variation in gas exchange: the balance between carbon fixation and water loss. *Plant Physiology* **174**(2): 614-623.
Mc Adam SAM, Brodribb TJ. 2015. The evolution of mechanisms driving the stomatal response to vapor pressure deficit. *Plant Physiology* **167**(3): 833-843.
Mc Ausland L, Vialet-Chabrand S, Davey P, Baker NR, Brendel O, Lawson T. 2016. Effects of kinetics of light-induced stomatal responses on photosynthesis and water-use efficiency. *New Phytologist* **211**(4): 1209-1220.
McAinsh MR, Brownlee C, Hetherington AM. 1990. Abscisic acid-induced elevation of guard cell cytosolic Ca2+ precedes stomatal closure. *Nature* **343**(6254): 186-188.
Medlyn B. 2004. *A MAESTRO retrospective*.
Medlyn BE, Duursma RA, Eamus D, Ellsworth DS, Prentice IC, Barton CVM, Crous KY, de Angelis P, Freeman M, Wingate L. 2011. Reconciling the optimal and empirical approaches to modelling stomatal conductance. *Global Change Biology* **17**(6): 2134-2144.
Medrano H, Tomas M, Martorell S, Flexas J, Hernandez E, Rossello J, Pou A, Escalona JM, Bota J. 2015. From leaf to whole-plant water use efficiency (WUE) in complex canopies: Limitations of leaf WUE as a selection target. *Crop Journal* **3**(3): 220-228.
Ministère de l'agriculture et de l'alimentation. 2019. Le gouvernement annonce la généralisation des projets de territoire pour la gestion de l'eau. [WWW document] https://agriculture.gouv.fr/le-gouvernement-annonce-la-generalisation-des-projets-de-territoire-pour-la-gestion-de-leau, accessed June 12 2019.
Ministère de la transition écologique et solidaire. 2016. Gérer la sécheresse. [WWW document] https://www.ecologique-solidaire.gouv.fr/gerer-secheresse, Accessed June 6 2019.
Monclus R. 2006. *Efficience d'utilisation de l'eau et tolérance à la sécheresse chez le peuplier.* PhD, Université d'Orléans Orléans.
Monclus R, Dreyer E, Delmotte FM, Villar M, Delay D, Boudouresque E, Petit JM, Marron N, Brechet C, Brignolas F. 2005. Productivity, leaf traits and carbon isotope discrimination in 29 Populus deltoides x P-nigra clones. *New Phytologist* **167**(1): 53-62.
Monclus R, Dreyer E, Villar M, Delmotte FM, Delay D, Petit JM, Barbaroux C, Le Thiec D, Brechet C, Brignolas F. 2006. Impact of drought on productivity and water use efficiency in 29 genotypes of Populus deltoides x Populus nigra. *New Phytologist* **169**(4): 765-777.
Mooney HA, Ferrar PJ, Slatyer RO. 1978. Photosynthetic capacity and carbon allocation patterns in diverse growth forms of Eucalyptus. *Oecologia* **36**(1): 103-111.
Mott KA, Cardon ZG, Berry JA. 1993. Asymmetric patchy stomatal closure for the 2 surfaces of Xanthium strumarium leaves at low humidity. *Plant Cell and Environment* **16**(1): 25-34.
Mott KA, Sibbernsen ED, Shope JC. 2008. The role of the mesophyll in stomatal responses to light and CO2. *Plant Cell and Environment* **31**(9): 1299-1306.
Muller E, Lambs L. 2009. Daily variations of water use with vapor pressure deficit in a plantation of I214 poplars. *Water* **1**(1): 32.
Naiman RJ, Décamps H, McClain ME. 2005. Riparia - ecology, conservation and management of streamside communities. *Aquatic Conservation: Marine and Freshwater Ecosystems* **17**(6): 657-657.
Navarro A, Portillo-Estrada M, Arriga N, Vanbeveren SPP, Ceulemans R. 2018. Genotypic variation in transpiration of coppiced poplar during the third rotation of a short-rotation bio-energy culture. *GCB Bioenergy* **10**(8): 592-607.
Ng PAP, Jarvis PG. 1980. Hysteresis in the response of stomatal conductance in Pinus sylvestris L needles to light - Observations and a hypothesis. *Plant Cell and Environment* **3**(3): 207-216.
Nickel UT, Winkler JB, Mühlhans S, Buegger F, Munch JC, Pritsch K. 2017. Nitrogen fertilisation reduces sink strength of poplar ectomycorrhizae during recovery after drought more than phosphorus fertilisation. *Plant and Soil* **419**(1): 405-422.
Nisbet EG, Manning MR, Dlugokencky EJ, Fisher RE, Lowry D, Michel SE, Myhre CL, Platt M, Allen G, Bousquet P, et al. 2019. Very strong atmospheric methane growth in the 4

years 2014-2017: implications for the paris agreement. *Global Biogeochemical Cycles* **33**(3): 318-342.

Norman JM, Welles JM. 1983. Radiative-transfert in an array of canopies. *Agronomy Journal* **75**(3): 481-488.

Normand M. 1974. Méthode d'étalonnage d'un humidimètre à neutrons utilisant les mesures de densité du densimètre gamma associé.: 53-69.

Nye PH, Tinker PB, Boast CW. 1979. Solute movement in the soil-root system. *Soil Science* **127**(4): 254.

Olbrich BW, Le Roux D, Poulter AG, Bond WJ, Stock WD. 1993. Variation in water use efficiency and δ13C levels in Eucalyptus grandis clones. *Journal of Hydrology* **150**(2): 615-633.

Olsen RL, Pratt RB, Gump P, Kemper A, Tallman G. 2002. Red light activates a chloroplast-dependent ion uptake mechanism for stomatal opening under reduced CO2 concentrations in Vicia spp. *New Phytologist* **153**(3): 497-508.

Ooba M, Takahashi H. 2003. Effect of asymmetric stomatal response on gas-exchange dynamics. *Ecological Modelling* **164**(1): 65-82.

Oren R, Sheriff DW 1995. Water and nutrient acquisition by roots and canopies. In: Smith WK, Hinckley TM eds. *Resource physiology of conifers. acquisition, allocation, and Utilization,*. San Diego, United States: Academic Press, Inc., 39-74.

Outlaw WH, Manchester J. 1979. Guard cell starch concentration quantitatively related to stomatal aperture. *Plant Physiology* **64**(1): 79-82.

Oxborough K, Baker NR. 1997. An instrument capable of imaging chlorophyll a fluorescence from intact leaves at very low irradiance and at cellular and subcellular levels of organization. *Plant, Cell & Environment* **20**(12): 1473-1483.

Palmgren MG. 2001. Plant plasma membrane H+-ATPases: powerhouses for nutrient uptake. *Annual Review of Plant Physiology and Plant Molecular Biology* **52**(1): 817-845.

Park S-Y, Fung P, Nishimura N, Jensen DR, Fujii H, Zhao Y, Lumba S, Santiago J, Rodrigues A, Chow T-fF, et al. 2009. Abscisic acid inhibits PP2Cs via the PYR/PYL family of ABA-binding START proteins. *Science (New York, N.Y.)* **324**(5930): 1068-1071.

Peak D, Mott KA. 2011. A new, vapour-phase mechanism for stomatal responses to humidity and temperature. *Plant Cell and Environment* **34**(1): 162-178.

Peters GP, Andrew RM, Boden T, Canadell JG, Ciais P, Le Quéré C, Marland G, Raupach MR, Wilson C. 2012. The challenge to keep global warming below 2 °C. *Nature Climate Change* **3**: 4.

Ponton S, Dupouey J-L, Nathalie B, Dreyer E. 2002. Comparison of water-use efficiency of seedlings from two sympatric oak species: Genotype x environment interactions. *Tree Physiology* **22**: 413-422.

Porcar-Castell A, Tyystjarvi E, Atherton J, van der Tol C, Flexas J, Pfundel EE, Moreno J, Frankenberg C, Berry JA. 2014. Linking chlorophyll a fluorescence to photosynthesis for remote sensing applications: mechanisms and challenges. *Journal of Experimental Botany* **65**(15): 4065-4095.

Prieto JA, Lebon E, Ojeda H. 2010. Stomatal behavior of different grapevine cultivars in response to soil water status and air water vapor pressure deficit. *Journal International Des Sciences De La Vigne Et Du Vin* **44**(1): 9-20.

Qu MN, Hamdani S, Li WZ, Wang SM, Tang JY, Chen Z, Song QF, Li M, Zhao HL, Chang TG, et al. 2016. Rapid stomatal response to fluctuating light: an under-explored mechanism to improve drought tolerance in rice. *Functional Plant Biology* **43**(8): 727-738.

Rasheed F. 2012. *Components of transpiration efficiency in poplars : genetic diversity, stability with age and scaling from leaf to whole plant level.* PhD, AgroParisTech Nancy.

Rasheed F, Dreyer E, Richard B, Brignolas F, Brendel O, Le Thiec D. 2015. Vapour pressure deficit during growth has little impact on genotypic differences of transpiration efficiency

at leaf and whole-plant level: an example from Populus nigra L. *Plant Cell & Environment* **38**(4): 670-684.

Rasheed F, Dreyer E, Richard B, Brignolas F, Montpied P, Le Thiec D. 2013. Genotype differences in C-13 discrimination between atmosphere and leaf matter match differences in transpiration efficiency at leaf and whole-plant levels in hybrid Populus deltoides x nigra. *Plant Cell and Environment* **36**(1): 87-102.

Rasheed F, Richard B, Le Thiec D, Montpied P, Paillassa E, Brignolas F, Dreyer E. 2011. Time course of delta C-13 in poplar wood: genotype ranking remains stable over the life cycle in plantations despite some differences between cellulose and bulk wood. *Tree Physiology* **31**(11): 1183-1193.

Raven JA. 2014. Speedy small stomata? *Journal of Experimental Botany* **65**(6): 1415-1424.

Ray IM, Townsend MS, Muncy CH, Henning JA. 1999. Heritabilities of water-use efficiency traits and correlations with agronomic traits in water-stressed alfalfa. *Crop Science* **39**(2): 494-498.

Rayment MB, Loustau D, Jarvis PG. 2000. Measuring and modeling conductances of black spruce at three organizational scales: shoot, branch and canopy. *Tree Physiology* **20**(11): 713-723.

Read JJ, Johnson DA, Asay KH, Tieszen LL. 1991. Carbon isotope discrimination, gas-exchange, and water-use efficiency in crested Wheatgrass clones. *Crop Science* **31**(5): 1203-1208.

Reich PB. 1984. Loss of stomatal function in ageing hybrid poplar leaves. *Annals of Botany* **53**(5): 691-698.

Richardson F, Brodribb TJ, Jordan GJ. 2017. Amphistomatic leaf surfaces independently regulate gas exchange in response to variations in evaporative demand. *Tree Physiology* **37**(7): 869-878.

Rodriguez-Dominguez CM, Buckley TN, Egea G, de Cires A, Hernandez-Santana V, Martorell S, Diaz-Espejo A. 2016. Most stomatal closure in woody species under moderate drought can be explained by stomatal responses to leaf turgor. *Plant Cell and Environment* **39**(9): 2014-2026.

Roelfsema MRG, Hanstein S, Felle HH, Hedrich R. 2002. CO2 provides an intermediate link in the red light response of guard cells. *Plant Journal* **32**(1): 65-75.

Roth-Nebelsick A, Grein M, Utescher T, Konrad W. 2012. Stomatal pore length change in leaves of Eotrigonobalanus furcinervis (Fagaceae) from the Late Eocene to the Latest Oligocene and its impact on gas exchange and CO2 reconstruction. *Review of Palaeobotany and Palynology* **174**: 106-112.

Roussel M, Dreyer E, Montpied P, Le-Provost G, Guehl JM, Brendel O. 2009a. The diversity of C-13 isotope discrimination in a Quercus robur full-sib family is associated with differences in intrinsic water use efficiency, transpiration efficiency, and stomatal conductance. *Journal of Experimental Botany* **60**(8): 2419-2431.

Roussel M, Le Thiec D, Montpied P, Ningre N, Guehl J-M, Brendel O. 2009b. Diversity of water use efficiency among Quercus robur genotypes: contribution of related leaf traits. *Annals of Forest Science* **66**(4): 408-408.

Sack L, Cowan PD, Jaikumar N, Holbrook NM. 2003. The 'hydrology' of leaves: co-ordination of structure and function in temperate woody species. *Plant, Cell & Environment* **26**(8): 1343-1356.

Sánchez-Gómez D, Robson TM, Gascó A, Gil-Pelegrín E, Aranda I. 2013. Differences in the leaf functional traits of six beech (Fagus sylvatica L.) populations are reflected in their response to water limitation. *Environmental and Experimental Botany* **87**: 110-119.

Sato A, Sato Y, Fukao Y, Fujiwara M, Umezawa T, Shinozaki K, Hibi T, Taniguchi M, Miyake H, Goto DB, et al. 2009. Threonine at position 306 of the KAT1 potassium channel is essential for channel activity and is a target site for ABA-activated SnRK2/OST1/SnRK2.6 protein kinase. *Biochemical Journal* **424**: 439-448.

Schroeder JI, Hagiwara S. 1989. Cytosolic calcium regulates ion channels in the plasma membrane of Vicia faba guard cells. *Nature* **338**: 427.

Schroeder JI, Hedrich R, Fernandez JM. 1984. Potassium-selective single channels in guard cell protoplasts of Vicia faba. *Nature* **312**(5992): 361-362.

Schroeder JI, Keller BU. 1992. Two types of anion channel currents in guard cells with distinct voltage regulation. *Proceedings of the National Academy of Sciences of the United States of America* **89**(11): 5025-5029.

Schroeder JI, Raschke K, Neher E. 1987. Voltage dependence of K+ channels in guard-cell protoplasts. *Proceedings of the National Academy of Sciences* **84**(12): 4108-4112.

Sheffield J, Wood EF. 2008. Projected changes in drought occurrence under future global warming from multi-model, multi-scenario, IPCC AR4 simulations. *Climate Dynamics* **31**(1): 79-105.

Sheriff DW. 1979. Water-vapor and heat-transfer in leaves. *Annals of Botany* **43**(2): 157-171.

Shimazaki K-i, Doi M, Assmann SM, Kinoshita T 2007. Light regulation of stomatal movement. *Annual Review of Plant Biology*, 219-247.

Solomon S, Plattner G-K, Knutti R, Friedlingstein P. 2009. Irreversible climate change due to carbon dioxide emissions. *Proceedings of the National Academy of Sciences of the United States of America* **106**(6): 1704-1709.

Sondergaard TE, Schulz A, Palmgren MG. 2004. Energization of transport processes in plants. Roles of the plasma membrane H+-ATPase. *Plant Physiology* **136**(1): 2475-2482.

Song JY, Wang Y, Pan YH, Pang JY, Zhang X, Fan JF, Zhang Y. 2019. The influence of nitrogen availability on anatomical and physiological responses of Populus alba x P-glandulosa to drought stress. *BMC Plant Biology* **19**.

Sperry JS, Hacke UG, Oren R, Comstock JP. 2002. Water deficits and hydraulic limits to leaf water supply. *Plant Cell and Environment* **25**(2): 251-263.

Sternberg T. 2011. Regional drought has a global impact. *Nature* **472**(7342): 169-169.

Stettler RF. 2009. *Cottonwood and the river of time.* . Seattle, WA: University of Washington Press.

Stobrawa K. 2014. *Poplars (Populus spp.): ecological role, applications and scientific perspectives in the 21st century*.

Stout AB, Schreiner EJ. 1933. Results of a project in hybridizing poplars. . *Journal of Heredity* **24**: 216-229.

Tardieu F, Simonneau T. 1998. Variability among species of stomatal control under fluctuating soil water status and evaporative demand: modelling isohydric and anisohydric behaviours. *Journal of Experimental Botany* **49**: 419-432.

Thivolle-Cazat A. 2002. A. T-C, ed. *Disponibilité en bois de peuplier en France de 2002 à 2020. Rapport AFOCEL*. Paris, France: Commission Nationale du Peuplier.

Tinoco-Ojanguren C, Pearcy RW. 1993. Stomatal dynamics and its importance to carbon gain in two rainforest Piper species. *Oecologia* **94**(3): 395-402.

Touma D, Ashfaq M, Nayak MA, Kao S-C, Diffenbaugh NS. 2015. A multi-model and multi-index evaluation of drought characteristics in the 21st century. *Journal of Hydrology* **526**: 196-207.

Tschaplinski TJ, Blake TJ. 1989. Water relations, photosynthetic capacity, and root shoot partitioning of photosynthates as determinants of productivity in hybrid poplar. *Canadian Journal of Botany-Revue Canadienne De Botanique* **67**(6): 1689-1697.

Tschaplinski TJ, Tuskan GA, Gebre GM, Todd DE. 1998. Drought resistance of two hybrid Populus clones grown in a large-scale plantation. *Tree Physiology* **18**(10): 653-658.

Turner NC, Palta JA, Shrestha R, Ludwig C, Siddique KHM, Turner DW. 2007. Carbon isotope discrimination is not correlated with transpiration efficiency in three cool-season grain legumes (pulses). *Journal of Integrative Plant Biology* **49**(10): 1478-1483.

Tuskan GA, DiFazio S, Jansson S, Bohlmann J, Grigoriev I, Hellsten U, Putnam N, Ralph S, Rombauts S, Salamov A, et al. 2006. The genome of black cottonwood, Populus trichocarpa (Torr. and Gray). *Science* **313**(5793): 1596-1604.

Tuzet A, Perrier A, Leuning R. 2003. A coupled model of stomatal conductance, photosynthesis and transpiration. *Plant Cell and Environment* **26**(7): 1097-1116.

Vahisalu T, Kollist H, Wang Y-F, Nishimura N, Chan W-Y, Valerio G, Lamminmäki A, Brosché M, Moldau H, Desikan R, et al. 2008. SLAC1 is required for plant guard cell S-type anion channel function in stomatal signalling. *Nature* **452**: 487.

Vanden Broeck A, Villar M, Van Bockstaele E, Van Slycken J. 2005. Natural hybridization between cultivated poplars and their wild relatives: evidence and consequences for native poplar populations. *Annals of Forest Science* **62**(7): 601-613.

Vialet-Chabrand S, Brendel O. 2014. Automatic measurement of stomatal density from microphotographs. *Trees-Structure and Function* **28**(6): 1859-1865.

Vialet-Chabrand S, Dreyer E, Brendel O. 2013. Performance of a new dynamic model for predicting diurnal time courses of stomatal conductance at the leaf level. *Plant Cell and Environment* **36**(8): 1529-1546.

Vialet-Chabrand S, Lawson T. 2019. Dynamic leaf energy balance: deriving stomatal conductance from thermal imaging in a dynamic environment. *Journal of Experimental Botany* **70**(10): 2839-2855.

Vialet-Chabrand S, Matthews J, McAusland L, Blatt MR, Griffiths H, Lawson T. 2017. Temporal dynamics of stomatal behavior: modeling and implications for photosynthesis and water use. *Plant Physiology* **174**(2): 603-613.

Vialet-Chabrand S, Matthews JSA, Brendel O, Blatt MR, Wang Y, Hills A, Griffiths H, Rogers S, Lawson T. 2016. Modelling water use efficiency in a dynamic environment: An example using Arabidopsis thaliana. *Plant Science* **251**: 65-74.

Vico G, Manzoni S, Palmroth S, Katul G. 2011. Effects of stomatal delays on the economics of leaf gas exchange under intermittent light regimes. *New Phytologist* **192**(3): 640-652.

Viger M, Rodriguez-Acosta M, Rae AM, Morison JIL, Taylor G. 2013. Toward improved drought tolerance in bioenergy crops: QTL for carbon isotope composition and stomatal conductance in Populus. *Food and Energy Security* **2**(3): 220-236.

Viger M, Smith HK, Cohen D, Dewoody J, Trewin H, Steenackers M, Bastien C, Taylor G. 2016. Adaptive mechanisms and genomic plasticity for drought tolerance identified in European black poplar (Populus nigra L.). *Tree Physiology* **36**(7): 909-928.

Viola P, Jones MJ. 2004. Robust real-time face detection. *International Journal of Computer Vision* **57**(2): 137-154.

Virgona JM, Farquhar GD. 1996. Genotypic variation in relative growth rate and carbon isotope discrimination in sunflower is related to photosynthetic capacity. *Australian Journal of Plant Physiology* **23**(2): 227-236.

Voltas J, Serrano L, Hernandez M, Peman J. 2006. Carbon isotope discrimination, gas exchange and stem growth of four euramerican hybrid poplars under different watering regimes. *New Forests* **31**(3): 435-451.

Walsh BD, MacKenzie AF, Buszard DJ. 1996a. Soil nitrate levels as influenced by apple orchard floor management systems. *Canadian Journal of Soil Science* **76**(3): 343-349.

Walsh BD, Salmins S, Buszard DJ, MacKenzie AF. 1996b. Impact of soil management systems on organic dwarf apple orchards and soil aggregate stability, bulk density, temperature and water content. *Canadian Journal of Soil Science* **76**(2): 203-209.

Wang H, Yang Z, Yu Y, Chen S, He Z, Wang Y, Jiang L, Wang G, Yang C, Liu B, et al. 2017. Drought enhances nitrogen uptake and assimilation in maize roots. *Agronomy Journal* **109**(1): 39-46.

Weih M, Bonosi L, Ghelardini L, Rönnberg-Wästljung AC. 2011. Optimizing nitrogen economy under drought: increased leaf nitrogen is an acclimation to water stress in willow (Salix spp.). *Annals of Botany* **108**(7): 1347-1353.

Welles J, Norman J, Martsolf JD. 1979. Orchard foliage temperature model. *Journal American Society for Horticultural Science* **104:5**.

Williams M, Law BE, Anthoni PM, Unsworth MH. 2001. Use of a simulation model and ecosystem flux data to examine carbon-water interactions in ponderosa pine. *Tree Physiology* **21**(5): 287-298.

Williams M, Rastetter EB, Fernandes DN, Goulden ML, Wofsy SC, Shaver GR, Melillo JM, Munger JW, Fan SM, Nadelhoffer KJ. 1996. Modelling the soil-plant-atmosphere continuum in a Quercus-Acer stand at Harvard forest: The regulation of stomatal conductance by light, nitrogen and soil/plant hydraulic properties. *Plant Cell and Environment* **19**(8): 911-927.

Wong SC, Cowan IR, Farquhar GD. 1979. Stomatal conductance correlates with photosynthetic capacity. *Nature* **282**(5737): 424-426.

Xu Cy, Lin Gh, Griffin KL, Sambrotto RN. 2004. Leaf respiratory CO2 is 13C-enriched relative to leaf organic components in five species of C3 plants. *New Phytologist* **163**(3): 499-505.

Yamauchi S, Takemiya A, Sakamoto T, Kurata T, Tsutsumi T, Kinoshita T, Shimazaki K. 2016. The plasma membrane H+-ATPase AHA1 plays a major role in stomatal opening in response to blue light. *Plant Physiology* **171**(4): 2731-2743.

Yoshida R, Umezawa T, Mizoguchi T, Takahashi S, Takahashi F, Shinozaki K. 2006. The regulatory domain of SRK2E/OST1/SnRK2.6 interacts with ABI1 and integrates abscisic acid (ABA) and osmotic stress signals controlling stomatal closure in Arabidopsis. *Journal of Biological Chemistry* **281**(8): 5310-5318.

Zhang X, Zang R, Li C. 2004. Population differences in physiological and morphological adaptations of Populus davidiana seedlings in response to progressive drought stress. *Plant Science* **166**(3): 791-797.

ABSTRACT

The number of drought events is expected to increase in intensity and frequency as a result of climate change. Since poplar productivity is closely linked to water availability, there is an increasing risk of decline in wood production from poplar plantations. Optimization of the ratio of biomass production to water used (i.e. water use efficiency, WUE) appears therefore as a relevant target for poplar research. Previous studies have shown the clonal diversity of WUE in poplar is driven mainly by stomatal conductance (g_s). However g_s and photosynthesis are not always tightly coupled which can result in large variations of WUE at leaf level. Additionally, because transpiration efficiency (TE) is laborious to measure, experiments are often conducted in pots in glasshouses. However in controlled conditions the environment is widely different than in the field and comparisons of WUE in controlled and field conditions are scarce in the literature.

We assessed the diversity of stomatal dynamics among poplar genotypes under control or drought conditions grown in a glasshouse and in the field. We investigated the link between physiological, morphological and molecular factors and stomatal dynamics, and their influence on TE. Furthermore, we examined the relation between different estimators of WUE and its components between controlled and field conditions. Element content and candidate gene expression in the guard cells were also quantified at two times during the day to analyze their link to stomatal conductance.

We found among the four genotypes studied significant genotypic variability of stomatal dynamics to irradiance and VPD which was altered by drought and growing conditions. Stomatal size and density as well as water use, but not WUE, were correlated to stomatal dynamics, emphasizing the importance and complexity of such mechanisms at the whole plant scale. Good agreements between leaf-level and whole-plant WUE among genotypes and between growing conditions were also found. Finally, distinct guard cell element contents and candidate gene expression, between leaf sides and time of day, linked with stomatal conductance draw attention to the diversity of components contributing to TE. These findings provides valuable information to better understand the diverse, sometimes unsuspected, leaf-level mechanisms driving water use efficiency at the whole plant scale.

Key words: water use efficiency, climate change, stomatal conductance, drought, upscaling

RÉSUMÉ

Il est prévu une augmentation de l'intensité et de la fréquence des sécheresses dans les années à venir à cause des changements climatiques. Puisque la productivité des peupliers est étroitement liée à la disponibilité en eau, il existe un risque de déclin de la production de bois dans les peupleraies. L'optimisation de la biomasse produite en regard de l'eau consommée (efficience d'utilisation de l'eau, WUE) apparaît alors être une question de recherche prometteuse. Des études précédentes ont montré une diversité clonale de WUE chez les peupliers, pilotée principalement par la conductance stomatique (g_s). Cependant, g_s et l'assimilation en CO_2 ne sont pas toujours connectés, ce qui peut conduire à de fortes variations de WUE au niveau foliaire. De plus, puisque la mesure de l'efficience d'utilisation de l'eau au niveau de la plante entière (TE) est laborieuse à mesurer, les expérimentations sont souvent réalisées en serre. Toutefois, les conditions contrôlées d'une serre conduisent à un environnementent très différent des conditions naturelles, et les comparaisons de WUE entre conditions contrôlées et naturelles sont rares dans la littérature.

Nous avons évalué la diversité des dynamiques stomatiques au sein de génotypes de peupliers sous conditions témoins et sous sécheresse en serre et en pépinière. Nous avons examiné le lien entre différents facteurs physiologiques, morphologiques et moléculaires et les dynamiques stomatiques, ainsi que leur influence sur TE. De plus, nous avons étudié la relation entre différents estimateurs de WUE et ses composantes entre des conditions contrôlées et naturelles. Le contenu en éléments minéraux et l'expression de gènes candidats ont également été quantifiés à deux moments de la journée pour analyser leur relation avec g_s.

Nous avons observé une variabilité génotypique significative des dynamiques stomatiques à la fois en réponse à l'irradiance et au VPD, de plus modifiée par la sécheresse et les conditions de croissance. La taille et la densité des stomates ainsi que la transpiration foliaire étaient fortement corrélées aux dynamiques stomatiques en serre, mais très peu en pépinière. Ces résulats soulignent l'importance et la complexité de ces mécanismes à l'échelle de la plante entière. WUE au niveau de la feuille et de la plante entière étaient relativement stables au sein des génotypes et entre conditions de croissance, mais bien moins avec la sécheresse. Enfin, des contenus en éléments et des expressions géniques distinctes ont été observées entre faces de la feuille et enter moments de la journée, en lien avec g_s. Ces résultats fournissent de précieuses informations pour mieux comprendre les divers mécanismes foliaires pilotant WUE au niveau de la plante entière.

Mot-clés: efficience d'utilisation de l'eau, changements climatiques, conductance stomatique, sécheresse, changement d'échelle.